THE WATER INSTITUTE
OF THE GULF®

A COMMUNITY-INFORMED TRANSDISCIPLINARY APPROACH TO MAXIMIZING BENEFITS OF DREDGED SEDIMENT FOR WETLAND RESTORATION PLANNING AT PORT FOURCHON, LOUISIANA

Quantifying Social, Ecosystem, and Carbon Emissions Reduction Benefits of Wetland Restoration, and Ecosystem Evolution through 2050

ABOUT THE WATER INSTITUTE OF THE GULF

The Water Institute of the Gulf is a not-for-profit, independent research institute dedicated to advancing the understanding of coastal, deltaic, river and water resource systems, both within the Gulf Coast and around the world. This mission supports the practical application of innovative science and engineering, providing solutions that benefit society. For more information, visit www.thewaterinstitute.org.

ABOUT THE PARTNERSHIP FOR OUR WORKING COAST

The Water Institute of the Gulf and partners established The Partnership for Our Working Coast with Chevron, Shell, Danos, and the Greater Lafourche Port Commission in 2017. The Partnership for Our Working Coast takes a science-based approach to maximizing the benefits of coastal restoration efforts to protect energy assets and critical infrastructure as a vital component of industry's risk management and sustainability business drivers. In close collaboration with companies to determine what areas in and around the Port are most important from a critical infrastructure perspective, the group has focused its efforts on science and engineering to answer questions around the port concerning (a) options for optimizing the placement of beneficially-used dredged material to create nature-based defenses for critical infrastructure and communities; (b) land subsidence; (c) quantification of the potential for blue carbon capture and sequestration potential of the coastal ecosystems created using the dredged material; and (d) community resilience.

SUGGESTED CITATION

The Water Institute of the Gulf (2022). Partnership for Our Working Coast: A Community-Informed Transdisciplinary Approach to Maximizing Benefits of Dredged Sediment for Wetland Restoration Planning at Port Fourchon, Louisiana. Prepared for and funded by The National Fish and Wildlife Foundation, Shell, Chevron, Danos, and the Greater Lafourche Port Commission. Baton Rouge, LA.

PREFACE

Port Fourchon is a vital staging area for Gulf of Mexico energy production that is strategically located in one of the most fragile and rapidly evolving landscapes in the United States. The Greater Lafourche Port Commission is aware of the challenges posed by ongoing land loss and sea level rise, and continues to adapt—as they have since the early days of Port Fourchon—to provide the essential services with minimal disruption. The 2020 and 2021 hurricane seasons brought multiple impacts to Port Fourchon and the surrounding areas, including hurricanes Zeta and Ida which both made landfall within the area of analysis for this project. These recent storms underscore the importance of a resilient Port Fourchon and nature-based solutions such as those evaluated within this study are a crucial to the Port's resilience strategy, future growth, and continuation of services rendered.

The Public-Private Partnership Plus (P3+) of the Partnership for Our Working Coast (POWC) used for this effort combines the resources and expertise of public, private, and non-governmental organizations with the aim of enhancing coastal habitat and enhancing community and industry resilience. The partners (The Water Institute of the Gulf, Greater Lafourche Port Commission, Shell, Chevron, Danos, National Fish and Wildlife Foundation) provided not only funding for this work, but valuable input into the scope and aims of the project. The close partnership of scientists, funders, decision makers, and community members has already demonstrated benefits result in better outcomes for all. This approach builds on Port Fourchon's 20-year history of holistic, nature-based resilience activities, and scales up these activities through the use of collaborative implementation and state-of-the-art science and nature-based engineering. The POWC will serve as a model across the Gulf and around the country with respect to collaborative planning and shared funding to design nature-based coastal restoration projects with benefits across a range of stakeholders.

The objectives of this study are to: 1) develop and employ a community stakeholder-driven process to inform and evaluate an ecosystem restoration and sediment management strategy that enhances the resilience of the Port Fourchon community and surrounding ecosystems; and 2) assess blue carbon potential capture and storage of wetlands (including the sustainability of existing wetlands) restored with dredge material produced during navigation channel deepening.

A transdisciplinary scientific approach was designed and implemented that involved development and use of various numerical and analytical models to address these objectives. Landscape evolution in coastal Louisiana is complex, but the application of scientific modeling that captures the relevant processes can give insight into better ways to prepare for future challenges. While no model can precisely predict the future, this modeling effort to predict long-term wetland processes aims to understand the broad landscape trends in land area and wetland vegetation changes in the future surrounding Port Fourchon. The ability for constructed or restored wetlands to capture and store carbon that would otherwise be stored in the atmosphere is important to quantify given the importance of reducing atmospheric CO_2 levels. Furthermore, understanding and assessing wetlands' ability to store carbon is timely research for the Louisiana coast in the context of an emerging carbon market. Specific attention was given to the carbon fluxes, ensuring that models developed could track carbon fluxes within habitats, and quantifying

projected carbon capture and storage of different wetland restoration configurations due to placement of dredge material as well as which type of wetland vegetation may colonize.

Members of the community who live and work around Port Fourchon were included at all stages of the scientific method, including development and prioritization of restoration areas, identifying important physical and ecological parameters that should be modeled, evaluation of model results, and evaluation of the potential societal benefit of the proposed wetland restoration alternatives under consideration. The results of the combined analyses demonstrate that not every potential wetland restoration configuration has equal benefits persisting into the future, mitigation of storm surge and waves, carbon sequestration, or community benefit. However, collectively the modeled restoration projects demonstrate the effectiveness of a systematic approach to wetland restoration and sediment management in the vicinity of Port Fourchon at mitigating negative impacts of wetland loss to community resilience and ecosystem sustainability. This study provides approaches and tools that can be adapted for use elsewhere to develop holistic solutions that maximize benefits and enhance resilience.

AUTHORS AND CONTRIBUTORS

AUTHORS

Melissa Baustian

Harris Bienn

Martijn Bregman

Zach Cobell

Soupy Dalyander

Christine DeMeyers*

Christopher Esposito

Ioannis Georgiou

Audrey Grismore

Scott Hemmerling

Hoonshin Jung

Lexie LaGrone

Diana Di Leonardo

Binqing Liu

Brett McMann

Mike Miner

REVIEWERS AND CONTRIBUTORS

Charley Cameron

Tim Carruthers

Andrew Courtois

Ryan Clark

Alyssa Dausman

Justin Ehrenwerth

Erin Kiskaddon

Adrian McInnis*

Francesca Messina

Leland Moss*

Jessi Parfait*

Cyndhia Ramatchandirane*

Jeremy Thompson*

Brendan Yuill

Shan Zou

*Denotes authors and contributors formerly of The Water Institute of the Gulf

ACKNOWLEDGEMENTS

Many partners contributed to this study, including Madeline Foster-Martinez (University of New Orleans) and the late Scott Duke-Sylvester (University of Louisiana-Lafayette) for vegetation modeling assistance, and Ed Piñero (Ecometrics LLC) for SROI assistance. The Institute would additionally like to thank our partners at Deltares (Anrejan Van Loenen, Arjen Markus, Freek Scheel, and Bob Smits) for technical support related to the Delft modeling suite.

This study was funded through a combination of support from the National Fish and Wildlife Foundation (Grant ID 0318.19.065625) and the Partnership for our Working Coast Public-Private Partnership Plus (Greater Lafourche Port Commission, Chevron, Danos, and Shell). Through the course of the study, a group of representatives from the National Fish and Wildlife Foundation and the Partnership for our Working Coast formed a group termed the *Kitchen Cabinet*. This group was instrumental in providing encouragement, guidance, and feedback for the effort. Participants included:

Leah Brown	Chevron
Tom Broom	Danos
Alexandra Cheramie	Chevron
Chett Chiasson	Greater Lafourche Port Commission
Felicia Frederick	Chevron
Lindsey Levine	Chevron
Samantha McGee	Danos
Frederick Palmer	Shell
Renee Piper	Danos
Jonathan Porthouse	National Fish and Wildlife Foundation
Pamela Rosen	Shell
Suzanne Sessine	National Fish and Wildlife Foundation
Ron Stone	Shell
Joni Tuck	Shell

Last but certainly not least, the Institute would like to thank the residents, local stakeholders, and the Port Fourchon community who participated in the Environmental Competency Group meetings and the social return on investment interviews: Blaise Pezold, Davie Breaux, Claudia Burregi, Curtis Cheramie, Windell Curole, Calvin Duet, Julie Falgout, Ted Falgout, Darren Faucheux, Donnie Garrison, Branden Goldman, Richard Hartman, Austin Langley, Casey Leblanc, Julia Lightner, Amanda Phillips, Joey Rogers, and Amanda Voisin. Their input was invaluable to the success of this endeavor.

TABLE OF CONTENTS

LIST OF FIGURES

LIST OF TABLES

LIST OF ACRONYMS

Acronym	Term
ADCIRC	ADvanced CIRCulation
ANPP	Aboveground Net Primary Productivity
AG	Alternative Groups
AR	Autotrophic Respiration
CDF	Cumulative Distribution Function
CIAP	Coastal Impact Assistance Program
CMP	Louisiana Coastal Master Plan
CPRA	Coastal Protection and Restoration Authority
CIMS	Coastal Information Management System
CRMS	Coastwide Reference Monitoring System
CWPPRA	Coastal Wetlands Planning, Protection and Restoration Act
ECG	Environmental Competency Group
EIS	Environmental Impact Statement
ERDC	Engineer Research and Development Center
ESLR	Eustatic Sea Level
FEMA	Federal Emergency Management Agency
FWOA	Future Without Action
FWP	Future With Project
GHG	Greenhouse Gas
GIWW	Gulf Coast Intracoastal Waterway
GLPC	Greater Lafourche Port Commission
GOMESA	Gulf of Mexico Energy Security Act
GPP	Gross Primary Productivity
HNC	Houma Navigation Canal
HyCOM GOFS	Hybrid Coordinate Ocean Model Global Ocean Forecasting System

Acronym	Term
ICM	Integrated Compartment Model
ICM-BI	Integrated Compartment Model – Barrier Islands
LAR	Lower Atchafalaya River
LDWF	Louisiana Department of Wildlife and Fisheries
MLLW	Mean Lower Low Water
NAM	North American Mesoscale Forecast System
NAVD88	North American Vertical Datum of 1988
NCEP	National Centers for Environmental Prediction
NDBC	National Data Buoy Center
NECB	Net Ecosystem Carbon Balance
NFWF	National Fish and Wildlife Foundation
NOAA	National Oceanic and Atmospheric Administration
NRDA	Natural Resource Damage Assessment
POWC	Partnership for Our Working Coast
REF	Restore the Earth Foundation
RMSD	Root Mean Square Difference
RMSE	Root Mean Square Error
RSLR	Relative Sea Level Rise
SLR	Sea Level Rise
SROI	Social Return on Investment
SVI	Social Value International
TWL	Total Water Level
USACE	U.S. Army Corps of Engineers
USEPA	U.S. Environmental Protection Agency
USFWS	U.S. Fish and Wildlife Service
USGS	U.S. Geological Survey
WSE	Water Surface Elevation

UNIT TABLE

Abbreviation	Term
cm	Centimeter
CY	Cubic yards
ft	Feet
in.	Inches
km	Kilometers
kts	Knots
LF	Linear Foot
m	Meters
m^2	Square Meter
mb	Millibars
MCY	Millions of cubic yards
MMT	Millions of metric tonnes
mm/yr	Millimeters per year
ppt	Parts per thousand
psu	Practical salinity unit

INTRODUCTION

The state of Louisiana is experiencing the highest rates of coastal wetland loss in the United States. The accumulated land loss between 1932 and 2016 was nearly 5,200 km^2 (Couvillion et al., 2017), an area that is larger than the state of Delaware. The highest rates of land loss over that 84-yr period of analysis occurred in the Barataria-Terrebonne Basin in which Port Fourchon is located. The Louisiana coast is economically important to both the state and nation, providing productive fisheries, recreational opportunities, and energy production. To adapt to these coastal changes and minimize impacts to habitats, communities, and the economy, Louisiana's Comprehensive Master Plan for a Sustainable Coast (CMP CPRA, 2017) was developed as the state's planning process for coastal protection and restoration.

Perhaps nowhere else on the Louisiana coast are these challenges felt more acutely than in the Barataria-Terrebonne Basin. It is a highly dynamic and productive coastal ecosystem, but is experiencing the highest rates of relative sea level rise (~9 mm yr^{-1}; RSLR; National Oceanic and Atmospheric Administration [NOAA], 2019), shoreline retreat (~3 km $century^{-1}$; Miner et al., 2009), and land loss (~28 km^2 yr^{-1} for 1932-2016; Couvillion et al., 2017) in the nation. It is also the location of Port Fourchon, a strategically positioned, critical service port for the U.S. Gulf of Mexico offshore oil and gas industry (Greater Lafourche Port Commission [GLPC], 2020). A 2014 economic analysis found that a three-week closure of Port Fourchon would cause the loss of 65,502 jobs nationwide (Loren C. Scott & Associates, Inc., 2014).

Operating in such a dynamic landscape requires resilience to disruptions based on adaptive, innovative approaches informed by reliable science. Resilience can be broadly conceptualized as a community's ability to recover to a comparable functional state after an event that disrupts relationships among people and the environment that they inhabit (Colten et al., 2018). Key to this is the development of adaptations that enable a community to persist, even if modified, over time. In natural resource-dependent communities, resilience is often tied to the ability of residents to pursue natural resources in alternate areas or to shift the object of natural resource collection (Colten et al., 2012).

The Water Institute of the Gulf (the Institute) and partners established The Partnership for Our Working Coast (POWC) with Chevron, Shell, Danos, and the GLPC in 2017 (Allison et al., 2018; The Water Institute of the Gulf, 2018). The POWC was formed to address their need for science to support decision making and ensure resilience into the future. The GLPC has a long history of using sediment dredged from the ship channel for beneficial uses, including restoration of the surrounding wetlands, which afford the Port and surrounding infrastructure protection from storms. Through their partnership with the Institute, the GLPC has been striving to advance science that will inform their decisions and strategies.

GLPC plans to deepen its channel to 50 feet to service larger vessels—which are currently receiving service in other countries—within the Port. This dredging project will initially generate millions of cubic yards of uncontaminated material (between 13 and 20 million cubic yards, depending on final design) as well as a smaller, more continuous supply from maintenance dredging (GIS Engineering, LLC, 2018; U.S. Army Corps of Engineers, New Orleans District, 2021). To ensure that the GLPC can make most of the opportunity presented by this dredging project, the Institute has worked to provide state-of-the-science

expertise in ecosystem and landscape dynamics to support the decisions that will be made by GLPC about the fate of the dredged sediment. With the vast quantity of sediment that will be available, the possibilities for what to build, how to build, and where to build are numerous. A full understanding of the landscape and ecosystem dynamics surrounding Port Fourchon is necessary for GLPC to select the most beneficial option

For POWC Phase 1, which occurred prior to the work documented in this report, Institute scientists gathered foundational data and information on the blue carbon potential for wetlands in the vicinity of Port Fourchon, as well as the risks posed by the geological setting of the Port (Allison et al., 2018). A numerical model was developed and applied to estimate the amount of sediment that the Port could expect to produce from the channel after deepening, and some preliminary beneficial use sites were selected based on distance from the channel deepening location and water depth at the potential placement sites.

This report documents POWC Phase 2, which involved a more ambitious transdisciplinary approach incorporating aspects of social and ecological resilience; hydrological, geomorphic, and ecological predictive modeling; social vulnerability and risk assessment; and participatory research that is applied to inform design of nature-based protection and restoration options. These nature-based project alternatives are intended to function within and in response to the drivers of change to the natural system, serving the long-term needs of local stakeholders and improving ecosystem services. The proposed work will prioritize optimal locations and configurations of placing dredge material for wetland restoration projects in the context of future coastal evolution, RSLR, and storm scenarios over the next 30 years. This type of long-term, participatory modelling is essential for maintaining the resilience of the Port, and all that the Port supports, into the future.

OBJECTIVES

The stated objectives of the Institute and POWC are to (1) protect critical infrastructure in and around the Port; (2) generate new, quantifiable ecosystem services; (3) improve community understanding and overall resilience from Port Fourchon to Larose; and (4) quantify the carbon-capture benefits.

A fully integrated landscape and ecosystem evolution model (the Coastal Systems Modeling Framework) was used to forecast long-term changes to the landscape and wetland vegetation communities surrounding Port Fourchon. In addition, this model framework was designed to simulate and quantify carbon sequestered by the created wetlands. Two environmental scenarios with and without two combinations of coastal restoration alternatives were evaluated over a 30-year period. These long-term forecasts of landscape and wetland evolution were combined with a hurricane and tropical storm model intended to assess how the proposed coastal restoration projects would perform in the face of future extreme events. Throughout the duration of this project, Institute scientists engaged closely with a small group of community members so that the technical work could benefit from their local knowledge. This group not only provided input into the specific locations that would benefit most from coastal restoration projects, but also participated in the development of the model inputs, ensuring that the Institute scientists were using the best possible data to build the models, while also building trust within the community.

Using science to inform decision making will help to maintain resilience into the future. While the POWC partners appreciate that constructing wetlands may represent a more expensive alternative to the traditional disposal of dredge material, it is understood that the multitude of additional benefits justifies the investment. Furthermore, this public-private partnership (P3+) approach in which a diverse group of stakeholders are incentivized to contribute capital to building greater coastal resilience is an important methodology to establish in south Louisiana with potential application in other locations across the Gulf Coast.

BACKGROUND

The Barataria-Terrebonne Basin (Figure 1) comprises the majority of Louisiana's south-central coast. The area is part of the Lafourche delta complex that has been degrading into an erosional headland with flanking barriers since its abandonment by the Mississippi River approximately 800 years ago (Penland et al., 1988a, 1988b). The modern Mississippi River channel lies to the east of Barataria Basin. Bayou Lafourche, the abandoned Mississippi River distributary responsible for constructing the Lafourche Delta Complex, separates the Barataria Basin from the Terrebonne Basin and meets the Gulf at the Caminada Headland, which is the site of Port Fourchon. Both basins are irregularly shaped, shallow interdistributary basins fronted by barrier islands. The sediment to build this landscape was originally delivered to the system by Bayou Lafourche when it served as the Mississippi River's primary distributary flowing to the Gulf. Modern artificial levees and water control structures regulate the flow from the Mississippi River into Bayou Lafourche at Donaldsonville and no new sediment is introduced to the Barataria-Terrebonne Basin from the modern Mississippi River with the exception of freshwater diversion at Davis Pond. These basins contain ecologically rich habitats and are home to migratory and nonmigratory species such as alligators, shrimp, oysters, blue crabs, brown pelicans, piping plover, red knots, and the seaside sparrow.

Figure 1. Map of the lower Barataria-Terrebonne Basin, including Barataria Bay and associated waterbodies, Terrebonne and Timbalier Bays and associated waterbodies, and the Port Fourchon area with landmarks for reference.

RSLR and wetland edge erosion are forcing the conversion of wetland habitats to open water habitats throughout Barataria-Terrebonne Basin. Anthropogenic modifications to the landscape, such as limiting sediment supply to the basin from the River due to levees and the excavation of canals for oil and gas development, have exacerbated this wetland loss (Craig et al., 1979; Gagliano et al., 1981; Penland et al., 2001). Barataria-Terrebonne Basin experienced the greatest amount of wetland loss in Louisiana between 1932-2016, approximately 1,120 km^2 and 1,302 km^2, respectively (Figure 2; Couvillion et al. 2017). Rates of RSLR in the southern portion of the basin, specifically for Grand Isle, LA, have been documented at 9.1 mm/yr for 1944-2019 (Byrnes et al., 2019). This area also experiences the highest rate of shoreline retreat in the nation (3 km/century; Figure 3; Miner et al., 2009b). Coastal engineering structures such as rock seawalls, jetties, and breakwaters along the Gulf shoreline contribute to shoreface steepening which eventually leads to larger waves impacting the shoreface fronting the hard structures and an increase in wave energy reflected in an offshore direction, exacerbating sediment losses in an already starved system (Beasley et al., 2019; List et al., 1994; Penland & Suter, 1988; Reynolds et al., 2007; Sabatier et al., 2009).

Figure 2. Land change for the study area 1932-2010 adapted from Couvillion et al. 2017.

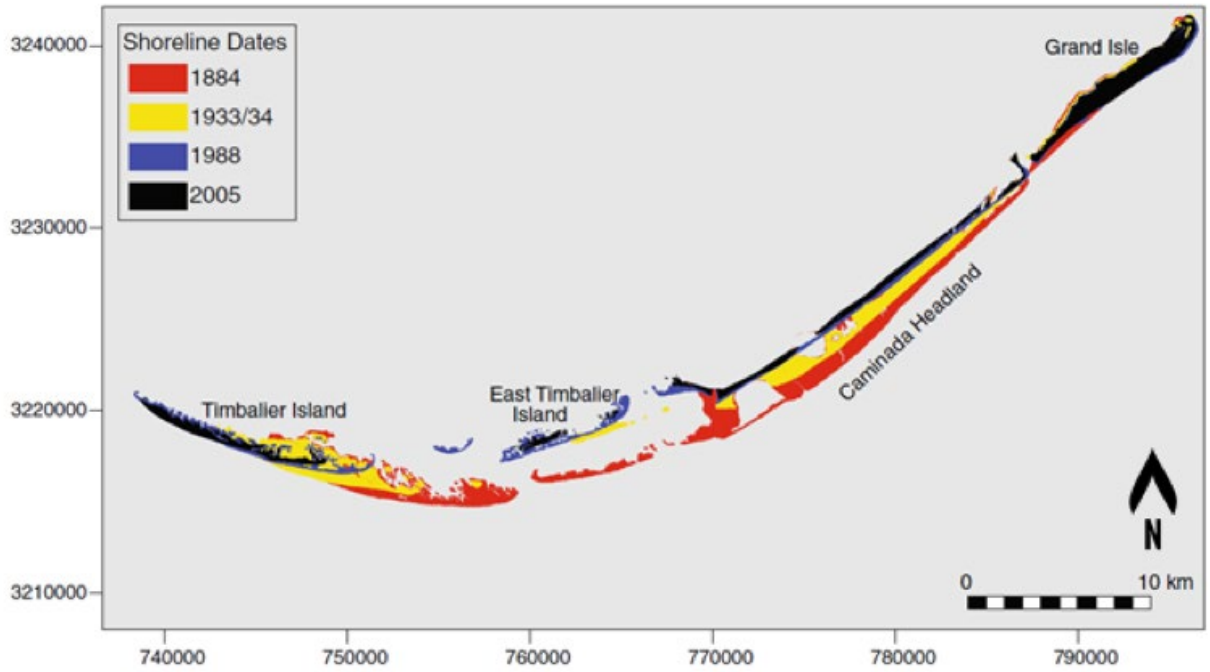

Figure 3. Shoreline change at Caminada Headland (including the Timbalier Islands and Grand Isle) for 1884-2005 (Miner et al. 2009). This area of coast is eroding at a rate of over 3 km/century and has been documented as the most rapidly eroding shoreline in North America by the U.S. Geological Survey (McBride et al., 1992).

While storm surges and waves associated with hurricanes can cause abrupt and significant changes to the landscape, the passage of winter frontal systems are far more frequent (~10-40 annually) and cumulatively have a greater influence on landscape evolution in coastal Louisiana (Dingler et al., 1993; Stone et al., 2004). As a cold front approaches the area, onshore winds result in water set up along shorelines and elevated water levels in the basin (Georgiou et al., 2005; Li et al., 2018, 2019). After the front passes, a strong outward flow into the Gulf develops, producing the maximum flow velocities at channels and inlets, draining the Barataria-Terrebonne Basin into the Gulf and lowering water levels in the basin. Water levels and currents in the basin influence waves and sediment transport which impacts erosion, deposition, and the overall total wetland area.

The brackish and saline wetlands surrounding Port Fourchon are dominated by *Spartina patens* (saltmeadow cordgrass), *Spartina alterniflora* (smooth cordgrass) and *Avicennia germinans* (black mangrove). Since the last major freeze event in 1989, black mangroves have been rapidly expanding near Port Fourchon into areas that were previously salt marshes dominated by smooth cordgrass (McKee & Vervaeke, 2017). Black mangrove areas are projected to continue to expand in response to warmer winters in the future (Osland et al., 2013).

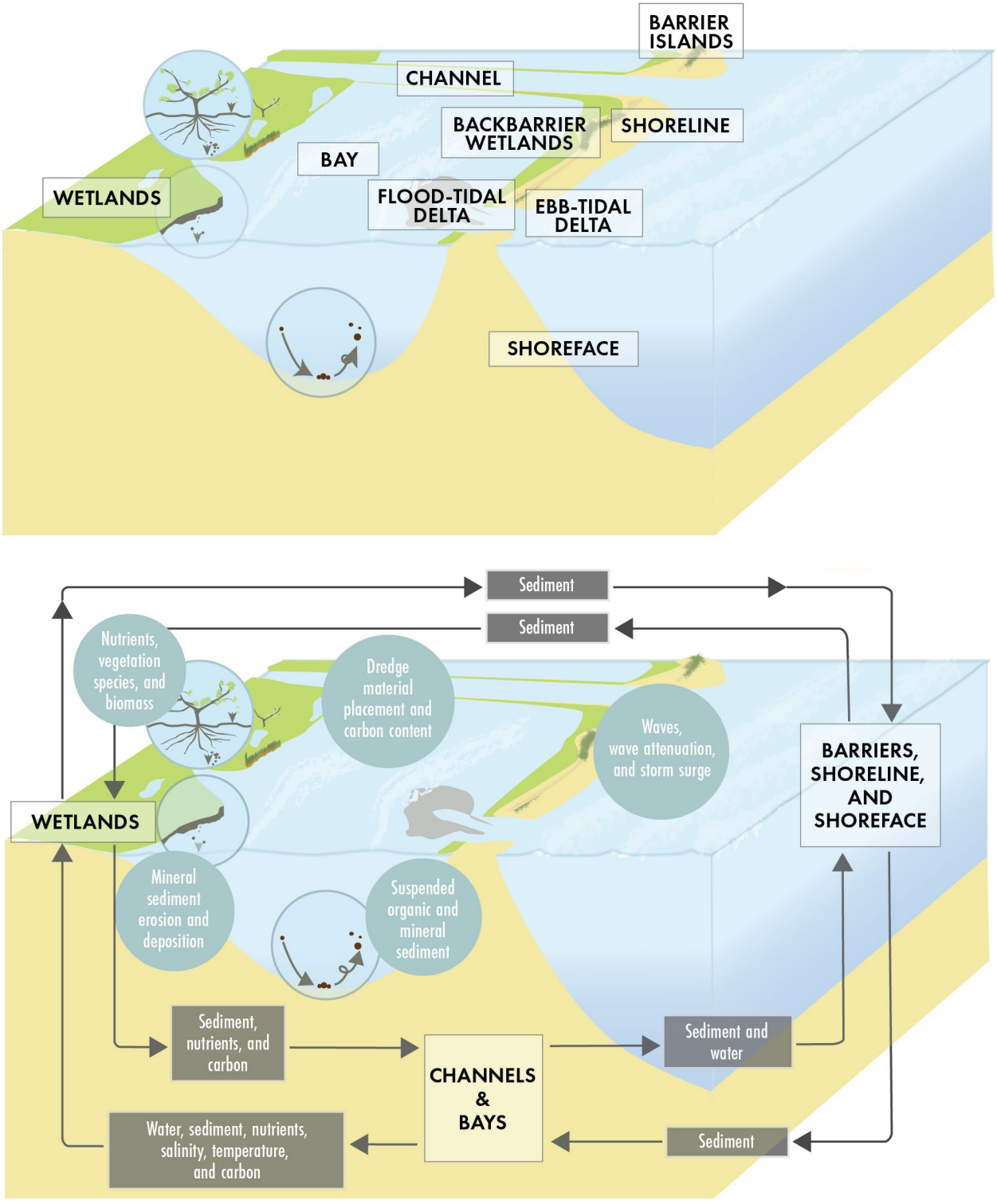

Figure 4. Conceptual diagrams of the landscape and ecological processes in an area such as Barataria-Terrebonne Basin. The upper image shows landforms in Barataria-Terrebonne Basin. The bottom image shows the physical and ecological interactions that drive landscape evolution.

Barrier island and wetland ecosystems support a wide variety of species of both commercial and recreational significance. The Barataria-Terrebonne Basin hosts the Mississippi Flyway, an important stopover location for migratory birds, such as the piping plover and red knot as well as providing critical habitat for resident species such as the brown pelican. The area surrounding Port Fourchon has been designated a Conservation Opportunity Area by the Louisiana Department of Wildlife and Fisheries for coastal mangrove and marsh shrubland habitat with several coastal bird species designated as Species of Greatest Conservation Need (Holcomb et al., 2015). Recreation activities that take advantage of the natural environment such as boating, birding, fishing, and hunting are popular with both residents and tourists (DeMyers et al., 2020), including a yearly migratory bird festival on Grand Isle. A resilient natural environment is essential to support these activities.

Commercial and charter fishing are important industries in Louisiana and the Barataria-Terrebonne Basin. About 20% of all commercial fish and shellfish landings in the United States are in Louisiana (Barataria-Terrebonne National Estuary Program, 2018). The ecosystems of the Barataria-Terrebonne Basin supports several species of commercial importance such as brown and white shrimp, oysters, and specked trout (Hijuelos et al., 2017; Patillo et al., 1997; Pattillo, Mark E. & et al., 1997; Stanley & Sellers, 1986). In 2017, approximately 12.4 million pounds of seafood valued at $13.7 million was landed from Barataria Basin consisting of blue crab, shrimp, oysters, saltwater fish, and freshwater fish (Louisiana Department of Wildlife and Fisheries, n.d.).

The oil and gas industry in Louisiana supports nearly one-third of crude oil production and one-fifth of natural gas production in the United States (DeMyers et al., 2020). Port Fourchon provides an important service port for the offshore oil and gas industry in Louisiana. Over 250 companies utilize Port Fourchon as a base of operations, including over 95% of the Gulf of Mexico's deepwater energy production (https://portfourchon.com/seaport/port-facts/; Greater Lafourche Port Commission, 2020). While production occurs offshore, land-based infrastructure is a necessary part of producing and refining these products (Hemmerling et al., 2021). The Port itself comprises 1,200 developed acres, a 300 ft wide dredged channel, and numerous docking slips. Approximately 15,000 people are flown to offshore locations from Port Fourchon every month. The Louisiana Offshore Oil Port pipeline offshore of Port Fourchon is a strategic location for unloading of imported oil and gas and delivery to the national strategic oil and gas reserve and uses Port Fourchon as its land base. Many pipelines come onshore at Port Fourchon from the expansive oil and gas fields across the northern Gulf. The Port also serves as a location for rig repair, and operations at the Port provide employment for many people in Lafourche Parish and the surrounding parishes.

The GLPC intends to deepen the Port's channels and slips to service larger vessels that are currently receiving service in other ports. Therefore, there will be opportunities to use the dredge material to create wetlands built from dredged material resulting from port expansion (Figure 5; GIS Engineering, LLC, 2018). At the time of this report, the Port has received authorization to dredge to -30 ft below Mean Lower Low Water (MLLW) datum. Future dredging plans include dredging the channel to -50 ft MLLW, with the possibility of also dredging a turning basin, slip, and deep loading hole to use for large rig repair (Figure 5). Because of the uncertainty related to the decision to build the turning basin, slip, and deep loading hole, these were excluded from this analysis. Only the -50 ft MLLW channel depth was

constructed in the model. The slip was originally envisioned to be dredged to -85 feet deep, but later revised to -30 ft MLLW (GIS Engineering, LLC, 2018; GLPC personal communication). The deep loading hole would provide a large portion of the dredged sediment. The amount of sediment produced, and thus the number of different wetland restoration projects that can be built, from these different alternatives ranges widely. The modeling approach considered sets of wetland restoration projects that could be built from the sediment likely to be generated, between 13.2 million and 20.1 million cubic yards from the first-cut excavation of the channel and slips only, with the understanding that additional sediment could be directed to multiple sets of projects or maintaining existing wetland over the long-term. Port capital planning and mitigation projects are summarized in Table 1.

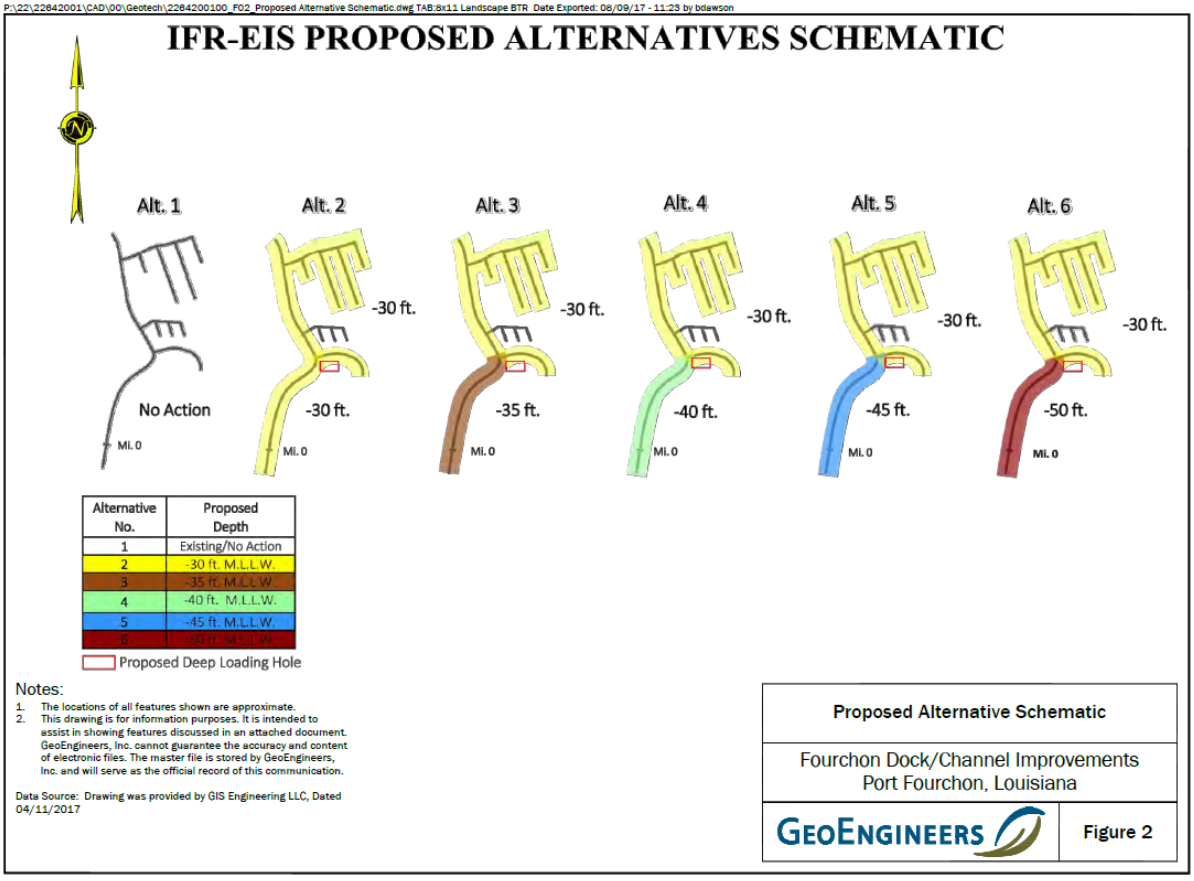

Figure 5. Proposed alternative dredging strategies at Port Fourchon (GeoEngineers, 2019).

Table 1 Greater Lafourche Port Commission capital improvement and mitigation projects. All project descriptions provided by the Port. FWOA = future without action.

Project	Status	Description	In FWOA?
30-foot deepening	Permitted	Deepening of the northern slips, Pass Fourchon, and Belle Pass to -30 ft. MLLW.	Yes
50-foot deepening	In Planning	Deepening of the northern slips, Pass Fourchon, and Belle Pass to -50 ft. MLLW.	No
Fourchon Island Slip and Mitigation	In Planning	Construction of a new deep loading hole ranging from -30 to -85 ft deep in the wetland area bounded by the Gulf of Mexico, Belle Pass, and Pass Fourchon.	No

Several recently constructed projects, as well as projects in various stages of planning, design, or construction exist in the immediate vicinity of Port Fourchon. These include projects led by CPRA, CPRA's federal partners such as the U.S. Environmental Protection Agency (USEPA), U.S. Fish and Wildlife Service (USFWS), the National Oceanographic and Atmospheric Administration (NOAA), and the Port. State and federal restoration projects are summarized in Table 2 and categorized based on their status.

Each of the proposed projects has been included in modeling analysis. Figure 6 depicts all proximal projects along with key stakeholder agencies and funding sources, as well as the projects modeled and the domain of the wetlands modeling area of interest for black mangroves and carbon.

Table 2. State and federal restoration projects in the vicinity of Port Fourchon, with notation of which projects were input into the POWC Future Without Action (FWOA) landscape in the models. All descriptions and costs taken from CPRA's Fiscal Year 2023 Annual plan (Coastal Protection and Restoration Authority, 2022) and the CPRA Coastal Information Management System (CIMS; CPRA, 2022) web portal.

Project (CPRA ID) in parenthesis)	Implementation Program	Status	Description	In FWOA?
Caminada Headlands Increment I (BA-0045)	CIAP	Constructed in 2014	This project restored 303 acres of beach and dune habitat on Caminada Headland in Lafourche Parish (beginning at Belle Pass and extends approximately 6 miles east towards Bayou Moreau) through the direct placement of approximately 3.3 million cubic yards of sandy material from Ship Shoal (an offshore borrow source). It cost $70.1 million.	Yes
Caminada Headland Beach and Dune Restoration Increment 2 (BA-0143)	NFWF	Constructed in 2016	This project restored 489 acres of beach and dune habitat on more than seven miles of Caminada Headland in Jefferson and Lafourche parishes through the direct placement of approximately 5.4 million cubic yards of sandy material from Ship Shoal (an offshore borrow source). It cost $147.1 million.	Yes
Caminada Headlands Back Barrier Marsh Creation Increment I (BA-0171)	CWPPRA	Construction ongoing as of March, 2022	This project will create and nourish 385 acres of back barrier intertidal marsh behind 3.5 miles of Caminada Headland in Lafourche Parish using material dredged from the Gulf of Mexico. This project will work synergistically with existing Caminada Headland dune and back barrier marsh projects (BA-0045 and BA-0143), expanding the restored back barrier marsh platform and improving the longevity of the barrier shoreline. It cost $32.3 million.	Yes
Caminada Headlands Back Barrier Marsh Creation Increment II (BA-0193)	CWPPRA	Construction ongoing as of March, 2022	This project will create and/or nourish 444 acres of back barrier intertidal marsh along Caminada Headland in Lafourche Parish and create a platform upon which the beach and dune can migrate. This project will work synergistically with existing Caminada Headland dune and back barrier marsh projects (BA-0045 and BA-0143), expanding the restored back barrier marsh platform and improving the longevity of the barrier shoreline. It is expected to cost $26 million.	Yes
West Belle Pass Headland Restoration (TE-0052)	CWPPRA	Constructed in 2012	This project reestablished the West Belle Headland in Lafourche Parish by rebuilding approximately 9,300 linear feet (362 acres) of beach, dune, and back barrier marsh using 4.2 million cubic yards of sediment dredged from the Gulf of Mexico. It cost $34.2 million.	Yes

Project (CPRA ID) in parenthesis)	Implementation Program	Status	Description	In FWOA?
Terrebonne Basin Barrier Island Restoration, West Belle Pass component (TE-0143)	NFWF	Constructed in 2020-2022	The original design included extending and renourishing the original West Belle Pass Barrier Headland Restoration (TE-0052) project. A sand spit extending from the fill limits of the original TE-0052 was used as a platform to construct the recommended design template, following the natural shoreline geometry for alignment. The original restoration template included approximately 545 acres of beach, dune, and marsh components and 3.1 miles of beach. The constructed template was heavily damaged in October 2020 by Hurricane Zeta. Prior to Hurricane Zeta's landfall, 442 acres of beach, dune, and marsh habitat and 2.4 miles of beach had been constructed. After the storm, the work plan was revised to construct a feeder beach near West Belle Pass, which includes 79-acres and 1 mile of beach. The new feeder beach provides high quality nesting habitat, helps protect West Belle Pass from flanking, and provides a sediment source to nourish West Belle Headland.	Yes[1]
West Fourchon Marsh Creation (TE-0134)	CWPPRA	Construction expected in 2023-2024	This project involves the creation of 302 acres and nourishment of 312 acres of marsh between Bayou Lafourche and Timbalier Bay in Lafourche Parish using sediment dredged from the Gulf of Mexico or Bayou Lafourche. It is expected to cost $30.7 million.	No
Port Fourchon Marsh Creation (TE-0171)	CWPPRA	In Planning	The primary goals of this project are to restore degraded wetland habitat and provide increased protection from storm surge and flooding. Specific goals of the project are to create approximately 514 acres and nourish approximately 91 acres of marsh with dredged material from Belle Pass. This project does not yet have an estimated cost.	No
East Leeville Marsh Creation and Nourishment (BA-0194)	CWPPRA	In Planning	The project goal is to create approximately 297 acres of saline marsh east of Leeville in Lafourche Parish using sediment dredged from Caminada Bay. It is expected to cost $35.1 million.[2]	No
Port Fourchon Shoreline Protection (BA-0251)	Gulf of Mexico Energy Securities Act (GOMESA)	In Planning	The goal of this project is to construct and repair shoreline protection features on the Caminada Headland to the south of Port Fourchon. It is expected to cost $2.0 million.[3]	No

[1] The original constructed template was included in the FWOA landscape. Hurricane Zeta made landfall after modeling for the project had already commenced.
[2] This project is on hold and not currently being advanced within the CWPPRA program.
[3] This project was not part of the analysis as it was proposed after the substantial completion of the modeling or report, and it did not yet have defined features.

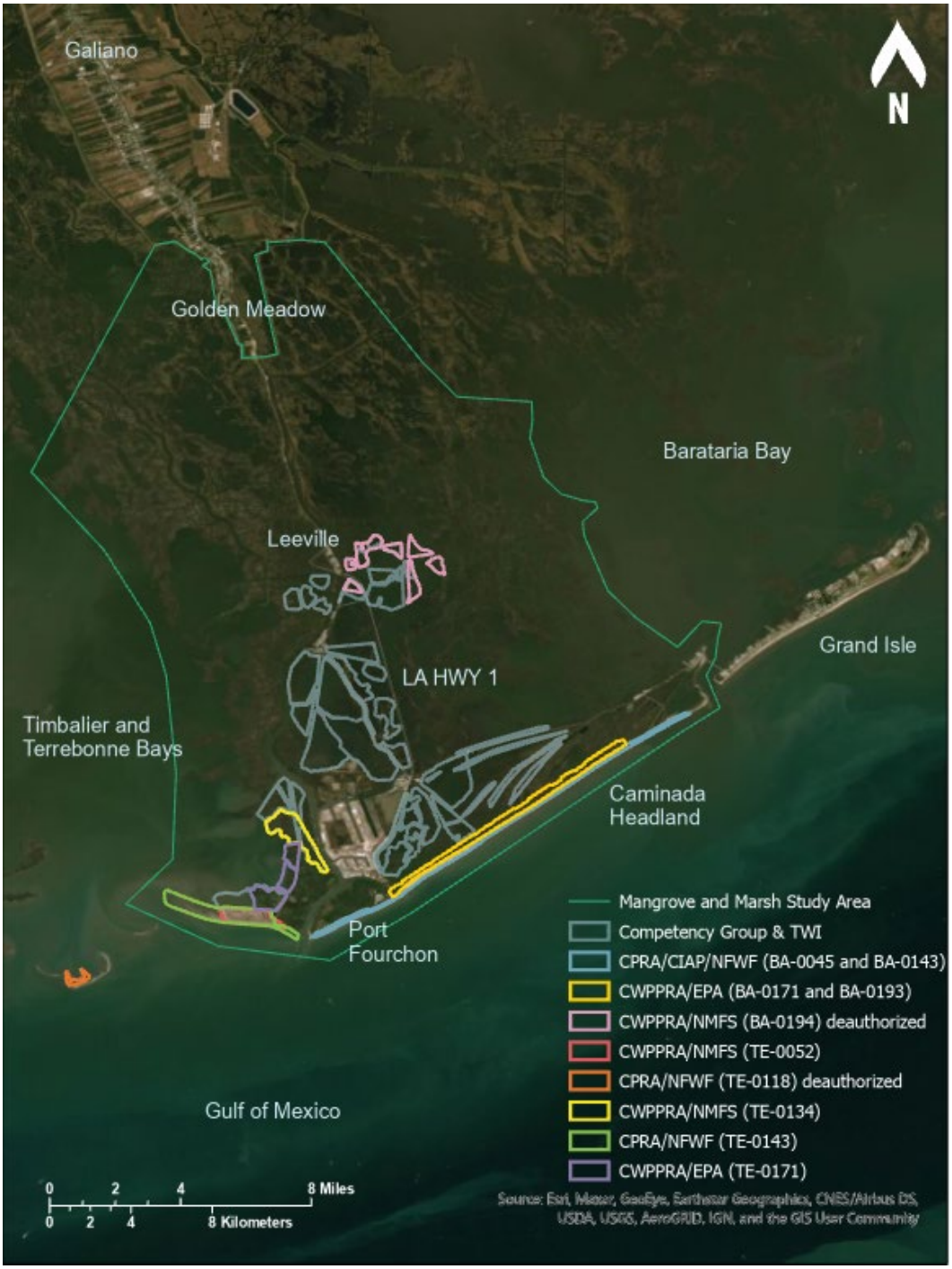

Figure 6. Built and proposed wetland restoration project polygons developed during this project and by state and federal agencies.

METHODS

The methods used in this study are summarized within this section. Additional details, such as specific model calibration procedures, are not included, but can be found in accompanying appendices.

TRANSDISCIPLINARY APPROACH

This study used a transdisciplinary approach for assessing and informing coastal resilience. In traditional research, technical science-based knowledge—including devices such as predictive models, risk indicators, monitoring instrumentation, ecosystem services calculations, and benefit cost analyses—is often granted priority over local experience-based knowledge (Barra et al., 2020). Transdisciplinary research, on the other hand, brings individuals from different scientific disciplines and from civil society together to actively collaborate in the production of knowledge (Krueger et al., 2016). This, by definition, requires local stakeholders and scientists from diverse fields to work on the same problem and co-develop solutions that fully integrate local and traditional knowledge with physical and social scientific knowledge, transforming traditional scientific disciplines into a combined new field. This process adds significant value by leveraging the approaches, knowledge, and principles of the individual disciplines as well as the accumulated local knowledge of residents and local stakeholders.

By integrating residents and other local knowledge experts into the scientific process, the results are much more actionable than those developed through traditional research (Bethel et al., 2014). This highlights another key aspect of transdisciplinary research: socially relevant issues, rather than scientific disciplines, define the frame of inquiry (Krueger et al., 2016). Because of the social relevance of transdisciplinary research, it requires a reconceptualization of public engagement and the traditional role that the public plays in scientific research. When traditional outreach and engagement methods are employed, coastal residents often feel disenfranchised by what they perceive to be a repetitive and ambiguous public engagement process that can leave residents feeling fatigued, frustrated, and ignored by policy makers and planners (Gotham, 2016; Hemmerling et al., 2020c). When local knowledge experts are not actively engaged in coastal research, a disconnect between local and traditional ecological knowledge and the hydrological and hydraulic science that underpins much of coastal management can develop. This disconnect has increasingly led to a lack of trust in science and the development of knowledge controversies where science fails to convince those whose direct experience contradicts scientific outputs and where policies based on that science fails to allay public concerns (Whatmore, 2009).

To address these shortcomings, the Institute developed an environmental competency group (ECG) methodology that has enabled residents and local stakeholders to work directly with scientists and engineers in the collaborative management of coastal projection and restoration projects (Barra et al., 2020; Hemmerling et al., 2020b, 2022b). From the outset of this project, the Institute team has adapted this methodology, directly including industry and other coastal decision makers to develop a fully transdisciplinary process that will result in the construction of a co-developed coastal protection and restoration project. The ECG approach allowed for active dialogue between local knowledge experts and technical knowledge experts and ensured that both sources of knowledge were included and valued throughout the process.

Incorporating local and traditional knowledge into the scientific process takes careful planning and consideration. For example, community members may not utilize the same terminology as scientists when discussing landscape processes or the technical details of a morphology model. It is contingent on project leadership to recognize the inherent value of both understandings of the landscape, facilitate conversations between participants, and develop a shared language. Scientists need to engage with community members in thoughtful and deliberate ways. The community engagement of any one project should be specific to the needs of that project but successful community engagement should strive to include: 1) opportunities for two-way engagement between scientists and community members, 2) deliberate solicitation of feedback from community members, and 3) open-minded attitudes from all parties. The ECG process, and transdisciplinary research in general, is designed to move beyond the positionality of individual group members and provide new insights into the challenges facing coastal communities and the solutions to address them.

CONVENING AN ENVIRONMENTAL COMPETENCY GROUP

Engagement activities followed a methodology that has been employed in Louisiana by the Institute before, and adapted it for this specific location and community. This methodology involved forming a small group of community members and scientists into an ECG that would work together over the course of several meetings to review model inputs, develop model alternatives, and review model results (Baustian et al., 2020; Hemmerling et al., 2020a). A "snowball" sampling method was employed to select local knowledge experts for the ECG, in which recommendations are solicited from the community and the most frequently mentioned persons are asked to join the group (Bernard, 2017). Technical knowledge experts for the ECG were selected from the Institute based upon their scientific knowledge of the area in and around Port Fourchon. The final ECG membership included local landowners, recreational and commercial fishermen, representatives from the GLPC and its tenants, representatives from local government, and the local Sea Grant representative, as well as modelers, geologists, and ecologists from the Institute (Table 3). Recognizing that the technical knowledge experts in the ECG were being paid by their employers for their time taking part in the meetings, the local knowledge experts were financially reimbursed for each meeting they attended, so as to appropriately acknowledge value of the time the local knowledge experts spent working on the study and providing key data to build and test the numerical models.

The first meeting took place on February 18, 2020, at the headquarters of the GLPC in the town of Cutoff, LA. This introductory meeting was focused on introducing the members of the ECG to one another and discussing the goals of the study with the group. This was also an opportunity for the technical knowledge experts to introduce the group to the types of models that would be developed through this process and what these are intended to measure. This was also an opportunity for the local knowledge experts to discuss the environmental changes that they have seen take place in and around Port Fourchon. Several maps set up around the meeting room served as discussion prompts for the group members.

Table 3. Stakeholders who participated in the ECG by type.

Stakeholder Type	Number of Stakeholders
Modelers	2
Researchers (e.g., geologist, ecologist)	3
Community Service & Outreach	1
Conservation Organization	2
Education & Research	1
Local Business	1
Local Government	1
Local Landowner	4
Port Employee	1
Recreational User (hunting, fishing, birding, boating, etc.)	2

In this first meeting, steps were taken towards developing a common language and establishing that the knowledge possessed by the technical knowledge experts was not going to be prioritized over the local and traditional ecological knowledge possessed by residents and local stakeholders. It was also necessary to set specific expectations for what can and cannot be accomplished given environmental and economic constraints, including the potential type and magnitude of project impacts and non-impacts. Early in the ECG planning process, the technical team (the scientists from the Institute) communicated with the stakeholders about their prior modeling experience with similar project types across Louisiana to set reasonable expectations for this modeling effort.

As noted in the *Project Alternatives and Environmental Scenarios* section of this report, the material available for dredging is most likely to consist of cohesive fines and organics, with sparse amounts of very-fine sand. The technical team discussed the dredged material's likely composition with the ECG and collectively the group decided to limit proposed restoration project types to wetland restoration (target of intertidal habitat consisting of marsh grasses and mangroves) as opposed to beach and dune restoration or ridge restoration based on the dredge material properties expected.

Project Expectations – Surge and Wave Reduction

Studies of wetlands' ability to decrease storm surge over various distances have sometimes caused public misunderstanding. One example is the 1965 Morgan City and Vicinity Interim Survey report published by the USACE, which stated 1 vertical foot of surge is reduced by every 2.75 miles of horizontal wetland transect (USACE, 1965). In Louisiana, the ability of wetlands to reduce storm surge is highly dependent on individual storm characteristics such as forward speed, radius to maximum winds, central pressure, and angle of approach, as well as the impact location's geographic characteristics, such as bathymetric and topographic elevations, ground slope, and vegetation cover (Alymov et al., 2017; Cobell et al., 2013). Proximal impacts from infrequent, powerful hurricanes with large storm surge often inundate coastal wetlands entirely under several feet of water, at which point the wetlands have no impact on surge or

wave reduction at all. The impact that wetlands have on reducing storm surge and wave heights are most noticeable for more frequent events with smaller storm surges. Similar modeling efforts such as those in CPRA's 2012 and 2017 CMPs, showed that more frequent, smaller surge and wave events resulted in reductions of surge and waves on the order of a few feet, however, these conditions can result in localized surge increases, which also are discussed in the *Results* section. During the project generation portion of the analysis, before project modeling commenced, the technical team communicated to the ECG that similar results would be expected around Port Fourchon.

Project Expectations – Barrier System Response

Since all proposed projects were focused on wetlands behind the barrier shoreline, the technical team communicated to the ECG that the projects may have impacts to net sediment transport into or out of the estuarine bay system (especially Terrebonne Bay) due to impacts on the changes in the tidal prism. Furthermore, certain proposed projects in the back barrier had the potential to capture wash over of sandy sediment from storm events and contribute to shoreface integrity. However, most projects were unlikely to directly affect barrier shoreface morphology or tidal inlet morphology.

Project Expectations – Land Loss

The primary area that the technical team and ECG agreed the proposed wetland restoration alternatives could have the most noticeable, direct impacts to was the land loss rates in the vicinity of Port Fourchon. All the proposed projects were expected to not only directly reduce land loss within the restoration footprints, but also potentially outside of the wetland restoration footprints indirectly through reduction of fetch and wave energy on adjacent, unrestored wetlands.

LOCAL KNOWLEDGE MAPPING AND PARTICIPATORY MODELING

The remainder of the ECG meetings followed a stepwise approach utilized in an earlier pilot project organized by the Institute (Barra et al., 2020; Baustian et al., 2020; Hemmerling et al., 2020a; Meselhe et al., 2020). Data collection efforts centered around the outputs of a series of local knowledge mapping workshops and subsequent participatory modeling activities. The outputs of these engagement activities were analyzed both qualitatively and quantitatively to translate workshop outputs into geospatial data that could be incorporated into the numerical models that would be used to assess the impacts of the proposed project, with the results reviewed by the local and technical knowledge experts that comprise the ECG.

Local knowledge mapping is an approach that aims to encourage community member participation in sharing knowledge and perceptions of a given area and has been shown to provide an effective means of incorporating community and traditional ecological knowledge into a coastal protection and restoration framework (Curtis et al., 2018). This is traditionally done in a face-to-face setting, using paper maps, markers, and other physical materials. However, weeks after the initial ECG meeting, the first case of COVID-19 was diagnosed in Louisiana and by March of 2020, Louisiana had one of the world's highest average COVID-19 daily growth rates (Madhav et al., 2020). The governor ordered that all nonessential businesses be closed to the public and issued a stay-at-home order for all residents. As a result, the rest of the ECG meetings were held virtually.

The second meeting, originally scheduled to take place in March 2020, was delayed until May as the technical team worked to develop tools to conduct the local knowledge mapping workshops virtually. The team ultimately settled on an online survey software called Maptionnaire, which allows users to interactively mark-up maps online in response to a number of survey questions (Maptionnaire, n.d.). The virtual meetings were hosted on Zoom and composed of two segments. The first segment provided participants with an overview of progress to date as well as an update on modeling activities that took place between meetings. The second segment directly engaged participants by collecting geospatial data through an online public participation GIS portal. The technical team also provided an overview of the mapping portal, the format and how to use it, and provided a link to the mapping site for participants to continue to add data to the maps on their own.

During the second segment of the meeting, the ECG divided into smaller breakout groups to engage the ECG more fully in deeper conversations and bring out greater details on the data developed through the public participation GIS activities. The breakout groups were organized such that each group had a representative grouping of technical and local knowledge experts. During this segment of the meeting, roles were assigned among the technical team members to optimize participant engagement. A lead facilitator asked questions and guided the discussion while a map manager navigated the map onscreen, focusing on specific areas of concern and drawing the points, lines, and polygons for participants, if they were unable to do so themselves.

The second meeting focused on the different inputs to the model. The Institute modeling team of technical knowledge experts presented maps of the model inputs (e.g., elevation maps, vegetation maps) to the full ECG while facilitators guided the conversation between the technical experts and local knowledge experts in order to interrogate the accuracy of the model input data more fully. All conversations were recorded with the permission of the ECG members. This allowed the technical knowledge experts to analyze the qualitative data outputs and link these to the geospatial outputs. Following this meeting, the technical knowledge experts reviewed the resultant data outputs and adjusted the model inputs as appropriate, providing detailed responses to the full ECG (Table 4). This served dual purposes. First, the process provided a valuable quality control check on the model inputs, utilizing the local knowledge of those who are on the ground every day. Secondly, this transparent process will enhance confidence in the models within the community and trust in the scientists that are developing them (Barra et al., 2020).

The third meeting discussed coastal restoration projects; both the types of projects and locations of project that could be built were discussed. As with the second meeting, the ECG divided into smaller breakout groups with a representative sampling of local and technical knowledge experts. In each breakout group, community members were able to discuss their concerns about different areas of the landscape with the modelers so that, together, they could design potential solutions. Again, using the public participation GIS portal, group members collectively identified locations where sediment placement might generate the most benefit (Figure 7). Group members all recognize that there are physical and financial limits to what can be constructed given the amount of sediment available.

Table 4. ECG review of model inputs

ECG Input Type	ECG Input	Modeling Team Response
Morphology	Land has changed in areas surrounding the barrier islands.	We will update topobathy to account for this and to include some of the other update features like the depth of the slips in the port, depth of a few certain canals mentioned in the meeting.
	Topobathy does not show recent construction of a park within Port Fourchon.	We will update topobathy to account for this and to include some of the other update features like the depth of the slips in the port, depth of a few certain canals mentioned in the meeting.
	The topobathy map appears to show a shallow place within Port Fourchon that participants confirmed has been dredged to a uniform 27 feet.	The models will be adjusted for the consistent depth.
	Bathymetry does not reflect many recent changes.	We are manually editing the DEM to include these updates as the datasets we are using are only globally updated every 5-10 years.
	The topobathy map shows uneven depths around the port	The models will be adjusted for the consistent depth.
	Last Island (directly south of Cocodrie) has been "washing out" really quickly the past few years.	This location is at the edge of the model domain. This may be updated depending on the location of the final project scenarios to be modeled.
	Can we include maintenance dredging as part of the production runs?	How maintenance dredging is incorporated will be discussed in the next internal modeling meeting.
Hydrology	The bayou ridges in the area are consistent and do not break until the east wet canal in Leeville. Generally, the bayous in the area are 10 feet deep but at that crossing it is believed to be 40 feet deep	We will verify that the model is representing this flow path
	The east west canal in Leeville plays an important role in the hydrology of the area. Multiple participants agree fresh water traveling down Bayou Lafourche is diverted east or west at Leeville, meaning everything traveling into Barataria has to cross in Leeville.	We will verify that the model is representing this flow path
	Participants expressed concern that Louisiana Highway 1 (LA 1) does not appear on the elevation maps mentioning that it is a higher elevation that surrounding land often acting as a buffer and channeling water and is the most continuous elevation from Grand Isle to the Lafourche ridge.	The new elevated LA 1 is included in the surge model although it shouldn't be because it is on piles. The old LA 1 can be added to the representation in the model using LIDAR elevations
Ecology	Participant mentioned there may be more mangroves than shown on the vegetation map, along LA 1 just south of Lake Laurier. This area is slightly northeast of Port Fourchon north of Elmer's Island	We will review the vegetation map and update to assure that the mangrove vegetation in this area is shown.
	Participants mention a space within Port Fourchon has been restored to "thick marsh vegetation." This is the same location east of the Flotation Canal that many other participants mentioned has been restored and will not be developed for industrial use.	We will review the vegetation map and update to assure that the created marsh in this area is shown.

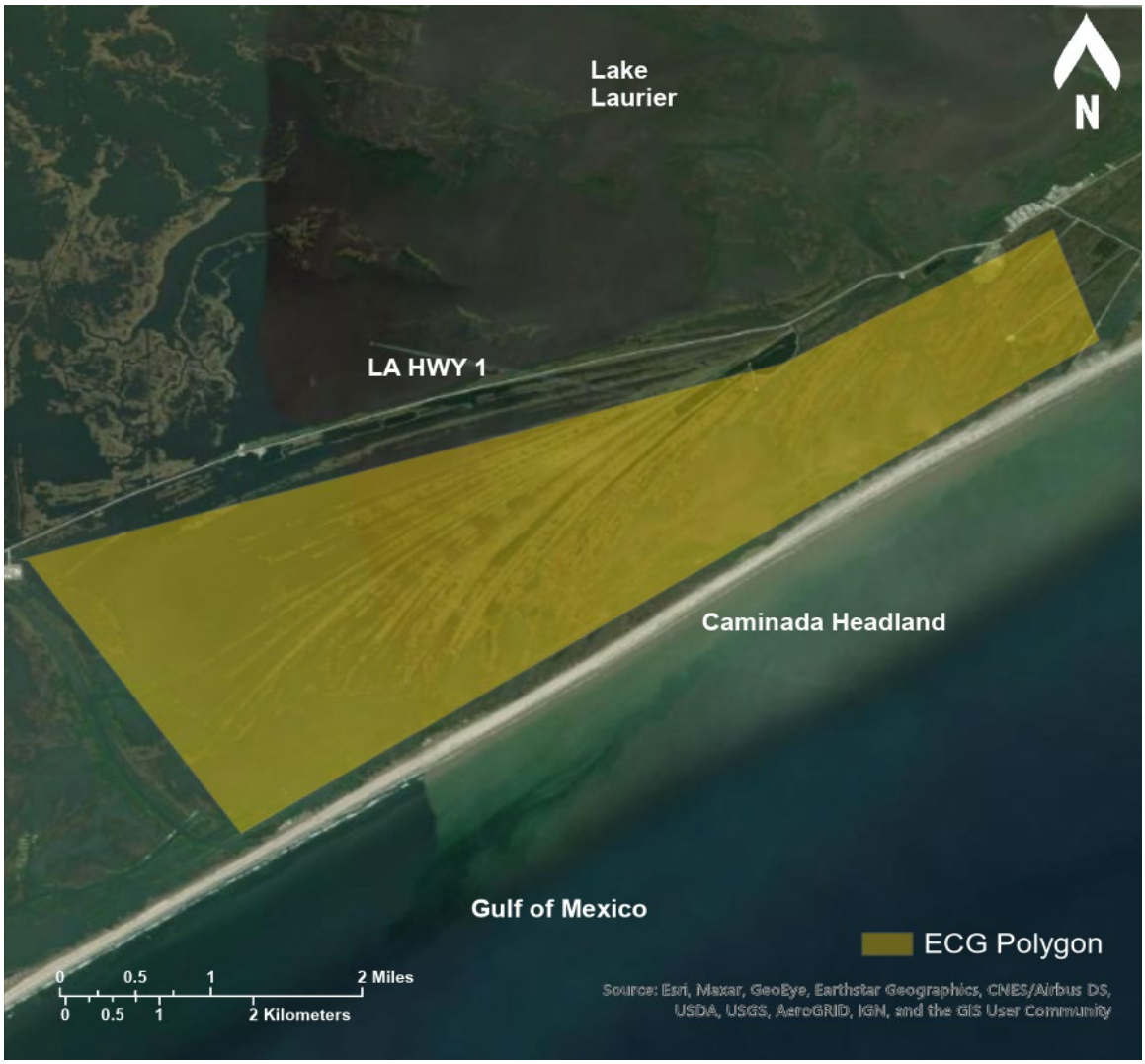

Local Landowner	With the natural ridges in the area, you could do a combined project and improve some of those ridges toward the back. The CWPPRA project is long and skinny, so there is an opportunity to do some additional marsh creation. You could find a way to do marsh creation along with something with the ridges…pretty much filling in the blanks of the CWPPRA project.
Local Wildlife Biologist	The back barrier bay project that CWPPRA is working on stops at the property line between Elmer's Island and the Wisner property. Any sediment that could be placed-it could be toward LA HWY 1 or it could be toward the beach-would be beneficial. It we wanted to take some of that sediment and extend the CWPPRA marsh creation project, that would be good.

Figure 7. Sample project idea developed by the ECG during Meeting 3 using the Maptionnaire online interface.

Following this meeting, the technical knowledge experts from the group collaborated with other engineers and ecologists from the Institute to refine the generalized project footprints and adapt them to the landscape. The Institute also assigned geographically appropriate attributes to each project, which assured data comparability with the numerical models being developed by the team. During this evaluation process, the modeling team noted all changes made to the initial project footprints and provided explanations and rationale for why these decisions were made; this reinforces confidence in the modeling and trust in the technical team. As the modeling team worked to refine the project footprints, Institute social scientists transcribed and coded the audio from the meeting, allowing the research to link the desired outcomes of each proposed project to the geospatial data.

SOCIAL VALUATION OF CO-DESIGNED PROJECTS

The final output of the participatory modeling phase of the project was a GIS database consisting of fully attributed project polygons developed and reviewed by the ECG. In total, 43 feasible sites were identified through this process, consisting of wetland creation and ridge restoration projects. Each project polygon was developed with specific goals in mind, ranging from protection of industrial infrastructure to protection of wildlife and fisheries habitat, to recreational utilization. The workshops were recorded, transcribed, and coded to allow for additional qualitative data analysis. Through this process, the goals and intentions detailed by ECG members during project development were identified and tagged in the GIS.

While this process allowed the technical team to identify and delineate the final set of project polygons, it did not allow for a final ranking of projects. To accomplish this, the technical team used a modified Social Return on Investment (SROI) framework to integrate community-based qualitative research, ecological site assessments, and economic proxies to calculate the social value of candidate projects. SROI is a performance measurement framework that directly accounts for the broad concept of social value, a measure of change that is relevant to people and organizations that experience it. Built upon a combination of traditional cost-benefit analysis and social accounting principles, the SROI process involves a systematic analysis of the effects of projects or programs on communities of interest and key stakeholders, with stakeholder input as part of the data that are analyzed (Nielsen et al., 2021). SROI encompasses a much broader concept of how change is created and valued, moving beyond what can be captured in pure, market-based financial terms. When used to assess environmental change, the process can be employed to help reduce inequality and environmental degradation and improve human health and wellbeing by incorporating social, environmental, and economic costs and benefits into project valuation (Teo et al., 2021).

SROI is classified into two types: evaluative analysis and forecast analysis. In the former, the goal is to evaluate the social value that has already been created by a project while the latter estimates how much social value a project could generate in the future (Teo et al., 2021). Forecast SROIs are especially useful in the planning stages of an activity. They can help show how investment can maximize social impact and are also useful for identifying what should be monitored and measured once the project is implemented (SROI Network, 2012).

For this study, the SROI process was adapted to allow the technical team to focus on potential impacts to key stakeholders who have a direct physical connection to the project. SROI analyses are often used by corporate funders and governmental agencies that have fiduciary responsibility to the public and may include social benefits such as improved company reputation and social license to operate to these funders as key outcomes. While these social benefits would certainly accrue to Port Fourchon and the POWC partners following project construction and implementation, this was not a key focus of this research. Building on the traditional SROI methodology, this process was undertaken in three primary stages:

1. *Identify and engage key stakeholders affected significantly by the proposed projects* – Understand what each stakeholder wants changed (objectives), what they contribute (inputs), what activities they do (outputs) and what changes for them (outcomes, intended or unintended);
2. *Measure and value the social impacts of the proposed projects* – Understand the value created because of the changes experienced by each stakeholder group by using indicators to measure the outcomes and financial proxies to value the outcomes; and
3. *Create a forecast analysis to measure and evaluate the impacts of the proposed projects* – Articulate the key drivers of social value and identify what data are needed to best measure and evaluate the impacts of activities.

Potential costs and benefits of each proposed wetland restoration project on nearby communities were assessed through qualitative research and stakeholder engagement including one-on-one interviews and questionnaire research. The technical team conducted a series of guided interviews using an option questionnaire to assess the social value that would be generated by each project. To simplify the process and reduce the amount of time that would be required for respondents to assess the projects, the initial 43 projects were grouped into five project clusters based upon geographical proximity and project type (Figure 8). Respondents were asked to review the project clusters and also to note if any of the constituent polygons differed significantly from the others in terms of outcomes generated.

An option questionnaire was constructed around the three broad categories identified through qualitative analysis of the workshop results: impacts on ecology, impacts on wildlife and fisheries, and impacts on human communities. Potential project outcomes within each of these categories were identified by the technical knowledge experts in the ECG (Table 5). Through the guided interview process, each respondent was instructed to review each project outcome and determine if that outcome would be beneficial or harmful, its severity, how likely it is to occur, and over what timeframe and spatial scale it would take place. Respondents were also given an opportunity to identify any other potential outcomes that were not included in the questionnaire.

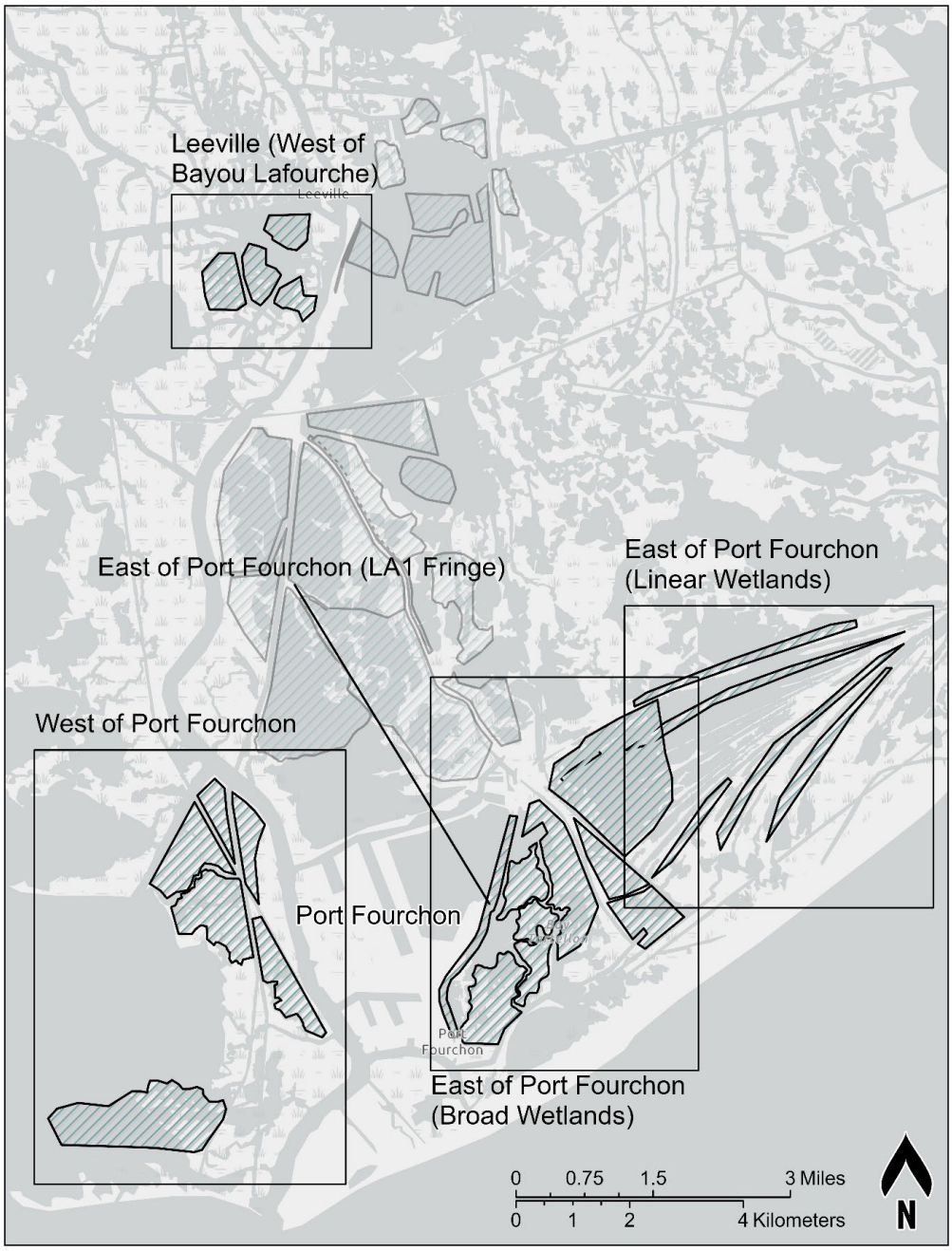

Figure 8. Project groupings used during stakeholder interviews.

Table 5. Option questionnaire assessment variables.

Impacts to wildlife and fisheries
Alter habitats for crabs, shrimp, oysters and fish
Alter spawning ground for finfish and shellfish
Alter habitat for bird species (e.g., migratory, threatened and endangered, secretive marsh)
Alter habitats for nesting reptile species (e.g., diamondback terrapins)
Affect the amount of mammals in the area (e.g., deer, fur-bearing mammals)
Impacts to ecosystems
Affect daily erosion of wetlands, bays, bayous, and canals (i.e., tidal prisms, changing salinity regimes, wind fetch)
Affect storm induced erosion of wetlands, bays, bayous, and canals
Impact existing and ongoing restoration projects
A change in plant and animal distributions and biodiversity (e.g., migration of more saline tolerant species)
Alter the number/distribution of invasive species.
Alter the acreage of saltmarsh
Alter the acreage of mangroves
Alter the water quality (e.g., harmful algal blooms, microalgae, and bacteria)
Impacts to humans
Alter storm surge and wave impacts on oil and gas infrastructure (port, pipelines)
Alter storm surge and wave impacts on essential facilities (grocery stores, schools, day cares)
Alter storm surge and wave impacts on critical facilities (water treatment facility, hospitals, police stations)
Alter storm surge and wave impacts on homes and camps
Affect seafood harvest for commercial fishermen
Affect recreational or subsistence catch (redfish, trout etc.)
Filling in of navigable waterways making locations more difficult or easier to get to
Create opportunities for recreation (e.g., birding, paddling, recreational fishing and hunting)
Create educational opportunities (e.g., ecotourism, K-12)
Alter sense of place/community

In total, 13 interviews were conducted[4]. Each interview lasted approximately 85 minutes and ranged from 65 minutes to 110 minutes. In addition, one respondent was unable to find time for the interview and opted to fill out the questionnaire on their own. In this case, the respondent was provided with background information on how the project polygons were derived and detailed instructions on how to fill out the questionnaire.

Upon completion of the interviews, the Institute developed a scripted workflow to analyze the option questionnaire spreadsheets. To convert the categorical data into quantitative scores, each attribute rank was translated into a corresponding numeric value, so that low, medium, or high were respectively translated into 1, 2, or 3 (Table 6). By converting the responses to numbers, the ranks could then be averaged across all surveys. The script then computed the average scores for all four attributes. To further refine risk averages, the scores were divided into three groups based on the average score. Averages ranging from 1.0-1.67 received an A grade; 1.68-2.33 received a B, and 2.34-3.0 were given a C grade.

Table 6. Example of possible responses and corresponding grade

	Likelihood of occurrence	Consequences of impact	How widespread	Over what period of time	Directionality of outcome
Low *Receives an A grade*	Unlikely to occur.	Life will go on, could adjust.	Limited-Site specific (e.g., small structure: dock, bridge, sewage plant).	30+ years away.	Less
Medium *Receives a B grade*	Moderate chance of occurrence.	Moderate impact.	Regional-Place or region (e.g., community, harbor, state park, wildlife refuge, sub-watershed).	10-15 years.	Same
High *Receives a C grade*	Already occurring.	Major disruption; goal out of reach or unattainable.	Widespread-Extensive (most of the watershed or most of the estuary).	Already occur-ring/ imminent or 0-10 years	More

After the survey results were compiled, the technical team worked with partners from EcoMetrics LLC to incorporate these into a social valuation methodology previously developed by the Restore the Earth Foundation (REF). This model was piloted by the Institute (Hemmerling et al., 2017a, 2017b) in conjunction with REF at two REF reforestation sites. EcoMetrics identifies, quantifies, and values all environmental, economic, and social benefits resulting from nature-based solutions projects. In this analysis, composite social value was quantified using part of the approach in the EcoMetrics

[4] Interviews took place during the spring and summer of 2021 and concluded after Hurricane Ida made landfall at Port Fourchon on August 29, 2021, as a category 4 storm.

methodology, which was built on the guiding principles of Social Value International's (SVI) SROI Methodology (SROI Network, 2012). The SVI approach concerns an in-depth, evidence-based understanding of change for a full range of community stakeholders with recognition of both positive and negative changes as well as intended and unintended outcomes.

Value in this context refers to the relative importance placed by a stakeholder group on one potential outcome over another and uses financial proxies as key performance indicators for each of the identified outcomes (Nielsen et al., 2021). The financial proxies used in this analysis were geographically based and focused on the amount of land built or lost, including acres of both saltmarsh and black mangrove (Table 7). The social value assessment also included an analysis of the social cost of carbon, defined by the USEPA as an "estimate of climate change damages and includes, among other things, changes in net agricultural productivity, human health, property damages from increased flood risk and changes in energy system costs, such as reduced costs for heating and increased costs for air conditioning" (USEPA, 2016). Utilizing the estimated tonnage of carbon calculated during the modeling phase of this research and the social cost values established by the USEPA for each specific year, the social value of carbon sequestered in dollars was calculated for each project grouping[5]. The financial proxies used to assess both the land built and carbon sequestered provided standard metrics by which each of the projects are ranked.

To account for the expected likelihood and consequence of each outcome among local stakeholders, the estimated social value generated by each outcome was weighted based upon the results of the option survey. The percentage of survey respondents that identified that specific outcome, the perceived likelihood of that outcome occurring, and the expected consequences of the outcome were all equally weighted in the final value calculation. If the perceived outcome is a benefit, then that outcome is assigned a positive value. Conversely, if the perceived outcome is a harm, then that outcome is assigned a negative value.

The maximum weighted social value would therefore be an outcome that all respondents identified as a benefit with a high likelihood of occurring and a high level of impact. The same scoring rubric was applied to establish the minimum social value, which would be an outcome that all respondents identified as harmful. If no survey respondents identified a specific outcome as a possibility or if all respondents deemed the anticipated impacts of an outcome to be inconsequential, the weighted social value was estimated to be zero. The final estimated costs and perceived social benefits of each project grouping were run through a modified version of part of the calculations component of the EcoMetrics model and calculated for 30 years into the future to coincide with the timeframe of the ecosystem models. This process resulted in a final Adjusted SROI score for each project grouping, a ratio of the expected construction costs to the perceived social benefits and costs estimated using the final weighted social value scores.

[5] For the SROI valuation, tonnes of carbon was calculated based on GHG flux (sinks) for vegetated habitats only (brackish and saline marsh + mangrove forest) of future with action (placement of dredge material) and future without action.

Table 7. Financial proxies used to rank project groupings

	Service	2022 US$/ha	Source
Human Impacts	Alter recreational or subsistence catch (redfish, trout etc.)	$1,510.96	(de Groot et al., 2012)
	Alter seafood harvest for commercial fishermen	$3,696.00	(Barnes et al., 2015)
	Alter sense of place/community	$1,757.12	(de Groot et al., 2012)
	Affect storm surge and wave impacts on critical facilities (water treatment facility, hospitals, police stations)	$7,277.36	(de Groot et al., 2012)
	Affect storm surge and wave impacts on essential facilities (grocery stores, schools, day cares)	$7,277.36	(de Groot et al., 2012)
	Affect storm surge and wave impacts on homes and camps	$7,277.36	(de Groot et al., 2012)
	Affect storm surge and wave impacts on oil and gas infrastructure (port, pipelines)	$7,277.36	(de Groot et al., 2012)
	Create educational opportunities (e.g., ecotourism, K-12)	$2,982.48	(de Groot et al., 2012)
	Create opportunities for recreation (e.g., birding, paddling, recreational fishing, and hunting)	$5,758.05	(Barnes et al., 2015)
	Filling in of navigable waterways making locations difficult to get to	$7,624.16	(de Groot et al., 2012)
Ecosystem Impacts	Alter plant and animal distributions and biodiversity (e.g., migration of more saline tolerant species)	$8,826.40	(de Groot et al., 2012)

	Service	2022 US$/ha	Source
	Alter daily erosion of wetlands, bays, bayous, and canals (i.e., tidal prisms, changing salinity regimes, wind fetch)	$5,343.44	(de Groot et al., 2012)
	Alter storm induced erosion of wetlands, bays, bayous, and canals	$5,343.44	(de Groot et al., 2012)
	Alter the acreage of mangroves	$21,096.32	(Salem & Mercer, 2012)
	Alter the acreage of saltmarsh	$23,307.68	(de Groot et al., 2012)
	Affect the number/distribution of invasive species.	$1,289.28	(de Groot et al., 2012)
	Alter the water quality e.g., harmful algal blooms, microalgae, and bacteria	$1,980.65	(Barnes et al., 2015)
	Impact existing and ongoing restoration projects	$7,277.36	(de Groot et al., 2012)
Wildlife Impacts	Alter the number of mammals in the area (e.g., deer, fur bearing mammals)	$1,453.08	(Barnes et al., 2015)
	Alter habitat for bird species (e.g., migratory, threatened and endangered, secretive marsh)	$1,453.08	(Barnes et al., 2015)
	Alter habitats for crabs, shrimp, oysters and fish	$1,453.08	(Barnes et al., 2015)
	Alter habitats for nesting reptile species (e.g., diamond back terrapins)	$1,453.08	(Barnes et al., 2015)
	Alter spawning ground for crab, fish, and shrimp (e.g., trout, redfish)	$14,481.28	(de Groot et al., 2012)

COASTAL SYSTEMS MODELING FRAMEWORK

Coastal communities need the capability to make long-term predictions about the persistence and function of their coastal wetlands and barrier islands to enable land use planning and management decisions. Numerical models that simulate coastal evolution are a common tool to facilitate planning, however, the large number of relevant coastal processes (e.g., Figure 4) interacting with one another at multiple temporal and spatial scales adds a significant obstacle to fully coupled modeling approaches.

Daily processes such as wind, waves, tides, nutrient flows, and sediment deposition influence land gain, loss, and ecosystem trajectory. In south Louisiana frequent cold fronts occur, which shape the landscape with large waves and unique current patterns. Less frequent tropical storms and hurricanes (hereafter, "tropical cyclones") impose short, punctuated disturbances on the landscape and ecosystem and threaten infrastructure. Coastal wetlands in particular pose a significant challenge in predictive numerical modeling because both their biology and their geomorphology depend on processes that occur at small spatial scales but large time scales. For example, wetland edge erosion occurs in response to wave conditions that are modeled on grids that are 10s of meters on a side and require timesteps as small as a few seconds. But the edge erosion that results from an entire year's worth of wave action might only be 1 or 2 meters, leading to difficulty in accommodating the wetland edge erosion inside of a physics-based numerical model that can also predict bay and shelf morphological processes.

It is therefore not feasible to dynamically model each relevant process and all their mutual interactions at high temporal and spatial resolution. In order to efficiently make realistic and useful projections of the entire ecosystem and landscape, and assess the sustainability of created wetland restoration projects over the 30-year analysis period, the Coastal Systems Modeling Framework was constructed such that important processes are grouped into sub-models that can be run independently while communicating through a reduced number of coupling points (Figure 9).

The Coastal System Modeling Framework consists of four component models: the Morphology Model, the Coastal Wetland Carbon Model, the Hydrodynamics Model, and the Storm Impacts Model. Each model is a combination of previously developed open-source codes and purpose-built software designed at the Institute. In addition, several of the models employ the Delft3D FM modeling suite. For clarity, the following terminology is used in this section. Delft3D FM is the name for a suite of modeling software that is principally developed by Deltares. Delft3D FM consists of tools to model the flow of water in coastal settings (D-Flow FM), waves (D-Waves, which is based on the SWAN model), and sediment transport and morphology (D-Morphology). For this analysis, two modeling grids were employed when using tools from Delft3D FM. The first, the "morph grid" is designed to run more quickly and is used for computationally intensive procedures within the Morphology Model. The second, the "hydro grid," has more grid cells and provides more spatial detail, but takes longer to run. Both grids are explained in detail in this section. The four component models (Morphology, Coastal Wetlands Carbon, Hydrodynamics, and Storm Impacts) are described separately below, with additional details available in Appendix A. Throughout this report there are references to the tools from the Delft3D FM suite as D-Flow FM, D-Morphology, or D-Waves as appropriate, and to their implementation on either the morph grid or the hydro grid.

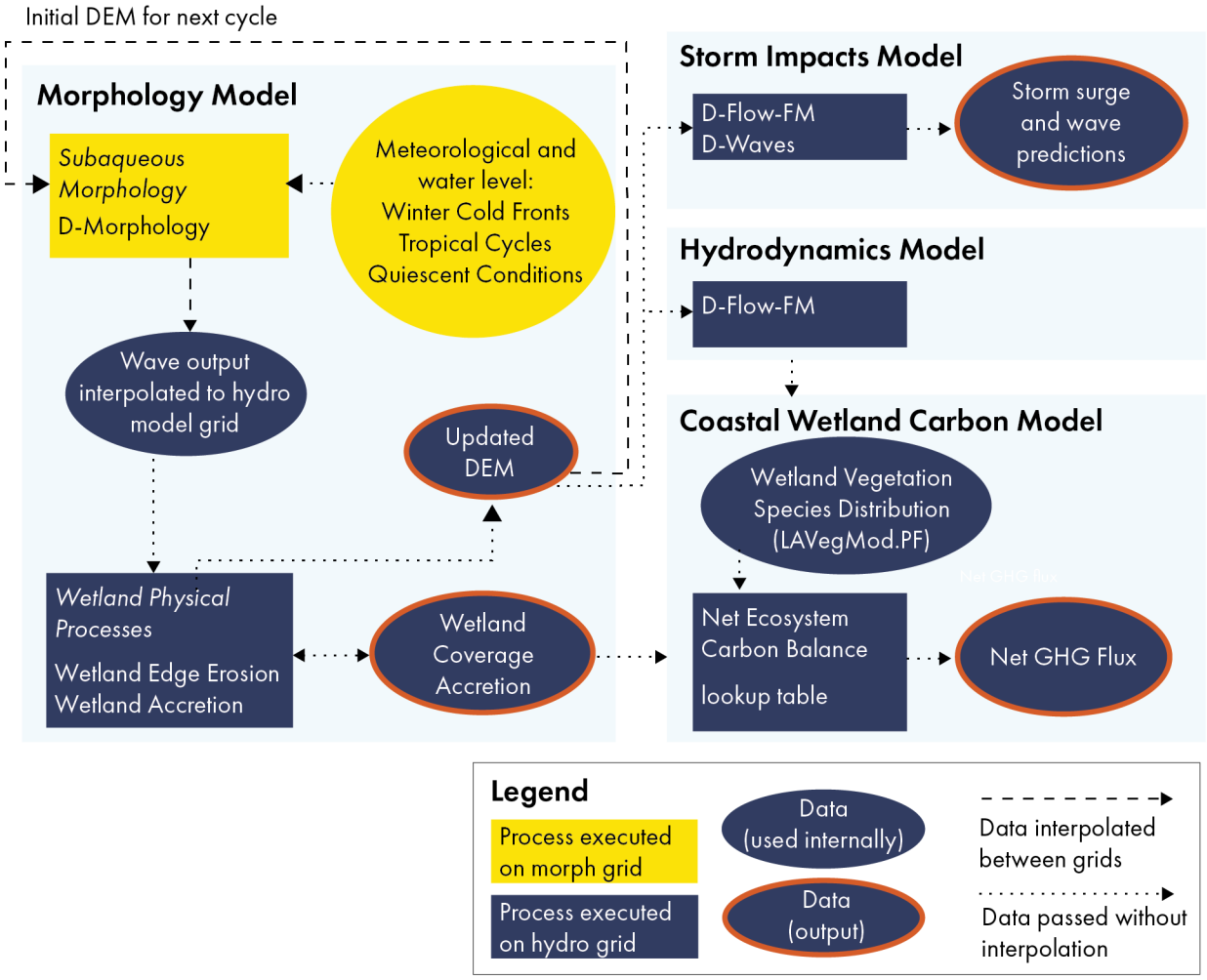

Figure 9. Schematic of the Coastal Systems Modeling Framework The Coastal Systems Modeling Framework consists of four independent models.The diagram shows how a single 5-year cycle of the Morphology Model is completed and the output passed to the other three models, as well as the input to the next 5-year cycle.

Model Integration

A model run is initiated with the Morphology Model, which simulates the influence of waves, tides, winter cold front conditions, and tropical cyclones for a schematized period of 5 years, as described in the *Subaqueous Morphology* section below. The 5-year interval, or "cycle", is the repeated functional unit of the modeling effort. Six cycles of the Morphology Model were executed to simulate the morphological evolution of the study site for 30 years. The Storm Impacts, Hydrodynamic, and Coastal Wetlands Carbon models use output from the conclusion of each cycle to initiate the following cycle.

The evolved morphology that results from a cycle of the Morphology Model includes updates to the elevation of all portions of the system, including tidal inlets, the shoreface, the shelf, the bay floor, and vegetated wetlands. The updated topography and bathymetry (hereafter "DEM," for Digital Elevation

Model) is used as the initial condition for the next cycle, and for initiating separate Delft3D FM hydrodynamic models that will be used in the other three models (Figure 9). The Morphology Model does not require input from the Coastal Wetlands Carbon Model.

The Hydrodynamics Model that creates input for the Coastal Wetlands Carbon Model can be run at the conclusion of any cycle of the Morphology Model, using maps of wetland accretion and coverage that are created from the Wetland Physical Processes component of the Morphological Model (Figure 9).

Morphology Model

The Morphology Model is run in two steps that together represent the morphological evolution of the landscape during a 5-year cycle. In the first step, the morphological response of the subaqueous environments (bay floor, tidal channels, shoreface, and shelf) to tides and waves is modeled using D-Flow FM with D-Waves and D-Morphology. This step includes a period of winter conditions where the basin is influenced by winter storms in the form of cold fronts, and a summer period during which the basin is meteorologically quiescent except for the occasional tropical cyclones. In the second step, the spatial coverage of wetland areas is adjusted to account for edge erosion, and the elevation of wetlands is adjusted to account for accretion. Both steps are described below, and the final DEM at the end of a 5-year run cycle is obtained by combining the results.

Subaqueous Morphology

The basic building block of the time-series inputs for the D-Flow FM, and D-Waves model is a 28-day period of two spring-neap tidal cycles that is then subdivided into seven four-day periods (Figure 10). During winter conditions, each four-day period is used to include either a meteorological event (i.e., cold front) or quiescent conditions. The inclusion of tropical cyclones during the summer is implemented in the same way except tropical cyclones do not directly impact the study area every summer and are not confined to four days.

Two sequences of 28 days (one for winter, and one for summer) were used to simulate morphological change as experienced by the area during 5 full years of morphological time, using a process called “morphological acceleration” whereby the rates of morphological change (erosion and deposition) are multiplied by an acceleration factor during the model run. Acceleration factors of 1, 20, and 45 were used during tropical cyclone, cold front, and quiescent conditions, respectively. This technique not only allows for significant savings in model run time but preserves the ability to allow for significant variability in the interaction and sequencing of meteorology and tides in driving water levels and waves throughout the basin.

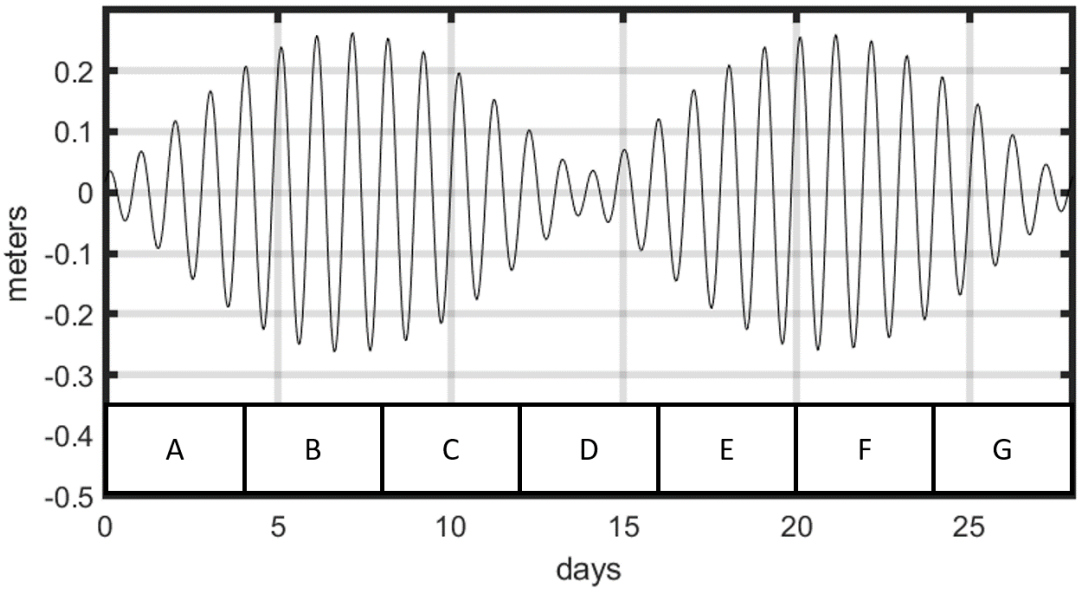

Figure 10. The 28-day spring neap cycle forms the basic unit of the morphology model's input time series. Shown here is the Winter period, in which each lettered block (A, B, C, …) represents a four-day slot that can be used for a cold front. Most studies of cold fronts in Louisiana estimate 20-30 frontal passages each winter (Georgiou et al., 2005; Hiatt et al., 2019; Walker & Hammack, 2000). The above scheme, with seven cold front slots per 28-day tidal period allows an effective maximum of 42 cold fronts to be included in each six-month winter period. Slots are filled with quiescent conditions to lower the number of frontal passages.

Wetland Physical Process

Following the subaqueous morphology step, the Wetland Physical Processes component then adjusts the elevation and spatial coverage of wetland cells to account for wetland loss due to edge erosion and wetland total vertical accretion due to organic and mineral accumulation. Both calculations are described below. This step is executed outside of Delft3D FM, via purpose-built software designed at the Institute.

Accretion

Coastal wetland vertical accretion depends on repeated inundation of sediment rich water and in-situ belowground organic production. The accretion values that are calculated by the Wetlands Physical Processes component are Total Vertical Accretion values that implicitly include both mineral and organic accretion. In this report the term "accretion" should be assumed to be Total Vertical Accretion unless otherwise specified.

Data collected over decadal timescales in coastal wetlands throughout the world (e.g. Kirwan et al. 2016; Kirwan and Guntenspergen 2010) has shown that when wetlands are flooded more frequently and to greater depths there is increased mineral sediment delivery, so as sea level rise (SLR) continues so too does inundation and sediment delivery. The models that are most commonly used to predict coastal wetland persistence (e.g. Clough 2016; Morris et al. 2002) are informed by decades-long measurements of sediment and organic matter accretion that are calibrated to records of wetland inundation, sediment availability, and wetland biology (Alizad et al., 2016; Clough et al., 2016; Kirwan & Murray, 2007; Morris et al., 2002; Mudd et al., 2009; Temmerman et al., 2003; Wu et al., 2015).

The modeling effort also exploits the relationship between accretion and inundation, doing so by predicting accretion as a function of the local rate of RSLR (Figure 11). In the base case environmental scenarios, accretion is set to be the same as local RSLR, thus keeping pace with SLR. In the "less optimistic" environmental scenarios, accretion is set to lag the local rate of RSLR by 2 mm/yr, thus leading to a slow drowning of lower elevation wetland cells during the course of the 30-year run. This approach is consistent with empirical observations in coastal marshes globally, and the choice of 2 mm/yr as the accretion deficit is drawn from measurements collected in nearby stations of the Coastwide Reference Monitoring System (CRMS) network (Figure 12; Figure 13). The environmental scenarios are discussed in detail in the *Project Alternatives and Environmental Scenarios* section below.

The amount of accretion that a given cell receives is further adjusted based on its elevation. Cells with an elevation at both the beginning and the end of a cycle greater than 35 cm above local eustatic sea level receive no accretion during that cycle because they are assumed to be infrequently inundated and thus receive mineral sediment input for only brief periods of time. Cells with an elevation less than 30 cm above current eustatic sea level receive the full component of accretion equal to RSLR. Finally, cells within the interval between 30 and 35 cm above eustatic sea level receive a linearly prorated amount of accretion. An example of accretion output is shown in Figure 14.

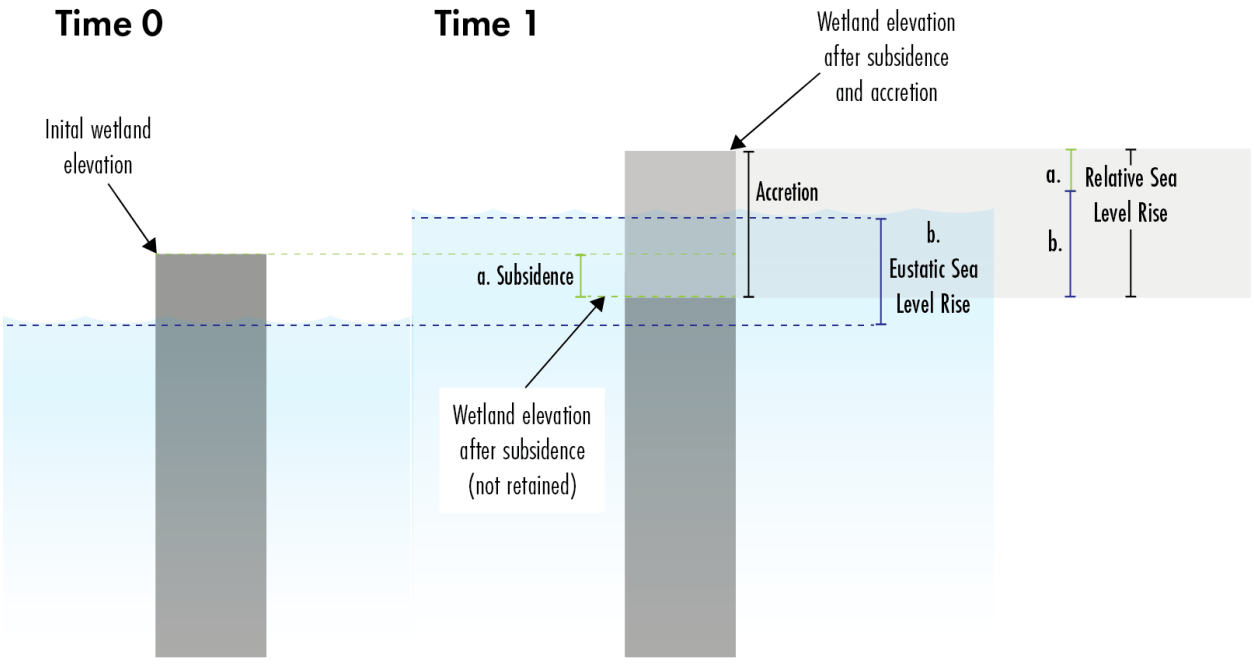

Figure 11. Schematic of the accretion calculation showing subsidence, eustatic sea level rise (ESLR), and RSLR as their sum. For environmental scenarios where wetlands keep up with RSLR (Table 18), the thickness of accretion that a wetland cell experiences is equal to the amount of subsidence plus the ESLR. For scenarios where wetlands do not keep up with RSLR, accretion is slightly less than RSLR, leading to drowning at low elevation cells.

Figure 12. Louisiana Coastwide Reference Monitoring System (CRMS) sites used for marsh accretion analysis.

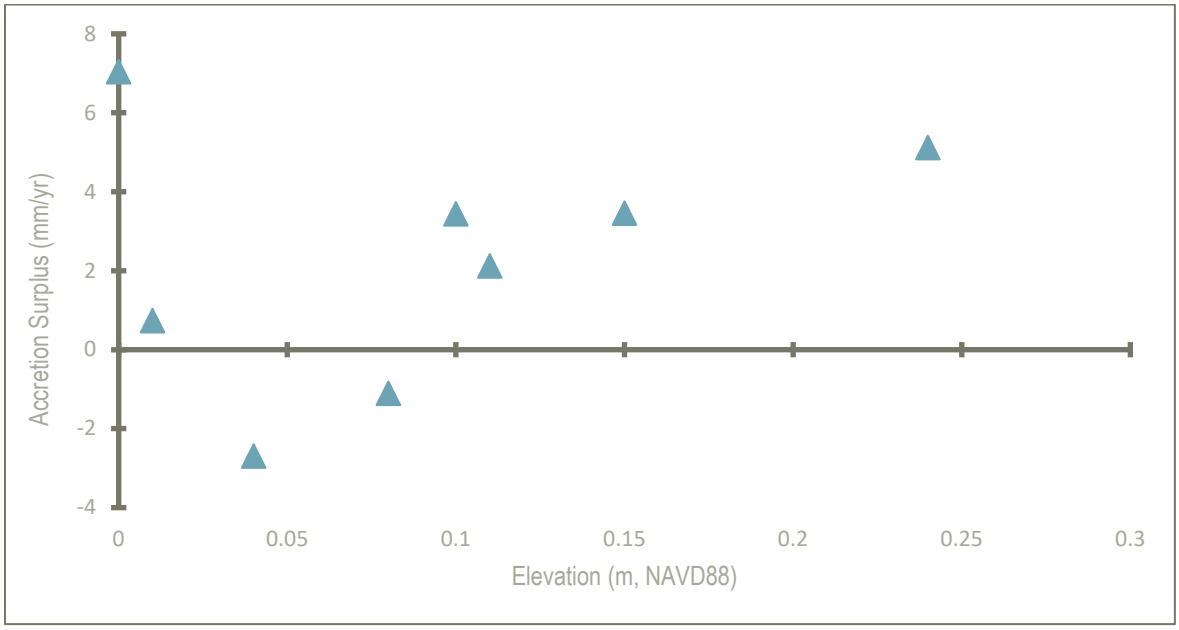

Figure 13. Accretion Surplus at CRMS stations near Port Fourchon. Accretion Surplus is defined as the local rate of RSLR subtracted from the Total Vertical Accretion rate. Stations with negative accretion surplus are vulnerable to drowning. Data points are from CRMS stations near Port Fourchon (Figure 12). Accretion rates for these stations were provided via personal communication from Gregg Snedden, U.S.G.S., and local rates of RSLR and station elevation are from (Jankowski et al., 2017).

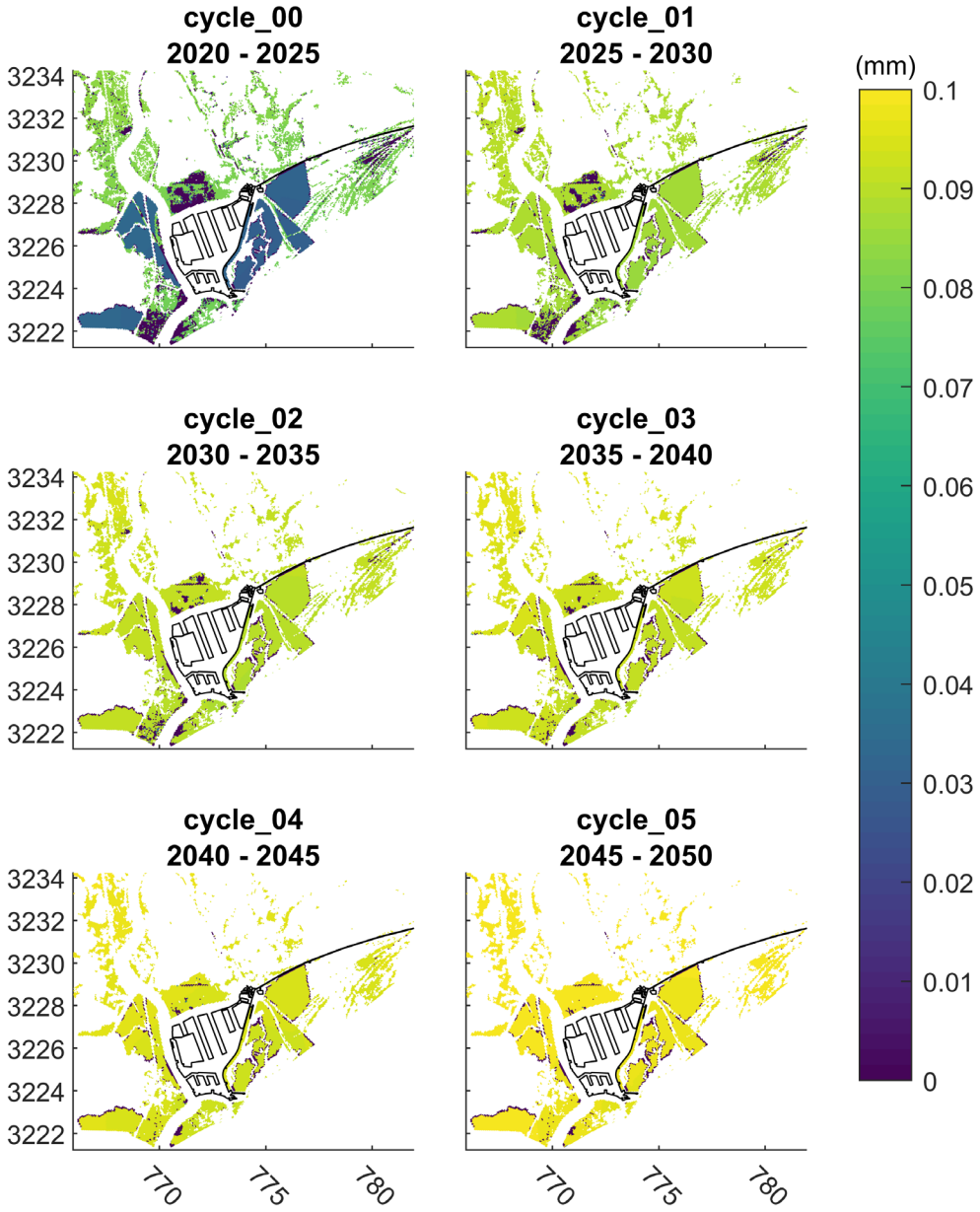

Figure 14. Wetland accretion, in mm, experienced during the five years simulated by the Morphology Model in the second model production run (PR2). Dark blue cells indicate locations that were elevated above mean high water either naturally or by restoration and therefore received no accretion. Intermediate colors indicate cells that are high enough in the tidal frame that they received a prorated amount of accretion, but not so high that they received none. Note that the overall rate of accretion increases toward the end of the production run, reflecting SLR acceleration that the wetland keeps up with. Note also that the overall wetland area decreases in response to edge erosion. Axes are shown in km UTM 15N. Port Fourchon facilities and portions of LA-1 are outlined in black.

Edge Erosion

One of the major modes of coastal wetland loss in the study area is due to wave driven erosion along the wetland edge (Mariotti & Fagherazzi, 2010; Penland et al., 2000; Valentine et al., 2021; Valentine & Mariotti, 2019). Observations in coastal wetlands worldwide show a linear relationship between incident wave power at the wetland edge and the amount of wetland that is eroded (Leonardi et al., 2016; Marani et al., 2011). The edge erosion component of the Wetlands Physical Processes component uses a wetland edge erodibility coefficient that was computed for Barataria Bay wetlands by Valentine and Mariotti (2019) to convert wave power density to an edge retreat rate (Figure 15). Wave power density is obtained from D-Waves in the Subaqueous Morphology step.

Because the rate of edge retreat is small (1s of meters per year) compared to the size of most wetland cells in the model domain (10s of meters), the amount of wetland erosion that has occurred in a given cycle must be retained for future cycles. This is accomplished through a bookkeeping system whereby a wetland cell is fully removed from the hydrodynamic model only after a cumulative 75% of its area has been eroded.

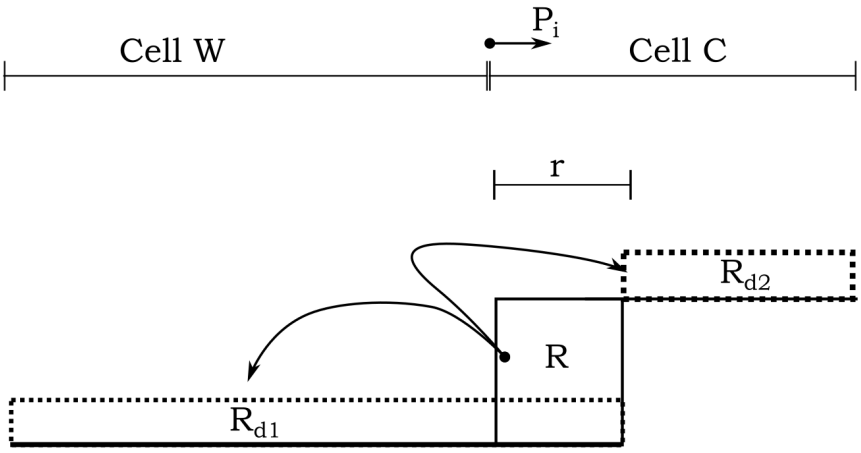

Figure 15. The incident wave power density (P_i) at the wetland edge is provided by the D-Waves model output for the open water cell (Cell W) and is used to calculate the linear retreat rate (r) of the wetland cell (Cell C). The hydrodynamic model grid geometry is used to convert the linear retreat rate (r) to a volume to be removed (R). An optional switch allows a portion of R to be redistributed to the adjacent open water cell (R_{d1}) and to the wetland top (R_{d2}). In the current model runs this switch is set to zero.

Restored Wetlands

Project alternatives were included in the Morphology Model by increasing the elevation of the entire project polygon to an elevation of 0.39 m NAVD88. This elevation was chosen to represent the 5-year post-construction elevation determined from settlement curves found in project design reports from nearby projects (Ardaman & Associates, 2018c, 2018a, 2018b; GeoEngineers LLC, 2018). Upon construction, restored polygons were governed by the same rules as unrestored wetlands. A detailed description of engineering considerations can be found in the *Project Alternatives Cost Evaluation* section.

Hydrodynamics Model

The Hydrodynamics Model was developed to represent hydrodynamics including salinity, water level, and temperature in the Barataria-Terrebonne Basin using a depth-averaged D-Flow FM model. The Hydrodynamics Model is used to represent the area of interest which includes the Caminada Headland between East Timbalier Pass and Caminada Pass extending up to Leeville (Figure 16). The area of interest is represented with a 50-meter resolution to adequately capture the spatial variability of local flow patterns.

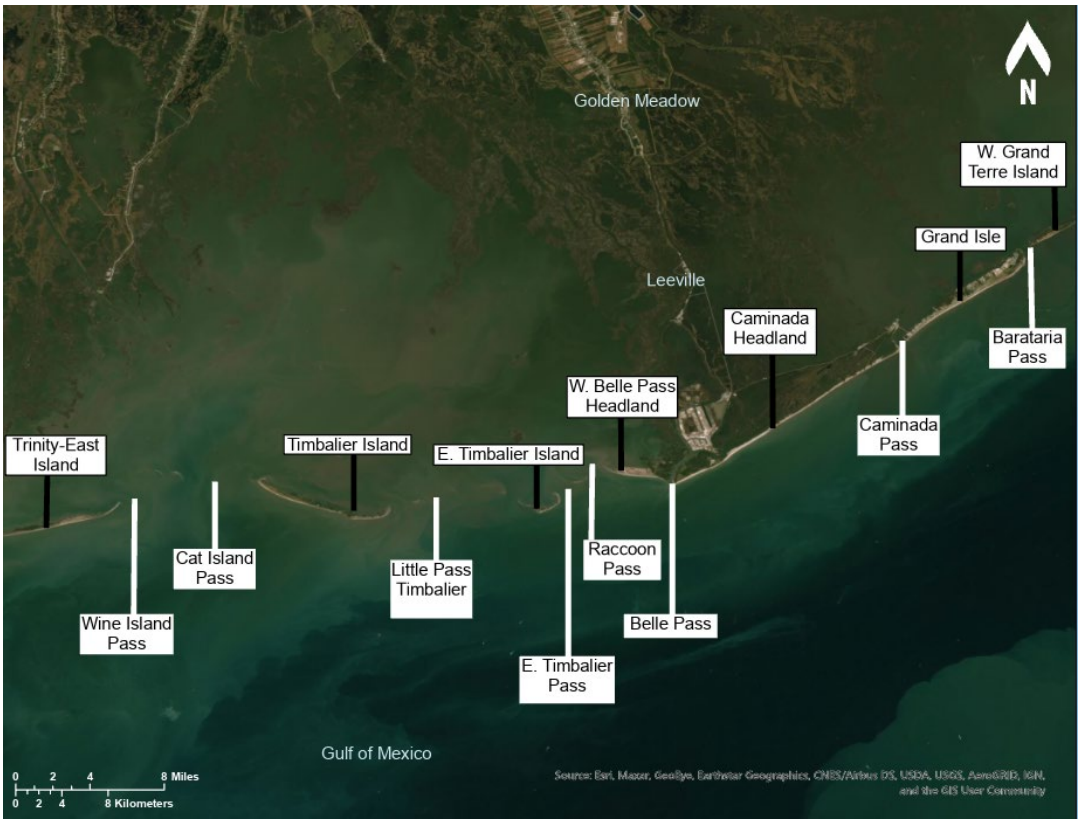

Figure 16. Tidal inlets and barrier shoreline landforms within the modeled area of interest in Lafourche and Terrebonne Parishes, LA.

Simulating hydrodynamics including salinity, water level, and temperature requires the input of several meteorological parameters including wind, relative humidity, air temperature, solar radiation, cloud coverage, precipitation, and evaporation, each of which is described in the *Meteorological Inputs* section. Additionally, the discharge and temperature of riverine and other freshwater inflows in the Barataria-Terrebonne Basin are included, along with spatially and temporally varying temperature and salinity data for the offshore boundary of the model domain.

The Hydrodynamics Model was run for the landscapes representing years 2020, 2025, 2030 and 2050 of every possible combination of project alternative and environmental scenario (six in total), amounting to a total of 21 simulations. All simulations were executed for a full calendar year to account for temporal and seasonal variability. The meteorological forcing, riverine inflows, and offshore temperature and salinity for the year 2015 were used as a representative year for each of the hydrodynamic simulations.

Coastal Wetland Carbon Model

In addition to predicting landscape and wetland vegetation changes over 30 years, estimates of the carbon capture potential of the wetlands surrounding Port Fourchon was a goal of this study. Louisiana's coastal wetlands are diverse (Sasser et al., 2014), productive in generating carbon, and their flooded, subsiding soils provide the perfect condition for the carbon to remain buried. Coastal Louisiana's ability to accumulate soil carbon may be underestimated because the carbon capture potential of mangrove habitats has not been well studied. Incorporating the characteristics of black mangroves (*Avicennia germinans*) into the modeling is necessary to represent the wetland habitats surrounding Port Fourchon that have been increasingly dominated by black mangroves (Osland et al., 2020) and is likely influencing the amount of carbon captured and stored in aboveground biomass and buried in soils.

To quantify the net greenhouse gas (GHG) flux of tidal wetlands currently and in the future, a Coastal Wetlands Carbon Model was developed that combines two key parts. The first part was a wetland vegetation species distribution model (LAVegMod.PF) that represents the mortality and establishment of dominant wetland species, such as Spartina patens, Spartina alterniflora and Avicennia germinans based on hydrological inputs, and the output is used to represent the area of coastal habitats based on dominant wetland vegetation species. The second part was a lookup table that provided the major carbon fluxes (aboveground net primary productivity, sediment/soil carbon accumulation, and greenhouse gas emissions) as a function of habitat type and a series of assumptions about habitat changes (Figure 17).

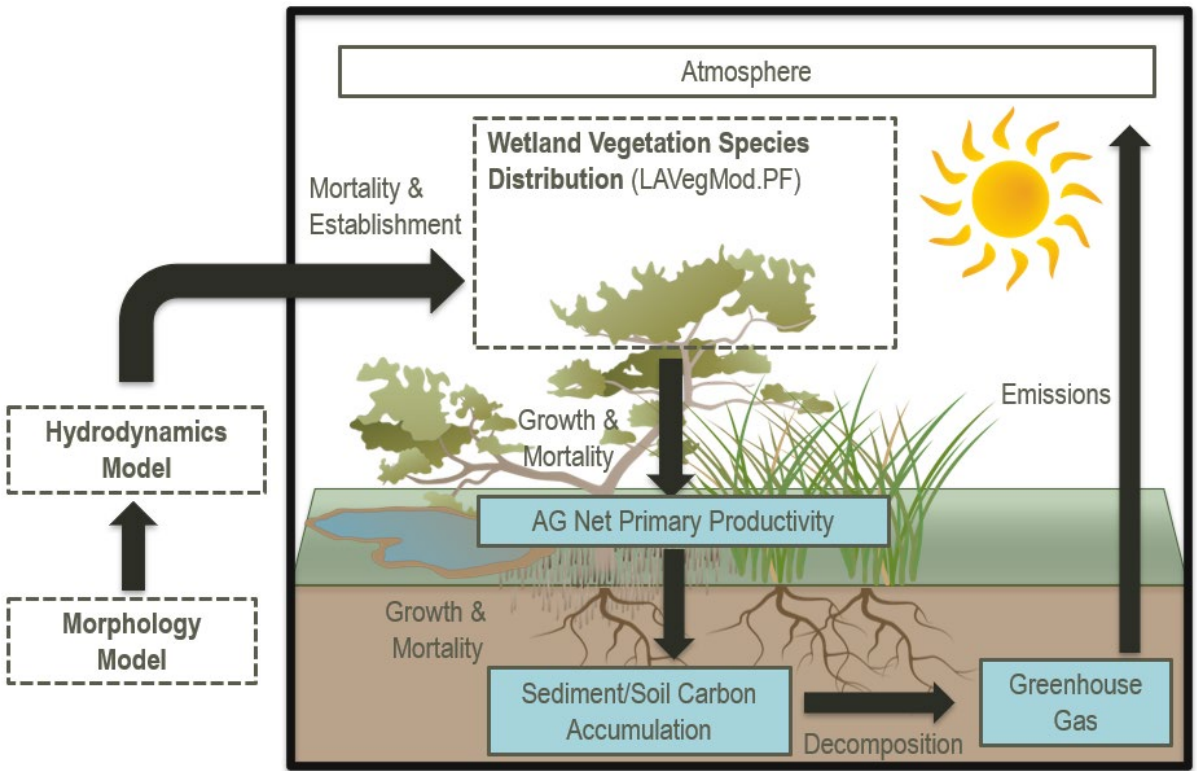

Figure 17. Conceptual diagram representing the information (models in dashed boxes) and ecological processes of the Coastal Wetlands Carbon Model that includes wetland vegetation species distribution that influences which carbon flux values (blue boxes) that inform net ecosystem carbon balance per habitat (see Table 8.

Wetland Vegetation Species Distribution

Three main wetland vegetation species were modeled in the LAVegMod.PF component (Table 8) Table 8. which was modified from LAVegMod that was previously developed for tracking vegetation shifts across coastal Louisiana given changing environmental conditions (Visser & Duke-Sylvester, 2017). The LAVegMod.PF operates on the same grid as the hydrodynamic model (D-Flow FM). Within each grid cell, the percent coverage of each wetland vegetation species is tracked on an annual basis. The initial percent coverage in each cell is derived from a 2014 land use land cover map with a 30 m resolution (Couvillion, 2017). The coverage changes are based on hydrodynamic model outputs of mean annual salinity and the standard deviation of water level. Each vegetation species has a set probability of mortality and probability of establishment for the given inputs that govern the coverage changes. The relationships that determine the probabilities were derived from observations of presence and absence of each wetland vegetation species at CRMS sites (Visser et al., 2013). If the environmental conditions cannot support any of the vegetation species, the cell was set to bare ground.

Net Ecosystem Carbon Balance

The Net Ecosystem Carbon Balance (NECB) flux method was modified from Chapin et al (2006) and based on previous studies (Poungparn et al. 2012; Taillardat et al. 2020; Troxler et al. 2013; Twilley et al. 2017, Hopkins, 2018). The modified Net Ecosystem Carbon Balance is based on habitat specific fluxes in carbon dioxide equivalents (CO_2e) and was calculated as follows:

$$Net\ Ecosystem\ Carbon\ Balance = NEE + GHG = ANPP + Sed/Soil_{accum.} + GHG\ (1)$$

where, *NEE = Net Ecosystem Exchange = ANPP* + sediment/soil carbon accumulation ($Soil/Sed_{accum.}$)

GHG = greenhouse gas emissions

ANPP = Aboveground net primary productivity which is the flux of gross primary productivity (GPP) minus the autotrophic respiration (AR) of the aboveground biomass of emergent vegetation.

$Sediment/Soil_{accum.}$ = Net carbon accumulation in the sediment/soils incorporates the net primary productivity of belowground biomass but also the accumulation of dead belowground biomass of roots and rhizomes, aboveground litter, as well as allochthonous carbon (Troxler et al., 2013).

Four main coastal habitats were considered, and the carbon fluxes were synthesized in a lookup table based on literature review to aid in estimation of the NECB of existing coastal habitats with common units of g C m^{-2} yr^{-1} that were converted to tonnes CO_2e ha^{-1} yr^{-1} to compare to other greenhouse gas (GHG) inventories (Table 8. The carbon was converted to CO_2e by multiplying by 3.67 (molecular weight ratio of CO_2 to C). Methane and nitrous oxide emissions were converted to CO_2e by multiplying their global warming potential (over 100 years) values of 25 and 298, respectively (IPCC, 2007; US EPA, 2021). For this study, it is assumed that the only carbon flux that will change in the future is the sediment/soil carbon accumulation flux. This flux will change in the future because of RSLR that will drive an accommodation space that allows for an increase in sediment/soil carbon accumulation (Herbert et al., 2021). Therefore, the simple linear regression from Herbert et al. (2021) was used that estimates

that the mean sediment/soil carbon accumulation rate is equal to 52.61 + 24.78*RSLR ($R^2 = 0.8$) to estimate the future sediment/soil carbon accumulation rate based on RSLR. ANPP and sediment/soil accumulation rates are represented as negative values because they represent a GHG sink from the atmosphere; values for GHG emissions are positive indicating a source to the atmosphere.

Table 8. Lookup table used to represent the carbon fluxes to estimate the net ecosystem carbon balance (NECB) of coastal habitats including dominant wetland vegetation taxa: Spartina patens *(SPPA),* Spartina alterniflora *(SPAL), and* Avicennia germinans *(AVGE).*

Habitat (w/ identifier and model code)	**Carbon Flux (mean ± 95% SE, tonne CO2e/ha/year)**				**References**
	Aboveground net primary productivity (ANPP)	Sediment/Soil (1 m) carbon accumulation	GHG emissions	NECB	
Brackish Marsh (i=1, SPPA)	-46.5 ± -5.5	-9.7 ± -1.4	+8.1 ± 3.2	-48.1± 21.0	(Cardoch et al., 2002; Cramer et al., 1981; Day et al., 2013; DeLaune et al., 1983, 1984; Delaune & Smith, 1984; Feijtel et al., 1985; Flynn et al., 1999; Herbert et al., 2021; Holm et al., 2016; Hopkinson et al., 1978, 1980; Krauss et al., 2016; Lane et al., 2016; Nyman et al., 1995; Pezeshki & DeLaune, 1991; Sasser et al., 2018; Sasser & Gosselink, 1984; Smith et al., 1983b; Stagg et al., 2016; White et al., 1978; White & Simmons, 1988)
Saline Marsh (i=2, SPAL)	-29.4 ± 2.6		+1.6 ± +0.7	-37.5± -17.6	(Cardoch et al., 2002; Darby & Turner, 2008; Day et al., 2013; DeLaune et al., 1983; Edwards & Mills, 2005; Feijtel et al., 1985; Herbert et al., 2021; Hopkinson et al., 1978, 1980; Kaswadji et al., 1990; Kirby & Gosselink, 1976; Lane et al., 2016; Pezeshki & DeLaune, 1991; Pham, 2014, 2014; Sasser et al., 2018; Sasser & Gosselink, 1984; Smith et al., 1983b; Stagg et al., 2016; Stagg & Mendelssohn, 2011; White et al., 1978)
Mangrove Forest (i=3, AVGE)	-45.9± -6.7		+1.6 ± +0.7	-54.0 ± -26.1	(DeLaune et al., 1983; Herbert et al., 2021; Lane et al., 2016; Lugo & Snedaker, 1974; Pham, 2014; Smith et al., 1983b; Weaver & Armitage, 2020)
Saline Open Water (i=4)	-3.67	-8.0± -0.7	+0.03	-11.6± -1.0	Day 1973; DeLaune et al. 1983; Smith et al. 1983

Existing, Restored, and Converted Habitats

Three main habitat-change categories were considered: existing, converted, and restored. Converted habitats are those that change because of no restoration or management action and restored habitats are those that change because of restoration or management actions. It was assumed that if a habitat remains the same habitat (existing habitat) or becomes restored to a different habitat (restored habitat) between years (e.g., 2020 and 2025) that the values in the lookup table will be used from the most recent habitat. Because LAVegMod.PF provides percent coverages of three dominant vegetation types in each cell, the NECB was estimated based on those fractions.

Two major conversions were also considered: 1) mangrove forest converted to brackish or saline marshes and 2) vegetated habitats converted to open water.

1. Mangrove forest converted to brackish or saline marshes

The changes in carbon fluxes through conversions of the mangrove forest to marshes were considered to describe the effect of the biomass loss to atmosphere and remaining standing stock as ghost trees in the converted habitats. In this calculation, the following assumption was used to describe the conversion of the black mangrove to marshes (Table 9).

Table 9. Assumption to prescribe to carbon fluxes of habitats that have been converted from black mangrove to marshes.

Converted habitats	Carbon Flux	Assumption	Literature cited
Mangrove Forest **converted** to Marsh Habitats	Aboveground Net Primary Productivity	50% becomes a source to atmosphere, dead organic matter or ghost trees can remain via 50% of standing stock	US EPA, 2021; Tampa Bay Blue Carbon Assessment, 2017; Domke et al., 2011
	Sed/Soil Accum.	Use values in new habitat look-up table	US EPA, 2021
	GHG Emissions		

Based on the assumptions in Table 9, the NECB equations of mangrove forest when converted to brackish or saline marshes were modified.

2. Vegetated habitats converted to open water

The changes in carbon fluxes through conversions of the vegetated habitats to open water were considered in the calculations of NECB (Table 10). It was assumed that the captured carbon in the aboveground biomass and the sediment/soils would be lost from the ecosystem and become a source to the atmosphere. To estimate the loss of the sediment/soil carbon stock, it was assumed that it took about 189 years to build 1 m of sediment/soil based on a mean long-term accretion rate of 0.53 cm yr^{-1} (Baustian et al. 2021). Therefore, the sediment/soil carbon accumulation rate from the vegetated habitat that was converted to open water was multiplied by 189 years to estimate the total carbon stock and a percentage of that stock was prescribed as a source of GHG to the atmosphere. It was also assumed that when the vegetated habitats convert to open water habitats, the estimates of GHG emissions from open water habitats would be an additional GHG source.

Table 10. Assumption of prescribing carbon fluxes of habitats that have been converted from vegetated habitats (saline wetlands, saline marsh, brackish marsh) to open water.

Converted habitats	Carbon Flux	Assumption	Literature cited
Mangrove Forest **converted** to Open Water	Aboveground Net Primary Productivity	50% becomes a source to atmosphere, DOM or ghost trees can remain, 50% of standing stock	US EPA, 2021;Tampa Bay Blue Carbon Assessment, 2017; Domke et al., 2011
	Sed/Soil Accum.	1) Mangrove converted to water means losing 1m soil, and it take 189 years to lose 1m soil 2) 50% of carbon in 1 m soil is source to atmosphere and 50% remains a sink	
	GHG Emissions	Depends on new habitat in the look-up table	US EPA, 2021
Marsh Habitats **converted** to Open Water	Aboveground Net Primary Productivity	100% is a source to atmosphere	US EPA, 2021
	Sed/Soil Accum.	1) Marshes converted to water means losing 1 m soil, and it take 189 years to lose 1 m soil 2) 75% of carbon in 1 m soil is a source to atmosphere and 25% remains a sink	(Baustian et al., 2021; Sapkota & White, 2021)
	GHG Emissions	Depends on new habitat in the look-up table	US EPA, 2021

Based on the assumptions in Table 10, the NECB from the mangrove forest and marshes to open water were modified.

Net GHG flux for Project Area

The term net GHG flux of emissions (MMT CO_2e) was used in the Louisiana's current GHG inventory (Dismukes, 2021) where negative values for a specific year signify removal of GHGs and positive values indicate a net source to the atmosphere for that year. The net GHG flux was determined by the product of the NECB for each habitat (Hopkinson, 2018) and its corresponding habitat area (ha) produced from the LAVegMod.PF for all habitat changes and based on model years 2020, 2025, 2030, and 2050. Therefore, the net GHG flux (MMT CO_2e) for project area for each of those snapshot years was calculated for a specific year based on the following equation:

$$\text{Net GHG Flux}_{(\text{year})} =$$

$$\sum_{N=4} \text{NECB}_{\text{existing habitats}} \times \text{Area}_{\text{existing habitats}} + \sum_{N=7} \text{NECB}_{\text{converted habitats}} \times \text{Area}_{\text{converted habitats}} + \sum_{N=3} \text{NECB}_{\text{restored habitats}} \times \text{Area}_{\text{restored habitats}} \quad \text{Eq. (4)}$$

Storm Impacts Model

To evaluate the effect of the nature-based project alternatives and morphological changes on the wave and flooding impacts associated with tropical cyclones, the evolved geomorphology and wetland cover that is produced by the Morphology Model was used as input to the Storm Impacts Model (see Figure 9). These simulations were performed with a coupled hydrodynamics and waves model using D-Flow FM and D-Waves.

For the Storm Impacts Model, six tropical cyclones were selected from a database of 645 synthetic storms that were developed by the USACE's Engineering Research and Development Center (ERDC) for use in the 2023 Louisiana CMP ADCIRC modeling analysis (Johnson & Geldner, 2020). Each storm consisted of time varying wind and pressure fields throughout the model domain, and offshore boundary conditions for water level, wave height, period, and direction. Storms were simulated for the initial (2020) and final (2050) landscapes of each production run, for a total of 54 unique run configurations.

The six storms were chosen through a two-step process. First, each storm in the database was ordered according to the root mean square difference (RMSD) between the storm's maximum surge elevation and a pre-defined set of elevation control points along LA 1 in the 2020 landscape DEM (Figure 18). The 30 storms with the lowest RMSD represent the storms where the maximum surge elevation is either close to overtopping LA 1 or has overtopped by a small amount. Therefore, for these storms, marginal changes in surge elevation due to project selection or changes to overall morphology and hydrology are likely to results in major changes to impacts. From this set of 30 storms, the final six (Figure 19, Figure 20) were selected to maximize variability in track relative to Port Fourchon. Three of the six selected storms have predicted maximum surges that exceed LA 1's 2020 elevation and three have predicted maximum surges that are slightly below the highway.

The six storms that were selected through this process represent a diverse set of storm approach trajectories, and produce surge elevations that are likely to be affected by the projects that are constructed and the changing morphology of the landscape. They therefore represent a strong test for the effectiveness of the proposed projects.

Figure 18. Data extraction points were located arbitrarily along the unelevated portion of LA 1 from Golden Meadow to Grand Isle.

Table 11. Properties of the six selected synthetic storms. Average water surface elevation at control points is the average surge that each storm produced at points shown in Figure 16. RMSD is the root mean square deviation.

StormID	Avg Water Surface Elevation at Control Points (ft)	Avg Err (ft)	RMSD (ft)	Forward Speed (kts)	Minimum Central Pressure (mb)	Radius of Maximum Winds (Nautical Mile)
149	3.0607	0.0752	0.0131	5	98	30.3
60	2.7803	-0.2052	0.0559	5.3	955	16
248	3.0892	0.1036	0.0776	10.2	955	28
34	3.1208	0.1352	0.1176	18.1	885	15.7
67	2.6422	-0.3434	0.1268	8.3	955	9.2
531	2.8689	-0.1166	0.1316	5.8	995	48.9

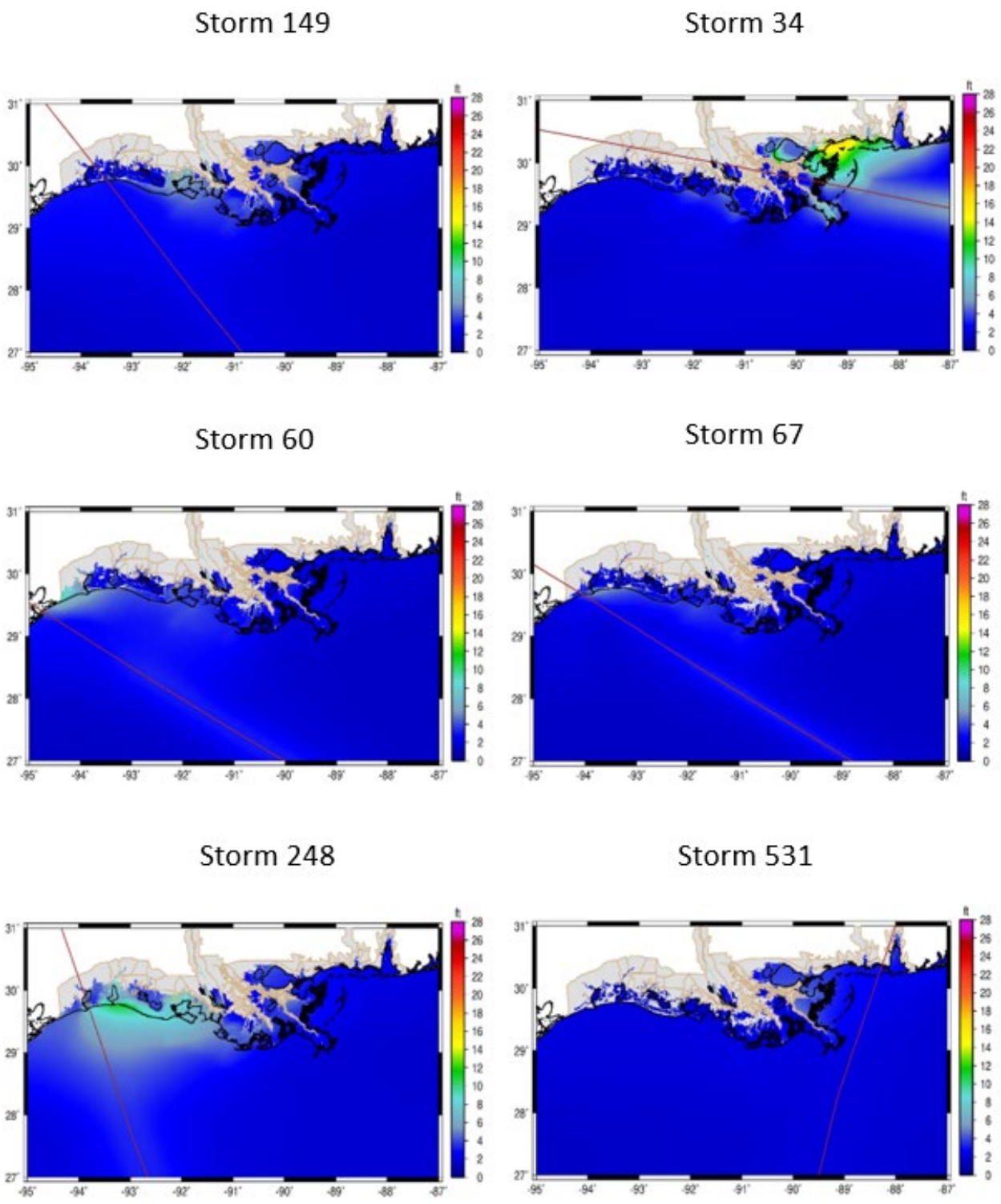

Figure 19. Tracks of the six selected tropical cyclones used. Colors show the maximum storm surge elevation in ft during the storm.

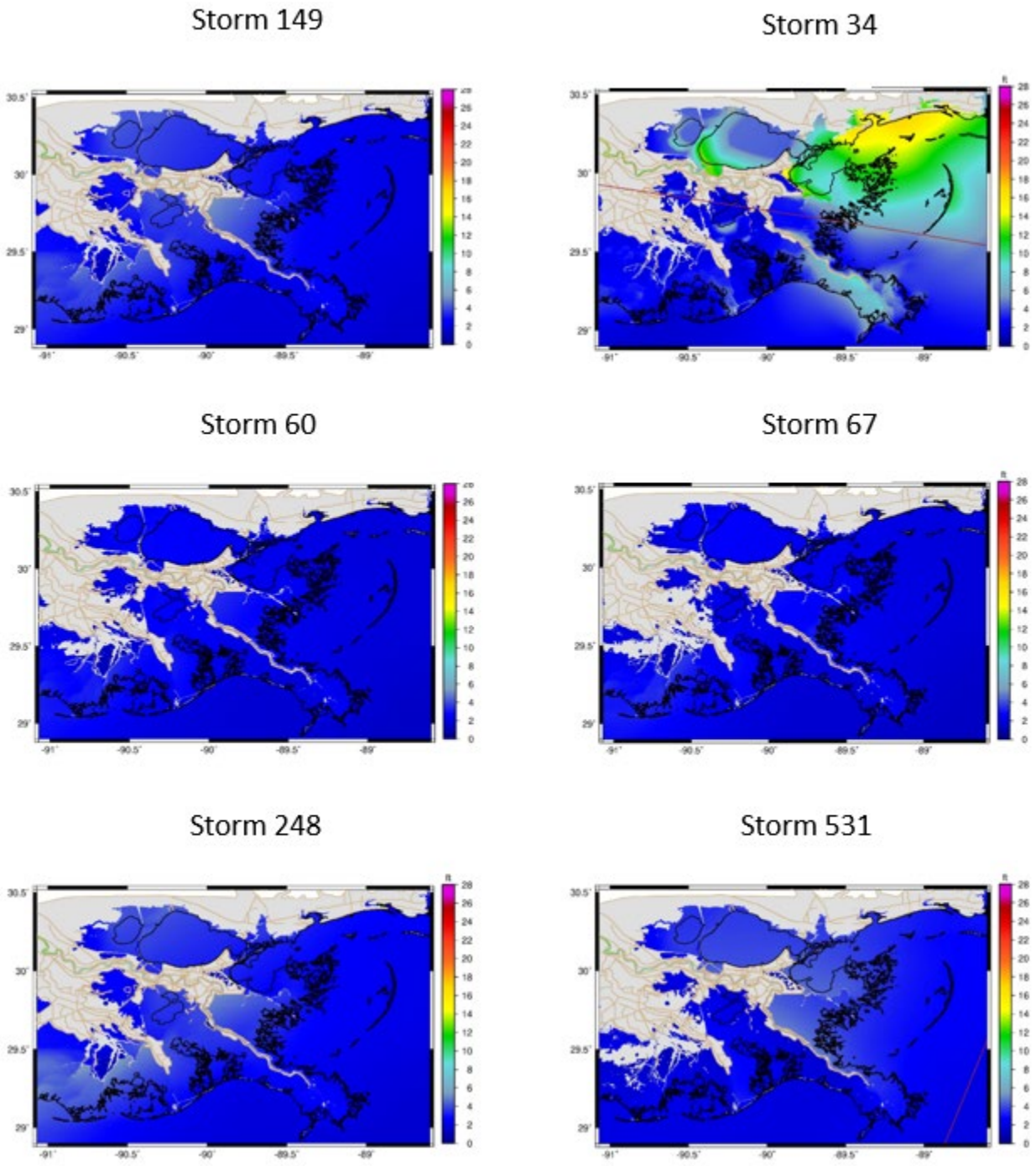

Figure 20. Maximum surge elevations in ft in southeast Louisiana for the six selected storms.

Delft3D FM Model Setup

The Delft3D FM model setup consisted of multiple steps:

- The setup of the extents of the model's analysis area (the domain);
- The setup of the variable resolution or density of the model's analysis grid points (the grid) within the domain; Balancing the selection of model domain and grid resolution is often a balancing act: higher resolution and larger domains may require increased computational resources and time.
- The calibration and validation of the model, which is a process of measurement and adjustment of the model's capability to recreate past events such that it can be trusted to predict future events.

Model Domain and Grid

The model domain (Figure 21) extends well beyond the area of interest to minimize potential interference of boundary conditions and to include external elements—such as riverine inflows—that are influential to the area of interest. The open domain boundary in the Gulf is located 100 km offshore of Port Fourchon. The subaqueous morphology component of the Morphology Model is simulated with the model grid (Figure 21) composed of approximately 113,000 grid cells. Grid cell resolutions are spatially varying, allowing for higher resolutions in areas of interest while keeping the number of grid cells elsewhere as low as possible to minimize computational burden. Resolutions range from 3.5 km in the offshore to 400 m in the nearshore and backbarrier. Higher resolution is used along the Caminada Headland with rectangular grid cells of 100 m in the longshore direction and 20 m in the cross-shore direction. Timbalier Island and East Timbalier Island have grid resolutions of 200 m in the longshore direction and 50 m in the cross-shore direction. These resolutions overlap one-on-one with the wave grids (Figure 22) used by the wave model (D-Waves) that was coupled online with the Hydrodynamics and Morphology models (D-Flow FM and D-Morphology).

The Hydrodynamics Model is used for simulations that are not coupled with waves or morphology, significantly reducing the computational burden. The model grid (Figure 23) consists of 350,000 grid cells and is an adapted version of the Morphology Model with higher resolutions in the back-barrier to enhance representation of hydraulic connectivity in tidal passes, bayous, channels, and canals. Significant portions of the Barataria-Terrebonne Basin have higher resolution with grid cell sizes of 100 or 200 m instead of 400 m as found in the model grid used for the Morphology Model. The focus area along the Caminada Headland, ranging from East Timbalier Pass in the west, and Caminada Pass in the east, and Leeville in the north, consists entirely of grid cells with a 50-m resolution.

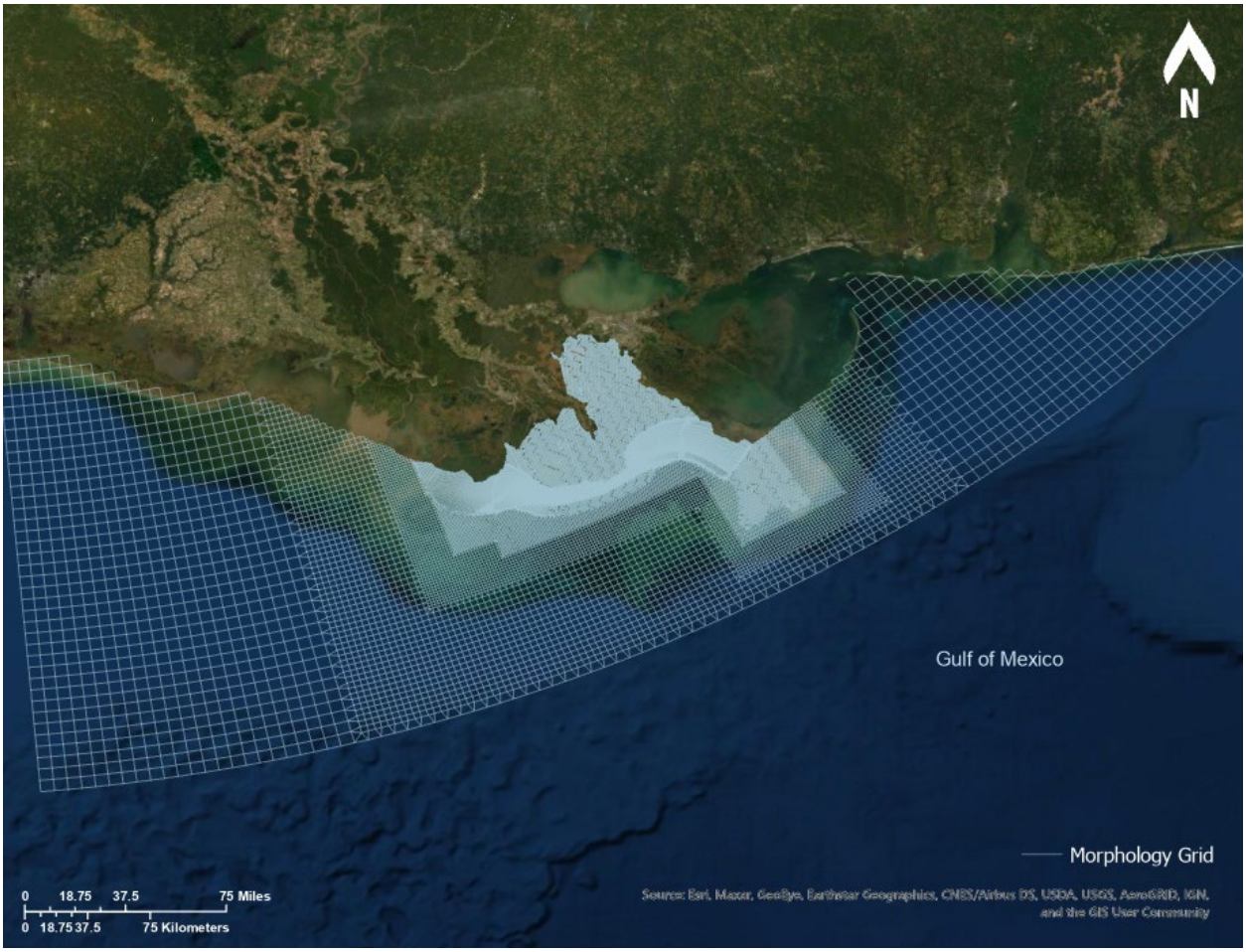

Figure 21. Delft3D FM domain and grid of the Morphology Model. Note the increased resolution within the area of interest.

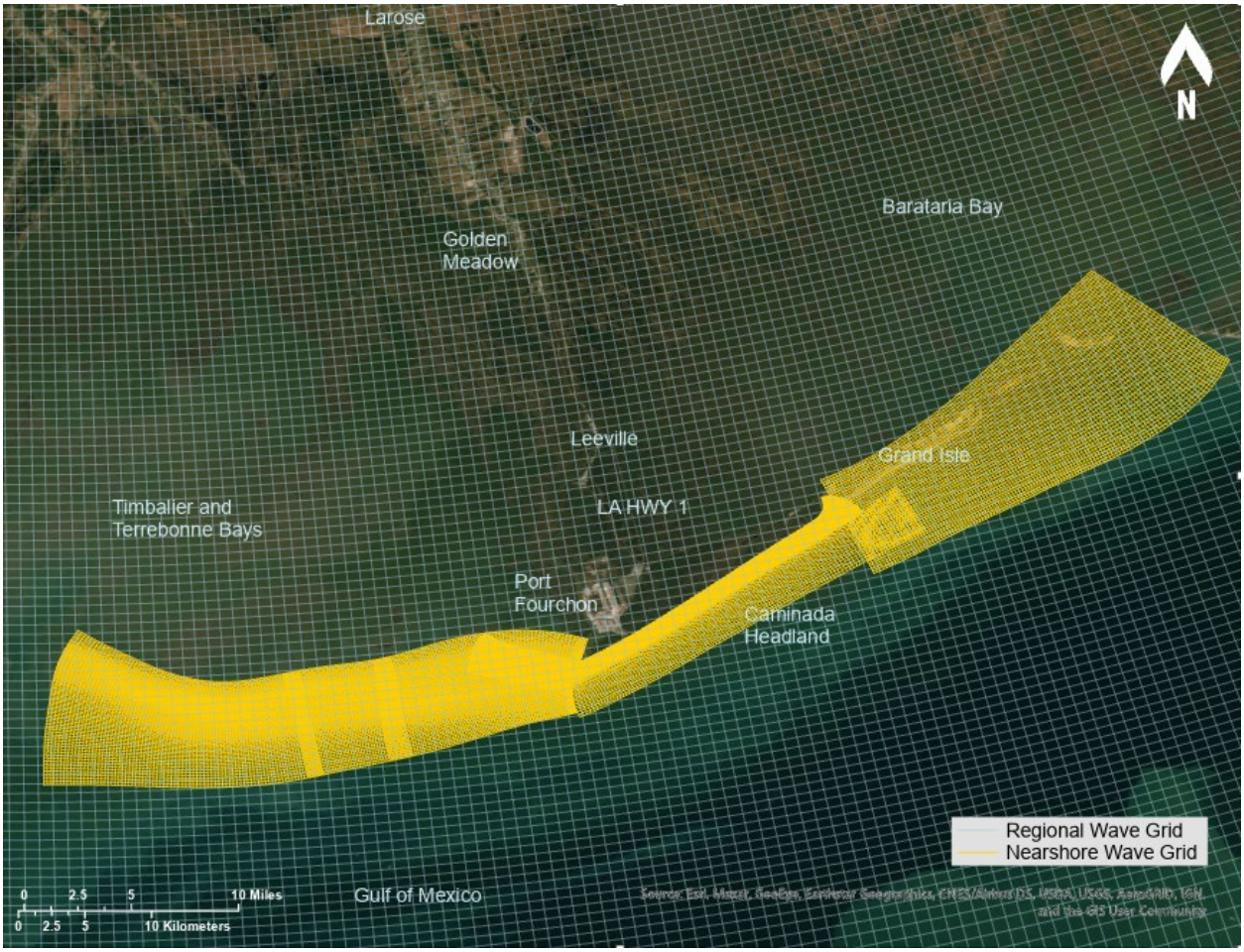

Figure 22. Nested wave grids used in Delft3D FM D-Waves (SWAN)

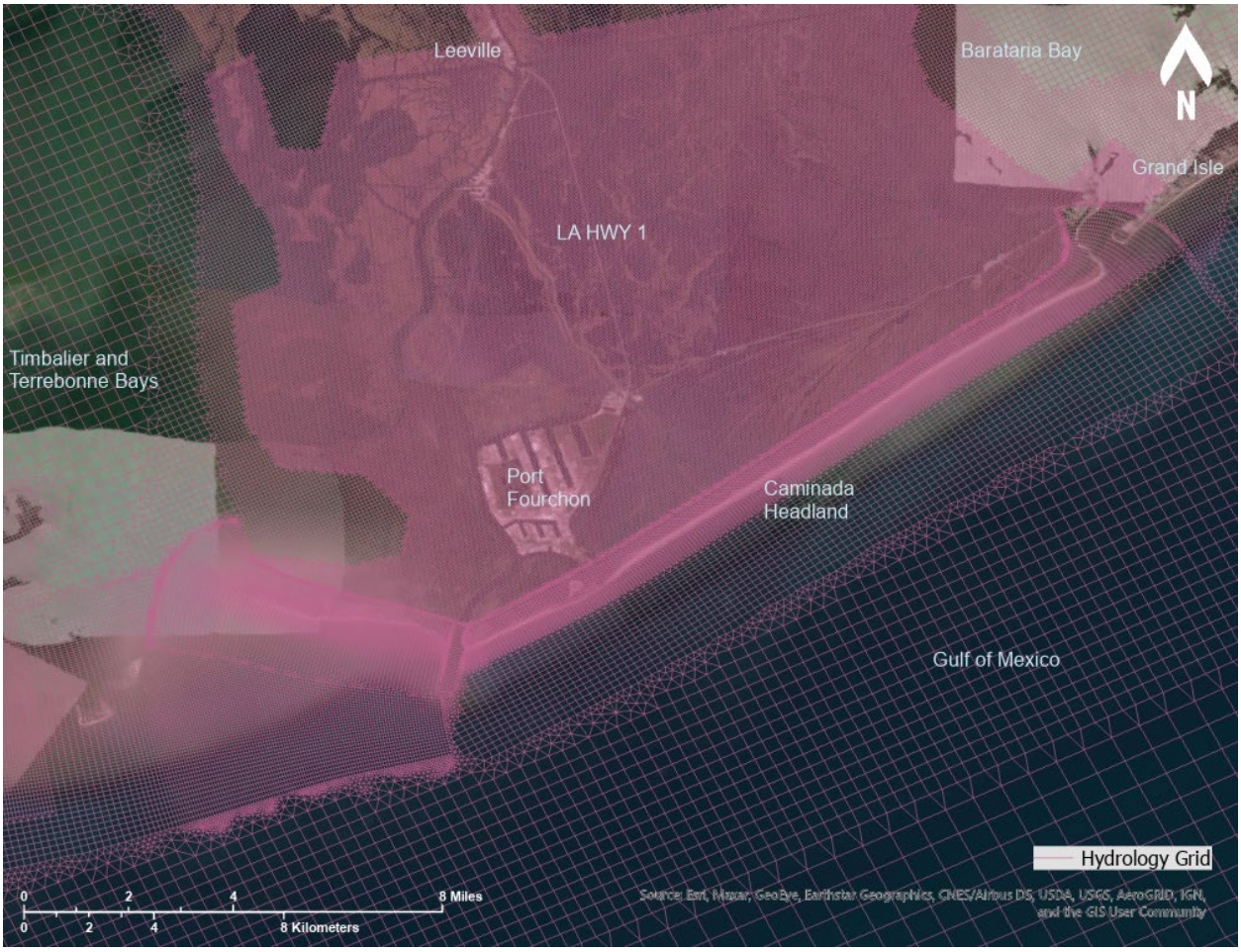

Figure 23. High-resolution Delft3D FM grid of the Hydrodynamics Model

Topography and Bathymetry

The topography and bathymetry used within the Coastal Systems Modeling Framework is based on the DEM from Byrnes et al. (2018). The bathymetry was supplemented by the U.S. Coastal Relief Model Vol.4 provided by NOAA (National Geophysical Data Center, 2001) for offshore areas that are not included in the DEM produced by Byrnes et al. (2018).

During inspection of the DEM, the Institute identified several waterways that appeared to be too shallow in the DEM (Figure 24). Based on open-source bathymetry datasets and expert judgement from ECG members, these waterways were classified into three categories based on the assumed depth: (a) 1-2 m, (b) 2-4 m, and (c) deeper than 4 m. The original depths of these waterways in the model grid were corrected with the assumed depth to prevent underrepresentation of hydraulic connectivity.

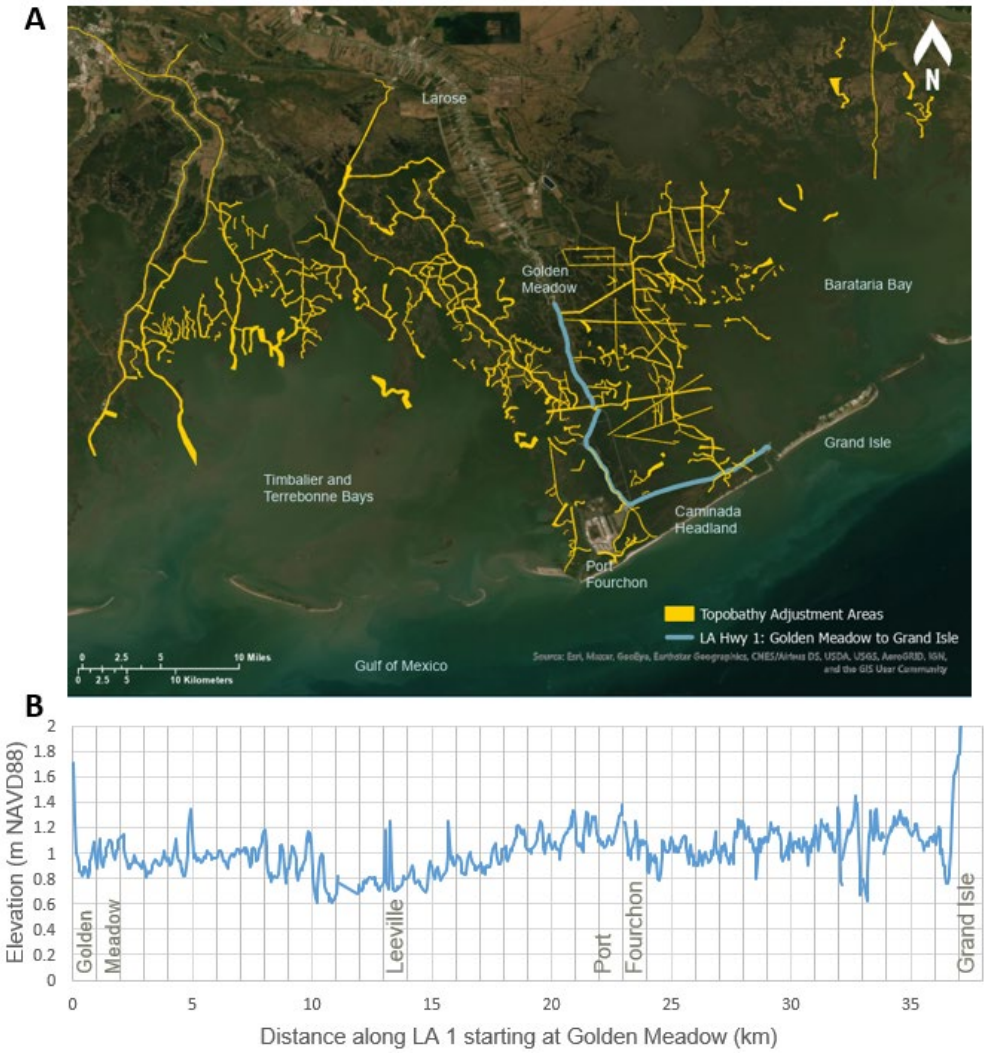

Figure 24. (A) Polygons indicating locations of waterways that are incorrectly or insufficiently represented by the DEM (orange), non-elevated portion of LA 1 (blue), and (B) the elevation profile of non-elevated sections of (old) LA 1 from Golden Meadow to Grand Isle

The non-elevated sections of LA 1 between Golden Meadow and Grand Isle, and the (non-elevated) old LA 1 between Leeville and Port Fourchon, had to be represented outside of the gridded topography because the road is typically too narrow to be resolved by the 50-m resolution of the model grid. Representing the highway position and elevation accurately is essential for the Storm Impact Model because it has the potential to influence the transmission of storm surge inland and between basins. Instead of elevating grid cells, a subgrid-scale polyline consisting of 6 sections was used (Figure 24). Each of these sections has a spatially varying crest elevation (Figure 24B) that allows for realistic overtopping if water levels exceed the local road elevation. The road elevation profile was kept the same from 2020 through 2050 landscapes.

Vegetation effect on flow velocity and bottom roughness were treated via the use of "trachytopes" in D-Flow FM, which locally enhance roughness based on vegetation parameters including vegetation height, stem diameter and stem density. These vegetation parameters were based on a 2014 land use land cover map with a 30 m resolution (Couvillion, 2017). A total of eight wetland vegetation taxa that represent five habitats in the model domain were considered (Table 12).

Table 12. Eight wetland vegetation taxa that represent habitats in the model domain.

Habitat	Dominant Wetland Vegetation Taxa
Fresh Marsh	*Sagittaria latifolia*, *Zizaniopsis miliacea*
Intermediate Marsh	*Typha* spp., *Phragmites* spp., *Sagittaria lancifolia*
Brackish Marsh	*Spartina patens*
Saline Marsh	*Spartina alterniflora*
Mangrove Forest	*Avicennia germinans*

Initial vegetation parameters (i.e., vegetation height, stem diameter and stem density) for each vegetation type and calibration settings in D-Flow FM were derived from Jung et al. (2019).

Offshore Boundary Conditions

The open domain boundary in the Gulf of Mexico, extending from 250 km south of Lake Charles, Louisiana, to Pensacola, Florida is forced by tidal conditions that were derived from the TOPEX/Poseidon Global database (Egbert & Erofeeva, 2002). Spatial variability in tidal conditions is accounted for by dividing the open boundary in 11 sections, each with a length of approximately 75 km, which are bounded by a total of 12 equidistant support points. A total of 13 astronomic tidal constituents (M2, S2, N2, K2, K1, O1, P1, Q1, MF, MM, M4, MS4, MN4) were extracted for each support point, of which K1, O1, P1, and Q1 are the most important because form the majority of the tidal amplitude. Interpolation between the support points is handled by the model to calculate the astronomic constituents for each grid cell along the open boundary. Additionally, the average seasonal cycle of mean sea levels in the northern Gulf of Mexico is incorporated to account for the effects of fluctuations in oceanic and atmospheric conditions on mean sea levels. The average seasonal cycle of mean sea level as provided by NOAA for the Grand Isle tide gauge (Figure 25) is superimposed on the tides and applied along the entire open boundary.

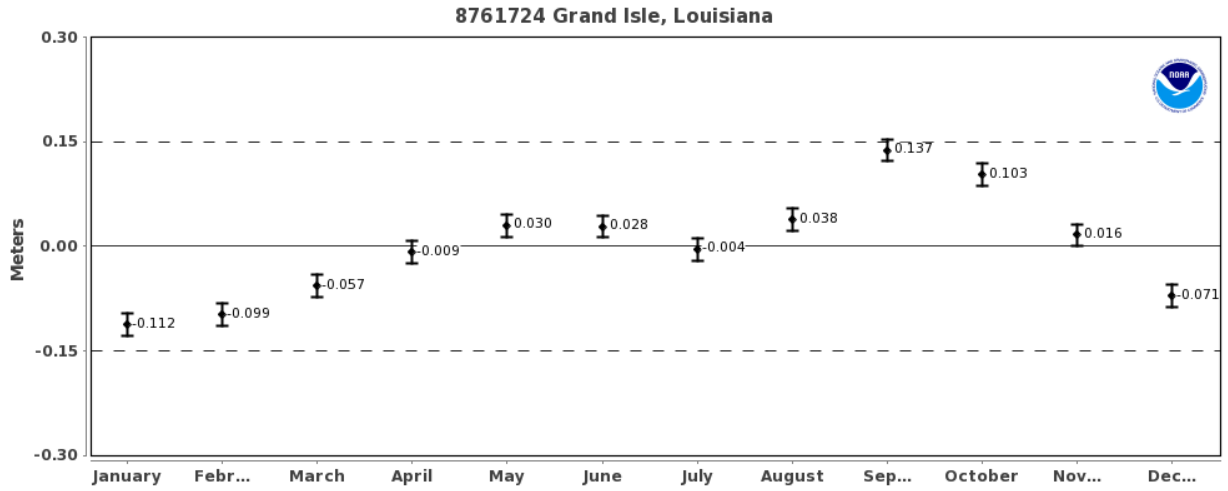

Figure 25. Average seasonal cycle of mean sea levels at Grand Isle (NOAA, n.d.). Note the seasonal variation in mean sea level varies by ~0.25 m during the year.

In addition to tidal conditions, salinity and temperature information is imposed at the offshore open boundary of the Hydrodynamics Model. Monthly average salinity and temperature values were derived from the Hybrid Coordinate Ocean Model Global Ocean Forecasting System 3.1 (HyCOM GOFS; National Ocean Partnership Program, n.d.) for each of the 12 support points along the offshore boundary. HyCOM GOFS also provided offshore current speed and direction.

Lastly, waves are imposed at the offshore boundary of the regional wave grid for simulations representing tropical storms as part of the Morphology Model and Storm Impacts Model to account for incoming waves that cannot be captured by local wave generation alone. Significant wave heights, wave periods, and wave directions are imposed every 20 minutes at the offshore boundary. The spatially varying boundary information is provided at 8 equidistant support points located along the boundary with a point-to-point distance of 40 km.

Riverine Boundary Conditions

The following freshwater inflows are included in the Hydrodynamics Model (Figure 26):

- Gulf Intracoastal Waterway (GIWW) west of the Houma Navigation Canal (HNC) – The discharge timeseries were generated by correlating the GIWW discharge west of HNC to the stage of the Lower Atchafalaya River at Morgan City, using measurements from Swarzenski and Perrien (2015). The following channels connect the GIWW with the Terrebonne Basin and are therefore represented by the grid:
    - Houma Navigation Canal
    - Bayou Petit Caillou
    - Bayou Terrebonne
    - Grand Bayou Canal

    - Bayou Lafourche
- Bayou Des Allemands (for which no discharge records are available) – Simulation output from CPRA's Integrated Compartment Model (ICM) from the 2017 CMP were used to compile a monthly discharge timeseries. This was done by correlating modeled discharges to precipitation in the local catchment area as observed during the simulation period.
- Davis Pond Diversion with discharges based on data of the local USGS station at this site (295501090190400).
- Naomi Siphon and West Pointe a la Hache Siphon with discharges based on records kept by CPRA.
- Mississippi River (at Venice) based on discharge data from the USGS station at Belle Chasse (07374525). A reduction of 20% was applied as a rough approximation of the loss of discharge between Belle Chasse and Venice caused by leakage through Mardi Gras Pass and passes in the Ostrica and Fort St. Philip area. The following passes and distributaries downstream of Venice are represented within the model grid:
    - Baptiste Collette
    - Cubit's Gap and Main Pass
    - Pass a Loutre
    - South Pass
    - Southwest Pass
    - West Bay Sediment Diversion
    - Grand Pass and Tiger Pass

The temperature timeseries of the freshwater inflows are based on USGS data of the nearest or most relevant station. All inflows originating from the Mississippi River use temperature information from the USGS station at Baton Rouge (07374000). The temperature timeseries of the GIWW and Bayou des Allemands inflows are based on USGS data at the GIWW in Houma (07381331).

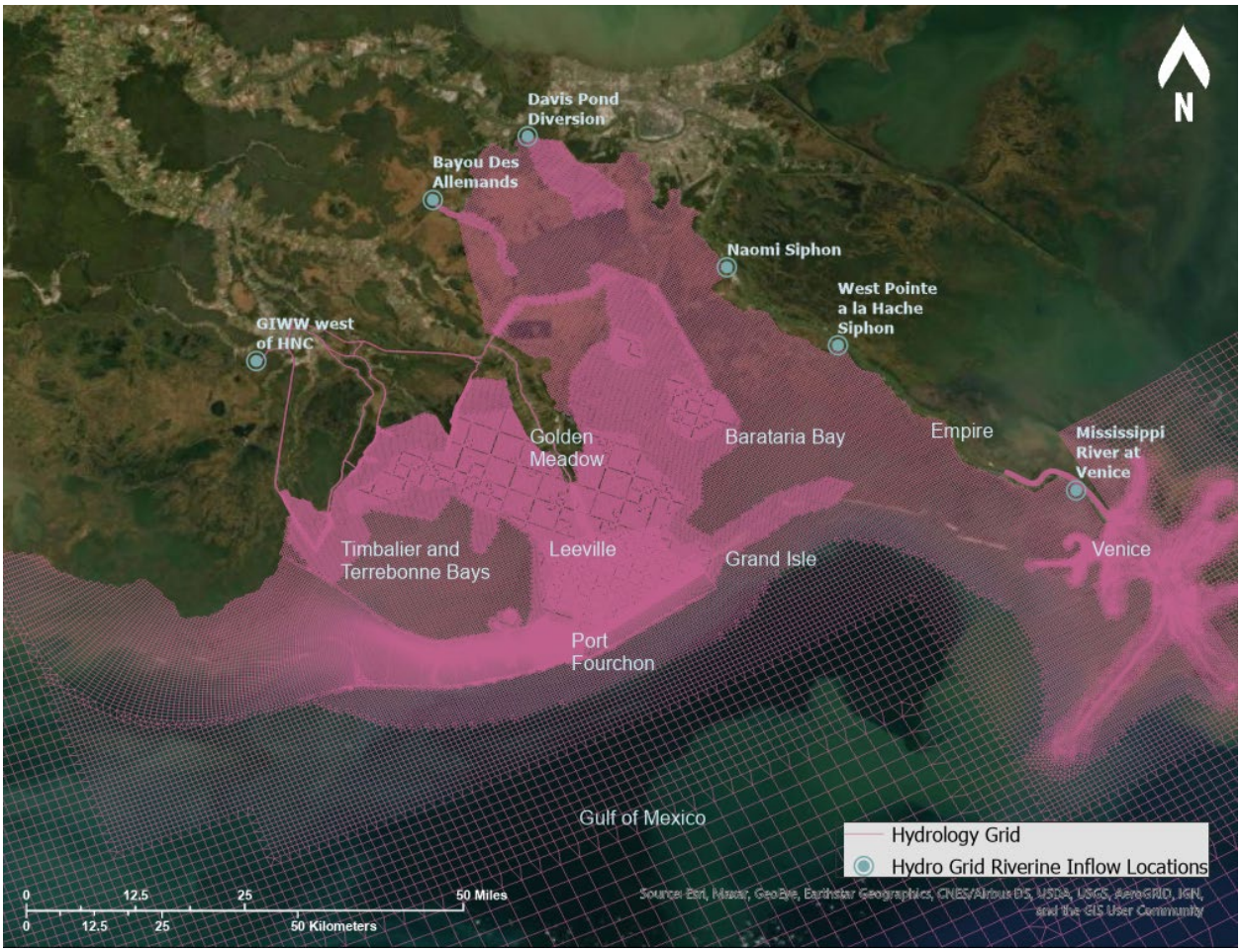

Figure 26. Locations of freshwater inflows in the Hydrodynamics Model. Note that for clarity that labels are omitted for additional connections between the Gulf Intracoastal Waterway (GIWW) and the Barataria-Terrebonne Basin. From west to east, these are the Houma Navigation Canal, Bayou Petit Caillou, Bayou Terrebonne, Grand Bayou Canal, and Bayou Lafourche.

Meteorological Inputs

Historical records of wind speed, wind direction, temperature and atmospheric pressure data were obtained from the National Data Buoy Center (NDBC) Grand Isle gauge for the period from 2005 to 2019. These data were used to develop wind forcings for quiescent periods and to choose representative cold front forcings. Each year was separated into the cold front season (October through March) and quiescent season (April through September). A statistical analysis was performed on the quiescent season data to find a 28-day period within the record that best represented the mean of the entire data record following the method of Cobell et al. (2020). The average cumulative distribution function (CDF) for the entire record, computed from the wind density function, was compared to the CDF calculated for a moving window of 28 days. The wind density function is the product of the mean wind speed for a given direction and the relative frequency of the wind blowing from this direction (Siegismund & Schrum, 2001). The magnitude of the difference between the two CDF's was used to rank the periods (Cobell et

al., 2020; Siegismund & Schrum, 2001). The period with the smallest difference (August 3, 2015, through August 31, 2015) was used to represent the quiescent periods in the model.

Individual cold fronts were identified using the method from Warner et al (2012). A cold front was defined as a low air pressure event accompanied by a drop in the temperature over 24 hours during the cold front season. The threshold for low air pressure was defined as two standard deviations below the mean for an air pressure record from 1948 through 2019 obtained from NOAA's National Centers for Environmental Prediction (NCEP)/National Center for Atmospheric Research Reanalysis 1 dataset (Kalnay et al., 1996; NCEP et al., 1994). To create the model forcings, identified cold fronts were categorized as weak, intermediate, and strong using the maximum wind speed within 12 hours of the air pressure low and the median and standard deviation of the cold front record. Cold fronts with maximum wind speeds within 1 standard deviation of the median were categorized as intermediate; strong and weak cold fronts were those with maximum wind speeds greater and less than the intermediate range, respectively. Each cold front was inspected visually for wind speed, wind direction, air temperature, and air pressure. A representative cold front from each category was chosen for the model forcing.

Data from the Grand Isle gauge are available at 20-minute intervals and were averaged to hourly data using the scalar average for wind speed and the unit vector average for wind direction (procedure as described by the NDBC; US Department of Commerce, 2018). The procedure used to address gaps in the Grand Isle record is described in Appendix A, as is the selection process for tropical cyclones.

Additional meteorological parameters are required to capture salinity and temperature within the Hydrodynamics Model, namely relative humidity, air temperature, cloud coverage, precipitation, evaporation, and solar radiation. Relative humidity, air temperature, cloud coverage, and precipitation are obtained from NOAA's NCEP/NCAR Reanalysis 1 Dataset (Kalnay et al., 1996; NCEP et al., 1994). Evaporation data from International Water Management Institute's World Water and Climate Data Atlas (International Water Management Institute, n.d.) is subtracted from the precipitation rate to obtain the excess rainfall boundary condition (Meselhe et al., 2015). Solar radiation is computed by D-Flow FM's composite heat flux model based on the latitude and longitude of the model grid.

Stratigraphy and Sediment Settings

The composition of the bed stratigraphy and selection of sediment fractions and properties is based on a review of available literature and datasets combined with expert judgement. A large number of scientific and engineering studies were reviewed to develop the bed stratigraphy and sediment classes (Ardaman & Associates, 2017, p. 20, 2018c; Eustis Engineering Services, LLC, 2015; Flocks et al., 2006; Fugro, 2018; Gahagan & Bryant Associates, Inc., 2013; GeoEngineers, 2010, 2017; Georgiou et al., 2019; GIS Engineering, LLC, 2019; Henry & Twilley, 2013; Kulp et al., 2002, p. 2002; Liu et al., 2018; Nyman et al., 1993; Wilson & Allison, 2008). Substantial simplifications are required to schematize the regional geology such that it is compatible with Delft3D FM's morphology component, D-Morphology, as used within the Morphology Model. A total of five sediment classes consisting of two non-cohesive (sand) and three cohesive classes (mud) were used in the model, shown in Table 13 with their characteristics.

Table 13. Sediment classes used in the Morphology Model

Sediment class	D50 (µm) (sand)	Grain Density	Dy bed density/bulk density	Settling velocity fresh water	Critical shear stress for erosion
Shoreface sand	130	2.65 g/cm^3	1.72 g/cm^3	(Calculated by model)	-
Beach sand	160	2.65 g/cm^3	1.72 g/cm^3	(Calculated by model)	-
Silt (cohesive)	-	2.65 g/cm^3	1.72 g/cm^3	0.0015 m/s	1.0 Pa
Clay (cohesive)	-	2.65 g/cm^3	1.72 g/cm^3	0.000025 m/s	1.0 Pa
Organic (cohesive)	-	1.14 g/cm^3	0.076 g/cm^3	0.00025 m/s	4.0 Pa

The initial bed stratigraphy of the Morphology Model included five unique sediment layers as listed in Table 14. The horizontal boundaries between these layers are visualized in Figure 27. Bed layer thicknesses were based on the elevation range of the corresponding stratigraphic unit (Table 14) and leveraged use of the spatially varying bed elevation of the DEM to establish spatially varying bed layer thicknesses. The bed stratigraphy consists of a muddy base layer below -1 m NAVD88 in the backbarrier and -3 m NAVD88 at the barrier and upper shoreface. Sediment units above -1 m NAVD88 in the backbarrier were assigned to brackish or saline wetland layers which consist of large amounts of organic sediments. Finally, sandy barrier island and upper shoreface layers were classified as very fine sand (130 µm) between -3 m and 0 m NAVD88 and fine sand (160 µm) if exist above 0 m NAVD88. The Morphology Model simulations were executed such that bed levels and compositions changed over time as a result of erosion and deposition of sediments.

Table 14. Sediment layers composing the bed stratigraphy of the Morphology Model

Sediment layer name	Shoreface sand (% by volume)	Beach sand (% by volume)	silt (% by volume)	clay (% by volume)	organic (% by volume)	Elevation range
Saline Wetland	14	0	42	24	20	Above -1 m NAVD88
Brackish Wetland	9	0	26	15	50	Above -1 m NAVD88
Bay and Lower shoreface	8	0	14	75	3	Below -1 m NAVD88 in bay, below -3 m NAVD88 at barrier and upper shoreface
Barrier Island	0	95	2.5	2.5	0	Above 0 m NAVD88
Upper Shoreface	85	0	7.5	7.5	0	Between -3 m and 0 m NAVD88

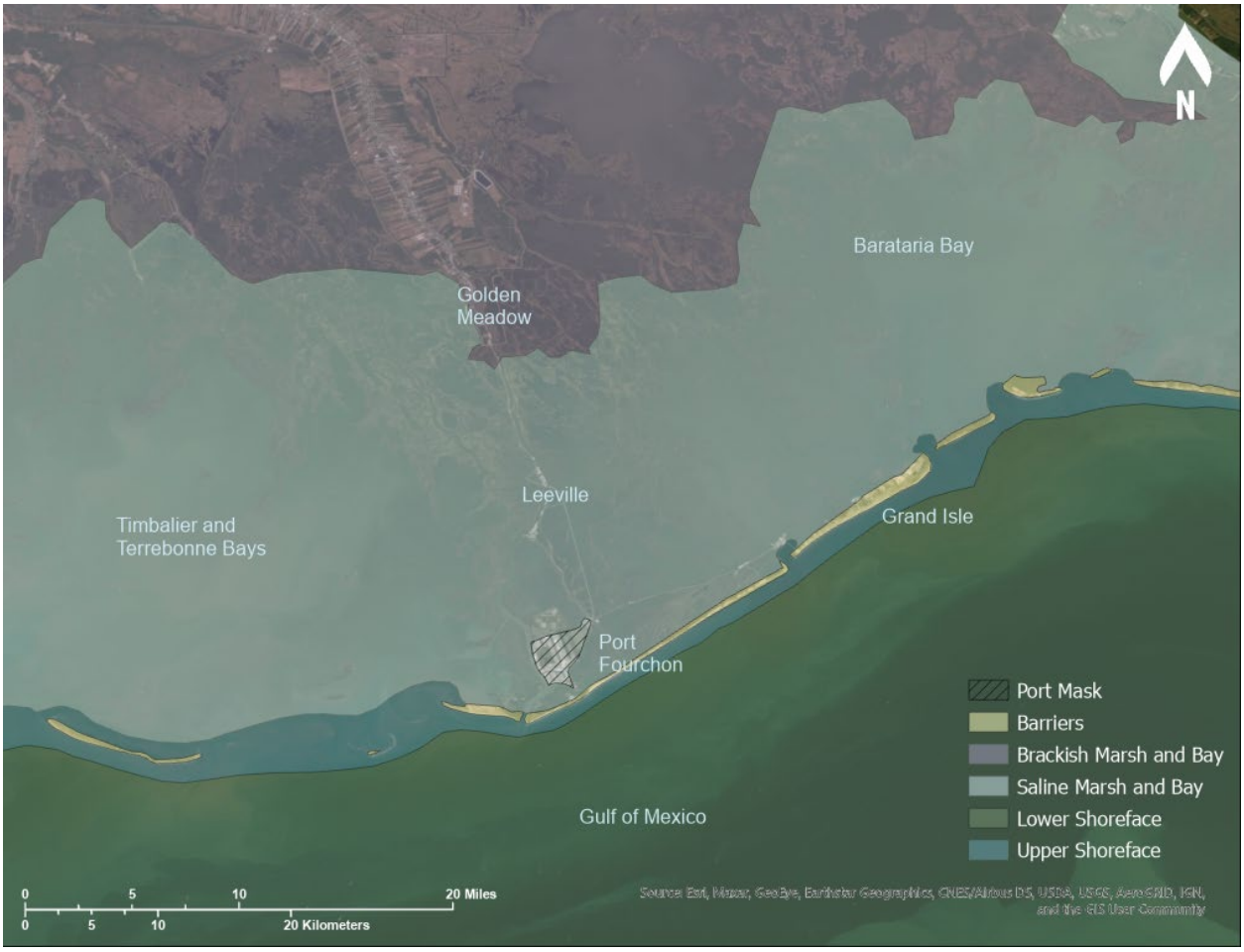

Figure 27. Spatial delineation of sediment layers. See Tables 13 and 14 for sediment layer classification by grain size. From north to south: brackish wetland (purple), saline wetland (teal), barrier (yellow), upper shoreface (blue), and lower shoreface (green).

Delft3D FM Model Calibration

Calibration of the Delft3D FM models was divided into multiple component: hydrodynamics, waves, morphodynamics, salinity, and temperature. Each component of the modeling framework required separate calibration as displayed in Table 15. For example, calibration of hydrodynamics is of relevance for all model components, but calibration of salinity and temperature only applies to the Hydrodynamics Model. Additional calibration figures and details are available in Appendix B.

Table 15. Applicability of calibration efforts for each of the Delft3D FM-based models that are part of the modeling framework

	Hydrodynamics calibration	Wave calibration	Sediment transport and morphology calibration	Salinity and temperature calibration
Hydrodynamics Model	x			x
Morphology Model	x	x	x	
Storm Impacts Model	x	x		

Hydrodynamics Calibration

The hydrodynamics calibration was focused on water levels that were analyzed for several calendar years and extreme events such as tropical cyclones Katrina and Rita, focusing on the representation of wind-driven water level set-up and set-down. Additionally, a tidal harmonic analysis was accomplished through decomposition of water level signals at various locations throughout the Barataria-Terrebonne Basin. This was done for modeled and measured water levels to validate representation of the modeled tidal signal across the entire basin. Lastly, flow velocities in tidal inlets, channels, and bayous, were inspected to ensure these fell within ranges that are typical for the area of interest based on hydraulic stability curves for inlets (Escoffier, 1940) and as reported in previous studies (Huang & Li, 2020).

Reference material and data consisted of water level data from open water (USGS, NOAA) and wetland (CRMS) gauges throughout the Barataria-Terrebonne Basin for calendar years 2015, 2016, and 2019. Water level data of tropical cyclones Katrina and Rita were obtained from measurements and previous results from the ADCIRC model (Cobell & Roberts, 2021).

Model calibration was performed through corrections in the model's input data and by adjustments of calibration parameters. Multiple corrections in the gridded topography and bathymetry were required to account for: 1) incorrect elevation data and 2) loss of hydraulic connectivity that resulted from interpolation of elevation data onto the model grid. Adjustments were made to the offshore water level boundary condition based on NOAA's records of monthly averaged water level fluctuations at Grand Isle, which are related to dynamics in ocean temperatures, salinities, winds, atmospheric pressures and oceanic currents (NOAA, n.d.). The representation of wind-driven water level set-up and set-down was improved by adjusting the model's wind drag coefficient. Lastly, a statistics analysis was performed to obtain a quantitative assessment of the model skill in terms of representing water levels at gauges for which measurements were available. This effort focused on open-water gauges in the Barataria Basin (Figure

28) because open water gauges in the Terrebonne and Timbalier Bays are scarce. The bias, Root Mean Square Error (RMSE), and correlation coefficient as shown in Table 16 were within acceptable range for coastal and estuarine systems based on guidance presented by Meselhe and Rodrigue (2013).

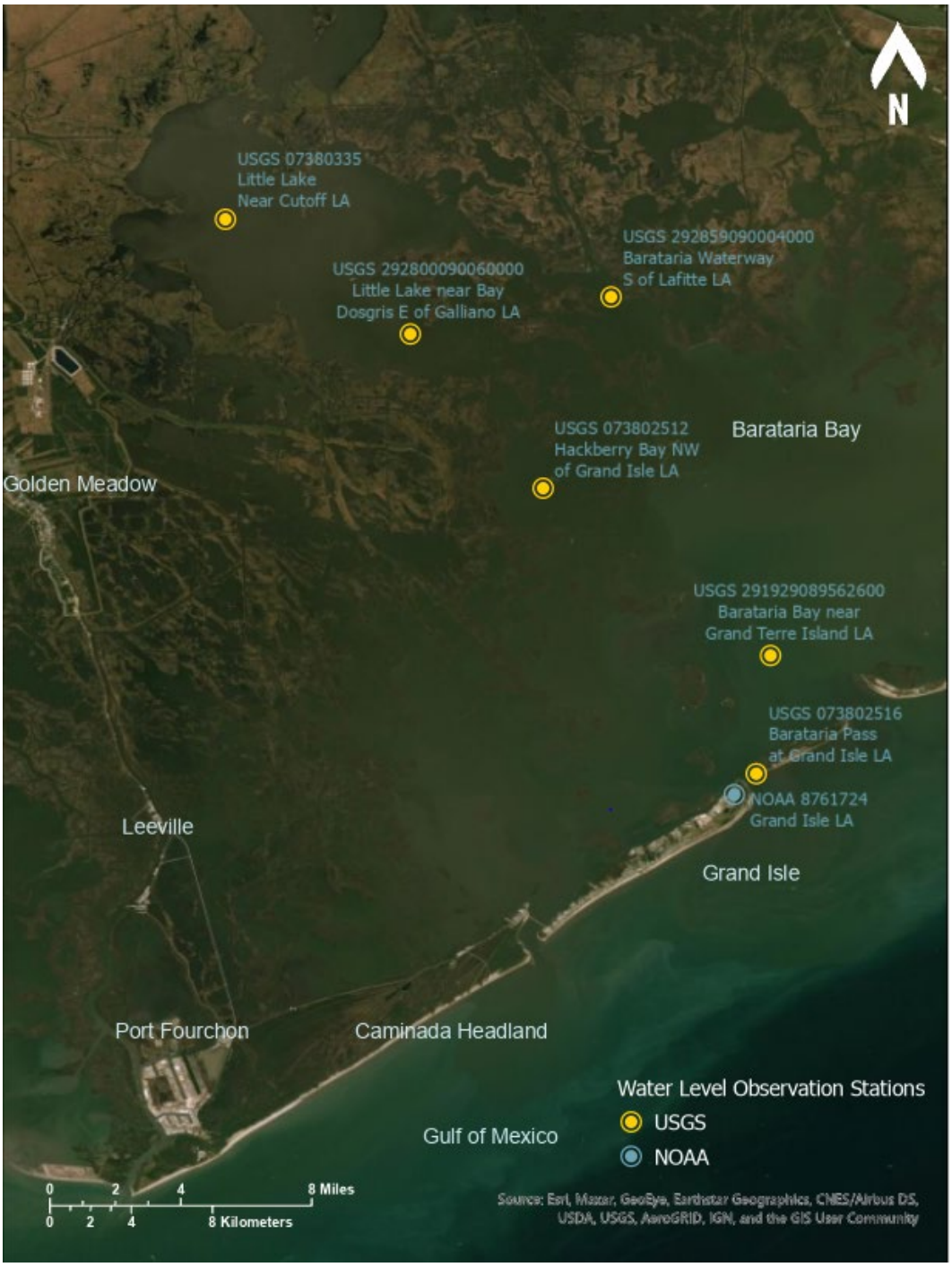

Figure 28. Location of USGS and NOAA stations used in the model calibration of water level

Table 16. Statistical analysis of model performance in representing water levels for the years 2015 and 2016

Station name	2015 (Jan-Dec)			2016 (Jan-Dec)		
	bias (m)	RMSE (m)	correlation coefficient R (-)	bias (m)	RMSE (m)	correlation coefficient R (-)
NOAA 8761724 Grand Isle LA	0.13	0.15	0.90	0.17	0.19	0.86
USGS 073802516 Barataria Pass at Grand Isle LA	-0.13	0.17	0.81	-0.06	0.12	0.83
USGS 291929089562600 Barataria Bay near Grand Terre Island LA	-0.01	0.09	0.85	-0.03	0.09	0.87
USGS 073802512 Hackberry Bay NW of Grand Isle LA	0.01	0.10	0.85	-0.02	0.09	0.86
USGS 292859090004000 Barataria Waterway S of Lafitte LA	0.00	0.09	0.86	-0.01	0.08	0.87
USGS 292800090060000 Little Lake near Bay Dosgris E of Galliano LA	0.00	0.11	0.79	-0.02	0.08	0.86
USGS 07380335 Little Lake Near Cutoff LA	-0.01	0.10	0.82	-0.02	0.07	0.90
AVERAGE	**0.00**	**0.11**	**0.84**	**0.00**	**0.10**	**0.86**

Wave Calibration

The wave model calibration assessed model skill in predicted wave heights during quiescent periods, cold fronts, and hurricanes Katrina and Rita. Additionally, visual inspection of combined (flow and waves) bed shear stresses along the shoreface, tidal inlets, and bays was conducted to ensure reasonable results.

Wave and water level instrument deployments near Port Fourchon conducted to inform restoration project design provided data in the offshore and in Timbalier Bay (Coastal Engineering Consultants Inc., 2016).

Sediment Transport and Morphology Calibration

Calibration of sediment transport focused on assessing sediment transport trends along the shoreface, tidal inlets, and back barrier bays. Morphology was calibrated by comparing erosional and depositional rates, trends, and patterns in the upper shoreface and bay floors.

Because the availability of reference material and data to calibrate sediment transport and morphology models is limited, morphology predictions were compared to previous studies of the geomorphic evolution of the Caminada Headland (Miner et al., 2009a). Model performance was assessed by visual inspection of maps showing sediment transport rates and bed level changes through a series of iterative model tests.

Calibration was performed through adjustment of sediment characteristics of cohesive classes (e.g, critical shear stress for erosion, settling velocity) and sand classes (e.g., median sand diameter), and by fine-tuning the horizontal and vertical delineation of the sediment (stratigraphic) layers.

Salinity and Temperature Calibration

Calibration of salinity and temperature typically involves investigation of the regional to local patterns and dynamics, from the nearshore areas of the headland throughout the entire Barataria-Terrebonne Basin. An important aspect of the calibration efforts was to obtain a correct representation of the discharge distribution from the Mississippi River into the distributary channels in the bird-foot delta, and from the GIWW into northern Terrebonne Basin.

Reference material and data consisted of salinity records from open water (USGS) and wetland (CRMS) gauges throughout the Barataria-Terrebonne Basin for calendar years 2015 and 2016. Additionally, visual comparisons were made between modeled salinity patterns and salinity maps from the Barataria Basin Hydrocoast Map Archives (Pontchartrain Conservancy, n.d.). Literature that was used during calibration consists of reports on the distribution of discharge in the Mississippi River's bird-foot delta (McCorquodale et al., 2010) and GIWW (Swarzenski and Perrien, 2015).

The salinity and temperature calibration approach consisted of two phases. First, adjustments were made to the bed elevation and roughness in the Mississippi River passes and distributary channels that connect GIWW with the Terrebonne Basin, to obtain a discharge distribution that is in line with findings of previously mentioned studies (e.g., McCorquodale et al. 2010; Swarzenski and Perrien (2015). Once that step was completed, adjustments were made to the horizontal eddy diffusivity coefficient to improve the model's ability to reproduce seasonal and interannual salinity patterns and dynamics. A statistical analysis was performed to obtain a quantitative assessment of the model skill in terms of representing salinity at gauges at or near open water where measurements were available in the Barataria-Terrebonne Basin (Figure 29). The bias, RMSE, and correlation coefficient of most gauges shown in Table 17 were within acceptable range for coastal and estuarine systems based on guidance presented by Meselhe and Rodrigue (2013).

Table 17. Statistical analysis of model performance in representing salinity for the years 2015 and 2016

Station name	2015 (Jan-Dec)			2016 (Jan-Dec)		
	bias (ppt)	RMSE (ppt)	correlation coefficient R (-)	bias (m)	RMSE (m)	correlation coefficient R (-)
CRMS0178	-0.5	4.6	0.51	0.2	3.6	0.54
CRMS0181	-0.7	4.1	0.88	-0.2	3.8	0.71
CRMS0224	-1.7	4.0	0.61	-1.7	3.4	0.59
CRMS0292	0.9	2.7	0.77	1.7	3.3	0.55
CRMS0338	-0.3	3.1	0.58	1.3	3.1	0.38
CRMS0341	-0.5	2.7	0.70	1.6	2.9	0.67
CRMS4690	-0.7	3.0	0.53	-1.0	3.0	0.48
USGS 291929089562600 Barataria Bay near Grand Terre Island LA	-1.6	4.6	0.81	-0.3	3.6	0.43
USGS 073802516 Barataria Pass at Grand Isle LA	-0.1	4.7	0.76	0.6	3.9	0.68
USGS 07380251 Barataria Bay N of Grand Isle LA	-2.5	5.3	0.69	-1.4	3.8	0.78
AVERAGE	**-0.8**	**3.9**	**0.68**	**0.1**	**3.4**	**0.58**

Figure 29. Location of USGS and CRMS stations used in the model calibration of salinity

PROJECT ALTERNATIVES AND ENVIRONMENTAL SCENARIOS

There was a total of six project alternatives and two environmental scenarios modeled. The wetland restoration project alternatives represent different potential locations or configurations for placement beneficially used dredged sediment produced during navigation channel deepening. For inclusion in the model, the alternatives were grouped into Alternative Grouping (AG) 2 and 3. AG 1 represents a Future Without Action scenario (FWOA). The environmental scenarios provide insight into project performance for two realistic possible climate futures.

PROJECT ALTERNATIVES

The list of proposed wetland restoration polygons was developed in consultation with community stakeholders. Virtual meetings were conducted during the 2020 COVID-19 pandemic to generate proposed project polygons with the ECG after participants were briefed by Institute staff members on constraints related to modeling limitations, the material composition of the borrow, and ongoing projects in the area where it was not necessary for them to propose further work (e.g., cohesive material not suitable for stacking on beaches or other tall features, not proposing in areas of active project construction, etc.). The analysis was guided by the ECG (stakeholders who are separate from the project's funders), the Kitchen Cabinet (a group of representatives from the POWC), federal agency stakeholders with ongoing projects in the area, and technical staff from the Institute. The complete list of project polygons and alternatives was developed collectively by the groups as follows:

1. The ECG was engaged virtually through which polygons of proposed wetland restoration were proposed on maps.
2. The Institute team then engaged with other stakeholders, including federal and state agencies involved with the CWPPRA program (namely NOAA, USEPA, USFWS, CPRA) after the ECG interactions to ensure other ongoing project proposal pursuits in the area were captured.
3. The Institute team then presented the summation of the proposed wetland restoration areas to the POWC Kitchen Cabinet, who provided comment and approval of the list to model.

From this list, the Institute team subdivided the proposed wetland creation polygons into six groupings of project alternatives (Figure 30) to be modeled and undergo cost estimation to serve a broader group of future stakeholders beyond the ECG (Figure 8), such as state and federal partner agencies. The alternatives in shown in Figure 30 include more polygons than were proposed by the ECG. These additional polygons were modeled to investigate a broader series of physical responses than those proposals undergoing the SROI analysis from the ECG. These project alternatives were generated through a combination of considerations, including geographic proximity, to limit project interactions during modeling simulation, as well as considerations on the amount of computational capacity, funding, and time available within this study's schedule. Figure 30 displays the six project groupings modeled under each of the two environmental scenarios. Polygon numbers are shown and were used for internal tracking purposes across various calculations such as costs, SROI, and carbon sequestration. Since the ECG was

only interviewed for the subset of proposals in Item 1 above, the arrangement of SROI analyses and reporting focuses only on those proposed wetland restoration areas proposed by the ECG (Figure 8):

- East of Fourchon – broad wetlands
- East of Fourchon – linear wetlands
- East of Fourchon – LA 1 fringe
- West of Port Fourchon
- Leeville – West of Bayou Lafourche

In cases where the ECG polygons differed from the six alternatives, project costs were applied on a cost-per-unit acre basis to the ECG derived areas for the SROI analysis.

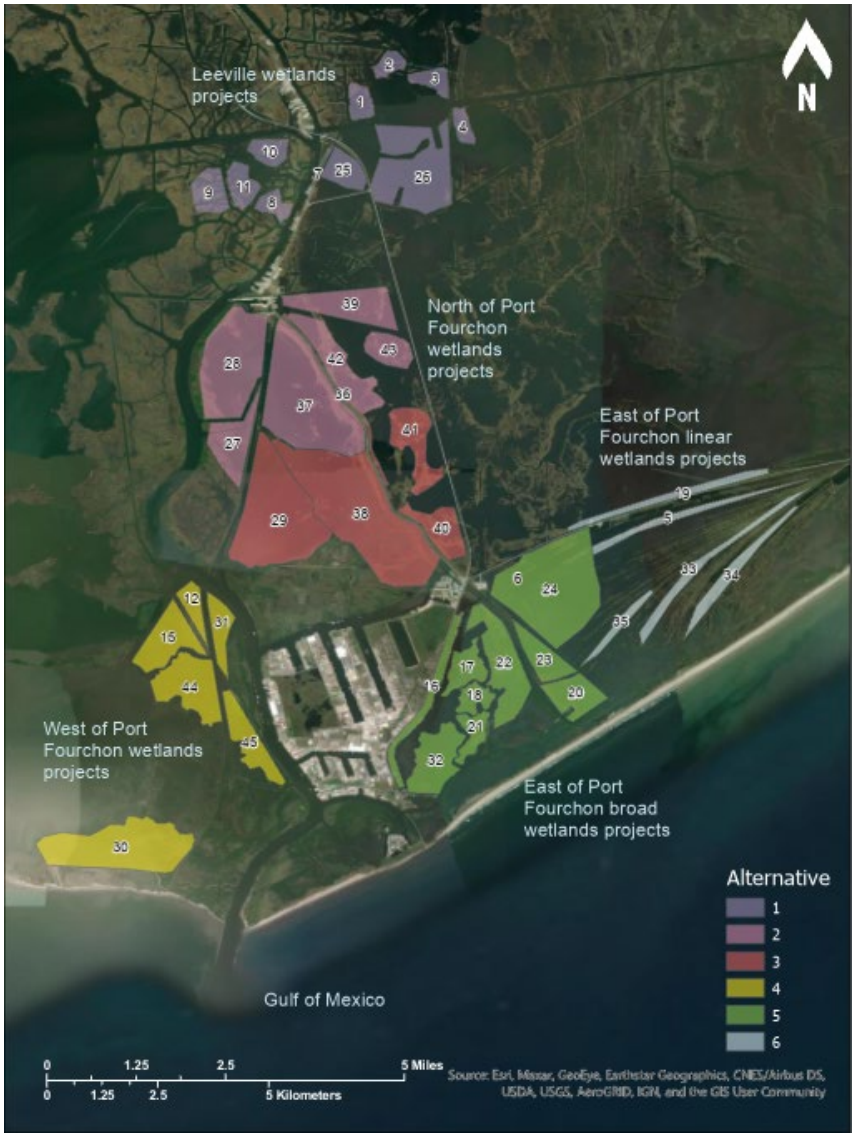

Figure 30. The six project alternatives used in the modeling and cost analysis

Although the six alternatives provide the basic level of naming for analysis and reporting, there are some key differences between the discussion of projects with regard to wetland vegetation and carbon, wetland morphology analysis, SROI analysis, and cost. Since the project list development occurred concurrently with stakeholder group feedback and comment on proposed projects as well as modeling analysis, some of the names used during the SROI interviews are different from those used in the morphological modeling:

- The ECG outlined several proposed project polygons to the south and west of Leeville, however, other CWPPRA project stakeholders suggested adding a former CWPPRA Phase I project's (East Leeville marsh creation, BA-0194) polygons east of Leeville to Alternative 1. Within the SROI discussion, the project grouping is focused on those polygons proposed by the ECG and referred to as the 'West Leeville' grouping (Figure 31).

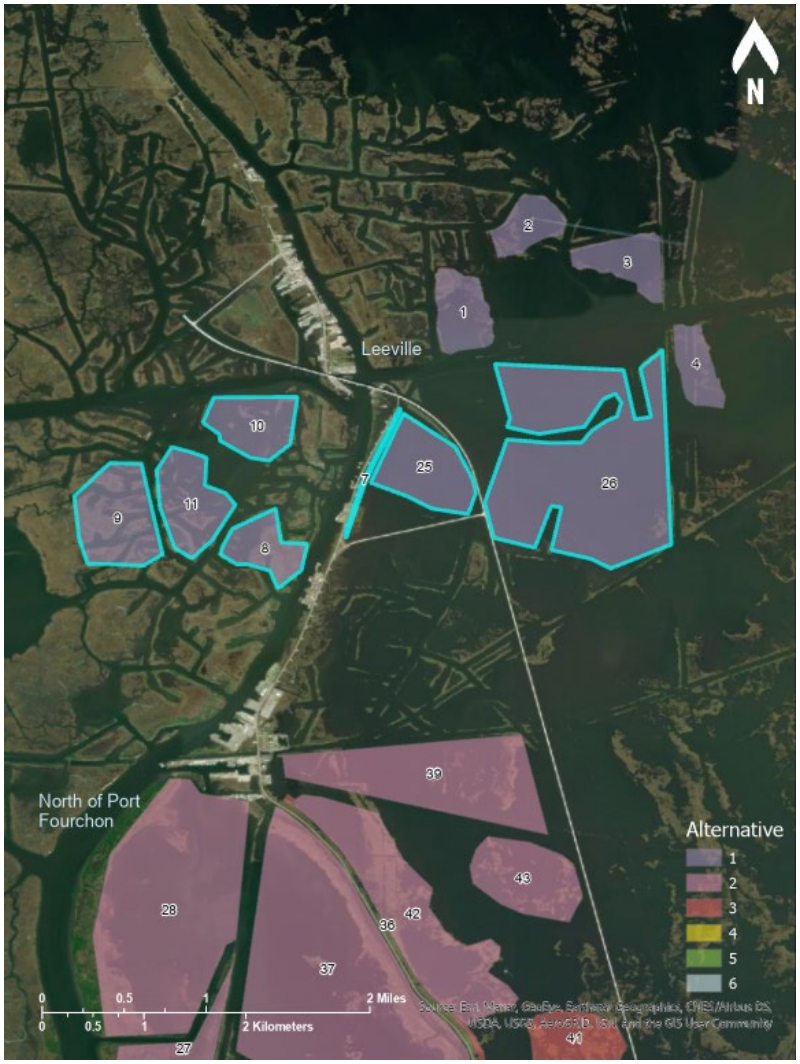

Figure 31. Alternative 1 polygons, with blue highlighted polygons representing the ECB-inspired project polygons and unhighlighted polygons representing those from the BA-0194 East Leeville CWPPRA Phase I project. This area is referred to as Leeville.

- Alternatives 2 and 3 were added by other stakeholders after the ECG had met to draw proposed projects. This group of polygons has been termed the 'North Fourchon' grouping (Figure 32).

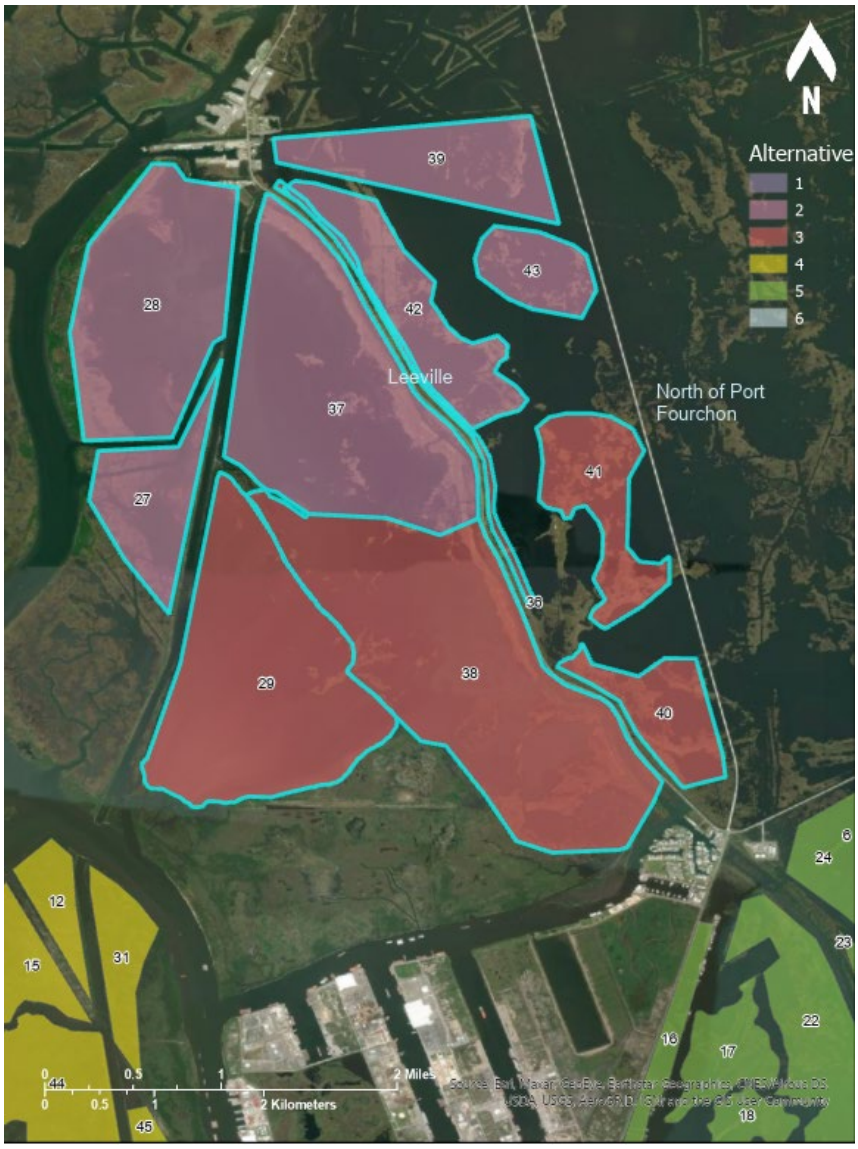

Figure 32. Alternative 2 and 3 polygons (highlighted in blue) developed after ECG interaction. This area is referred to as North of Port Fourchon.

Alternatives 5 and 6 also had various polygons which tended to be grouped in stakeholder discussion and have thus been termed 'East Fourchon' within the SROI analysis. ECG members had particularly negative reactions to one proposed project polygon, which is a strip of proposed wetland restoration near existing camps along LA Highway 3090 and was termed the 'Fourchon Fringe' project (Figure 33).

All results are grouped and presented geographically.

Figure 33. Alternative 5 East Fourchon Fringe polygon area (highlighted in blue) as discussed in the SROI analysis. This area is referred to as East of Port Fourchon.

ENVIRONMENTAL SCENARIOS

Two environmental scenarios were developed to evaluate the performance of the wetland restorations, a base case scenario and a less optimistic scenario (Table 18). Cold front and quiescent period forcings as well as the subsidence rate were the same for both scenarios. Cold front and quiescent forcings are described in the model framework section above. Spatially varying subsidence rates were derived from the deep subsidence values from Louisiana's 2023 CMP (Fitzpatrick et al., 2021). Deep subsidence values are highest Terrebonne Basin (7.6 to 9 mm/yr), lower in Barataria Basin (6.1 to 7.5 mm/yr) and lowest at Caminada Headland (3 mm/yr). Shallow subsidence values from the 2023 CMP were also applied (4 mm/yr).

The less optimistic scenario differed from the base case scenario for ESLR wetland accretion, and tropical storms. ESLR rates were chosen from Louisiana's 2023 CMP. Scenario S07-RCP 4.5 NOAA Intermediate Regionally Adjusted was used for the base case scenario, and scenario S08-RCP 8.5 NOAA Intermediate-High Regionally Adjusted was used for the less optimistic scenario (White et al., 2021). Both scenarios describe nonlinear rates of SLR. At 2030, the sea level described by Scenario S08 is only 0.025 m greater than Scenario S07; however, by 2050, Scenario S07 results in 0.25 m of ESLR, while Scenario S08 results in 0.36 m of ESLR.

In the base case, wetlands accrete at a rate equal to subsidence plus ESLR; the result is wetlands that maintain their elevation with respect to sea level. For the less optimistic scenario, wetlands accrete at a rate 2 mm/yr less than subsidence plus ESLR; the result is wetlands that slowly lose elevation with respect to sea level. These two scenarios were chosen to represent the uncertainty in the long-term ability of wetlands to maintain elevation with rising sea levels (Jankowski et al., 2017; Keogh et al., 2021; Kirwan et al., 2016; Törnqvist et al., 2020, 2021a).

A 30-year sequence of synthetic tropical storm events was generated that accounts for storm intensity and frequency, extending the same methodology as used for the 2023 CMP (Johnson & Geldner, 2020). This sequence includes storms of varying intensity and distance to the study area. Storms that were unlikely to overwash or inundate (Sallenger Jr., 2000) the barrier islands in the study area were removed from the sequence to reduce model runtime. To create a stormier sequence for the less optimistic environmental scenario, storms with lower total water level impacts along the coast in the study area were replaced with storms that had greater total water level impacts. The resulting storm sequence maintains the number of storms between the two scenarios, while increasing the storm energy that impacts the study area. Detailed methods descriptions can be found in Appendix A.

Table 18. Comparison of modeled environmental scenarios.

Environmental Scenario	ESLR	Accretion	Storm Choice
Base Case	S07-RCP 4.5 0.25 m at 2050	Keeps up with SLR	Lower Energy
Less Optimistic	S08-RCP 8.5 0.36 m at 2050	Lags SLR by 2 mm/yr	Higher Energy

Table 19. The six Production Runs

Production Run	Project Grouping	Environmental Scenario
PR1	AG1; Future Without Action	Base Case
PR2	AG2; Alternatives 4 and 5	Base Case
PR3	AG3; Alternatives 1, 2, 3, and 6	Base Case
PR4	AG1; Future Without Action	Less Optimistic
PR5	AG2; Alternatives 4 and 5	Less Optimistic
PR6	AG3; Alternatives 1, 2, 3, and 6	Less Optimistic

RESULTS

This section describes modeling results. It also has a subsection which describes the strengths, limitations, and uncertainties inherent in the modeling, as well as certain implications as to how these factors relate to the interpretation of results. All of the modeling results are summarized in this section and are described in two ways:

- Regional results, which are broad, basin-scale responses that are either model predictions which occur in the FWOA simulations or are independent of the implementation of any single proposed wetland restoration alternative.
- Project-specific results, which are directly caused by the implementation of a wetland restoration alternative.

COASTAL SYSTEMS MODELING FRAMEWORK

The results from the Coastal Systems Modeling Framework's simulation of coastal system dynamics and evolution through year 2050 are presented at two different scales: 1) regional or basin-scale (i.e., Terrebonne and or Barataria basins) modeling and analysis results and 2) local results in the vicinity of the proposed restoration project alternatives.

Model Strengths, Limitations, and Uncertainties

Deterministic numerical models are frequently used to help forecast how natural systems would evolve or respond to various environmental forcings over time. All models are a simplified representation of actual processes. While models offer a reasonable prediction of a system's response to external drivers, results have limitations and uncertainties that depend on model setup, choice of initial conditions, selection of coefficients and constants during model calibration, implementation of boundary conditions, parameterization of processes, and theoretical formulations. Knowledge and awareness of these limitations are essential when interpreting model results.

The strengths of the Coastal Systems Modeling Framework include the use of state-of-the-art models for essential hydrodynamic, sediment transport, and wetland processes, employing fully coupled procedures. The model integration, interaction, sequencing, and feedback between all modeling elements also constitute a strength and as discussed previously, incorporate flexible, efficient, and robust methods. The Coastal Systems Modeling Framework is sufficiently vigorous and reproduces surface processes operating on the shoreface, the shelf, inland back-barrier bays, and wetlands. As such, the Coastal Modeling Framework simulates the overall landscape evolution of the basin well.

All numerical models have limitations. There are several ways to evaluate or quantify some of the limitations; this can be conducted using model skill or through an exhaustive matrix of sensitivity simulations. Models also have uncertainties, related to their inputs, and assumptions that were used in the model setup and development. This section outlines limitations and uncertainties for this application of the Modeling Framework.

Evolution of coastal shorelines in sandy systems and wetland systems are implicitly complex. Accurate simulation of shoreline evolution in sandy systems relies on inclusion of all processes governing the morphology of beaches, berms, and dunes, operating at timescales of minutes to decades. The Coastal Systems Modeling Framework used here can simulate the overall shoreline position, but lacks the non-linear wave-current interaction and the nearshore processes necessary to capture more complex coastal interactions that would improve predictions of short-term response to storms. This includes barrier breaching, dune over washing and the role of infragravity waves on beach and dune morphology. Moreover, the Coastal Systems Modeling Framework lacks recovery processes following storms, which control the gradual recovery of beaches, aeolian processes that rebuild dunes, and together return the shoreline to a more robust state. The lack of recovery processes also hinders accurate prediction of barrier retreat. For example, the model correctly predicts trends of barrier retreat but lacks the complexity to reproduce historical rates of barrier retreat over the long term.

Another limitation in the Coastal Systems Modeling Framework is related to Belle Pass, the channel geometry, and the lack of maintenance dredging operations. Without dredging, model predictions are less accurate, and they tend to underestimate future channel depth. Limitations also exist in the way the projects were evaluated, and specifically the approach to project groupings. It was not computationally feasible to evaluate all projects individually and as such, projects were evaluated as three separate groups. This approach may underestimate individual project performance, or disguise project low performance if grouped with projects that dominate the benefit.

The Coastal Systems Modeling Framework and its component models also have uncertainties. As is the case with other predictive models, assumptions and hypotheses are made to inform model inputs when attempting predictions for the next 30 years. There is uncertainty in those assumptions because conditions in the future may not occur as assumed. Some examples of assumptions include subsidence, ESLR, wind patterns, rainfall, the frequency and magnitude of winter storms, and tropical cyclones. In addition, the type of wetland vegetation or the area of wetlands converting to open water may not occur as assumed. Any departure from the assumed conditions will influence the results.

While many of the necessary physical processes that govern landscape evolution are included in, and simulated by the Coastal Systems Modeling Framework, some processes are not fully represented in the framework. The lack of inclusion is either due to limited data to initialize or calibrate the models, knowledge gaps related to the underlying processes, or complexities in the spatiotemporal variability of the processes. Some examples of processes that are not included are bank erosion from vessel traffic in navigable channels, complexities and feedbacks with future wetland vegetation growth and decay processes, more comprehensive feedbacks between processes that contribute to marsh accretion (which is solely dependent on SLR in the model), and more comprehensive global-scale climate perturbations. Future climate predictions are uncertain, and as such further influence uncertainty related to many of the processes within the Coastal Systems Modeling Framework. For example, the assumptions of accretion processes in the Morphology Model to keep up/not keep up with RSLR while consistent with historical observational data, lack the ability to predict changes in marsh response that might occur as a result of future conditions such as the fertilization effect to wetland vegetation with increased atmospheric CO_2, higher air and water temperatures that can influence growth and decomposition processes, less frequent

freeze events, or altered nutrient loads. Additionally, the majority of the observational data upon which the marsh accretion model developed for this study are based are from temperate locations with high tidal range. In warm locations with low tidal range, such as Louisiana, soil organic production and resulting wetland accretion might be less dependent on RSLR. This remains an important and open research question.

Simulating these processes requires complex parameterization and comprehensive field data that is largely beyond the capabilities of any existing modeling software that attempts long-term morphology change at this spatial scale. Nevertheless, these processes can improve long-term landscape evolution, and they are essential when attempting forecasts at multi-decadal timescales.

Regional Results

Comparing the FWOA model results for 2020 and 2050 helps to better understand and give context to the landscape changes around Port Fourchon at a regional scale. Results are discussed for hydrodynamics, salinity, morphology, and habitat area changes.

Hydrodynamics and Salinity

Water Level and Tidal Prism

Hydrodynamics in the Barataria-Terrebonne Basin are influenced by the changes in topography and bathymetry as predicted by the Morphology Model, which includes the effect of RSLR. Predicted water levels (Figure 34) show an overall increase over time. Commensurate with the gradual increase of water levels, tidal amplitudes (range) in the Terrebonne and Barataria bays also increase. Figure 34 shows an increase in tidal range during the month January noting varying magnitude of change for neap to spring tide conditions. After harmonic analysis (a method that decomposes all the components of the tidal signal) is performed for an entire year of simulation, the model predicts that tidal range will increase by 30% in Barataria Bay and approximately 15% in Terrebonne Bay by 2050 (Table 20). Changes in tidal phase between the base environmental scenario and other alternatives are shown in Table 21. Tidal phase changes for the dominant harmonics from 2020 through 2050 are of the order of 3-7 degrees, suggesting that the time to high tide by 2050 will differ by up to 28 minutes compared to 2020. The water level differences in these simulations, between the 2020 and 2050 landscape simulations, are due to changes in topography, bathymetry, and mean sea-level, and do not reflect additional potential changes due to meteorology or inflow of freshwater. Figure *35* depicts the locations of the analysis found in Figure 34, Table 20, and Table 21.

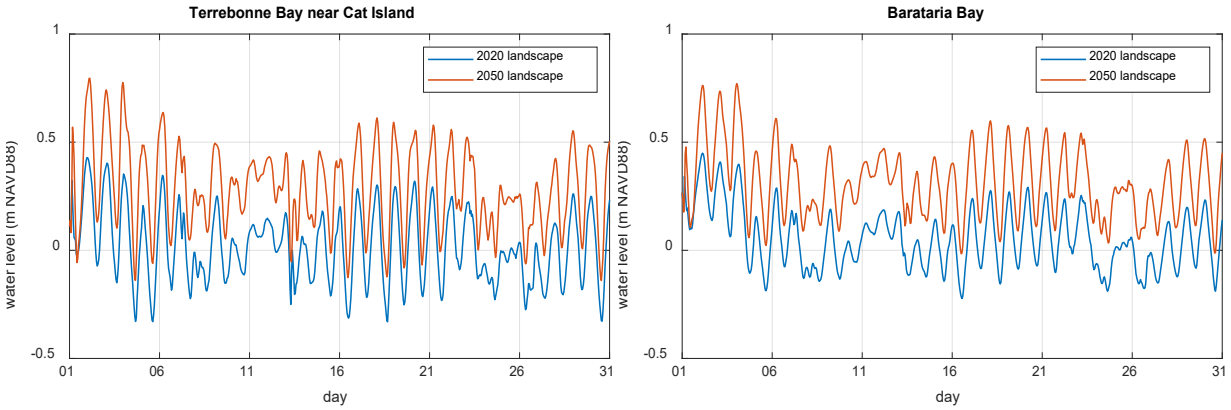

Figure 34. Instantaneous water levels during the month of January for Terrebonne Bay (left) and Barataria Bay (right) for the 2020 and 2050 landscape and for the base case environmental scenario (FWOA). Locations for these measurements are indicated in Figure 35. Model results show an increase of mean sea level from 2020 to 2050 of approximately 0.25 m, as well as increase in tidal range for neap and spring conditions.

Table 20. Tidal amplitudes (m) for various alternatives in the 2020 and 2050 landscapes for the base case environmental scenario. This table only lists the constituents (Q1, O1, P1, K1) that had amplitudes larger than 1 cm, and are dominating the tidal signal. Tidal harmonic analysis was performed using T_TIDE (Pawlowicz et al., 2002)

Tidal amplitude in meters		**2020 landscape**			**2050 landscape**		
Location (Figure 35)	**Tidal constituent**	FWOA	AG2 (Alternatives: 4,5)	AG3 (Alternatives: 1,2,3,6)	FWOA	AG2 (Alternatives: 4,5)	AG3 (Alternatives: 1,2,3,6)
Barataria Bay	Q1	0.02	0.02	0.02	0.03	0.03	0.03
	O1	0.09	0.09	0.09	0.12	0.12	0.12
	P1	0.03	0.03	0.03	0.03	0.03	0.03
	K1	0.10	0.10	0.10	0.12	0.12	0.12
	Sum of Q1, O1, P1, K1	**0.23**	**0.23**	**0.23**	**0.30**	**0.30**	**0.30**
Terrebonne Bay near Cat Island	Q1	0.03	0.03	0.03	0.03	0.03	0.03
	O1	0.13	0.13	0.13	0.15	0.15	0.15
	P1	0.04	0.04	0.04	0.05	0.05	0.05
	K1	0.14	0.14	0.14	0.16	0.16	0.16
	Sum of Q1, O1, P1, K1	**0.34**	**0.34**	**0.34**	**0.39**	**0.39**	**0.39**
Bayou Lafourche at Port Fourchon	Q1	0.03	0.03	0.03	0.03	0.03	0.03
	O1	0.13	0.13	0.13	0.14	0.14	0.15
	P1	0.04	0.04	0.04	0.04	0.04	0.04
	K1	0.13	0.13	0.14	0.15	0.15	0.15
	Sum of Q1, O1, P1, K1	**0.33**	**0.33**	**0.34**	**0.37**	**0.37**	**0.38**

Table 21. Tidal phases (degrees) for various alternatives in the 2020 and 2050 landscapes for the base case environmental scenario. Tidal harmonic analysis was performed using T_TIDE (Pawlowicz et al., 2002).

Tidal phases in degrees		2020 landscape			2050 landscape		
Location (Figure 35)	**Tidal constituent**	FWOA	AG2 (Alternatives: 4,5)	AG3 (Alternatives: 1,2,3,6)	FWOA	AG2 (Alternatives: 4,5)	AG3 (Alternatives: 1,2,3,6)
Barataria Bay	Q1	37	37	37	29	29	29
	O1	53	53	53	47	47	47
	P1	60	59	60	53	53	53
	K1	59	59	59	53	53	53
Terrebonne Bay near Cat Island	Q1	18	18	18	14	13	13
	O1	35	35	35	32	32	32
	P1	40	40	40	37	37	37
	K1	41	41	41	38	38	38
Bayou Lafourche at Port Fourchon	Q1	6	6	4	9	9	7
	O1	23	22	20	26	26	24
	P1	27	27	25	31	31	29
	K1	29	29	27	33	33	31

Figure 35 Locations of water level and salinity analysis in Barataria and Terrebonne Bays, LA.

The expansion of open water area associated with wetland erosion and gradual basin submergence increases the tidal prism, which is the total volume of water that enters and exits the tidal inlets during each tidal cycle (consisting of the flood and ebb tides between the Barataria-Terrebonne basin and the Gulf of Mexico). This increase in tidal prism is not only due to increase in bay area but also the loss of marsh islands and land bridges within the lower and central basin that help to attenuate the tidal wave as it propagates to the upper basin. The increased discharge at the inlets associated with increasing tidal prism also results in wider, deeper inlets and increased volumes of sediment stored offshore in ebb tidal deltas that would otherwise contribute to more robust barrier islands. The increase of tidal amplitudes is apparent when comparing the tidal prism of the Barataria-Terrebonne Basin between the 2020 and 2050 landscapes (Figure 36) as well as increasing instantaneous discharge at the tidal inlets (Figure 37 and Figure 38). The increase in tidal discharge peaks is readily apparent for the 2050 landscape during spring tides, with larger discharge excursions generated by subtidal events such as cold fronts, indicating that the basin is predicted to become increasingly influenced by the Gulf in the future. A summary of present (2020) and predicted (2050) tidal prism is presented in Table 22 and Table 23. The analysis for the results presented uses the annual hydrodynamic simulations and reflect the average tidal prism for the Barataria-Terrebonne Basin. Model results show an increase in tidal prism from 2020 to 2050, reflecting the instantaneous increase in tidal inlet discharge (Figure 36) with an increase of approximately 52% for Barataria Basin, 39% for Terrebonne Basin, and approximately 17% for Belle Pass near the entrance to Port Fourchon. Across alternative groups (AG) of projects (Table 24) tidal prism decreases appreciably for tidal inlets proximal to the AG cluster. For instance, Belle Pass is influenced the most due to proximity, exhibiting tidal prism decrease across AG of the order of 4-10% (±2%), while the remaining tidal inlets show a negligible influence across AG.

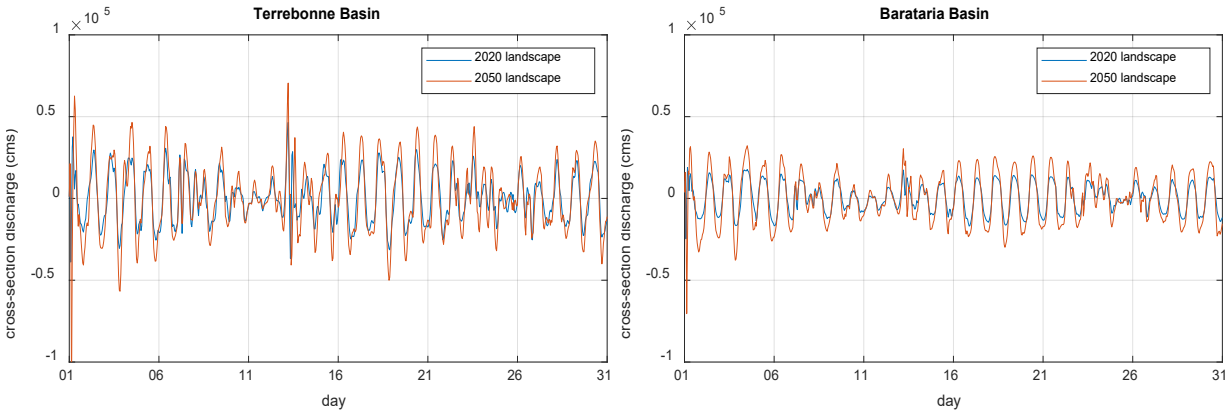

Figure 36. Instantaneous discharge for the Terrebonne Basin (left) and Barataria Basin (right) during the month of January for the 2020 and 2050 landscape and for the base case environmental scenario (FWOA). Model results show that both basins experience an increase in tidal prism by 2050, as evidenced by the increase in the flood (positive) and ebb (negative) flows. Note that the difference in the peak magnitude between 2020 and 2050 is not constant across spring and neap conditions, and neither is the difference between flood and ebb peaks. Refer to Figure 16 for the location of the basins and to Figure 37 and Figure 38 for the location of the cross sections along which these measurements were extracted from model output. Model output data are in Table 22, Table 23, and Table 24.

Table 22. Tidal prism (millions of cubic meters) for alternatives groupings in the 2020 and 2050 landscapes for the base case environmental scenario. Calculations were performed via trapezoidal integration of absolute hourly cross-sectional discharges modeled for both flood and ebb tides over a full calendar year, divided by the number of flood and ebb tides that occurred during this period.

Tidal prism (million cubic meters)	2020 landscape			2050 landscape		
Cross-section location (Figure 16)	FWOA	AG2 (Alternatives: 4,5)	AG3 (Alternatives: 1,2,3,6)	FWOA	AG2 (Alternatives: 4,5)	AG3 (Alternatives: 1,2,3,6)
Barataria Bay at barrier islands	330	330	330	502	501	499
Terrebonne Bay at barrier islands	493	492	492	683	682	682
East Timbalier and Raccoon Passes	61	61	61	101	102	102
Little Pass Timbalier	159	159	159	220	219	220
Belle Pass	14	14	13	17	15	16

Table 23. Increase of tidal prism between 2020 and 2050 (FWOA)

Cross-section location (Figure 16)	Increase of tidal prism between 2020 and 2050 (FWOA)
Barataria Bay at barrier islands	52%
Terrebonne Bay at barrier islands	39%
East Timbalier and Raccoon Passes	64%
Little Pass Timbalier	38%
Belle Pass	17%

Table 24. Impact of Project Alternatives on tidal prism relative to FWOA; positive percentiles indicate increase in tidal prism, and negative indicate reduction. Note that tidal prism changes of 1-2% are within the model variance.

	Change in tidal prism relative to FWOA (2020 landscape)		Change in tidal prism relative to FWOA (2050 landscape)	
Cross-section location (Figure 16)	AG2 (Alternatives: 4,5)	AG3 (Alternatives: 1,2,3,6)	AG2 (Alternatives: 4,5)	AG3 (Alternatives: 1,2,3,6)
Barataria Bay at Barrier Islands	0%	0%	0%	-1%
Terrebonne Bay at barrier islands	0%	0%	0%	0%
East Timbalier and Raccoon Passes	0%	0%	1%	1%
Little Pass Timbalier	0%	0%	0%	0%
Belle Pass	-1%	-10%	-8%	-4%

Figure 37. Cross-section along which model output were extracted for quantifying water and sediment fluxes along the barrier islands and tidal inlets of the Terrebonne Basin. Fluxes in southern (offshore) direction are positive as indicated by the yellow arrow

Figure 38. Cross-section along which model output were extracted for quantifying water and sediment fluxes along the barrier islands and tidal inlets of the Barataria Basin. Fluxes in southern (offshore) direction are positive as indicated by the yellow arrow.

The model predicted similar trends in tidal prism for tidal inlets to the west of Port Fourchon, namely Little Pass Timbalier, located between Timbalier Island and East Timbalier Island, and East Timbalier Pass and Raccoon Pass, located between East Timbalier Island and the West Belle Pass Headland (Figure 39; see Figure 16 for locations). East Timbalier Pass and Raccoon Pass experience the largest relative increase in tidal prism, where the maximum tidal discharge nearly doubles between 2020 and 2050, likely related to large morphological changes at these inlets and proximal environments.

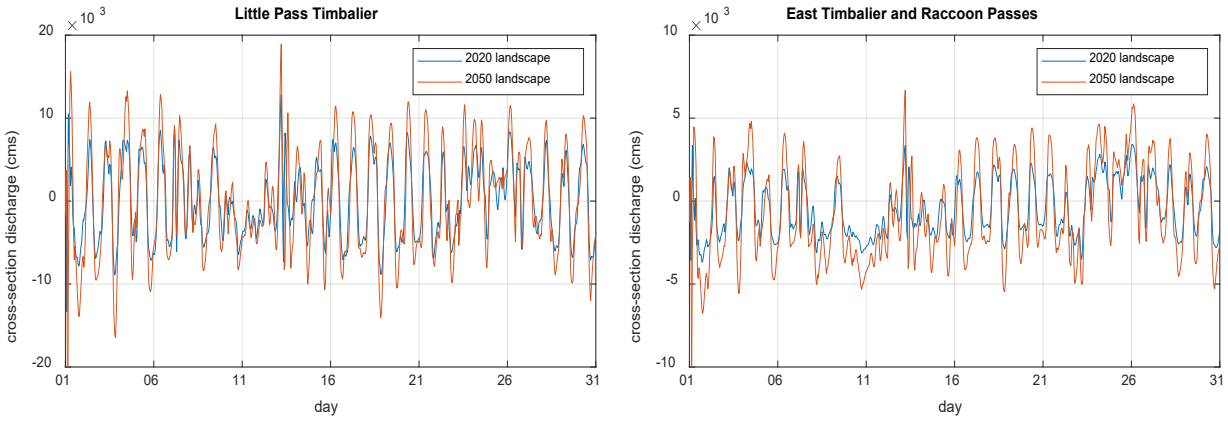

Figure 39. Instantaneous discharge for the Little Pass Timbalier (left) and combined East Timbalier and Raccoon Passes (right) during the month of January for the 2020 and 2050 landscapes in the base case environmental scenario (FWOA). Model results show that both basins experience an increase in tidal prism by 2050, as evidenced by the increase in the flood (positive) and ebb (negative) flows. Note that the difference in the peak magnitude between 2020 and 2050 is not constant across spring and neap conditions, and neither is the difference between flood and ebb peaks. Also evident are subtidal excursions during winter storms, which enhance water exchange through the inlets. Refer to Figure 16 for the location of the tidal passes.

The water levels in Bayou Lafourche near Port Fourchon (Figure 40) and tidal prism at Belle Pass (Figure 41) are also influenced by landscape evolution and mean sea level. Similar to other locations examined, tidal range and tidal discharge through Belle Pass are predicted to increase considerably in the future.

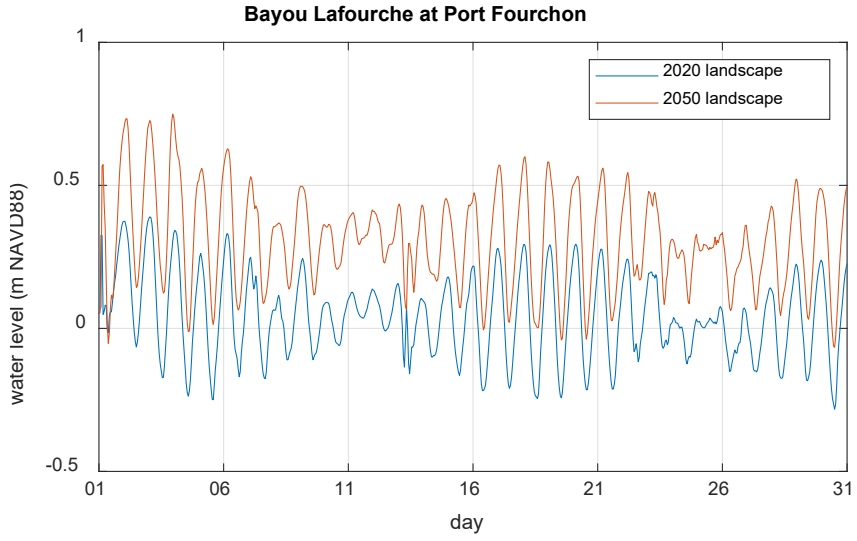

Figure 40. Instantaneous water levels during the month of January for Bayou Lafourche at Port Fourchon (location indicated in Figure 35) for the 2020 and 2050 landscapes in the base case environmental scenario (FWOA). Model results show an increase of mean sea level from 2020 to 2050 of at least 0.25 m, as well as increase in tidal range for neap and spring conditions.

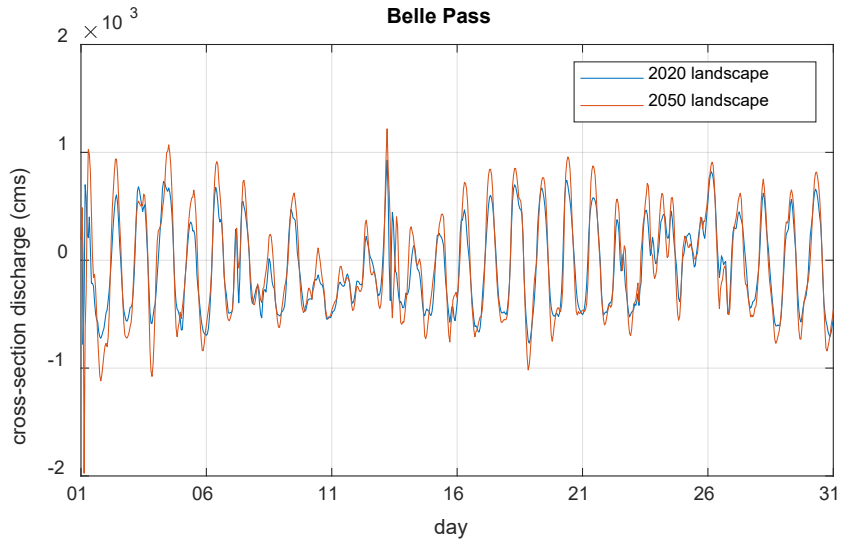

Figure 41. Instantaneous discharge for Belle Pass (refer to Figure 16 for location) during the month of January for the 2020 and 2050 landscape and for the base case environmental scenario (FWOA). Model results show that Belle Pass experiences an increase in tidal prism by 2050, as evidenced by the increase in the flood (positive) and ebb (negative) flows. Note that the difference in the peak magnitude between 2020 and 2050 is not constant across spring and neap conditions, and neither is the difference between flood and ebb peaks. Additionally, during subtidal excursion (related to water level fluctuations associated with meteorological forcings instead of astronomical), the water exchange through Belle Pass is amplified.

Salinity Patterns and Dynamics

The changes in topography and bathymetry as predicted by the Morphology Model and gradual rise of mean sea levels also influence salinity patterns and dynamics in the Barataria-Terrebonne Basin. Annual average salinity maps are shown in Figure 42 for the 2020 landscape and Figure 43 for the 2050 landscape. Figure 44 shows the difference in annual average salinities between the two landscapes. As previously mentioned, the differences between the 2020 and 2050 landscape simulations are limited to changes in topography, bathymetry, and mean sea level alone, and do not include any changes made to other model forcing parameters related to meteorology or inflow of freshwater.

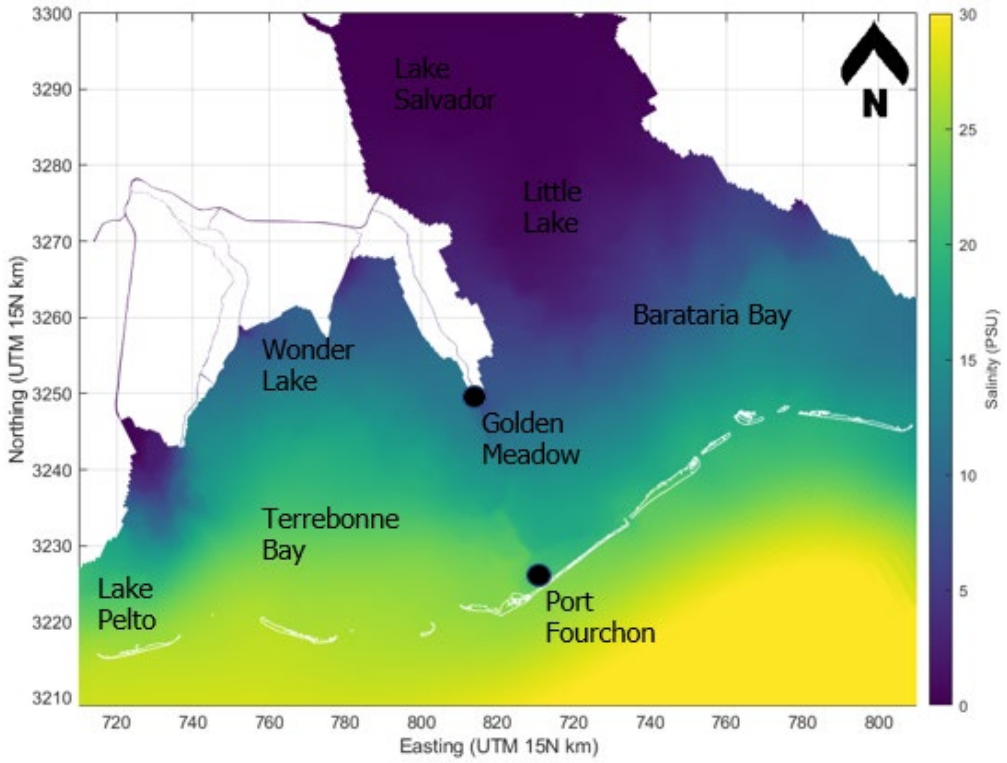

Figure 42. Annual average salinity patterns as modeled for the 2020 landscape

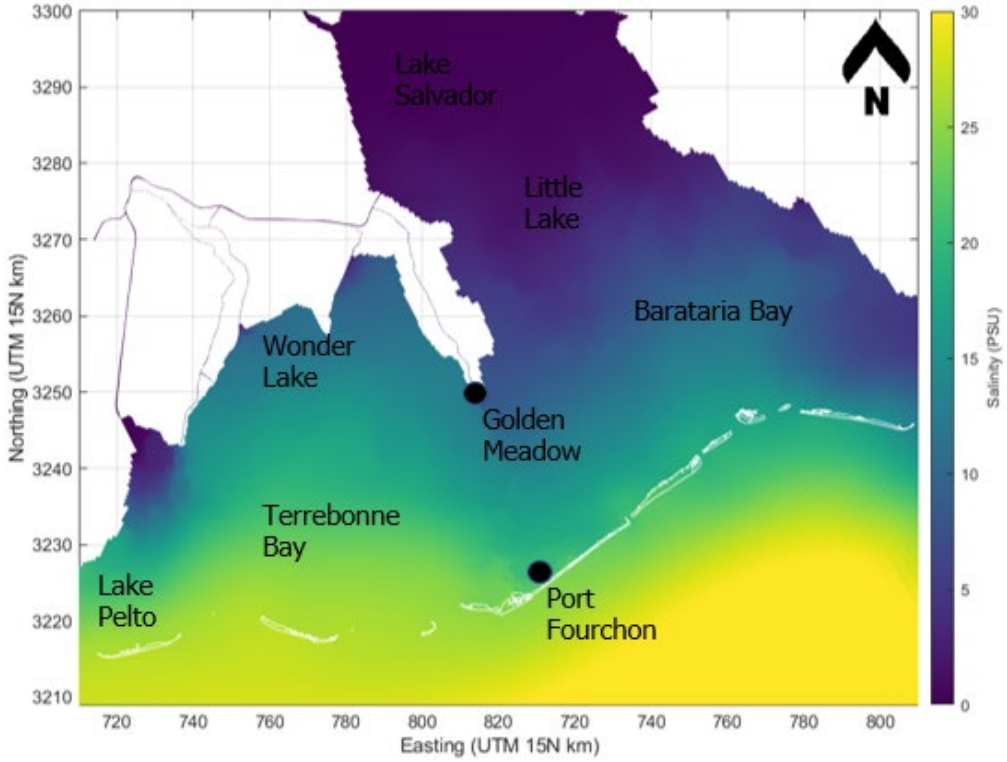

Figure 43. Annual average salinity patterns as modeled for the 2050 landscape

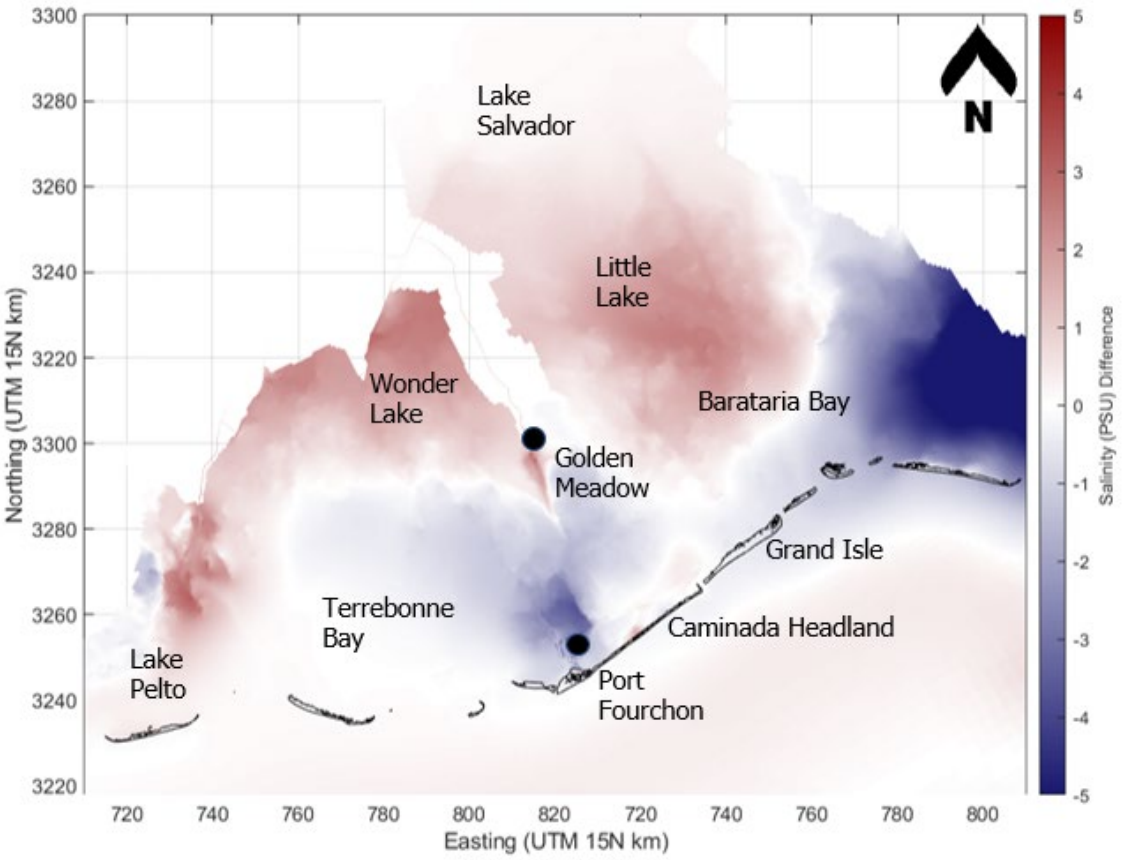

Figure 44. Differenced annual average salinity based on model predictions for the 2050 landscape relative to the 2020 landscape. Red colors as found in upper Terrebonne and between Barataria Bay and Lake Salvador in the Barataria Basin indicate increased salinities and blue colors as found in southeast Barataria and near the Caminada Headland indicate decreased salinities as predicted for the 2050 landscape relative to the 2020 landscape.

Comparisons of modeled salinity for the 2020 and 2050 landscapes show an increase of salinity north of the Terrebonne Basin, and parts of the Barataria Basin located north of Barataria Bay (Figure 44). This is expected as conversion of estuarine wetlands to open water due to erosion and SLR will bring about saltwater intrusion. The magnitude of saltwater intrusion varies through the basin. For instance, salinity increase in the western and northern Terrebonne Basin ranges from 1 to 3 psu, while in the southwest part of the basin, near Lake Pelto, salinity increase is approximately 1 psu. Similarly, in the Barataria Basin north of Barataria Bay, near Barataria Waterway and Little Lake, salinity increases by 1 – 3 psu. Salinity increase in these areas can be attributed to the increased tidal prism. The model predicted a decrease in salinity for southeast Barataria Basin, which becomes increasingly influenced by a freshwater introduction from the Mississippi River's modern delta. Through time, higher discharges at Grand Pass and Tiger Pass, active distributaries of the Mississippi River, affect the southeastern part of the Barataria Basin. In addition, the model predicts a decrease in salinity at the east and west sides of Bayou Lafourche between Golden Meadow and Port Fourchon, the result of increased hydraulic connectivity between Barataria-Terrebonne Basin associated with wetland loss. The connectivity increase enhances water flow from the relatively less saline Barataria Basin into the somewhat more saline Terrebonne Basin, resulting in reduced salinities in the southeast of the Terrebonne Basin, including the area near Port Fourchon.

Annual salinity time series at Wonder Lake in the Terrebonne Basin (Figure 45, left) and Little Lake in the Barataria Basin (Figure 46, left) show the salinity increase in these areas, with salinity values that are consistently higher throughout the year for the 2050 landscape. The salinity time series confirm the decrease in salinity around Port Fourchon at the eastern part of Timbalier Bay (Figure 45, right), which shows lower salinity values for the 2050 landscape during the majority of the calendar year. The trend is less clear for the salinity time series north of Barataria Bay (Figure 46, right) which does not show a consistent shift between the 2020 and 2050 landscapes. However, it does show a significant decrease in temporal variability of salinity when comparing the signals of the 2020 and 2050 landscapes.

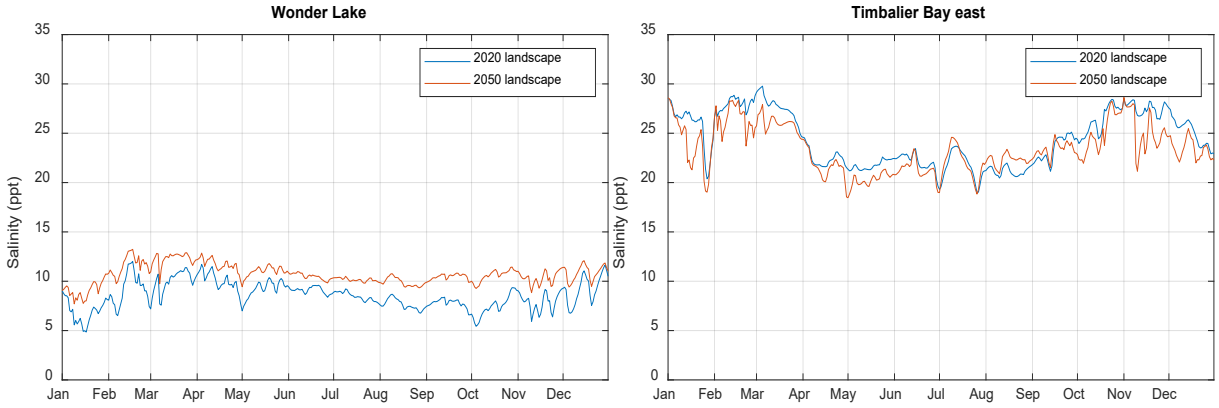

Figure 45. Annual salinity timeseries from the Terrebonne Basin (locations indicated in Figure 35) showing a predicted year-round future increase of salinity in Wonder Lake and a predicted future decrease of salinity during much of the year for the eastern part of Timbalier based on model results for the 2020 and 2050 landscapes. The 2050 results are based on the base case environmental scenario (FWOA). Salinity increase at Wonder Lake (left) varies from 1-3 psu in the winter months and 2–4 psu in the summer months, while at Timbalier Bay, salinity decreases by 1 psu averaged over the year without showing a consistent pattern over time.

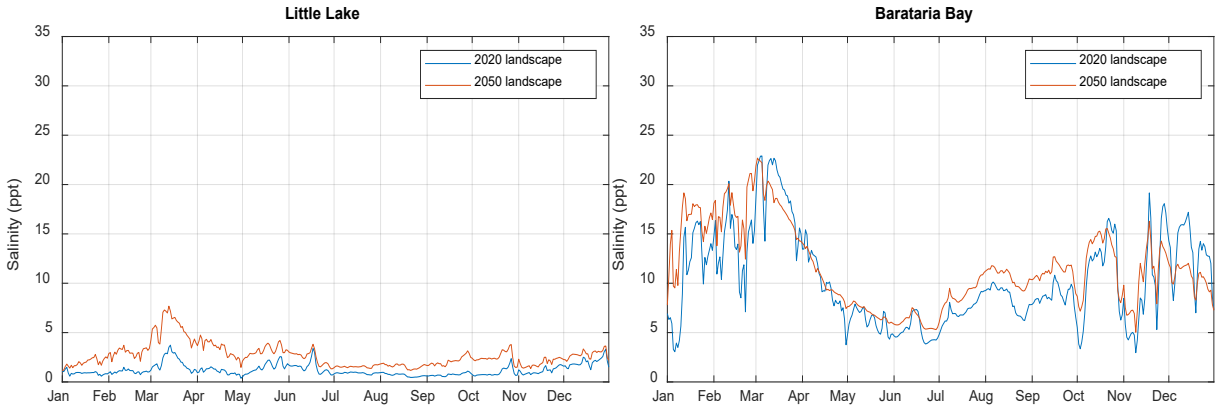

Figure 46. Annual salinity timeseries from the Barataria Basin (locations indicated in Figure 35) showing a predicted year-round future increase of salinity at Little Lake and a predicted reduction of temporal variability of salinity at the northern part Barataria Bay based on model results for 2020 and 2050 landscapes. The 2050 results are based on the base case environmental scenario (FWOA). Salinity increase at Little Lake (left) varies from 0.5 - 2 psu during most of the year and 2 – 4 psu in the month of March and April, while in the northern part of Barataria Bay, salinity increases by 1 psu averaged over the year.

Morphology

Regional morphology changes are closely related to basin hydrodynamics. Morphology is influenced by the exchange of water flow through the tidal inlets, the interaction of flow and waves in the backbarrier bays, and the influence of surge and waves along the shoreline. Wind, tidal, and wave-generated currents in the basin and along the shoreline erode and suspend sediment in the water column. Currents transport and deposit suspended sediment to change the landscape over long time periods. Strong currents can also erode and suspend sediment that may be exported from the basin. The dramatic changes in water levels and wind-generated waves associated with winter storms (cold fronts) are primary drivers sediment erosion and transport in coastal Louisiana (aside from large magnitude tropical cyclones), and the results below demonstrate their important role in the overall morphology change from 2020 to 2050.

In model year 2020, half of the major tidal inlets import sediment during cold fronts (Barataria and Caminada passes; Figure 47; Figure 48). Between 2020 and 2050 all the tidal inlets show increasing sediment fluxes (Figure 47; Figure 49; Figure 51; Figure 52). By 2050 all major tidal inlets near Port Fourchon (Barataria Pass, Caminada Pass, Belle Pass, and East Timbalier, and Raccoon passes) begin to export sediment (Figure 49; Figure 50). Most of the total sediment flux is composed of the clay fraction (extremely fine sediment; <4 μm); little to no change is seen in the amount of the sand and silt fractions exported from the basin. The changes in sediment import and export are largely attributed to the increasing tidal prism resulting from wetland loss in Barataria-Terrebonne Basin, as documented in the *Hydrodynamics and Salinity* section (Figure 53).

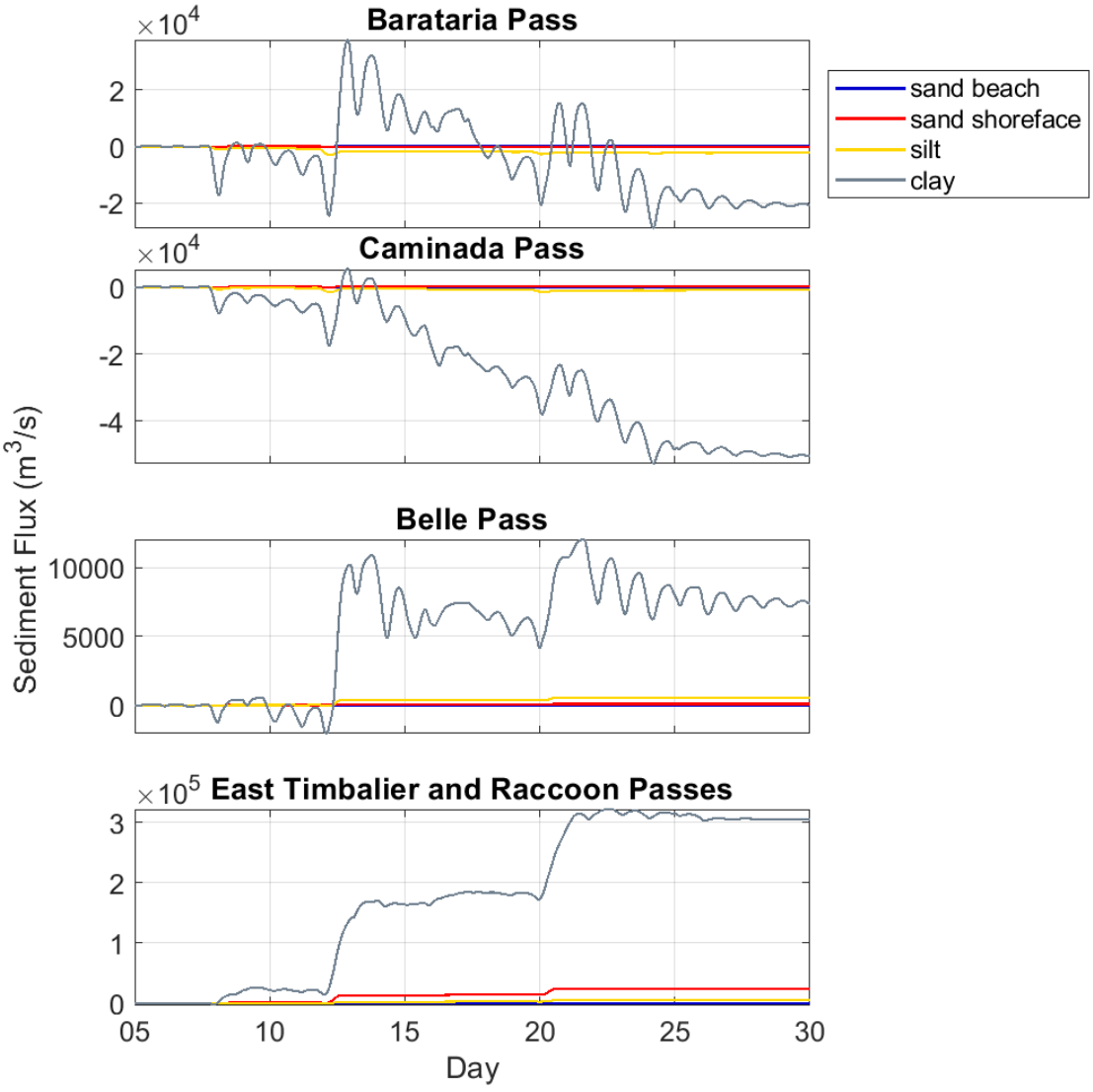

Figure 47. Cumulative sediment flux through the major passes in Barataria-Terrebonne Basin for the base case environmental scenario in 2020 for the FWOA alternative and for all sediment classes. Positive fluxes are transport toward the Gulf. Negative fluxes are toward the basin. The majority of the sediment flux is composed of clays for all major passes. The model results highlight the role of winter storms in dominating the transport through the inlets with rates that increase two to threefold during these events.

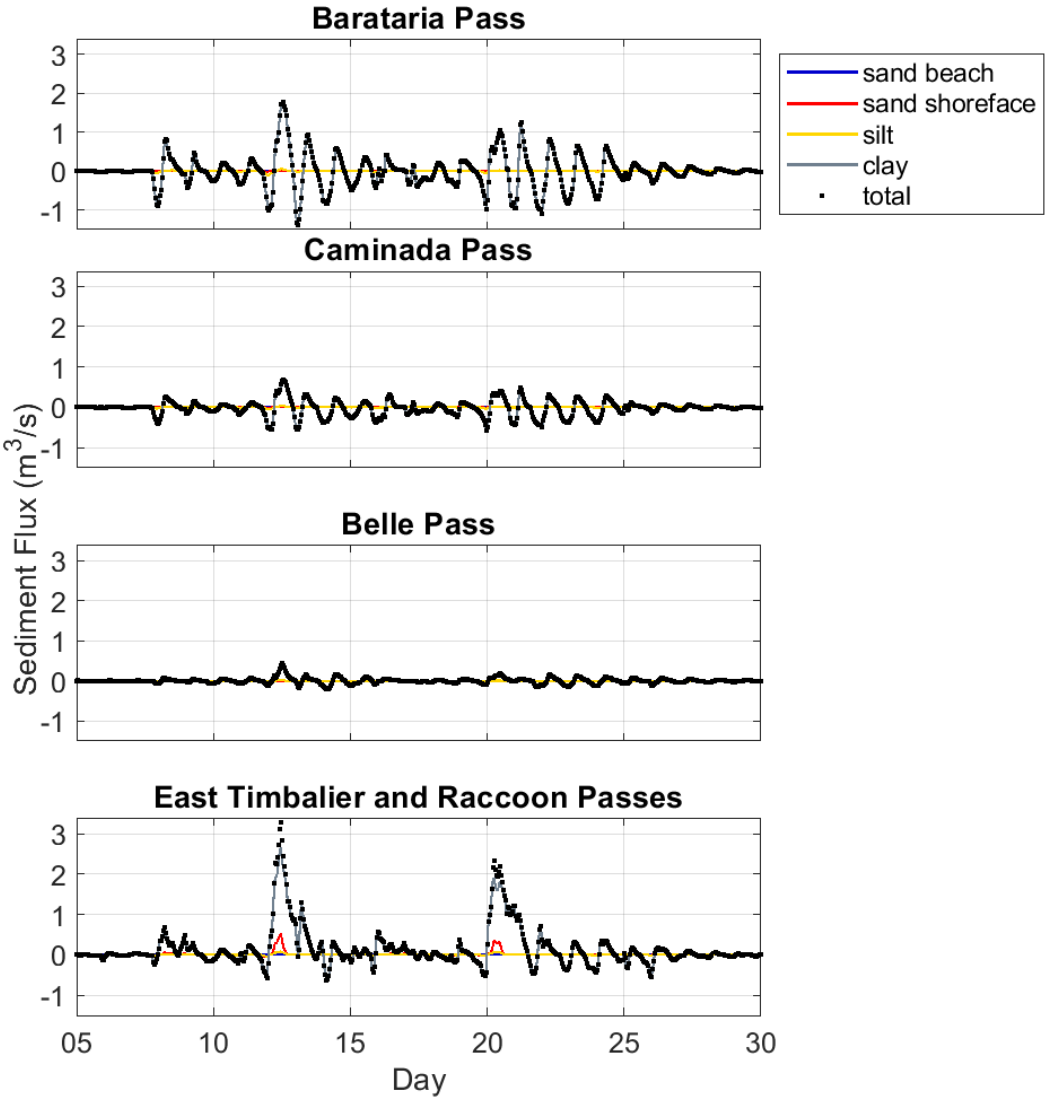

Figure 48. Hourly average sediment flux for the FWOA alternative during cold fronts in 2020 at four major inlets in the study area for all sediment classes. Positive fluxes are transport toward the Gulf. Negative fluxes are toward the basin. Note that sediment fluxes are highest through East Timbalier and Raccoon Passes, the only passes that show noticeable sand movement. The model results highlight the role of winter storms in dominating the transport through the inlets with rates that increase two to threefold for some inlets during those events. Note that the clay fraction tracks closely with the total sediment flux indicating the significant export of clays from the basin.

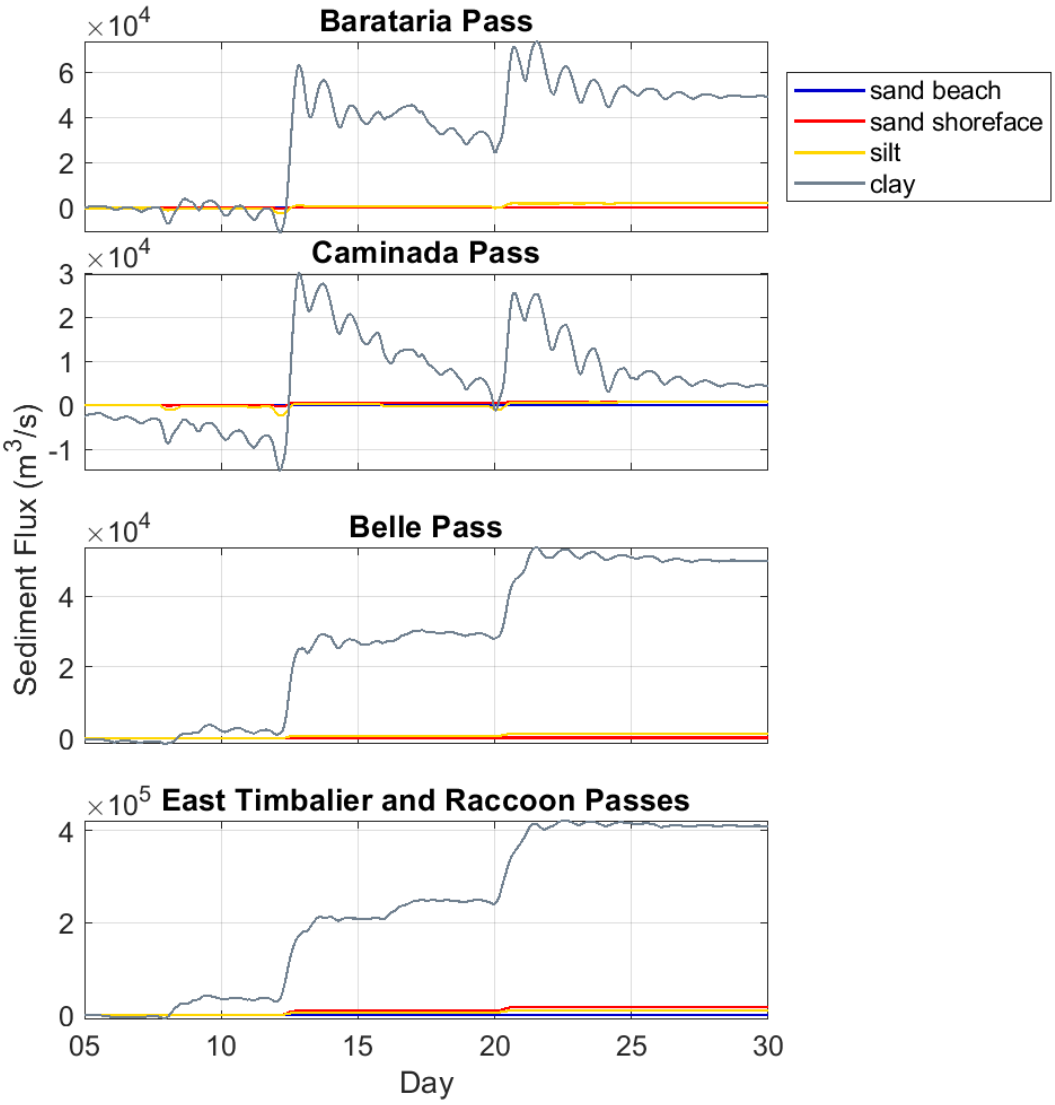

Figure 49. Cumulative sediment flux through the major passes in Barataria-Terrebonne Basin in 2050 for the base case environmental scenario in the FWOA alternative for all sediment classes. Positive fluxes are transport toward the Gulf. Negative fluxes are toward the basin. The majority of the sediment flux is composed of clays for all major passes. The model results highlight the role of winter storms in dominating the transport through the inlets with rates that increase two to five times for some inlets during these events.

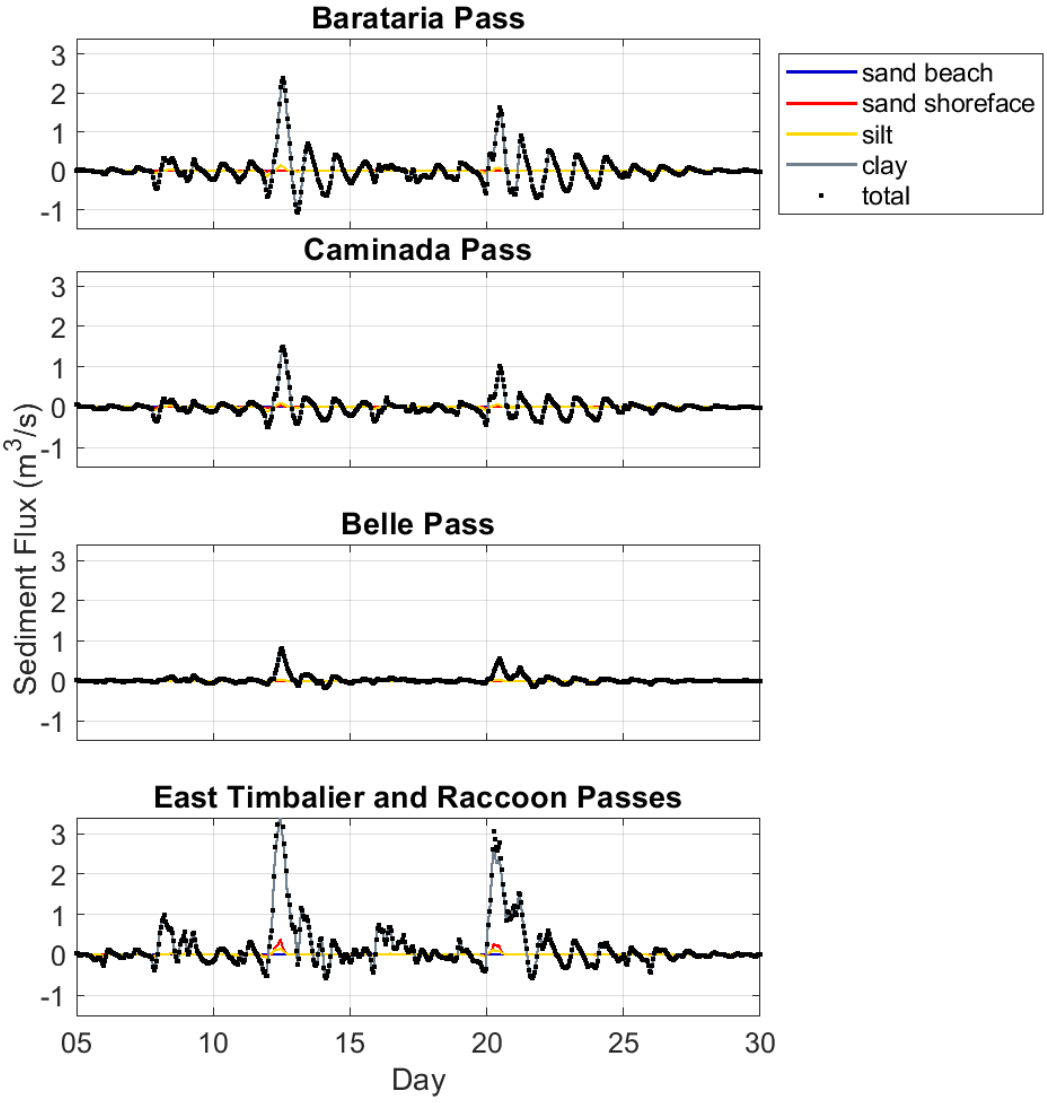

Figure 50. Hourly average sediment flux for the FWOA alternative during cold fronts in 2050 for the base case environmental scenario at four major inlets in the study for all sediment classes. Positive fluxes are transport toward the Gulf and negative fluxes are toward the basin. The model results highlight the role of winter storms in dominating the transport through the inlets with rates that increase two to threefold for some inlets during these events. Note that the clay fraction tracks closely with the total sediment flux indicating the significant export of clays from the basin.

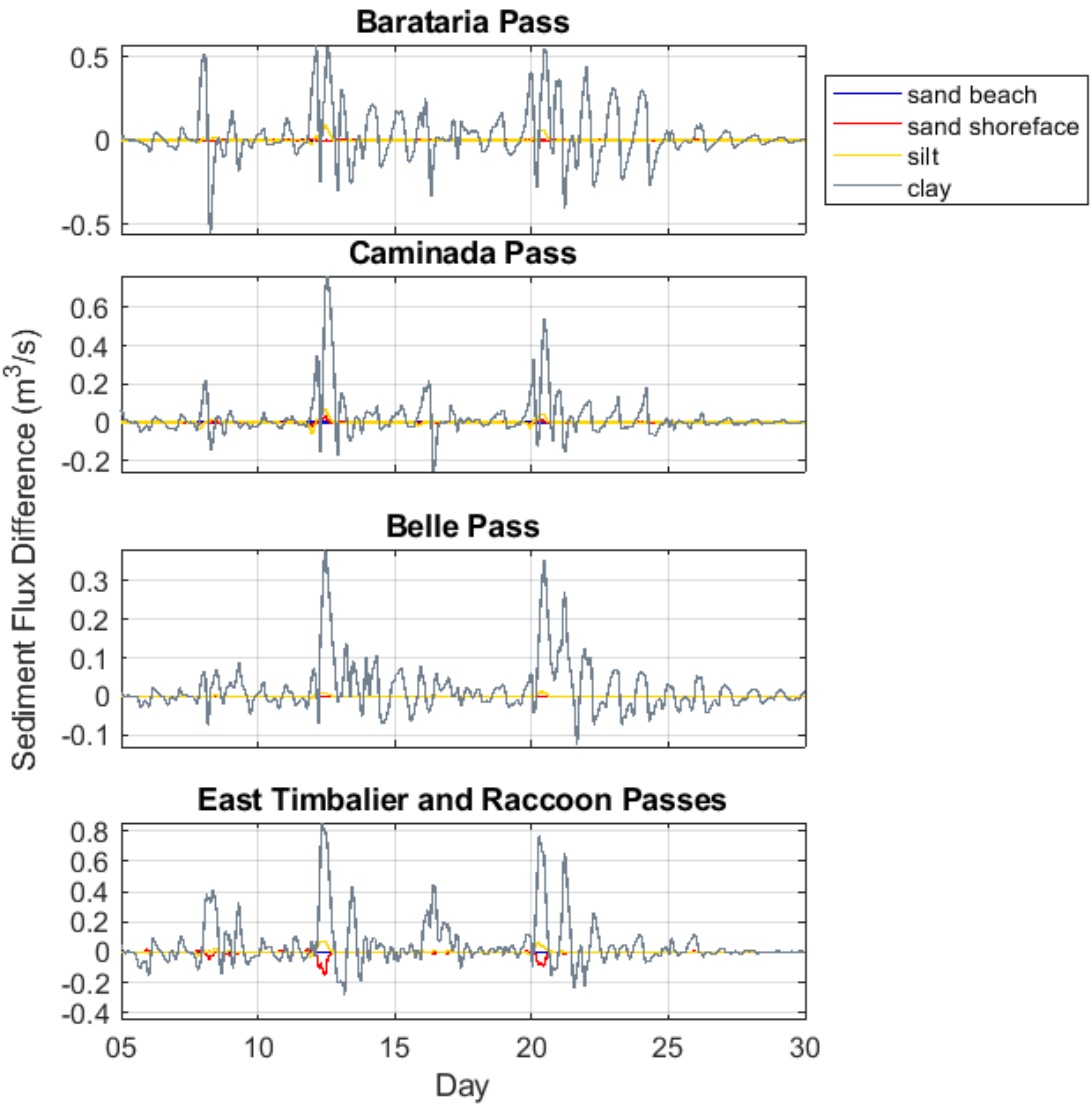

Figure 51. Hourly average sediment flux difference between 2020 and 2050 for the FWOA alternative during cold fronts for the base case environmental scenario at four major inlets in the study. Positive values are where 2050 fluxes are larger than 2020 and negative fluxes are where 2020 fluxes are larger than 2050. Fluxes in 2050 are generally larger than those in 2020.

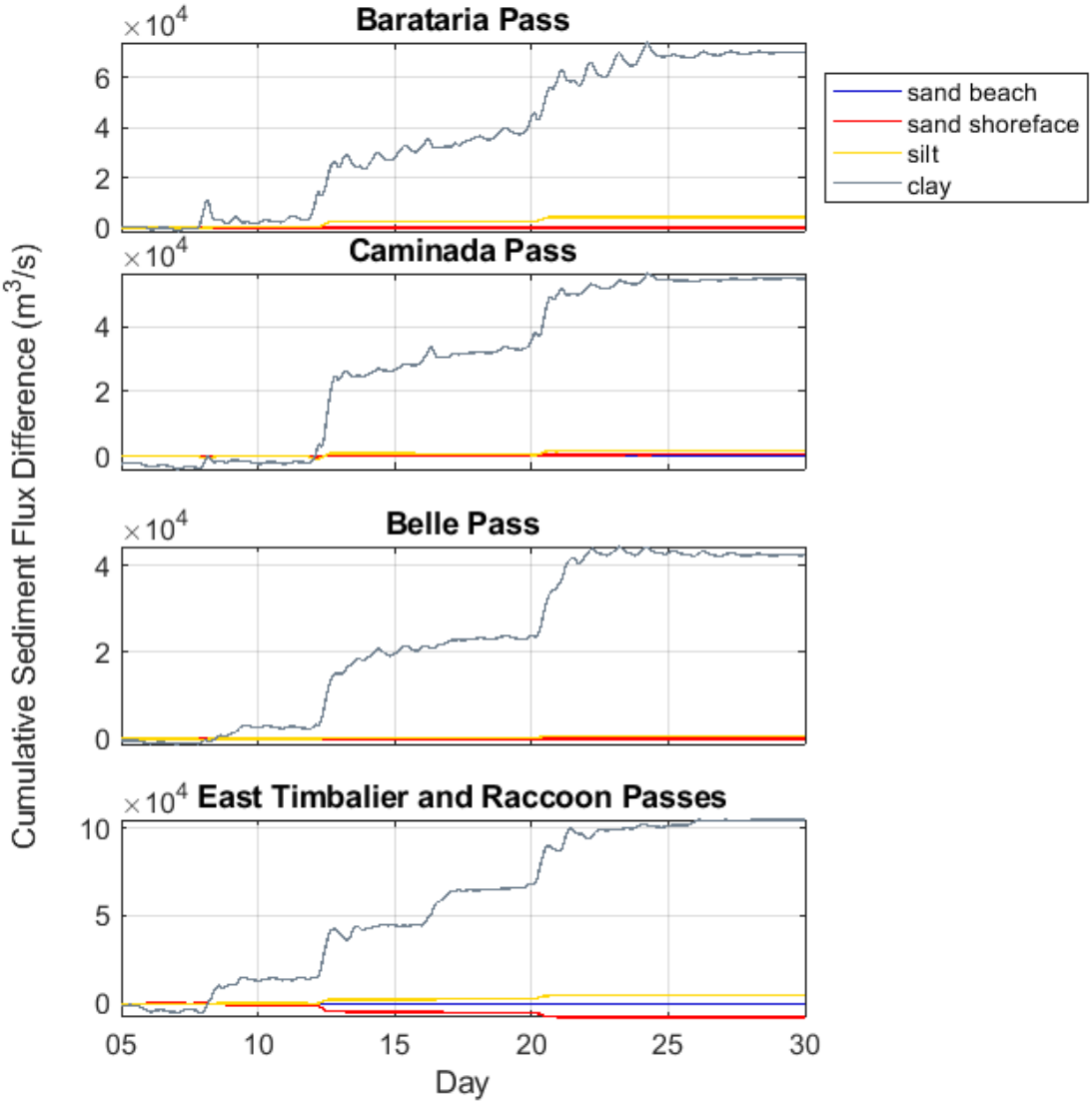

Figure 52. Cumulative sediment flux difference between 2020 and 2050 for the FWOA alternative during cold fronts for the base case environmental scenario at four major inlets in the study. Positive fluxes indicate 2050 fluxes that are larger than 2020 fluxes.

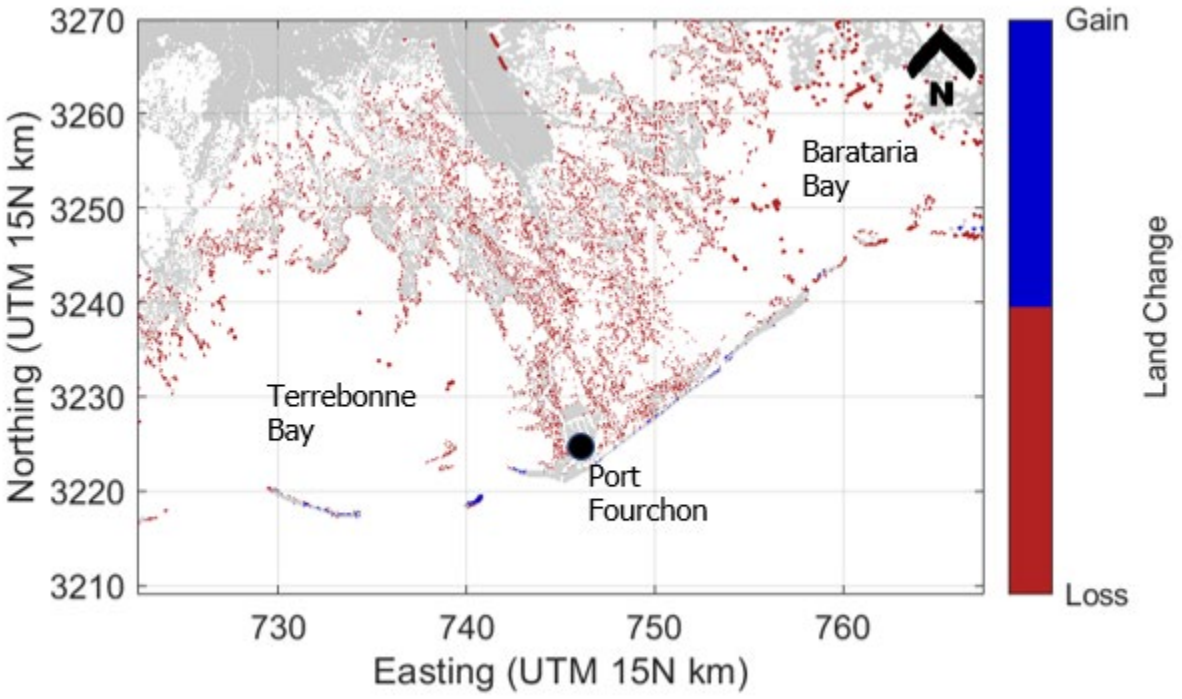

Figure 53. Modeled land change in Barataria-Terrebonne Basin from 2020 to 2050 for the base case environmental scenario in the FWOA alternative.

Sediment exported from the basin leads to an overall deepening of the bays from 2020 to 2050 (Figure 54). Some of this sediment is deposited in ebb tidal deltas at the outlets of East Timbalier and Raccoon Passes (Figure 54 A), and to a lesser extent, Caminada Pass (Figure 54 B). Figure 54 depicts a graph of the flux at the tidal inlets (see Figure 16 for locations of tidal inlets). Caminada Pass tends to deepen over the 30-year model run (Figure 54, Figure 54 C). East Timbalier and Racoon Pass tend to narrow and deepen (Figure 54 A). These changes are expected given the increasing tidal prism as wetlands degrade into open water in the basin. Increasing tidal prism will leads to increased current velocities through the major passes, making sediment export from the basin more efficient. Like the interior bays, the shoreface also tends to degrade and become deeper by 2050 (Figure 54). During storms this will lead to larger, higher energy waves breaking closer to the shoreline as well as larger waves propagating through the bays and impacting the wetland edges (Figure 55; Figure 56). Increased wave energy at the shoreline will be able to suspend and transport more sediment and have a greater potential for island breaching. Increased wave energy at wetland edges will tend to accelerate wetland edge erosion.

Wetland loss is overwhelmingly due to edge erosion rather than drowning. For every alternative / environmental scenario combination, the fraction of marsh loss that is attributable to drowning is less than 5% of the total wetland loss in the analysis polygon. This result is consistent with other modeled (Mariotti, 2020) and observational (Ganju et al., 2020; Törnqvist et al., 2021b) studies that have shown wetland losses to drowning to be uncommon over decadal timescales except for extreme rates of RSLR or sediment starvation.

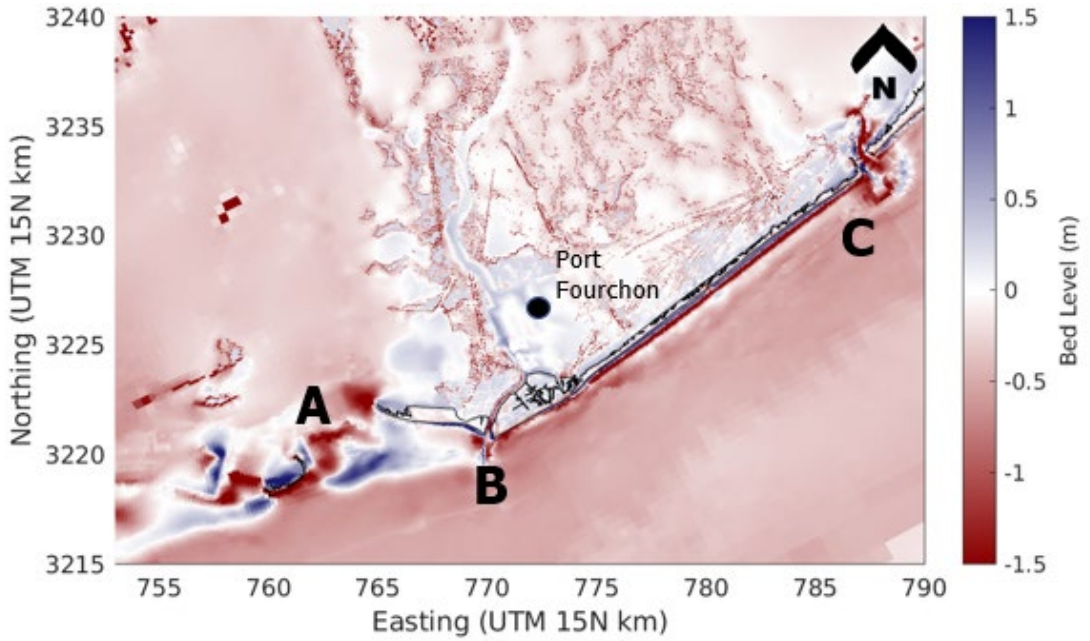

Figure 54. Bed change in the FWOA alternative from 2020 to 2050 for the base case environmental scenario. Blue colors show deposition. Red colors show erosion. Significant ebb tidal delta deposition is predicted for East Timbalier and Raccoon passes (A) is the location of those passes and blue region on the Gulf side of those tidal inlets indicates ebb tidal delta deposition). The tidal inlets increase in cross-sectional area over time in the model simulation, consistent with historical trends (Miner et al., 2009). Minimal ebb-tidal delta deposition is predicted at Belle Pass (B). Caminada Pass (C) deepens over time in the model simulation and the ebb tidal delta migrates down-drift as indicated by the red (erosion) on its western (updrift) flank and deposition on its eastern (downdrift) flank.

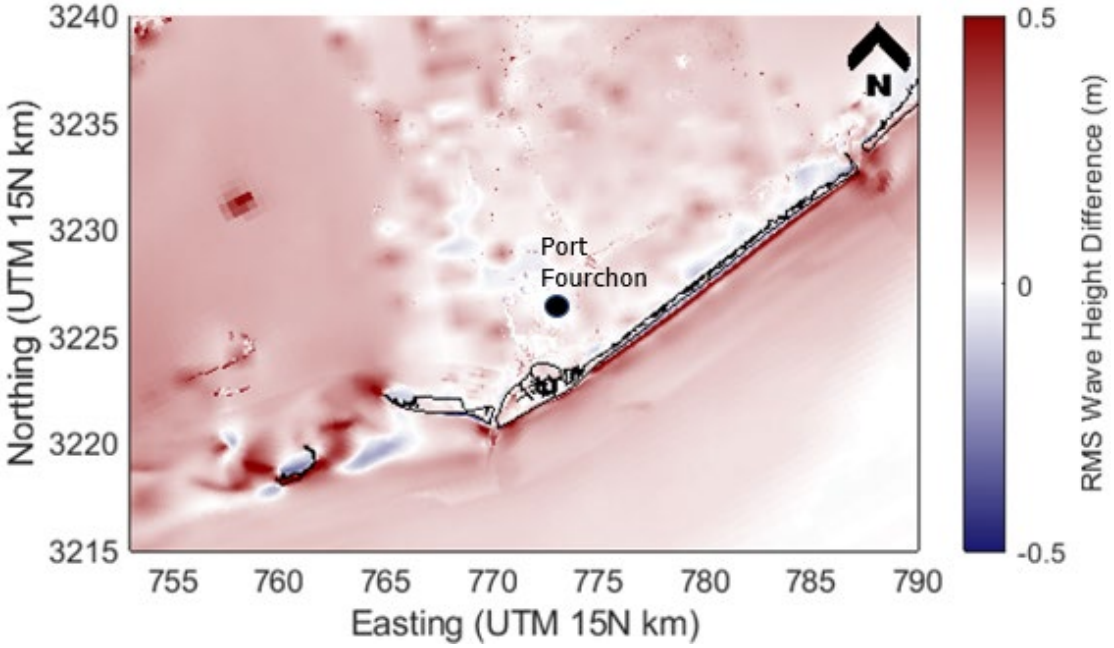

Figure 55. Peak wave height difference between 2020 and 2050 for the FWOA alternative during Storm 34 in the base environmental scenario. Red colors show areas where wave height is larger in 2050 and blue areas show where wave height is lower in 2050. Note the increased wave height along the Caminada Headland shoreline related to shoreface steepening and decreased wave height offshore East Timbalier and Raccoon passes due to ebb tidal delta growth and attendant wave sheltering effects of that bathymetric change between 2020 and 2050.

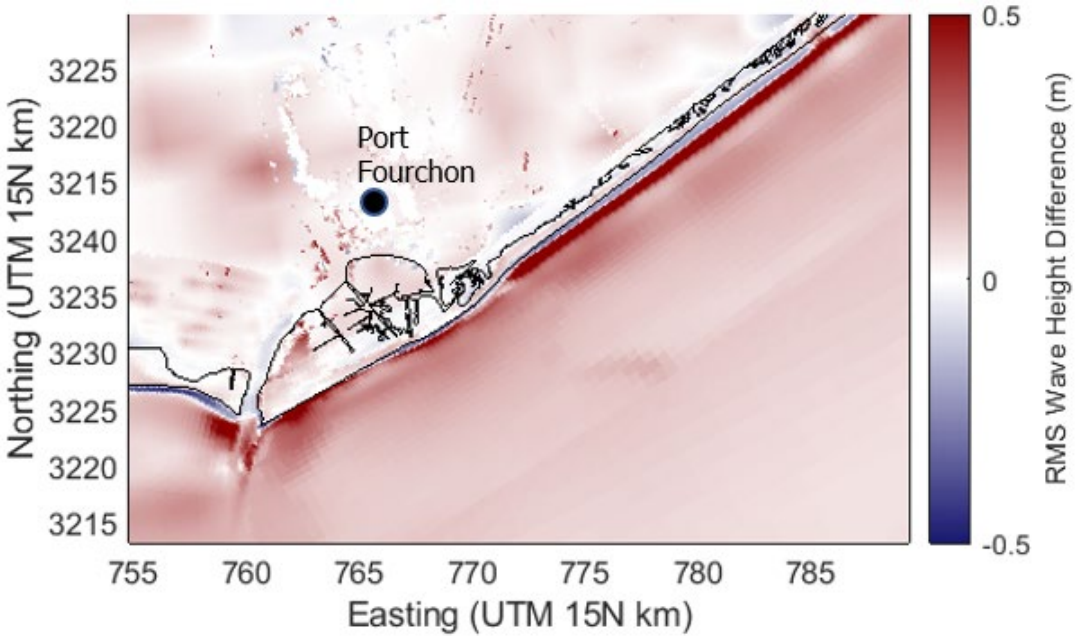

Figure 56. Peak wave height difference zoomed in to Caminada Headland between 2020 and 2050 for the FWOA alternative during Storm 34 in the base environmental scenario. Red colors show areas where wave height is larger in 2050 and blue areas show where wave height is lower in 2050. Note the significant increase in wave height along the shoreface.

Habitat Area Changes

From years 2020 to 2050 in both the FWOA and FWP simulated cases, the total area has a higher portion of open water habitats over time. In addition, the mangrove forest areas also decreased over time in model runs of FWOA and FWP (Figure 57).

From years 2020 to 2050, it was projected that with the habitat area changes within the project area of Port Fourchon, the total area would change from a net GHG sink at year 2020 to a net GHG source at year 2050 for both FWOA and FWA (Figure 58). By placing dredge material to develop six restoration project alternatives between AG2 and AG3, it was estimated that larger net GHG sinks could occur over time. At year 2050, it was projected that 0.2 MMT CO_2e could be avoided because of the alternatives that restored coastal wetlands (Figure 58).

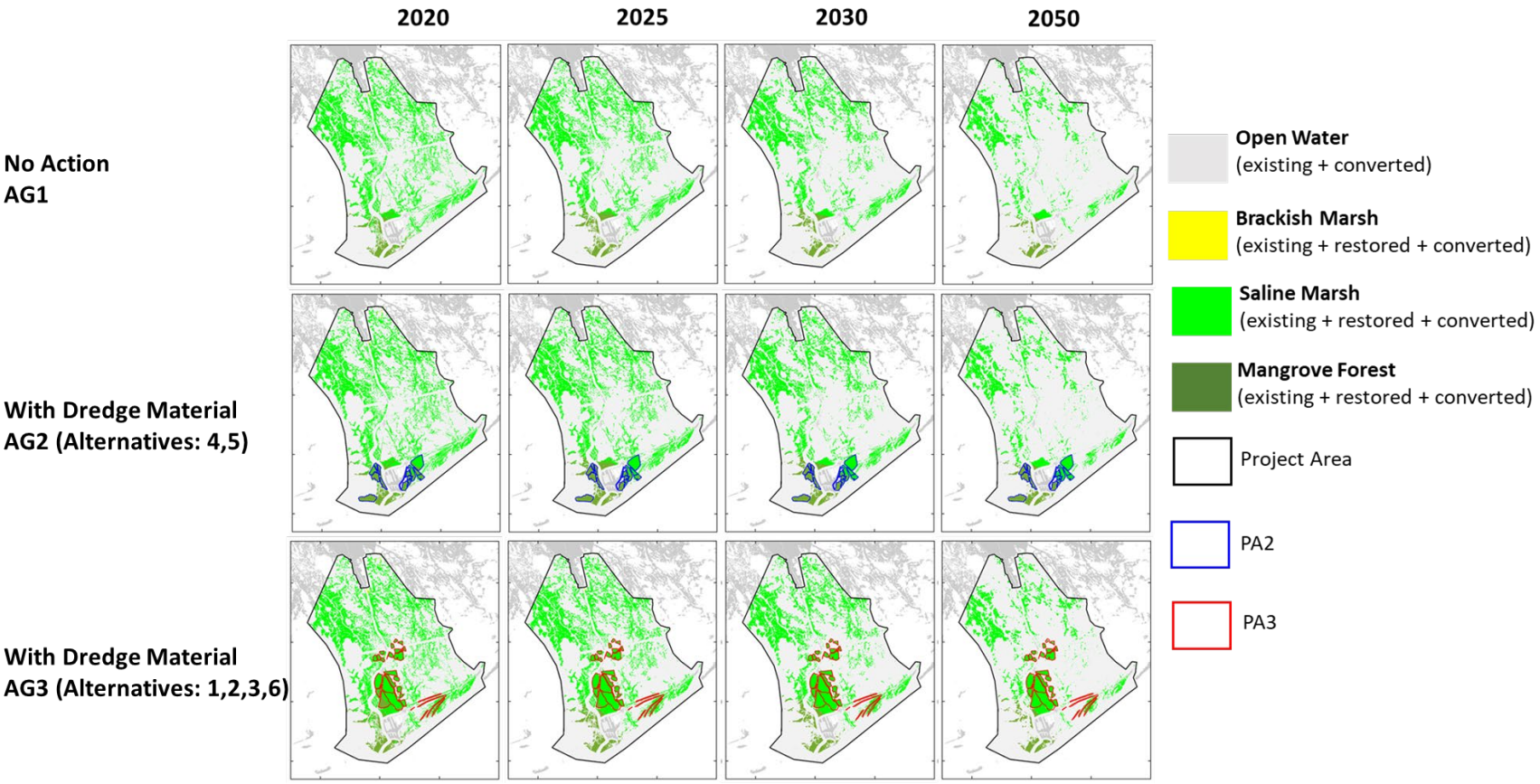

Figure 57. Timeseries of modeled habitat areas (open water, brackish marsh, saline marsh, and mangrove forest) in the project area including habitats that were existing, restored or converted at years 2020, 2025, 2030, and 2050 with a future without action of restoration (FWOA, AG1) and with the restoration via the project alternative (AG2 and AG3) of dredge material (model runs of PR2 and PR3).

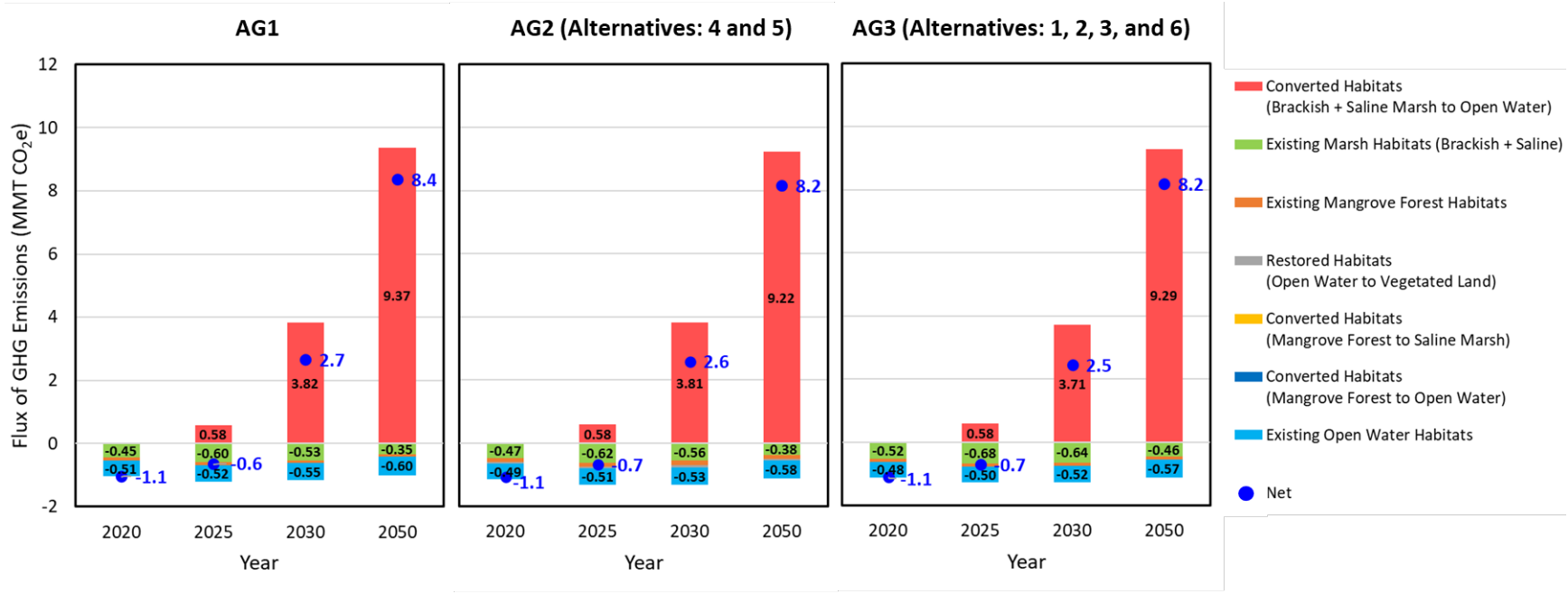

Figure 58. Modeled net flux of GHG emissions (MMT CO2e) at snap shot years of 2020, 2025, 2030, and 2050. Results are shown for FWOA – AG1 and future with project alternatives of placing dredge material for restoration (AG2, AG3) in the total project area. At 2020 for AG1, AG2, and AG3 the project area is a net sink (net GHG flux is negative), and at year 2025 remains a net sink for all three alternative groups. At 2050 the flux of GHG emissions are positive (indicating a net source) for AG1 is +8.4 MMT CO_2e, compared to +8.2 for AG2 and AG3, implying an avoidance of +0.2 MMT CO_2e that can be achieved through the construction of the either the projects in AG2 or in AG3. Most of the increase of net emissions from 2020 to 2050 is the result of the loss of carbon in aboveground biomass and in soils when wetlands convert to open water.

Restoration Projects Compared to FWOA Case

The proposed wetland restoration templates can be compared to the FWOA alternative to assess project performance, the persistence of the project after 30 years, project impact to storm surge and waves, and how it influences habitat changes for the estimation of the net GHG flux. Project persistence is evaluated based on land change maps which show gain and loss of area above mean low water for a given year. Storm surge (water level) and wave heights for the modeled storms can also be compared between the wetland restoration alternatives and the FWOA alternative. Storm surge heights and wave heights are considered by the peak value at any time during a storm and as the average value over the whole course of the storm. The net GHG flux comparisons must consider not only the initial net ecosystem carbon balance by habitat type in the project area, but also the habitat area changes over time. The net ecosystem carbon balance of wetland habitats can vary because woody plants like mangrove forests tend to store more carbon aboveground than herbaceous vegetation. Additionally, when a given area of wetland is eroded, it was assumed that certain percentages of captured carbon in the aboveground biomass and soils would be mineralized and released back to the atmosphere; thus, how well existing habitat areas are maintained greatly influences the net GHG flux estimate of the project area.

An important note about the project alternative evaluations discussed here is that because multiple wetland restoration projects (e.g., Alternatives 1, 2, 3, and 6) were modeled together, it is not possible to disentangle the performance or effects of any single project area from the others in the same area. Any single location where wetlands are restored is likely receiving some benefit—especially in terms of reduced wetland edge exposure tow waves—from other restoration areas in its vicinity. Results for each alternative are described below organized by geographic groupings (e.g., west of Port Fourchon). See Figure 30 for a map of the geographic project groupings.

West of Port Fourchon

The wetlands to the west of Port Fourchon lose land area and transition to a more open water environment between 2020 and 2050 in the FWOA alternative. Only a thin strip of wetland separates Bayou Lafourche from Timbalier Bay. Within the location of proposed restoration project areas in the FWOA, over 230 acres of land is lost (note that the projects are never constructed in the FWOA), primarily through edge erosion (Figure 59). In Alternative 4, which builds 6 different wetland restorations, approximately 980 acres of land is created, while only 160 acres are lost by 2050 (Figure 60). Because edge erosion is the major driver of wetland loss in the model, the unbroken area of restored wetlands erodes less than the unrestored wetlands. Less sediment is exported from this area with the restoration projects in place. All wetland restorations are largely intact in 2050.

The habitat total area (Alternative 4, 1,670 acres) was a net sink of GHG emissions from years 2020 to 2050 with a range of -0.03 to -0.04 MMT CO_2e (Figure 61). Because these wetlands remain largely intact (with little conversion to open water habitats), the net GHG emissions captured at 2050 was estimated at -0.03 MMT CO_2e for Alternative 4. The area of wetlands was projected to be dominated (nearly 70% over time) by mangrove forests which was parameterized to capture more carbon than saline marshes due to the greater aboveground biomass in woody trunks and stems compared to herbaceous vegetation (marsh grasses).

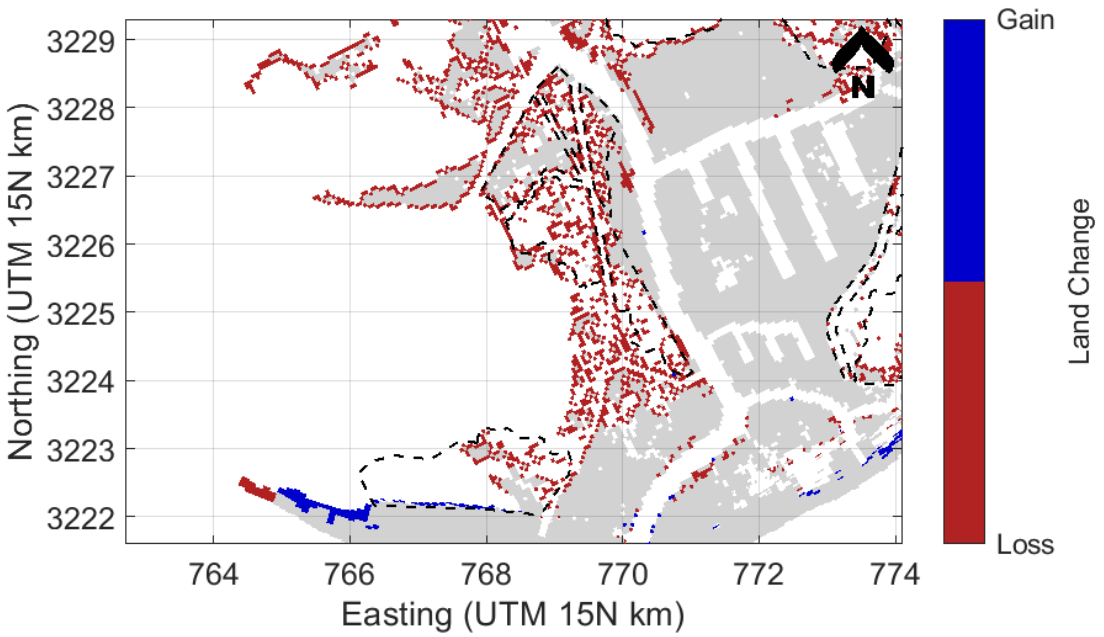

Figure 59. FWOA land change from 2020 to 2050 in Alternative 4, west of Port Fourchon. Dashed lines show the locations of projects that were modeled in the other alternatives. Over 230 acres of landloss occurred during the simulation.

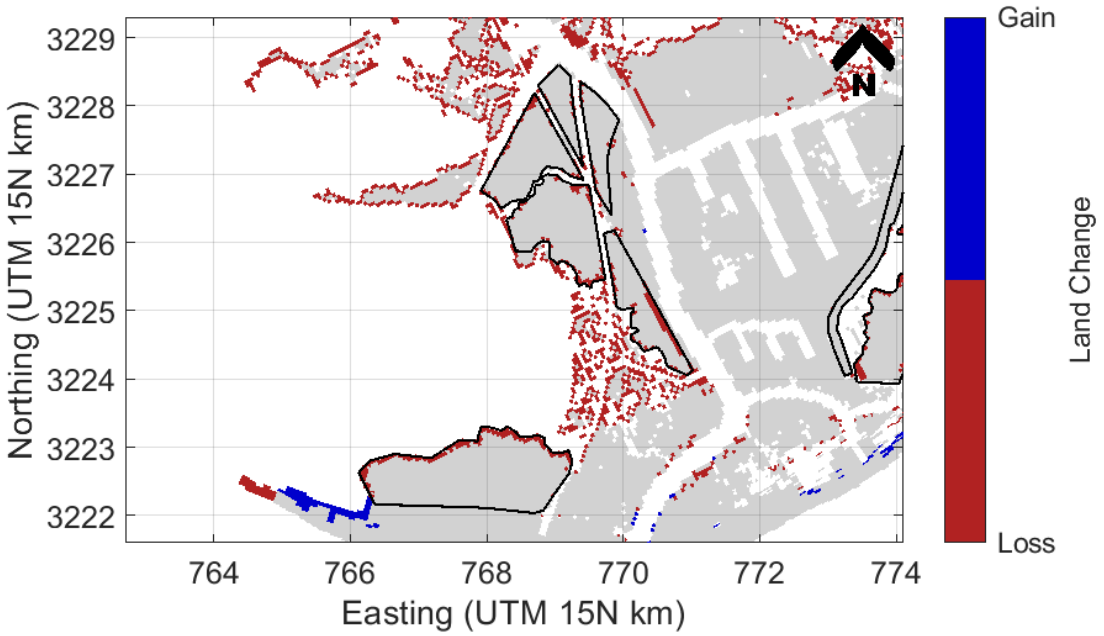

Figure 60. Land change to the west of Port Fourchon from 2020 to 2050 with Alternative 4 projects constructed. This model run used the base case environmental scenario; the land change seen in the higher SLR and storminess scenario is similar. Approximately 980 acres of land was created by restoration and 160 acres of wetland loss occurred during the simulation.

Figure 61. Modeled net GHG flux and wetland habitat areas (mangrove forest and marshes) from snapshot years of 2020, 2025, 2030, and 2050 of Alternative 4 in the West of Port Fourchon area. Positive net GHG flux values represent a source and negative values represent a net sink.. The habitat total area (Alternative 4, 1,670 acres) was a net sink of GHG emissions from years 2020 to 2050 with a range of -0.03 to -0.04 MMT CO_2e. Because these wetlands remain largely intact (with little conversion to open water habitats), the net GHG emissions captured at 2050 was estimated at -0.03 MMT CO_2e for Alternative 4.

As soon as these projects are constructed (model year 2020) their influence on storm surge and wave heights are observed at the Port. The reductions in peak storm surge heights are modest in 2020 (<5 cm; not shown), while the reductions in peak and average wave height are greater (5–25 cm, in the project area; not shown). The greatest reductions are seen in the southernmost area, immediately behind West Belle Headland (wetland creation 30, as referenced in Figure 30), where a large open water area was filled. The time-averaged water level inside the project area increases, compared with no projects; this change is expected because vegetated areas will drain more slowly than open water. These restoration projects that remain largely intact in 2050 continue to provide storm surge and wave height reduction in the model; the project benefits with respect to mitigating storm surge and wave heights observed in 2020 persist through model year 2050. Peak water levels (surge heights) are slightly lower, and time-averaged water levels are slightly higher with restorations in place (Figure 62; Figure 63). Reductions in peak wave height continue to be seen in 2050 (Figure 64). A slight increase in the wave heights in the bay immediately west of the constructed projects results from slightly increased depths in the open water area (compared to FWOA) due to less sediment leaving the project areas and settling in the bay. The results from storm 34 are shown for the base case environmental scenario; the less optimistic scenario shows similar results. All storm directions also show wave height reductions resulting from these projects. The effects of these projects on water level are more variable with storm direction, but none show large increases in water levels.

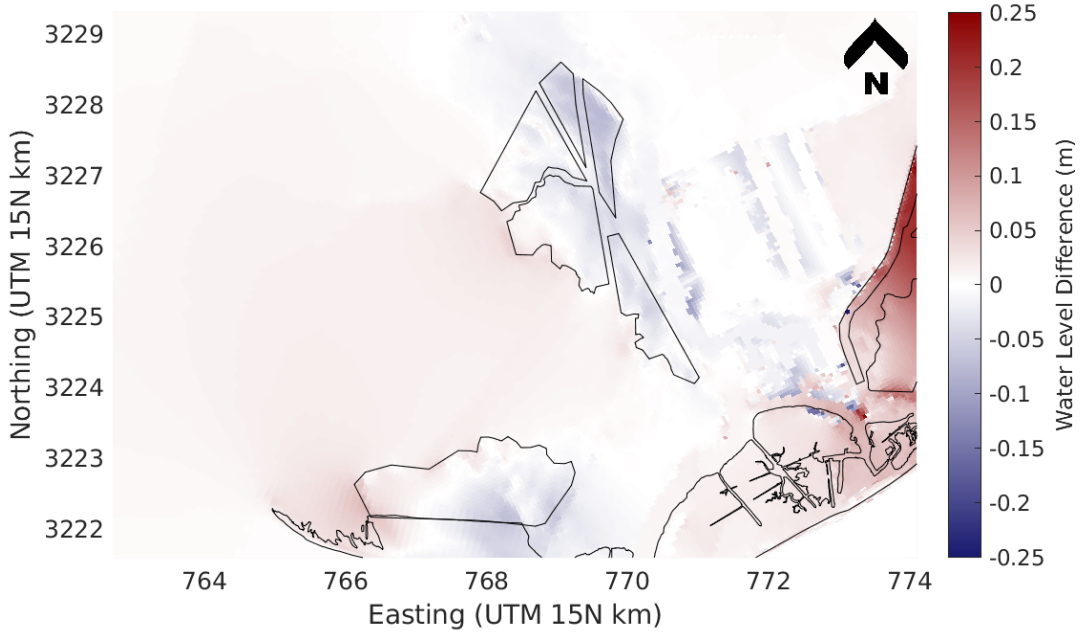

Figure 62. Peak water level difference for Alternative 4 projects compared with FWOA for the base case environmental scenario in 2050. Blue areas show where water levels during storm 34 are lower in Alternative 4 compared with FWOA. Red areas show where water levels are higher in Alternative 4 compared with FWOA. A slight reduction in peak water levels is predicted in most of the project areas.

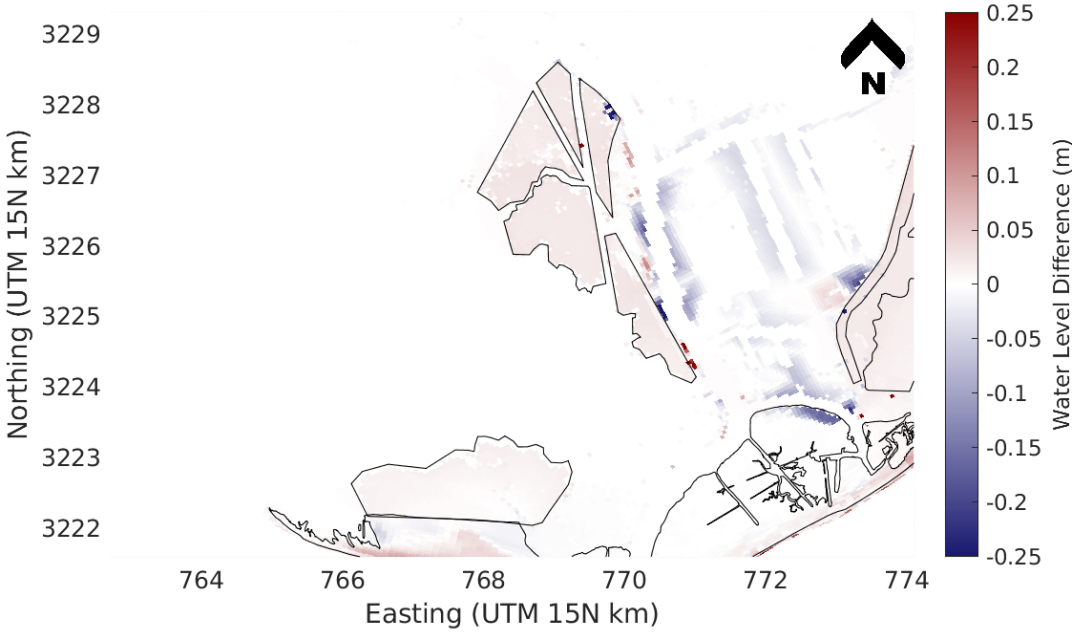

Figure 63. Time averaged water level difference for Alternative 4 projects compared with FWOA for the base case environmental scenario in 2050. Blue areas show where water levels are lower during storm 34 in Alternative 4 compared with FWOA. Red areas show where water levels are higher in Alternative 4 compared with FWOA. Higher time averaged water levels are expected after wetland creation because open water drains more quickly than wetland.

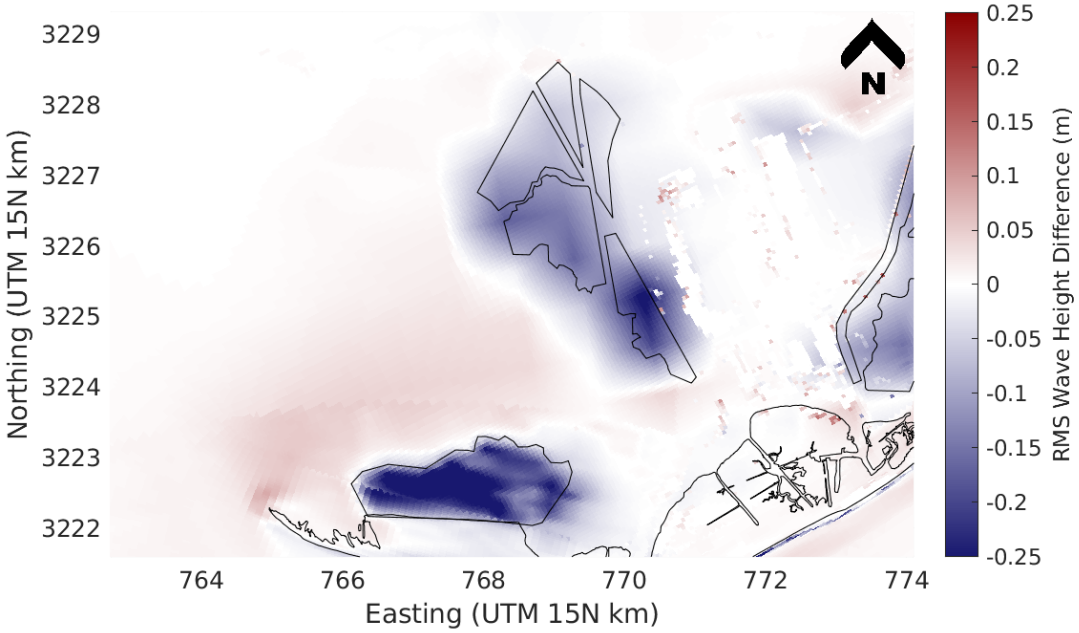

Figure 64. Peak wave height difference for Alternative 4 projects compared with FWOA for the base case environmental scenario in 2050. Blue areas show where wave heights are lower during storm 34 in Alternative 4 compared with FWOA. Red areas show where wave heights are higher in Alternative 4 compared with FWOA. The greatest wave height reductions are seen behind West Belle Headland.

North of Port Fourchon

The area north of Port Fourchon where restoration projects were modeled in Alternatives 2 and 3 was mostly shallow open water in the FWOA alternative. Most of the existing wetlands disappear by 2050 in FWOA, a loss of nearly 600 acres, in both environmental scenarios (Figure 65). In Alternatives 2 and 3, wetlands were constructed that largely fill in the open water areas creating over 4,000 acres of wetlands. Less than 400 acres are lost within the project areas by 2050 in both environmental scenarios for the restoration alternatives, with the loss concentrated at the southeast and northern edges (Figure 66). Like Alternative 4 west of Port Fourchon, loss of constructed project area is likely limited due to the large amounts of interior wetland created. Interior wetlands are protected from open water wave attack, decreasing the overall edge erosion.

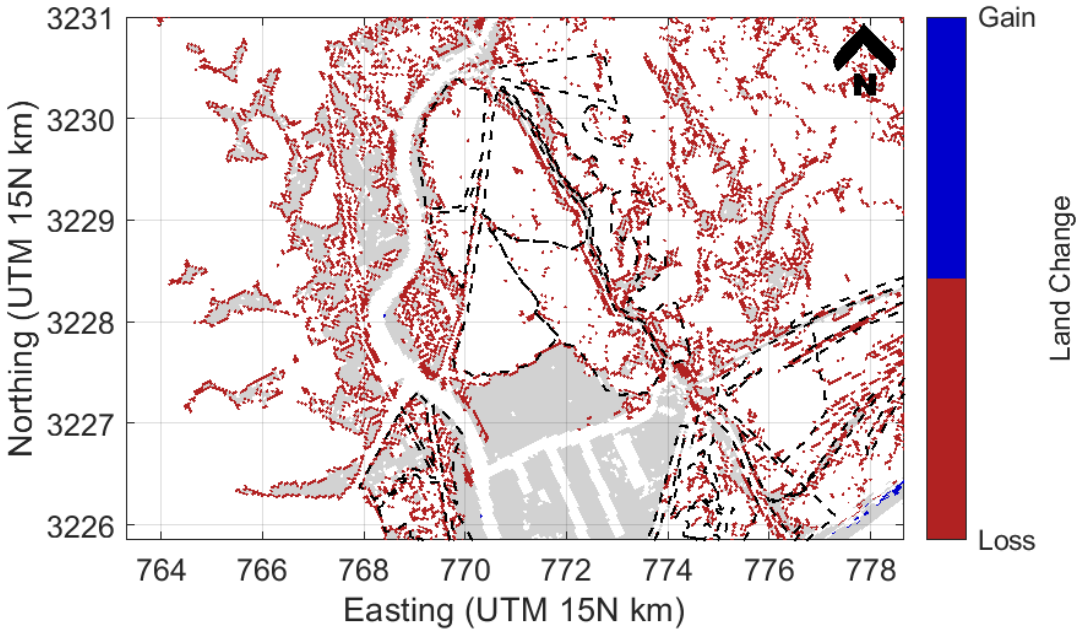

Figure 65. FWOA land change from 2020 to 2050 in the area of the wetland creation polygons to the west of Port Fourchon. Dashed lines show the locations of projects that were modeled in the other alternatives. Approximately 550 acres are lost in the project areas during the simulation.

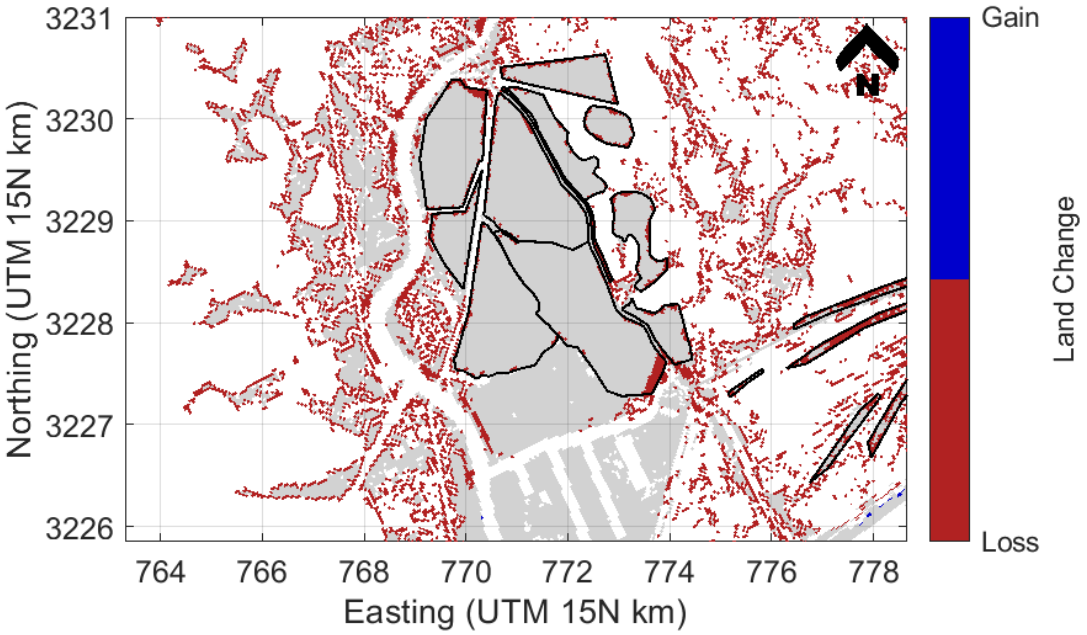

Figure 66. Land change to the north of Port Fourchon from 2020 to 2050 with Alternative 2 and 3 projects constructed. This model run used the lower SLR and storminess model scenario; the land change seen in the higher SLR and storminess scenario is similar (not shown). Approximately 380 acres are lost in the project areas during the simulation.

The total habitat area (4,941 acres for Alternative 2 and 3) was a net sink of GHG emissions from years 2020 to 2050 with a range of -0.03 to -0.09 MMT CO_2e (Figure 67). Because these restored wetlands remain largely intact (with little conversion to open water habitats), the net GHG emissions captured at 2050 was estimated at -0.03 MMT CO_2e for Alternatives 2 and 3. The area of wetlands was projected to be dominated (range between 76-86% over time) by brackish and saline marshes.

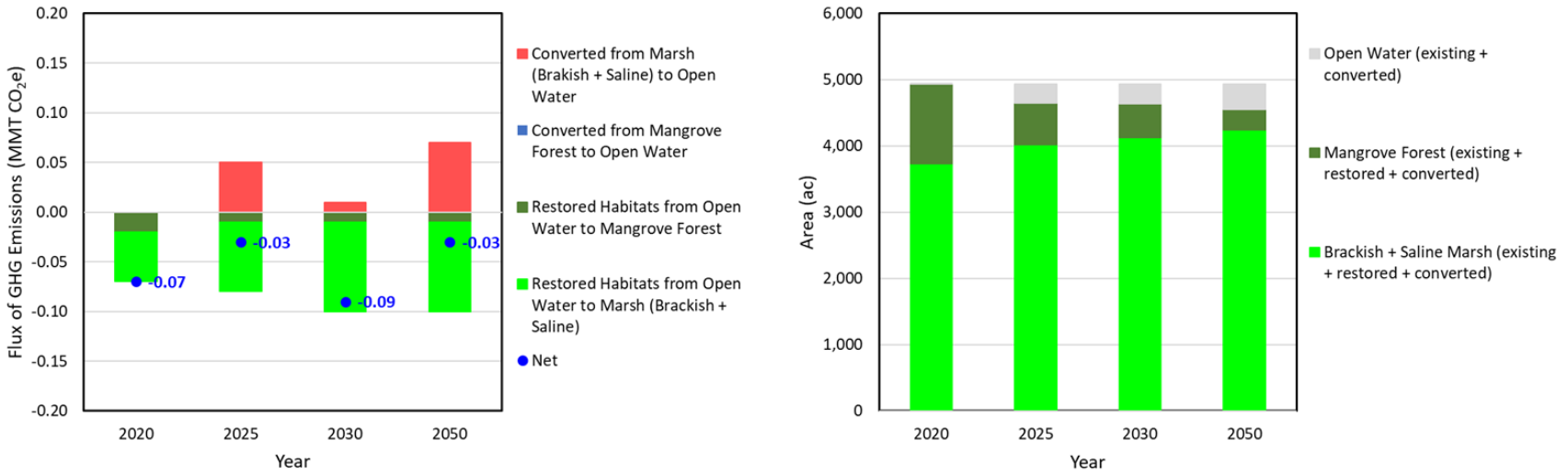

Figure 67. Modeled net GHG flux and wetland habitat areas (mangrove forest and marshes) at snapshot years of 2020, 2025, 2030, and 2050 of Alternatives 2 and 3 in the North of Port Fourchon area. Positive net GHG flux values represent a source and negative values represent a net sink. The total habitat area (4,941 acres for Alternative 2 and 3) was a net sink of GHG emissions from years 2020 to 2050 with a range of -0.03 to -0.09 MMT CO_2e. Because these restored wetlands remain largely intact (with little conversion to open water habitats), the net GHG emissions captured at 2050 was estimated at -0.03 MMT CO_2e for Alternatives 2 and 3.

The peak and time-averaged water level impacts associated with Alternatives 2 and 3 wetland creations depends on the storm direction, landfall location, and proximity. Storm 34, which makes landfall in Barataria Basin has increased peak and time-averaged water levels near the Port in Alternative 2 and 3 (Figure 68). Storm 67, which makes landfall west of the Port, has lower peak water levels and unchanged time averaged water levels in Alternative 2 and 3 (Figure 69). Storms 60 and 149 also show lower peak water levels. Storm 248 shows a mixture of higher and lower peak water levels across the projects. Storm 531, which also makes landfall to the east of Port Fourchon, shows the greatest increase in peak water levels of all modeled storms (about 0.25 m). Similar to results for the projects west of the Port, there is also potential for these projects to retain more water introduced to the basin during storms for longer periods when compared to open water, resulting in higher average water levels during storms (Figure 70). Decreases in both peak and time-averaged wave heights from 5 to 25 cm are observed all modeled storms (Figure 71). The storm effects are very similar in both 2020 and 2050 model years because the projects remain intact.

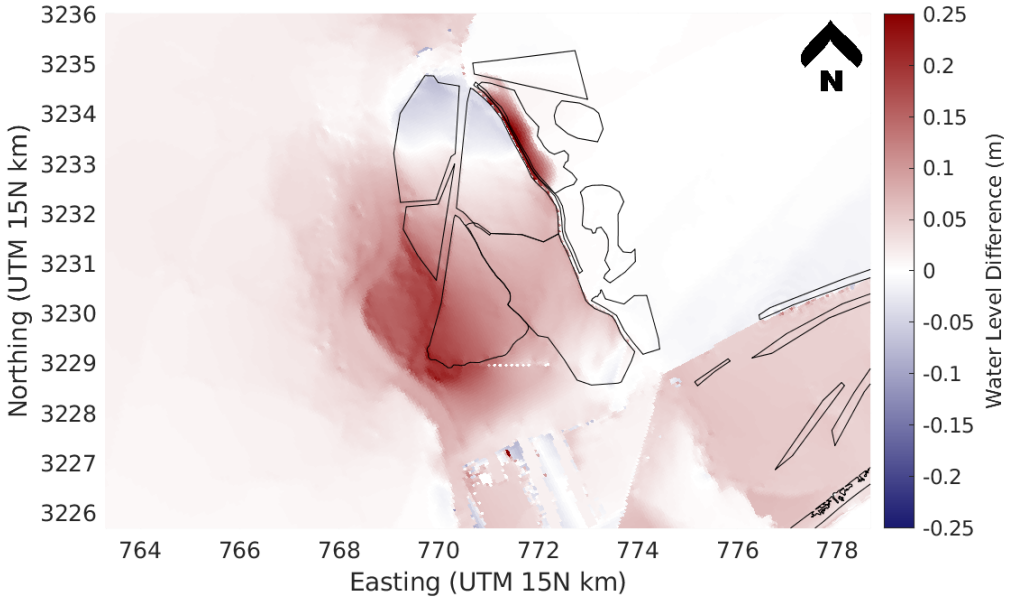

Figure 68. Peak water level difference for Alternatives 2 and 3 compared with FWOA for the base environmental scenario during Storm 34 in 2050. Blue areas indicate where water levels are lower compared with FWOA. Red areas indicate where water levels are higher compared with FWOA. Storms that make landfall to the east of the Port have higher peak water levels with these projects in place.

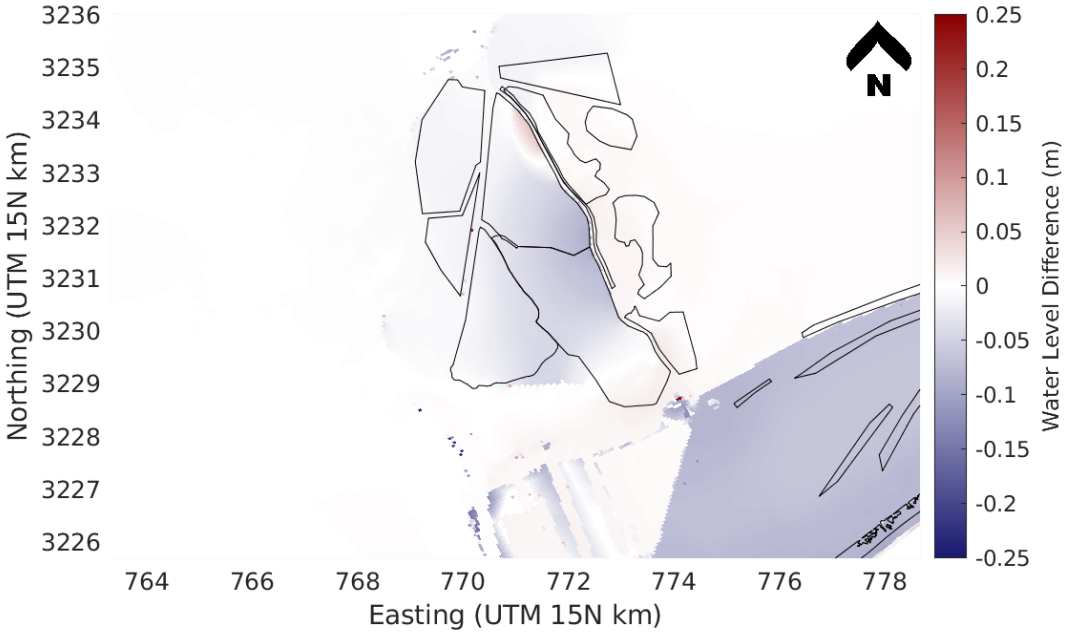

Figure 69. Peak water level difference for Alternatives 2 and 3 compared with FWOA for the base case environmental scenario during Storm 67 in 2050. Blue areas indicate lower water levels compared with FWOA. Red areas indicate higher water levels compared with FWOA. Storms that make landfall west of the Port have lower peak water levels with these projects in place.

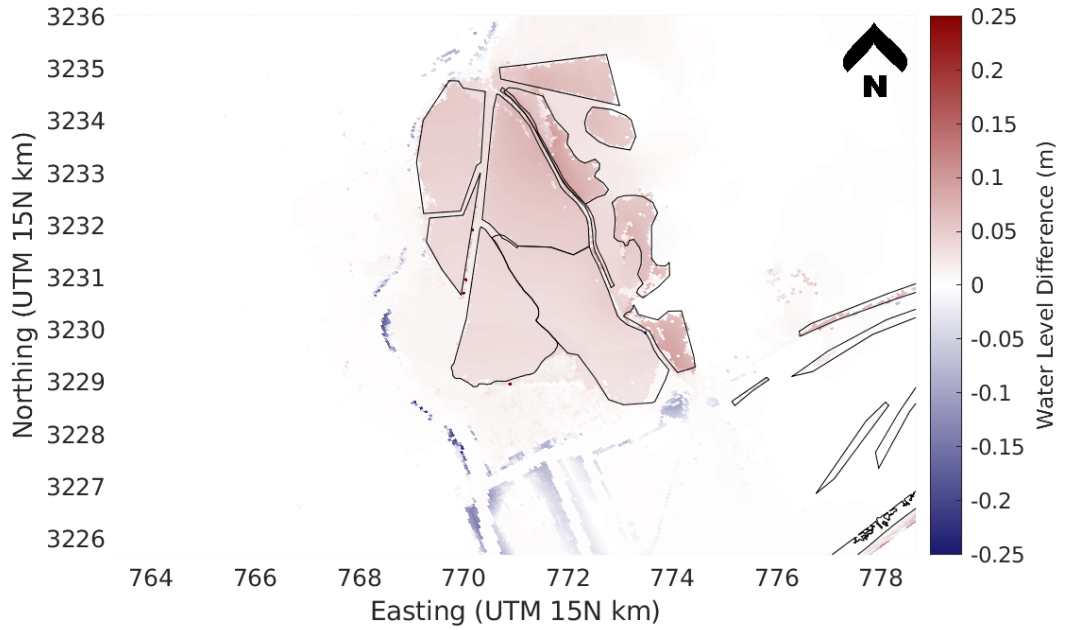

Figure 70. Time averaged water level difference for Alternatives 2 and 3 compared to FWOA for the base case environmental scenario during Storm 34 in 2050. Blue areas indicate lower water levels compared with FWOA. Red areas indicate higher water levels compared with FWOA. Higher time-averaged water levels in project areas are expected because open water drains faster than wetland areas.

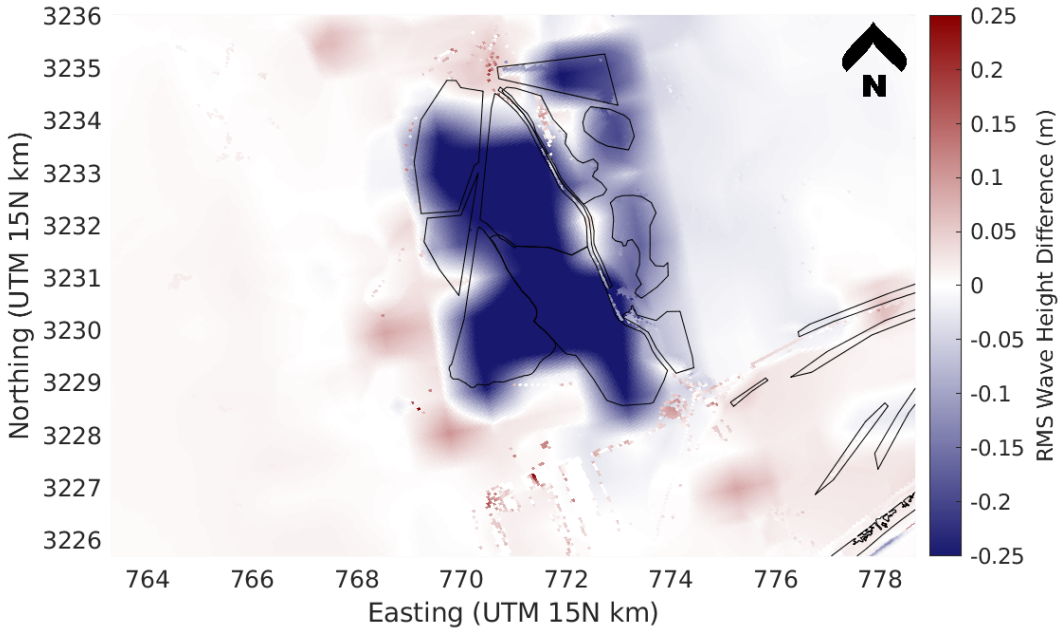

Figure 71. Peak wave height difference for Alternatives 2 and 3 compared with FWOA for the base case environmental scenario during Storm 34 in 2050. Blue areas indicate where wave heights are lower compared with FWOA. Red areas indicate where wave heights are higher compared with FWOA. Decreases in both peak and time-averaged wave heights from 5 to 25 cm are observed all modeled storms.

East of Port Fourchon

Two different geometries of restoration were modeled for East of Port Fourchon: broad wetland polygons (Alternative 5), which are located closer to the Port, and narrow linear wetland polygons (Alternative 6) near LA 1 and along existing ridges. Because the material available for construction is mostly finer sediments that will not stack at high angles, it is not possible to construct high, narrow ridges; thus, Alternative 6 wetlands were constructed to the same height as all other modeled wetland restoration projects. In the FWOA alternative, about 250 acres of land is lost in the area in which Alternative 5 would have been constructed, and about 230 acres is lost where Alternative 6 wetlands would have been constructed (Figure 72). Alternative 5 creates nearly 1800 acres of wetlands, but by 2050, more than 250 acres are lost in both environmental scenarios (Figure 73). Land loss occurs around the edges of project areas and especially closer to open water areas. Alternative 6 created about 320 acres of land and lost about the same amount of land area as was created in both environmental scenarios (Figure 74). These linear features have a larger proportion of edges to interior wetland and thus were more susceptible to edge erosion compared to most other restoration projects modeled.

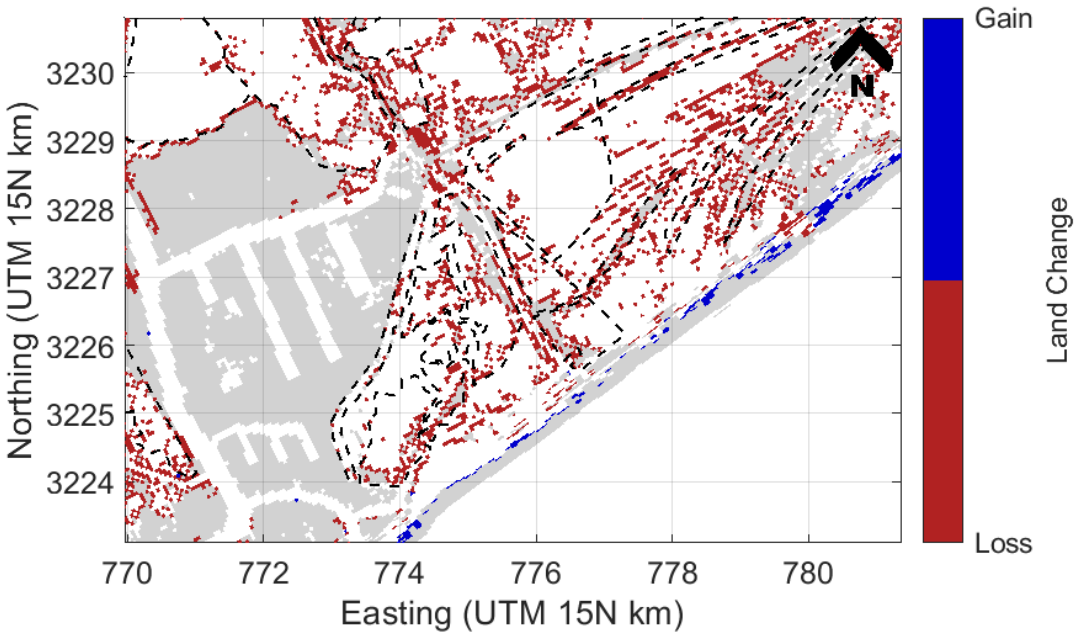

Figure 72. Land change in the FWOA alternative for the area to the east of Port Fourchon in the base case environmental scenario. Dashed lines represent the wetland creation projects modeled in the other alternatives. Approximately 475 acres are lost between 2020 and 2050 in the areas of Alternative 5 and Alternative 6 during the simulation.

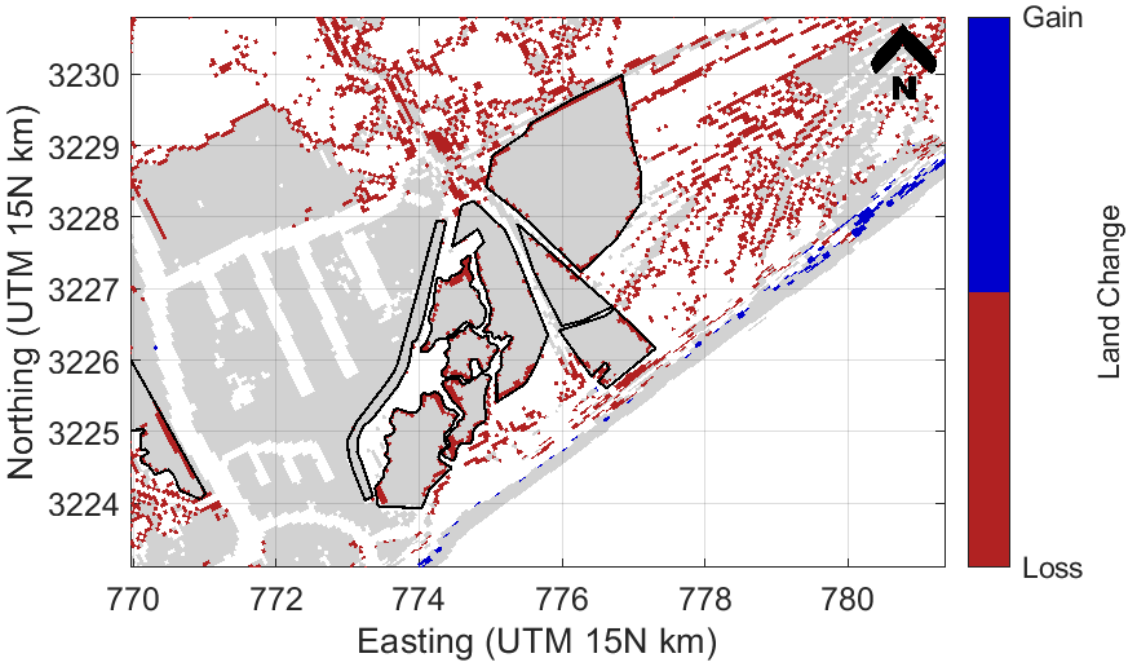

Figure 73. Land change for 2020 to 2050 for Alternative 5 wetlands creation to the east of Port Fourchon for the base case environmental scenario. Approximately 250 acres are lost during the simulation.

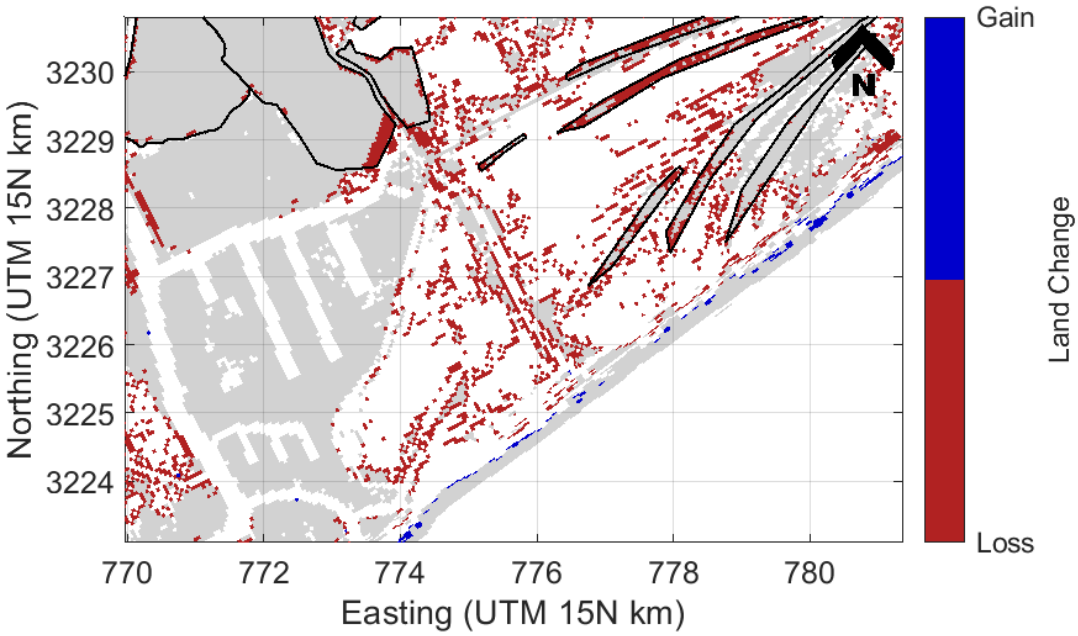

Figure 74. Land change for Alternative 6 wetlands for 2020 to 2050 to the east of Port Fourchon for the base case environmental scenario. Approximately 305 acres are lost during the simulation.

The habitat total area (Alternative 5, 2356 acres) referred to as the broad wetlands were a net sink of GHG emissions from years 2020 to 2050 with a range of -0.02 to -0.05 MMT CO_2e (Figure 75). These wetlands were co-dominated by mangrove forests and brackish and saline marshes that largely remained intact (with relatively little conversion to open water habitats) over time and thus at year 2050, it was estimated that this Alternative 5 was a net GHG sink of -0.02 MMT CO_2e.

Alternative 6, the linear wetlands, had a lower habitat total area (697 acres) compared to the other five alternatives. This habitat area was estimated to be a net sink of GHG emissions (-0.01 MMT CO_2e) at year 2020 (Figure 75). With continual wetland edge erosion from 2025 to 2050, the habitat area had a high proportion of wetlands converted to open water habitats, thus driving a loss of stored carbon from the aboveground biomass and the soils and creating a source of GHG emissions into the atmosphere (see red bars in the left bottom panel of Figure 75). Therefore, this habitat area with the linear wetlands was projected to switch from a net GHG sink at year 2020 to a net GHG source at years 2025 to 2050, with a range of +0.01 to +0.08 MMT CO_2e (Figure 75). These wetlands were projected to mainly be dominated by brackish and saline marshes overtime with mangrove forest area decreasing from 2020 to 2050 (Figure 75).

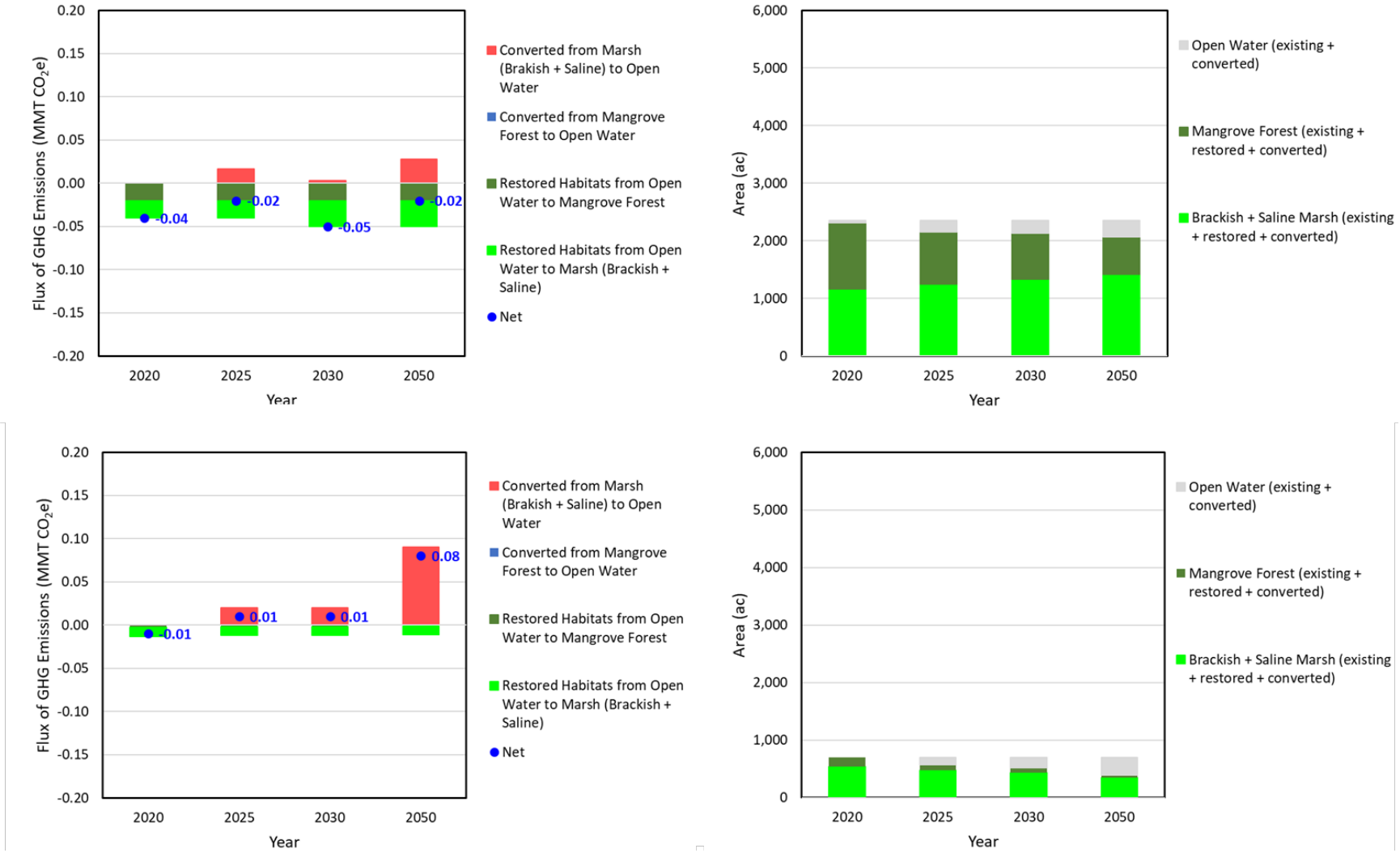

Figure 75. Modeled net GHG flux and wetland habitat areas (mangrove forest and marshes) at snapshot years of snap shot years of 2020, 2025, 2030, and 2050 of Alternatives 5 (broad wetlands, top panels) and 6 (linear wetlands, bottom panels) in the East of Port Fourchon area. Positive net GHG flux values represent a source and negative values represent a net sink. The habitat total area (Alternative 5, 2356 acres) referred to as the broad wetlands were a net sink of GHG emissions from years 2020 to 2050 with a range of -0.02 to -0.05 MMT CO_2e.

Reduced storm surge and wave height benefits are not clearly recognized from the Alternatives 5 and 6 east of Port Fourchon. In Alternative 5 increased water levels are observed in both 2020 and 2050 for both the peak and time averaged (not shown) water levels (Figure 76; Figure 77). This is the case for Storm 34 (Figure 76), Storm 67, and Storm 149 (not shown) in 2020; however, some storm surge reduction is observed in 2050 during Storm 67 (Figure 78), Storm 149, and Storm 248 (not shown). In Alternative 6, when the projects are first built in 2020, peak water levels are increased during Storm 34, but are similar to the FWOA values for all other storms. By 2050, peak water levels are increased during Storm 34 and Storm 531, but decreased during Storm 60, Storm 67, and Storm 149.

Wave heights are reduced by up to 0.25 m within the project footprint for Alternative 5 even when surge heights are increased; however, where increased water levels are observed near the project footprint, wave heights increase (Figure 80). This effect is observed in both in 2020 and 2050 cases; overall higher water levels in the less optimistic environmental scenario, compared to the base case, result in the projects having less effect on wave heights by 2050. Wave height reductions by Alternative 6 are minimal, at best, for all storms in 2050, in both environmental scenarios; in some cases, wave heights are increased, likely due to increased water depths associated with higher surge allowing larger waves to propagate through the area (Figure 81). Slightly better performance in wave height reduction is observed in 2020, when the projects are more intact than in 2050.

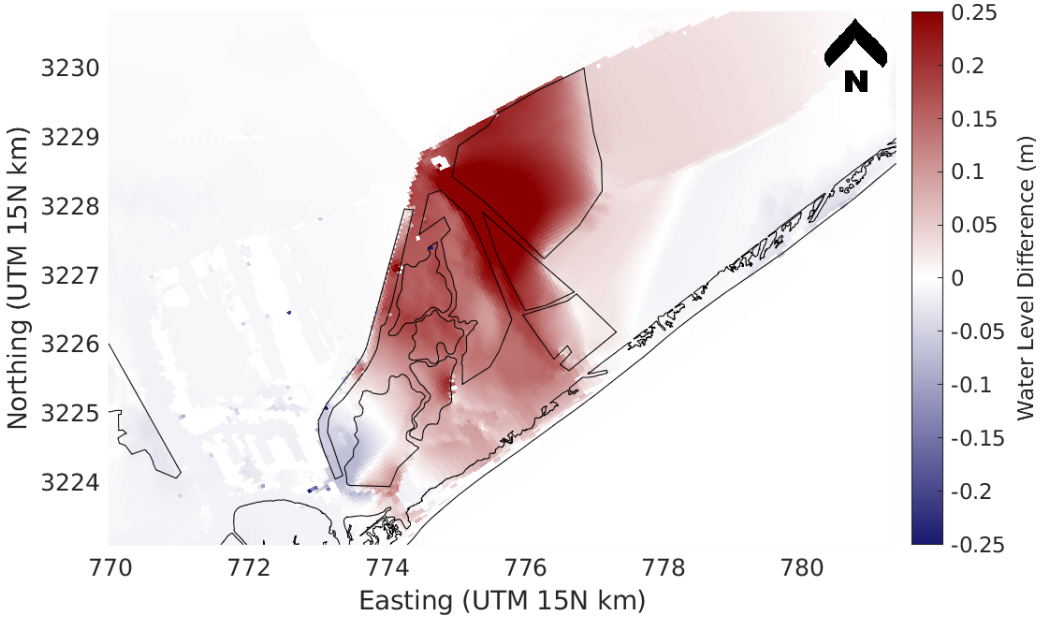

Figure 76. Peak water level difference for Alternative 5 compared to FWOA for the base case environmental scenario during Storm 34 in 2020. Blue areas show where water levels are lower compared with FWOA. Red areas show where water levels are higher compared with FWOA. Higher peak water levels are observed with projects in place in 2020 for Storm 34 (this figure) as well as Storm 67 and Storm 149.

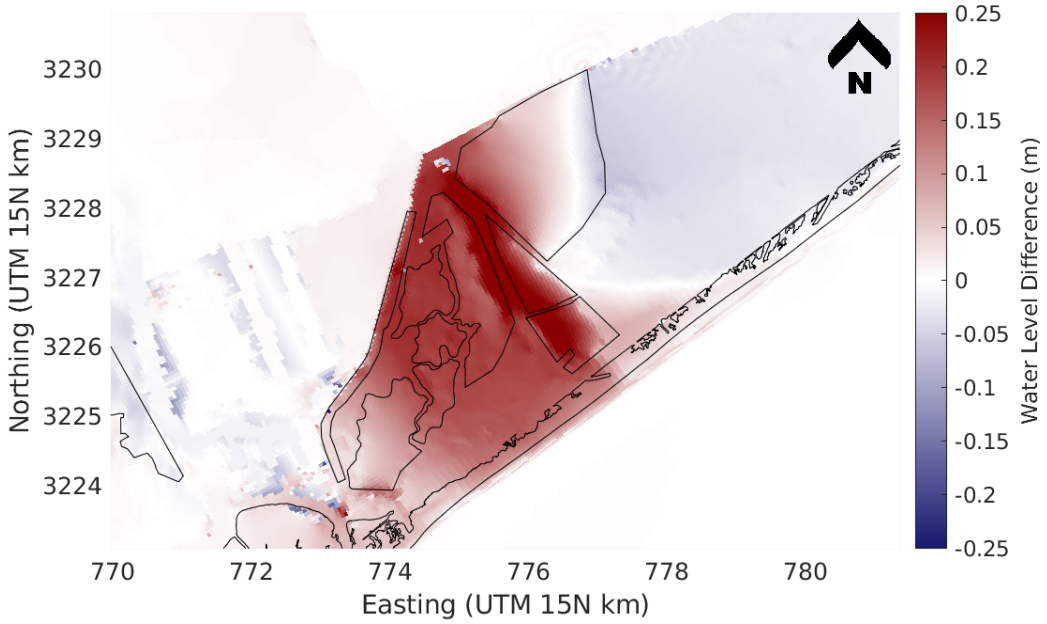

Figure 77. Peak water level difference for Alternative 5 compared with FWOA for the base case environmental scenario during Storm 34 in 2050. Blue areas show where water levels are lower compared with FWOA. Red areas show where water levels are higher compared with FWOA. Higher peak water levels are observed with projects in place in 2020 for Storm 34 (this figure) as well as Storm 67 and Storm 149.

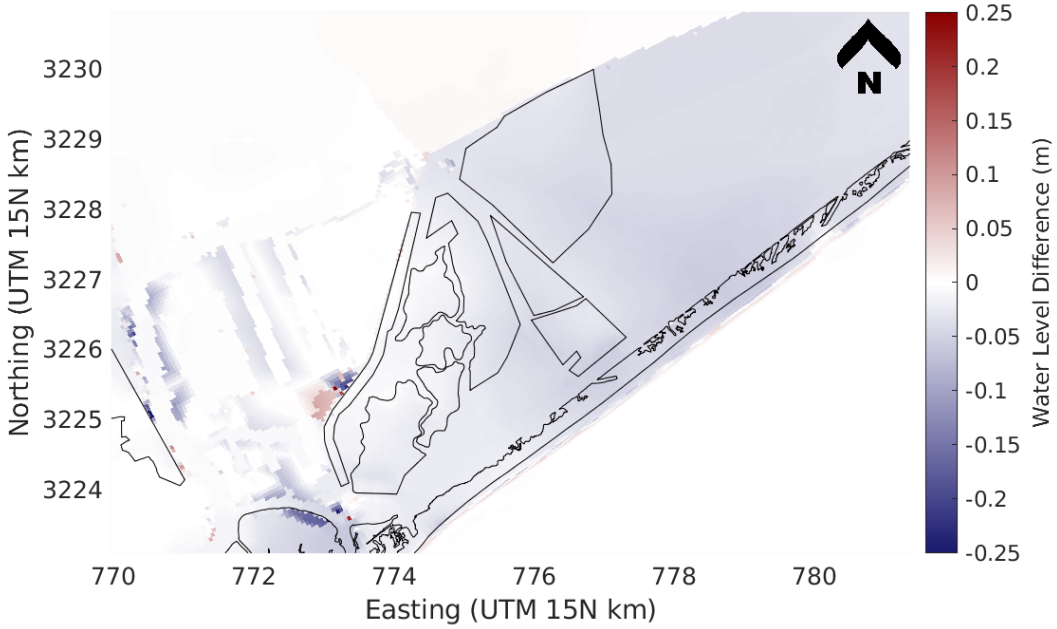

Figure 78. Peak water level difference for Alternative 5 compared with FWOA for the base case environmental scenario during Storm 67 in 2050. Blue areas show where water levels are lower compared with FWOA. Red areas

show where water levels are higher compared with FWOA. Lower peak water levels are observed with projects in place in 2050 for Storm 67 (this figure) as well as Storm 149 and Storm 248.

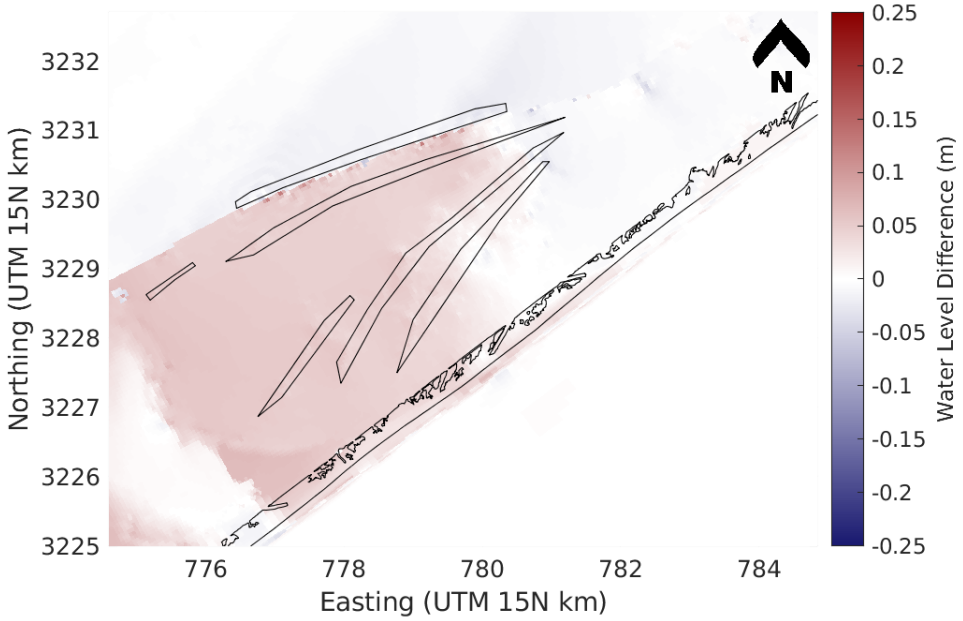

Figure 79. Peak water level difference for Alternative 6 compared to FWOA for the base case environmental scenario during Storm 34 in 2050. Blue areas show where water levels are lower compared with FWOA. Red areas show where water levels are higher compared with FWOA. Peak water levels are higher when projects are built in 2050.

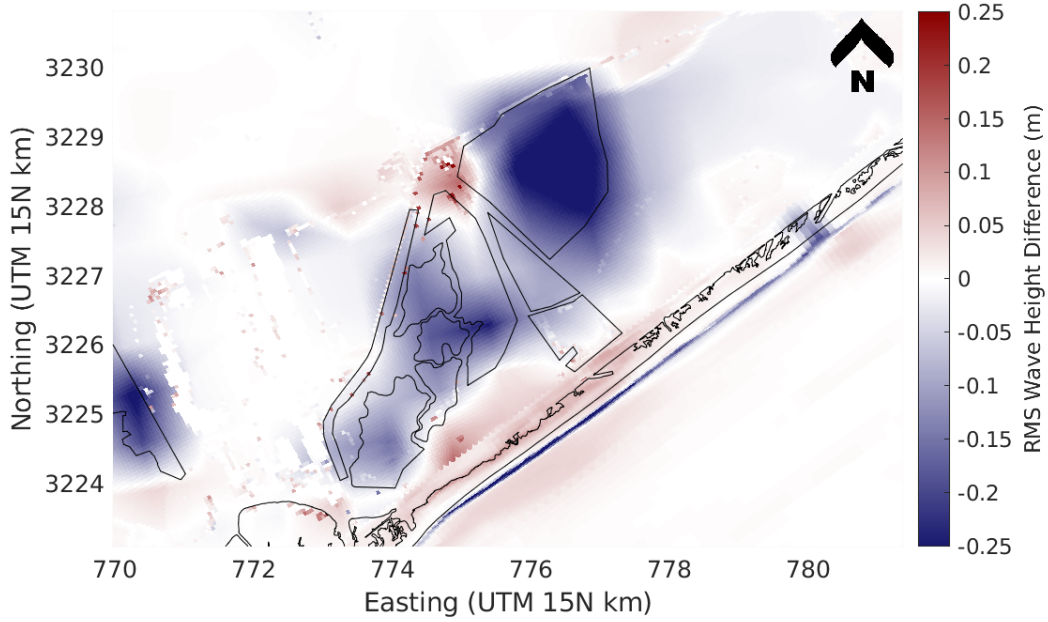

Figure 80. Peak wave height difference for Alternative 5 compared with FWOA for the base case environmental scenario during Storm 34 in 2050. Blue areas show where wave heights are lower compared with FWOA. Red areas show where wave heights are higher compared with FWOA. Wave heights are reduced up to 0.25 m within the project footprint; however, where increased water levels are observed near the project footprint, wave heights increase.

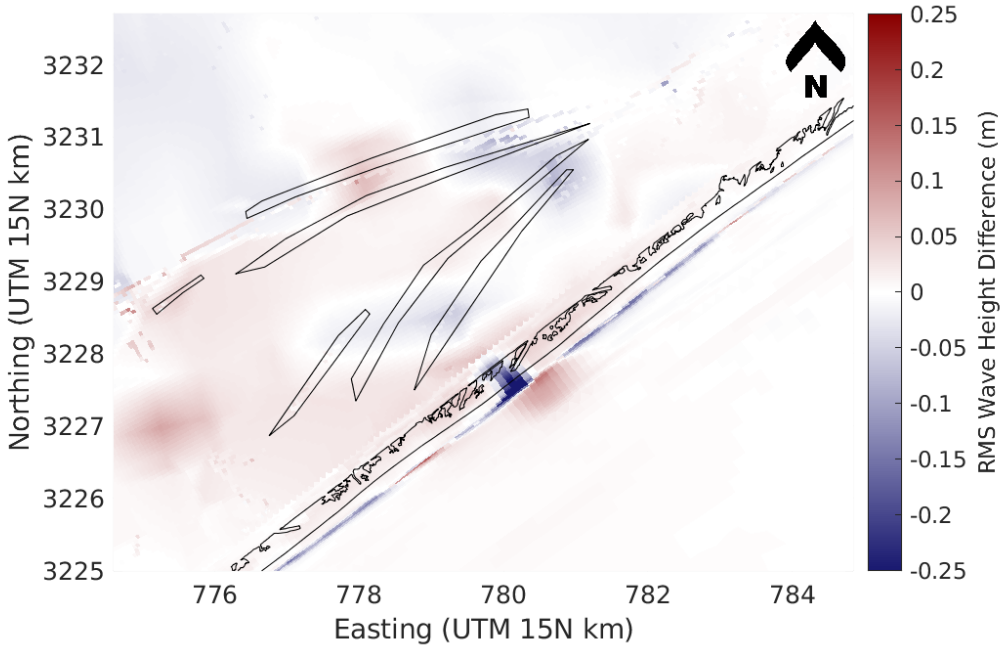

Figure 81. Peak wave height difference for Alternative 6 compared with FWOA for the base case environmental scenario during Storm 34 in 2050. Blue areas show where wave heights are lower compared with FWOA. Red areas show where wave heights are higher compared with FWOA. Wave height reductions are minimal Storm 34 (this figure) and for all storms in 2050. Wave heights are increased when increased water depths associated with higher surge allowing larger waves to propagate through the area.

Leeville

Restoration projects near Leeville (Alternative 1) both nourish existing wetlands and create new wetlands in open water. These projects create over 1,200 acres of land compared to the FWOA alternative (Figure 82) and result in about 1,140 additional acres of land within the project footprints in 2050; however, these wetlands do not persist on the landscape to 2050 as well as other alternatives modeled (Figure 83). The total wetland lost in the FWOA case is about 130 acres. In Alternative 1, more land is lost than in the FWOA (about 230 acres), likely because construction in open water with only fragments of existing wetlands increased the amount of wetlands able to be lost at this location. The creation of additional wetlands in this area does not result in long-term land gain in the model. Some smaller areas of wetland creation are almost entirely lost over 30 years. The wetland creations east and west of Bayou Lafourche perform similarly, each losing about 18% of the constructed wetland area by 2050.

The total habitat area of Alternative 1 was estimated to be about 1,421 acres and a net sink of GHG emissions (-0.02 MMT CO_2e) at year 2020 due to the brackish and saline marshes (Figure 84). At year 2025, it was projected that some of that marsh area would be lost to open water habitat and subsequently the carbon from the vegetation and soils would be lost to the atmosphere (Figure 84), resulting in net zero GHG emissions. However, over time more marsh area would be lost and converted to open water habitats and at year 2050, the habitat total area was projected to be a net GHG source of +0.05 MMT CO_2e (Figure 84).

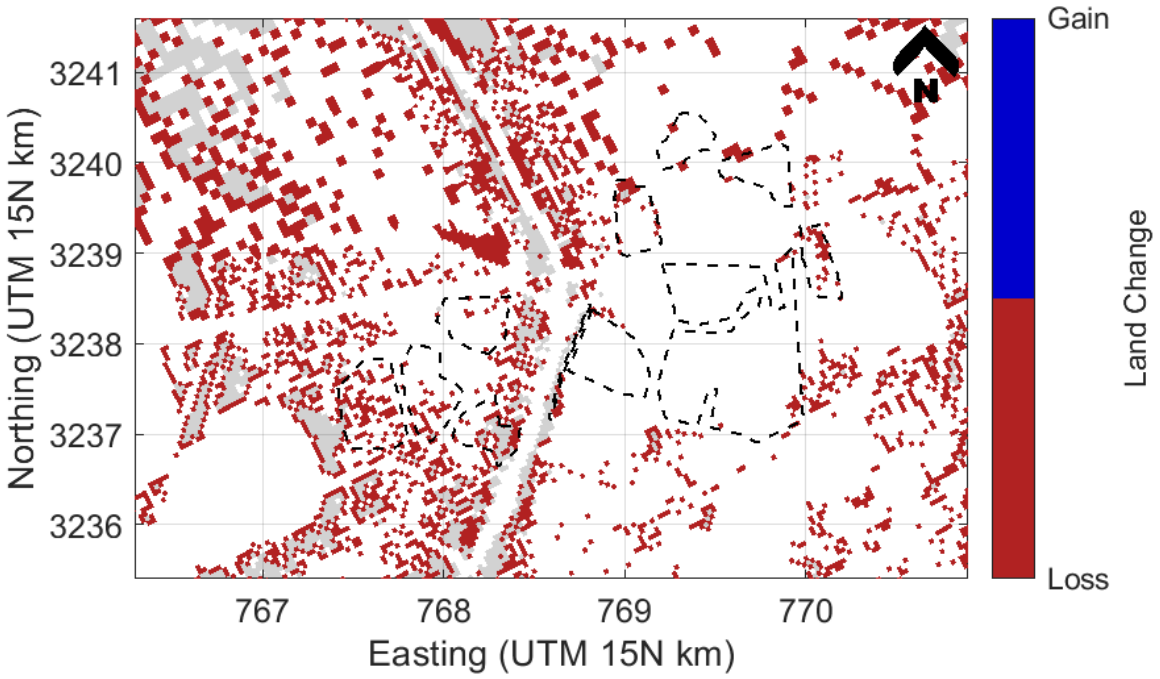

Figure 82. Land change near Leeville in the FWOA alternative from 2020 to 2050 for the base case environmental scenario. Dashed lines show the projects modeled in other alternatives. Approximately 120 acres are lost in the project areas during the simulation.

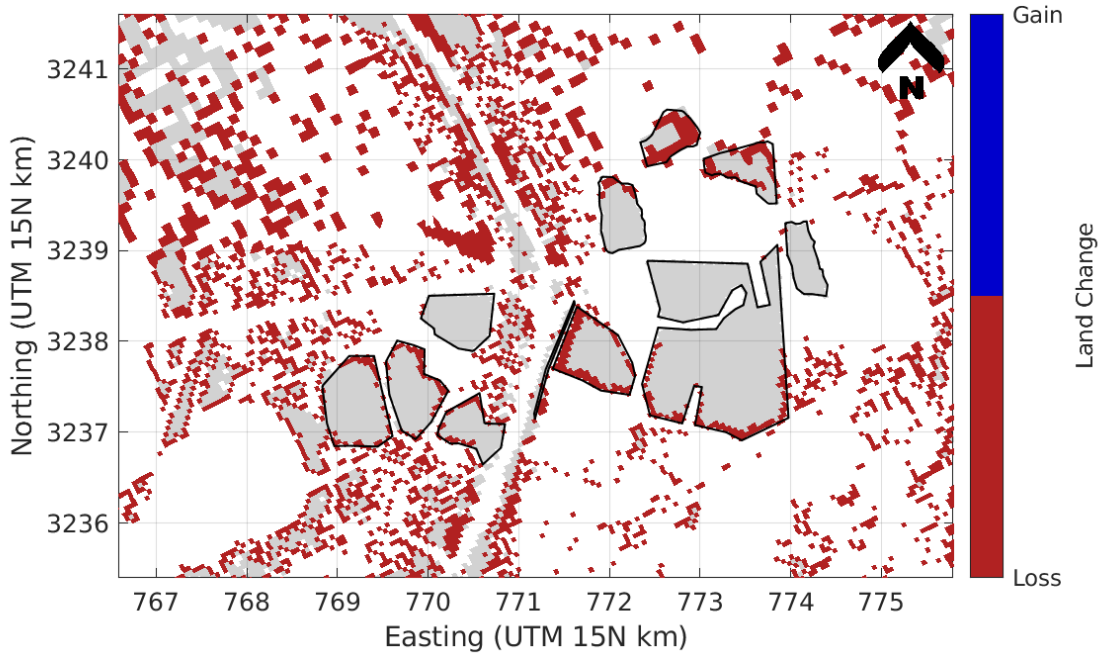

Figure 83. Land change near Leeville from 2020 to 2050 for modeled wetland restoration (Alternative 1). Approximately 225 acres are lost in the project areas during the simulation.

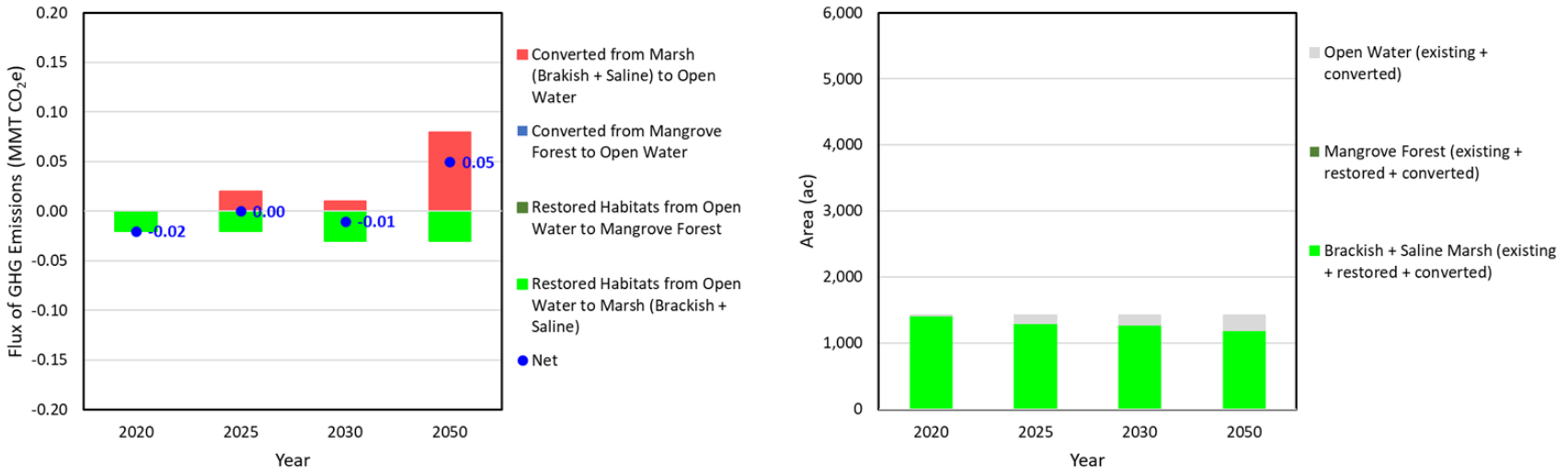

Figure 84. Modeled net GHG flux and wetland habitat areas (mangrove forest and marshes) at snapshot years of 2020, 2025, 2030, and 2050 of Alternative 1 in the North of Leeville area. Positive net GHG flux values represent a source and negative values represent a net sink. The total habitat area of Alternative 1 was estimated to be about 1,421 acres and a net sink of GHG emissions (-0.02 MMT CO_2e) at year 2020. Since more marsh area would be lost and converted to open water habitats and at year 2050, the habitat total area was projected to be a net GHG source of +0.05 MMT CO_2e.

There is not a consistent reduction in storm surge heights and wave heights resulting from construction of Alternative 1. The magnitudes of the effects are generally small and localized to the project areas. The largest effects are observed for Storm 34 and Storm 531, which both make landfall to the east of the Port (Figure 85). Both peak and time-averaged water levels are higher for these storms than the FWOA alternative. During storm 67, there is less than 5 cm of reduction in water levels in both 2020 and 2050 (Figure 86). Additionally, because vegetated marsh drains more slowly than open water areas, time-averaged water levels can be increased by these projects (Figure 85). Wave height is more often generally reduced by these wetland restorations but can be increased in the vicinity of these projects, likely due to increased water depths associated with increased surge heights as well as increased sediment trapping and retention of the restored wetlands (Figure 87). Similar wave height effects are observed for all storms in 2020 and 2050 and for both environmental scenarios.

Figure 85. Peak (left) and time averaged (right) water level difference for Alternative 1 projects compared with FWOA for the base case environmental scenario in 2050 during Storm 34. Blue areas indicate where water levels are lower compared with FWOA. Red areas indicate where water levels are higher compared with FWOA. Both peak and time averaged water levels are higher for this storm, with minimal reduction in peak water level to the northwest of the project area.

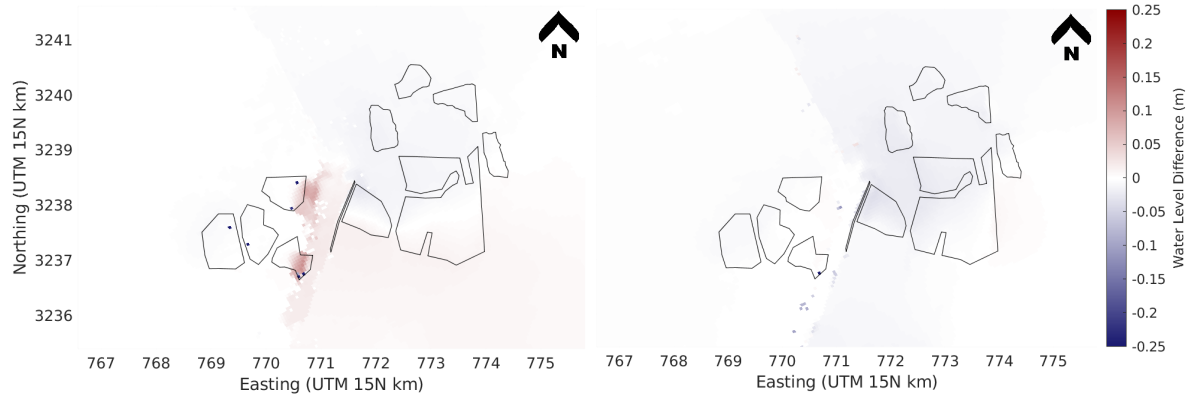

Figure 86. Peak water level difference for Alternative 1 compared with FWOA for the base case environmental scenario during Storm 67 in 2020 (left) and 2050 (right). Blue indicates where water levels are lower compared with FWOA. Red areas indicate where water levels are higher compared with FWOA. These project areas show very little (<5 cm) effect on peak water levels compared to FWOA.

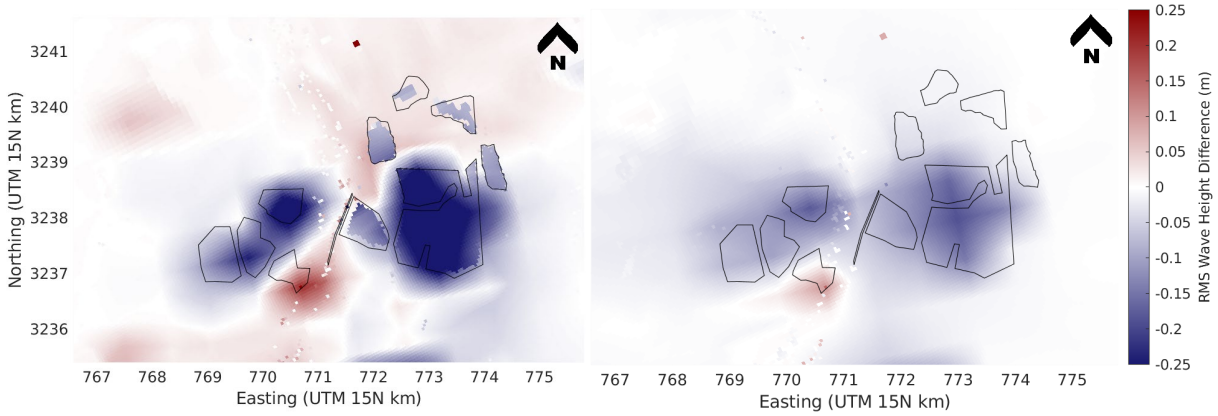

Figure 87. Peak wave height difference for Alternative 1 compared to FWOA for the base case environmental scenario during Storm 34 (left) and Storm 67 (right) in 2050. Blue areas indicate where wave heights are lower compared with FWOA. Red areas indicate where wave heights are higher compared with FWOA. Wave height reductions within in the project footprints are common, but increased water heights near the projects are also common.

Table 25. Summary of land change by project alternative for the time period 2020 – 2050. Acres of 2020 land includes the acres built by the alternative. Acres of land created is defined as acres of land that is newly above mean low water after construction of the project.

Project Alternative	2020 Land (acres)	Land Created for Alternative (acres)	2020 – 2050 Change: Scenario 1 (acres)	2020 – 205 Change: Scenario 2 (acres)
1	1419	1256	-226	-232
2	2539	2125	-238	-248
3	2397	1977	-144	-151
4	1663	987	-167	-178
5	2320	1784	-249	-261
6	697	315	-305	-319

PROJECT ALTERNATIVES COST EVALUATION

In order to define the set of characteristics necessary to estimate project costs and to insert project alternatives into the modeling suite, a series of assumptions was required. These assumptions characterize the shape and elevation of the features, the methods for estimating dredge fill volumes, and the geotechnical properties of the sediment and underlying soils in borrow and placement areas, which impact settlement, subsidence, and cut/fill dredging ratios. A summary of the assumptions and rational behind each assumption is presented in this section.

Typical Section

There are a number of other restoration projects that have been conducted within the study area, as detailed in Table 2. Design materials from projects BA-0193, BA-0194, TE-0134, and TE-171 were consulted in the analysis and were reviewed to confirm the expected behaviors of the borrow sediment and design characteristics of the fill areas. In general, fine grained, cohesive sediments conducive to wetland restoration are expected. As such, all projects analyzed were assumed to conform to the typical section shown in Figure 88, with a design elevation, containment dikes, and interior containment dike borrow channels. All geometries in Figure 88 are for illustrative purposes.

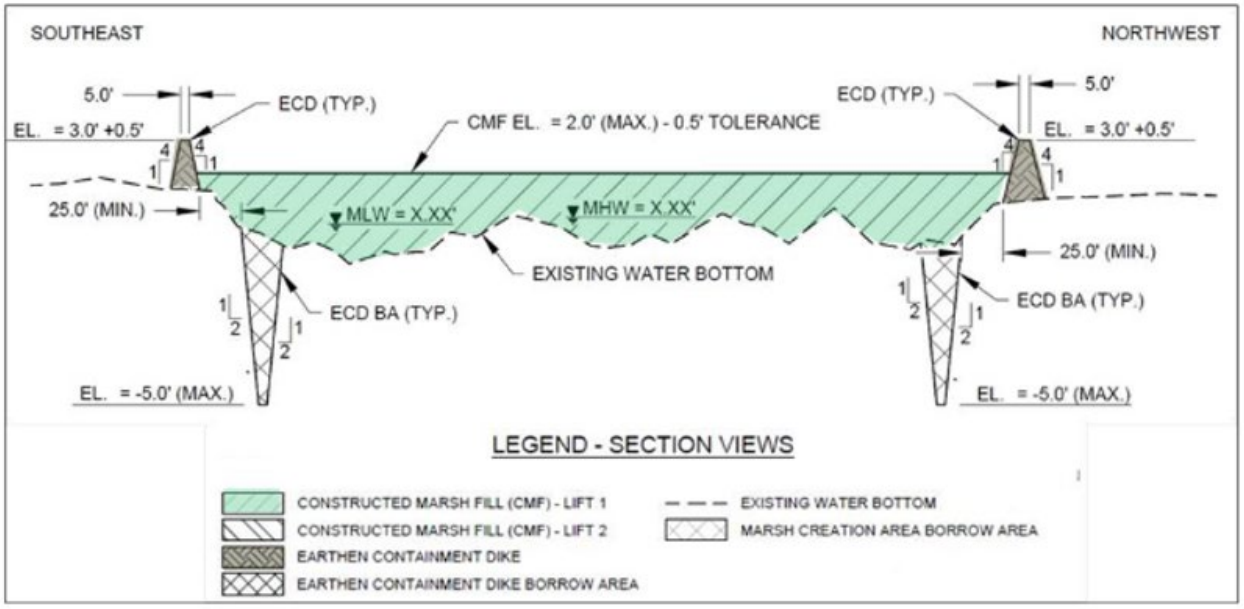

Figure 88 Wetland creation typical section. All elevations and dimensions are for illustrative purposes only. Project-specific geometries are discussed later in this document. Adopted from CPRA's Marsh Creation Design Guidelines (Coastal Protection and Restoration Authority, 2017).

Sediment Properties at the Borrow and Fill Areas

Due to the varied nature of the proposed wetland fill areas, simplifying assumptions were made concerning the geotechnical properties of available wetland fill material. Of the nearby projects, the East Leeville Marsh Creation project (BA-0194) had borrow area characteristics with the greatest similarity to what may be expected from dredging of the Port Fourchon water bottoms, consisting of very soft clays, silty clays, organic materials, and sparse amounts of very fine sands (GeoEngineers LLC, 2018).

Proximal project geotechnical investigations and design reports were used to inform assumptions for constructed wetland elevation, the settled year 5 elevation of the restored wetland, and the cut/fill ratio for the dredged material (often more borrow is required to be dredged than the volume of the receiving area to account for issues such as sediment losses in transport and settlement of the underlying soils due to the placed overburden). Averaged values were used to inform both cost estimation of the projects as well as how the projects were inserted into the model DEMs at the initiation of model runs. A summary of how each table element was used in project definition is shown in Table 26 and Table 27 below.

Constructed elevation and cut/fill ratio: Constructed elevation was used in conjunction with GIS analysis of existing topography and bathymetry of the project polygons to generate estimates of dredge fill quantities for wetland restoration areas. Initial 1:1 fill volume estimates were then increased by the cut/fill ratio to account for losses in the dredging process and the consolidation of underlying soils which occurs under the weight of placed material, causing volume losses in the fill template. Constructed elevations implicitly account for RSLR as well as local geotechnical conditions since they are averaged from multiple nearby projects' geotechnical investigations.

Year 5 elevation: Since the model runs occurred at 5-year timesteps over the 30-year planning horizon and because the modeling suite was unable to represent the drastic post-construction self-weight consolidation and settlement of wetland fill areas, the projects were inserted into the DEM at the 5-year post-construction elevations from settlement curves found in the project design reports for BA-0171, BA-0193, BA-0194, and TE-0134 (Ardaman & Associates, 2018c, 2018a, 2018b; GeoEngineers LLC, 2018).

Earthen containment dike cut/fill ratio and fill volume per linear foot: Since earthen containment dike fill is typically excavated from the interior of the wetland restoration fill cells as shown in Figure 88, dredged volumes must account for filling the excavated containment dike borrow channels in addition to the wetland fill area itself. This information was used in conjunction with the containment dike length to estimate the additional fill volume required.

Table 26. Fill characteristics used for project costs. All elevations are in ft, NAVD88, geoid 12b.

Design Item	Constructed elevation (first lift)	Year 5 elevation	Cut/fill ratio
Averaged value from existing projects	2.5	1.0	1.23

Table 27. Containment Dike characteristics used for project costs. All elevations are in ft, NAVD88, geoid 12b.

Design Item	containment dike top elevation	cont. dike side slope H:V	cont. dike cut volume (cy/LF)	cont. dike fill volume (cy/LF)
Averaged value from existing projects	3.9	3.9:1	8.0	5.2

Dredge Fill Volumes

Fill volumes for wetland restoration were calculated by superimposing the constructed elevation from Table 26 over the initial conditions DEM used for the modeling. The volumetric difference in surfaces was then calculated using GIS software. Certain limitations to the fill assumptions were added in the calculation:

All areas within the project polygon less than -5 ft (-1.5 m) NAVD88 (GEOID 12b) were filled to 100%.

Open water areas greater than -5 ft (1.5 m) deep were not filled, as common construction practice in south Louisiana is limited in deeper waters, where containment dike construction becomes increasingly difficult.

Areas with elevations greater than the design elevation had no material placed.

In addition to the GIS-based volume calculation, the GIS lengths of containment dike were multiplied by the cut volume (CY/LF from Table 27 above) since containment dike excavation occurs on the interior of the fill area as shown in Figure 88.

Project Cost Development

Costs were estimated for the proposed wetland restoration areas through two basic methods:

- Direct quantity estimation for materials or discrete construction activities and the application of parametric unit costs to the quantities derived, and
- Percentage-based estimation for cost items that are often labor-related activities an unable to be directly quantified.

These costs are all reported in 2020 dollars and are estimated over a 30-year project expected life.

Unit-based Cost Items

Wetlands creation in open water areas through placement of dredged material and vegetative plantings restore landscape and ecosystem processes and may provide storm surge and wave attenuation in certain cases. The cost of wetland restoration projects in Louisiana is influenced by the type of material to be dredged, the distance from the dredge location to the fill location, fuel costs, and mobilization/demobilization cost (the cost for the contractor to bring equipment to the site before construction and remove all equipment after construction). Mobilization and demobilization cost are influenced by project size, borrow source, dredging distance, pipeline corridor, dredging equipment, and dredging volume. All costs reported are in 2021 dollars. Where necessary, the USACE's Civil Works Construction Cost Index System was used to inflate costs from prior years to present day dollars (USACE, 2021). All costs presented are intended to provide planning level insights under significant uncertainty and are not intended to represent design or bid levels of detail or accuracy. Table 28 below provides a summary description of how each main cost item was calculated.

Table 28. Unit Cost Item Summary

Cost Item	Description of Method
Mobilization and Demobilization Cost	Mobilization and demobilization costs are a function of the type and amount of equipment required to accomplish the construction project. For the wetland restoration projects analyzed, assumptions were made that all work would consist of a 30-inch cutterhead suction dredge, as is typical in inland channel excavation projects in coastal Louisiana. Most dredges' inboard pumps can move material through discharge pipes for a distance, after which, booster pumps are required for increases in incremental pumping distance from the borrow location to the fill location. Cost calculations used standard values from CPRA's 2017 CMP, which assume a dredges onboard pumps can move material through 25,000 ft of pipeline, and each incremental booster pump can move material an additional 15,000 ft. (McMann et al., 2017). Pipeline lengths and types (pre-lay line, pickup line, subline, and pontoon line) used the 2017 CMP's GIS-based estimating rubric, where lengths for each are calculated in GIS and unique to each proposed fill polygon within a project alternative. The costs for the dredge plant, boosters, accoutrement such as marsh buggies and excavators, and all pipeline are then summed for the mobilization and demobilization cost as a lump sum.
Dredge Fill Unit Cost	Fill unit costs, typically reported in dollars per cubic yard ($/CY) for the dredging, transportation, and placement of fill material is the largest cost item for wetland restoration projects. For this planning level analysis, parametric cost relationships from CPRA's 2023 CMP (which is yet to be published), were provided via personal communication with CPRA's CMP team (Heather Sprague, CPRA, personal communications, November 2021). CPRA maintains an internal database of bid tabulations from constructed projects and has built relationships between the unit cost of material (in $/CY) versus the distance to transport the dredged material and type of material (such as offshore sand, Mississippi River sand, interior mixed sediments, etc.). The parametric unit cost relationship has a static base price over a certain initial distance (e.g., within a certain distance, $/CY unit costs remain constant), but then increases with added distance. Unit costs for the 6 alternatives ranges from $5.31/CY to $7.86/CY.
Containment Dike Unit Cost	Containment dikes are employed to capture the dredged slurry within the ordained restoration area and allow the sediments to fall out of suspension, commonly referred to as dewatering. Containment dikes ring the perimeter of the wetland restoration area. Additionally, interior containment dikes are required to avoid deep waterbodies or other areas not desired to be filled, such as oil and gas pipeline corridors, within the wetland restoration area. Perimeter calculations for each wetland restoration area were performed in GIS. Since the analysis is at a planning level, interior containment dikes were not specified for each wetland restoration area; instead, a multiplier of 1.5 was added to the perimeter length to account for interior containment dikes required. A parametric cost relationship of $60.10/LF from CPRA's 2017 CMP (McMann et al., 2017).
Other Miscellaneous Cost	As part of the cost estimation, several other parametric unit costs were employed to account for minor activities or materials required, such as settlement plates ($/plate based on 1 plate per 50 acres of the fill area) and vegetative plantings ($/acre based on planting 60% of the fill area).

Percentage-based Cost Items

Standard industry practice for some cost items for wetland restoration projects is to designate cost estimates based on a percentage of the estimated construction cost. Such cost items include construction surveys, project contingency, engineering and design costs, construction management costs, and operations and maintenance costs. A summary of percentage values employed is provided in Table 29 below.

Table 29. Percentage-based cost items.

Cost Item	Percentage Add-on to Construction Cost	Cost Item Description
Construction Surveys	2.5%	A 2.5% multiplier is applied to the sum of the cost of all construction items except mobilization and demobilization to calculate this cost item, which includes activities related to surveying the borrow and fill areas of the project during construction.
Project Contingency	20%	A 20% multiplier is applied to the sum of the cost of all construction items to calculate this cost item, which is used to capture uncertainties and unexpected costs outside of the quantifiable aspects of the cost estimate.
Engineering and Design	10%	A 10% multiplier is applied to the sum of the cost of all construction items (but before contingency is applied) to calculate this cost item.
Construction Management	5%	A 5% multiplier is applied to the sum of the cost of all construction items (but before contingency is applied) to calculate this cost item.
Operations and Maintenance	5%	A 5% multiplier is applied to the sum of the cost of all construction items (but before contingency is applied) to calculate this cost item, which is related to surveying and monitoring after construction completion.

A detailed breakdown of project costs can be found in Appendix D.

SOCIAL RETURN ON INVESTMENT (SROI) RESULTS

Stakeholders believe that each of the project groupings will generate positive social outcomes overall, although the project alternatives featuring broad wetlands to the east and west of the port are expected to generate the greatest social value (Figure 89). The West of Port Fourchon project grouping is expected to generate the greatest social return, with almost all respondents stating that utilizing the dredge material for marsh creation in this area will result in an increase in saline marsh and mangrove forest habitat areas (Figure 90). As a result, it is anticipated that bird and mammal habitat will increase. Many survey respondents would expect a concurrent improvement in crab, shrimp, oyster, and fish habitat if this area were restored, suggesting that they view these wetland areas as ecological systems supporting both aquatic and terrestrial species. It should be noted that there was not a consensus on this last point, however, with several respondents noting that they believe this project will harm aquatic habitats. Finally in terms of co-benefits, a majority of respondents believe that this project will reduce wave impacts on both fishing camps and oil and gas infrastructure while providing enhanced opportunities for recreation in the area.

The East of Port Fourchon (Broad Marsh) project grouping is expected to have many of the same beneficial outcomes as the West of Port Fourchon project groups with some notable exceptions (Figure 91). Many more stakeholders expect that this project will ultimately harm crab, shrimp, oyster, and fish habitat with a trickledown effect on subsistence, recreational, and commercial fisheries than seen in the West of Port Fourchon results. Conversely, more respondents believe that building marsh in this location will protect more homes, fishing camps, and oil and gas infrastructure than any other project grouping examined here. The additional negative outcomes related to fishers, however, coupled with higher planned construction costs for this area, reduce the overall return on investment for this location (Figure 89).

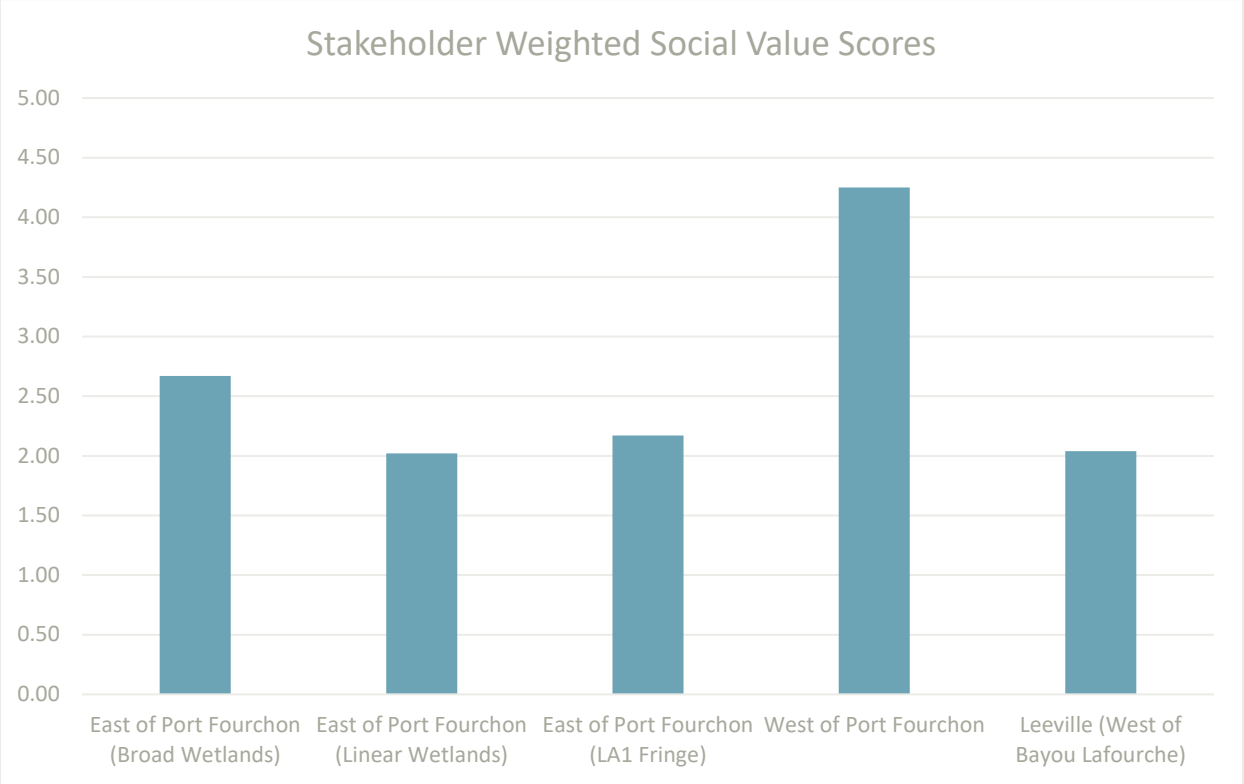

Figure 89. Final stakeholder weighted SROI scores for each project grouping analyzed during stakeholder interviews.

The third broad marsh features project grouping examined in this study was in Leeville (West of Bayou Lafourche). Like the other broad marsh project groupings, survey respondents expect to see an increase in saltmarsh with fewer anticipating an increase in mangrove habitat (Figure 92). Given that this location is the farthest north of the areas surveyed, it is not surprising that fewer stakeholders anticipate improved mangrove forest habitat here. Beyond this, the results for this area are similar to those seen in the East of Port Fourchon (Broad Marsh) project grouping, with many respondents believing that harm to crab, shrimp, oyster, and fish habitat will result from this project, directly impacting subsistence, recreational, and commercial fisheries. Though not a majority, other respondents believe work in this area will directly impact navigability and boating access and will also result in more invasive species in the area. These negative impacts are balanced out however, by a belief that march creation projects constructed in this area will reduce erosion and also protect homes and camps from storm surge. This project grouping is expected to have the greatest cost per acre to build however, resulting in the second lowest social returns on investment among the project groups analyzed (Table 30).

The linear marsh and ridge features, including those immediately adjacent to LA 1 and those further to the east of the proposed broad wetland features, are expected to generate less social value than broader wetland features. In general, the survey results show that the primary anticipated impacts of these projects are on reducing erosion. The East of Port Fourchon (LA 1 Fringe) feature, a proposed linear feature located directly adjacent to LA 1 and Port Fourchon itself, is expected to have the added benefit of reducing wave impacts on oil and gas infrastructure (Figure 93). These protection benefits are seen as

coming at the expense of access to the area for recreational and subsistence fishing. However, even as stakeholders see minimal benefits of these project for the area's coastal fisheries, they recognize that they do have the potential to generate saline marsh and mangrove forest habitats, which are valuable for birds and mammals.

Despite having the lowest planned construction cost per acre, the East of Port Fourchon (Linear Wetlands) project grouping is expected to generate the lowest social return on investment of all the project groupings examined (Table 30). Most stakeholders see this project grouping as having a positive impact on the ecosystem and the wildlife that depend on that ecosystem (Figure 94). Additionally, they recognize that these ridges will result in more saline marsh and mangrove forests and improve bird habitat. They also expect that this project grouping will reduce both daily and storm induced erosion of wetlands, bays, bayous, and canals in the region. However, most respondents do not see this project grouping generating benefits for local residents and communities, nor do they see additional co-benefits to the area's oil and gas infrastructure.

Table 30. Final model input values, outcome values, and stakeholder weighted SROI scores for each project grouping analyzed during stakeholder interviews.

	East of Port Fourchon (Broad Wetlands)	East of Port Fourchon (Linear Wetlands)	East of Port Fourchon (LA 1 Fringe)	West of Port Fourchon	Leeville (West of Bayou Lafourche)
Investment	$239,651,892	$29,367,664	$16,719,252	$107,409,736	$50,099,000
Total Present Value (PV)	$639,262,529	$59,388,542	$36,235,556	$456,494,303	$102,036,393
Net Present Value (PV minus the investment)	$456,758,637	$42,606,478	$23,502,104	$396,020,967	$73,408,393
Social Return ($ return per $ invested)	2.67	2.02	2.17	4.25	2.04

Additional output from the SROI process is provided in Appendix C.

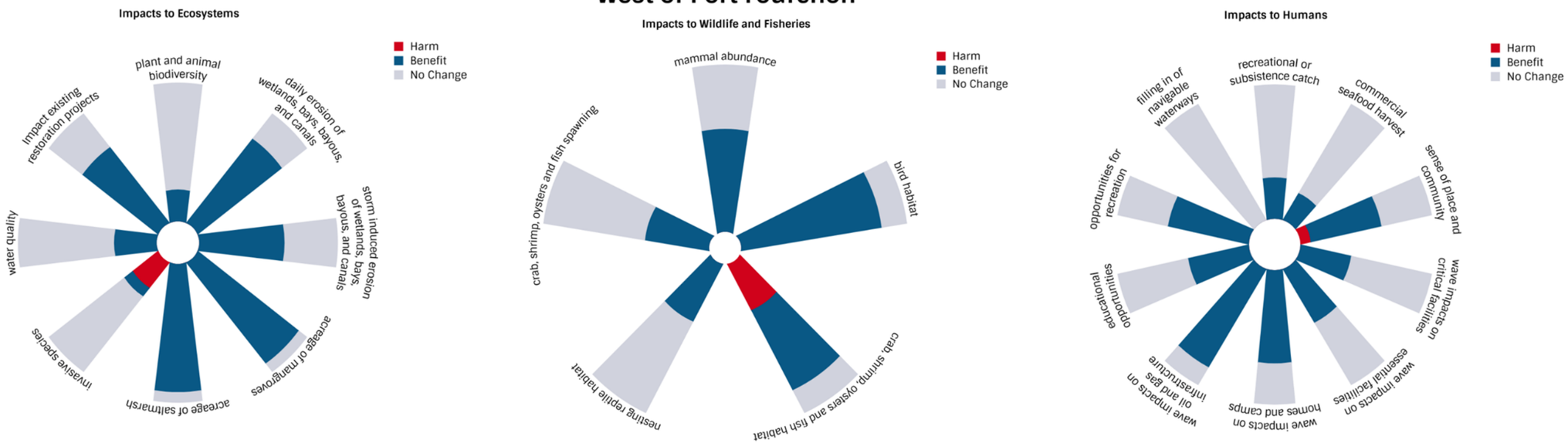

Figure 90. Expected ecosystem, wildlife and fisheries, and human impacts of the West of Port Fourchon project grouping based on survey results

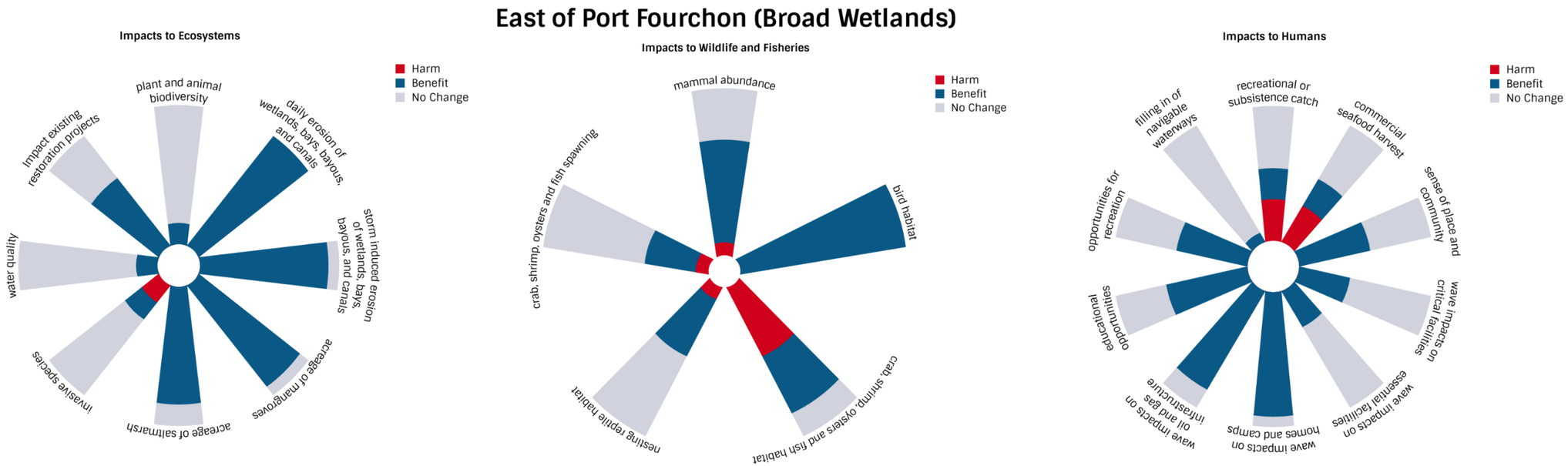

Figure 91. Expected ecosystem, wildlife and fisheries, and human impacts of the East of Port Fourchon (Broad Wetlands) project grouping based on survey results

Leeville (West of Bayou Lafourche)

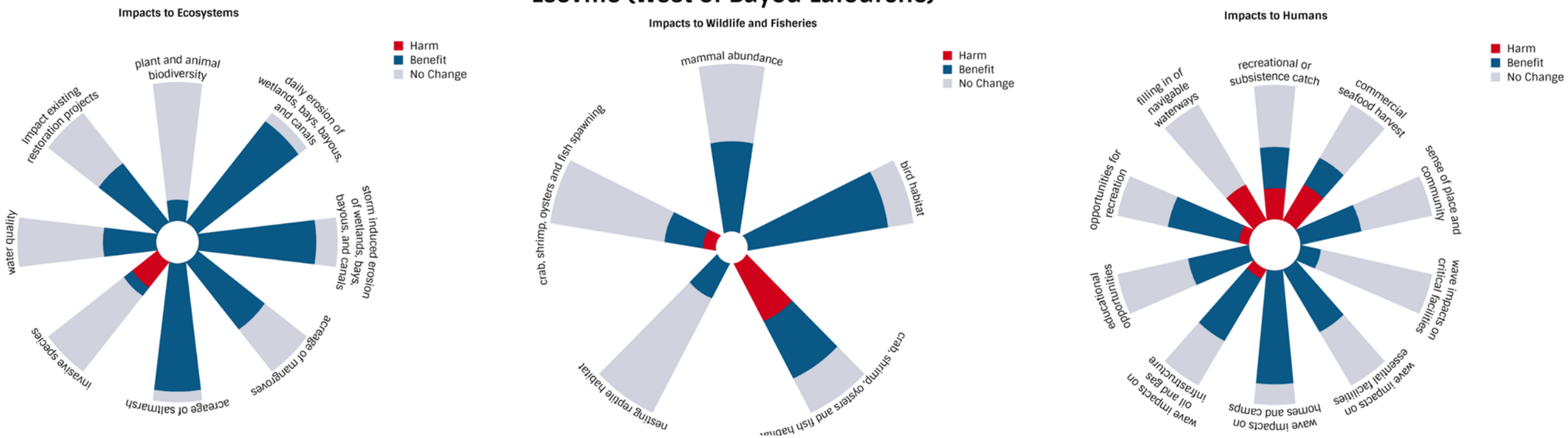

Figure 92. Expected ecosystem, wildlife and fisheries, and human impacts of the Leeville (West of Bayou Lafourche) project grouping based on survey results

East of Port Fourchon (LA1 Fringe)

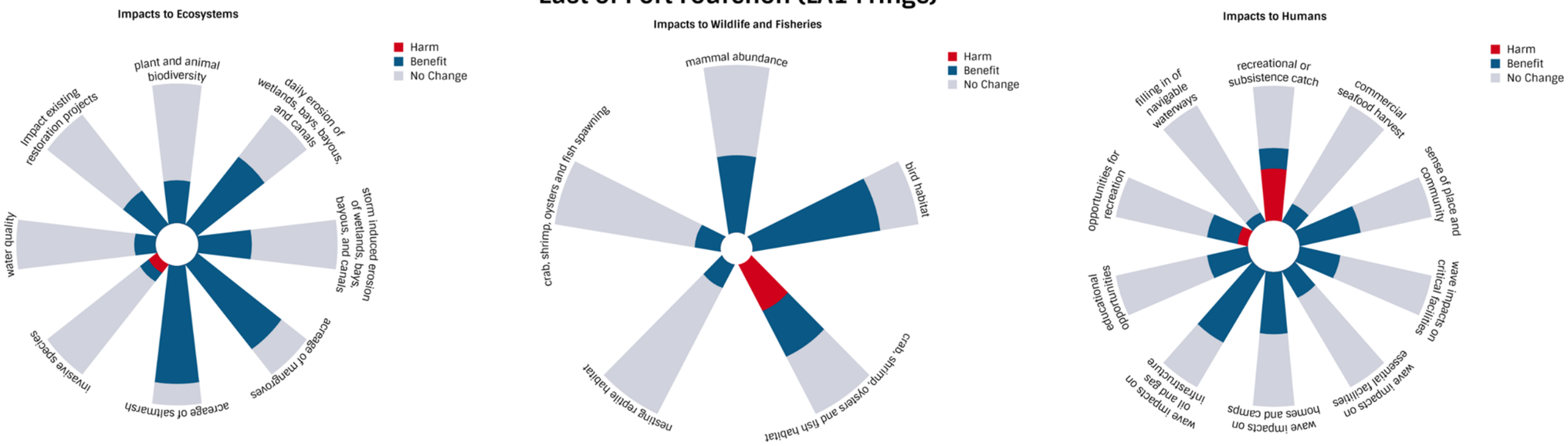

Figure 93. Expected ecosystem, wildlife and fisheries, and human impacts of the East of Port Fourchon (LA 1 Fringe) project grouping based on survey results

East of Port Fourchon (Linear Wetlands)

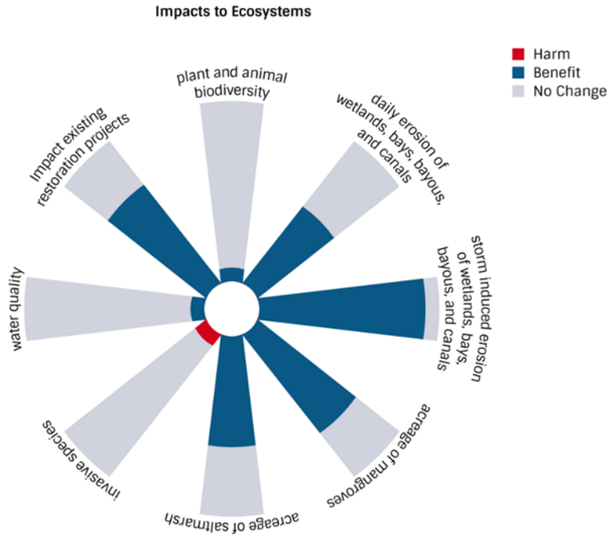

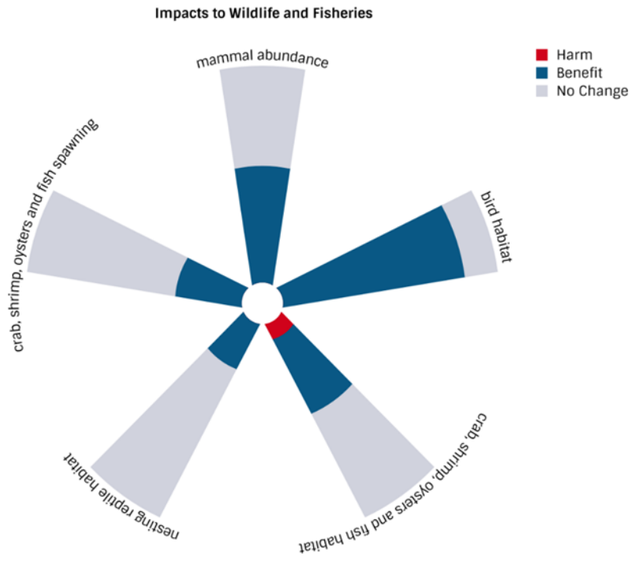

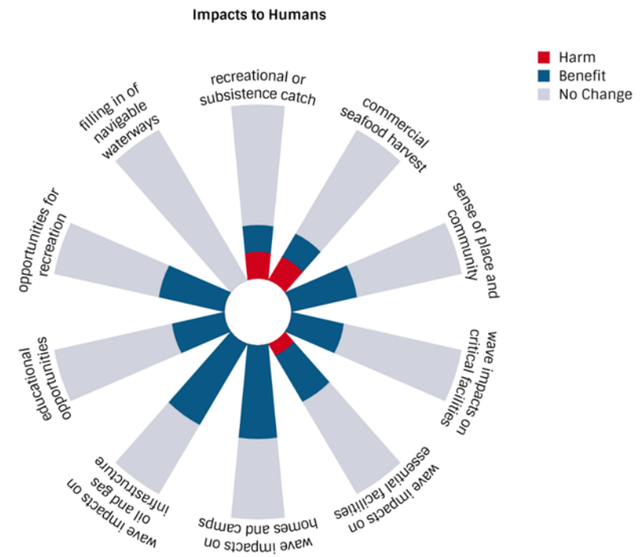

Figure 94. Expected ecosystem, wildlife and fisheries, and human impacts of the East of Port Fourchon (Linear Wetlands) project grouping based on survey results

DISCUSSION AND CONCLUSIONS

The transdisciplinary approach developed and operationalized in this study resulted in a suite of wetland restoration project alternatives that are all expected to generate a range of ecological and societal co-benefits. The ECG approach to participatory modeling actively encouraged residents and local stakeholders to work with scientists and other technical knowledge experts to co-design a suite of projects that, by their very nature, support local values and concerns (Hemmerling et al., 2022a). This work progressed in an iterative fashion, with the full ECG developing and reviewing each of the final project polygons. A key finding of this research is that the collaborative management approach resulted in a suite of project alternatives that are all expected to generate positive social value for stakeholders.

In addition, there is general agreement between the results of the social valuation model and those of the ecological and hydrodynamic models, highlighting the scientific value of local knowledge (Table 31). These results highlight that coastal protection and restoration planning that is supported by the generation and incorporation of reliable knowledge drawn from both the scientific community and from the local knowledge of community members who reside and work in the systems of which they are a part will result in more effective and sustainable outcomes (Hemmerling et al., 2020c).

Table 31. Summary of Cost and Outcomes of Project Groupings

	Restored Wetlands (acres at Y2030)	Restored Wetlands (acres at Y2050)	Carbon benefit from Restored Wetland (FWA-FWOA; tonne CO2e in Y2030)	Carbon benefit from Restored Wetland (FWA-FWOA; tonne CO2e in Y2050)	Cost for Wetland Restoration (over 30-year project life from Y2020)	Social Value Rating (at Y2050)
East of Fourchon - broad wetlands	1,809	1,745	41,391	40,890	$239,652,000	2.67
East of Fourchon - linear wetlands	353	226	7,500	4,951	$29,368,000	2.02
East of Fourchon - LA1 fringe	151	151	3,706	3,706	$16,719,000	2.17
West of Port Fourchon	1,253	1,193	32,408	31,964	$107,410,000	4.25
Leeville - West of Bayou Lafourche	367	344	7,652	7,499	$50,099,000	2.04

Each project grouping has a unique cost required to transfer the dredge material and construct and maintain the wetlands. The social value rating accounts for these costs as well as the anticipated value of a range of ecosystem, wildlife and fisheries, and human outcomes. These outcome values utilize financial proxies that are based upon model outputs, namely acres of wetlands restored, and the net carbon flux generated by these wetlands. The social value generated is weighted based on the perceived likelihood and severity of the anticipated changes generated by each project. While still accounting for cost differentials, this stakeholder weighting effectively shifts the valuation process from a more output-based to an outcome-based assessment. As such, while the acres of wetland restored and the net carbon flux are important and easily measurable outputs of these projects, the final valuation looks at the outcomes generated and ways these outcomes will affect residents and the natural resources they rely upon for their sustenance and wellbeing. For example, the proposed linear wetlands project east of Port Fourchon has the lowest cost per acre to construct and maintain among the project groupings analyzed. A pure cost-based model might be expected to prioritize these linear wetlands over more costly project alternatives. However, qualitative research found that the wetlands restored by this project grouping, while expected to generate a number of ecosystem and wildlife benefits, would not provide as much direct social value for human communities as some of the other groupings. The participation of local knowledge experts in this planning process provided insight into social and cultural values that could not be gained through scientific approaches alone, allowing the technical team to generate more alternatives, resulting in flexible actions and mutual co-benefits similar to the findings of (Stringer et al., 2006; Zedler, 2017).

LOCATION IMPLICATIONS ON PROJECT PERFORMANCE

While all projects had positive SROI values, project cost variation and land retention (of acres constructed remaining at year 30) differed due to geographic location and exposure to physical conditions. Project location has several implications for the results in the cost, modeling, and SROI analysis.

Construction costs were higher for the areas farthest from the channel deepening project that will provide sediment for restoration project construction. These areas also tended to be relatively deep open water, which requires more fill per unit area to create wetland acres than other restoration areas considered, more costly and more difficult to construct containment dikes, and more pipe and booster pump equipment to transport material to the restoration site. Project alternatives 1,2, and 6 in Figure 30 were estimated to have the highest costs per acres created, ranging from $104,00 to $189,000 dollars per acre of the 30-year life cycle of the project. Alternatives 3-5 had significantly lower costs per acres created, ranging from $87,000 to $92,000 over the 30-year life cycle of the project.

The main driver of wetland loss in the models was edge erosion and not submergence due to RSLR. Thus, projects with the greatest amount of edge habitat exposed to open water wave attack tended to retain the least amount of land by year 30 of the analysis. The East of Fourchon linear wetlands along remnant ridges were estimated to cost the least to construct but due to their geometries, have high exposure to wave attack and were predicted to lose the largest percentage of created wetland by year 30 of all the projects examined. Other project areas, such as those in the East of Fourchon broad wetlands and North of Fourchon, which have lower fetches due to existing geographic features protecting them, experienced less land loss.

NET GREENHOUSE GAS FLUXES

Examining the various habitat types and the potential changes (existing, restored, or converted) within alternatives helps to estimate the potential net GHG flux and if the habitat area remains a net GHG source or sink over time (Crooks et al., 2018; Holmquist et al., 2018). The six alternatives examined in this study suggest that those habitat areas that are restored have lower conversion to open water habitats (and thus lower sources of GHG emissions) and they tend to have a large percentage of brackish and saline marsh areas as well as mangrove forest areas that influence the area remaining as a net GHG sink over time. For example, Alternatives 2, 3, 4, and 5 were all projected to have wetland areas with marsh and mangrove forest vegetation and did not have large areas converted from wetlands to open water. Alternatives 1 and 6 had low areas of mangrove forest, were dominated by brackish or saline marsh vegetation, and tended to have large wetland areas that were converted to open water. Because the area surrounding Port Fourchon area has higher salinity waters (> 15 ppt) than those locations located toward the upper basin, the wetland areas there are dominated by brackish and saline marshes as well as mangrove forests. These habitat types have been demonstrated to produce lower methane and nitrous oxide emissions relative to the intermediate and fresh wetlands that occur further up in the basin (DeLaune et al., 1983; Poffenbarger et al., 2011; Smith et al., 1983a). Major sources of GHG emissions to the atmosphere from these natural lands was driven by the conversion of wetland habitats to open water habitats and the loss of stored carbon in aboveground biomass and soils (using assumptions commonly applied in GHG inventories [Domke et al., 2011; RAE, 2017; Sapkota & White, 2021; US EPA, 2021]). Some of the carbon in the aboveground biomass and soils could be laterally transported or buried in channels, bays, and offshore sediments, thus remain buried and stored in the system, and not necessarily released to the atmosphere. Field observations about these potential carbon losses or redistribution and retention processes are needed in the Port Fourchon area to test the assumptions that significant amounts of carbon are released to the atmosphere and to reduce uncertainties in the projected estimates of net GHG fluxes.

RESPONSE OF STORM SURGE AND WAVES TO RESTORED WETLANDS

Port Fourchon is expected to continue to face increasing risk from various sources of coastal threats, including RSLR, wetland loss, and storm impacts. Modeling results for the study area indicate that coastal forces will continue to cause bay deepening and steepening of the water bottom slopes in the vicinity of Port Fourchon, allowing large waves to attack its protective adjacent wetlands and facilities. The storm surge water level modeling often depicts potentially contradictory results: all of the wetland restoration proposals analyzed result in certain areas of water level or wave height increases and other areas of water level and wave decreases. These results highlight the nature of storm surge and wave impacts in coastal areas: impacts are highly situationally dependent on the nature of the storm (wind speeds, track relative to point of interest, etc.) and the nature of the landscape (bathymetric and topographic features). Water levels in Figure 77, Figure 78, and Figure 79 are perfect examples, where differing storm tracks may actually cause the wetlands to increase storm surge setup against elevated features such as LA Highway 3090. Similarly, the wetland restoration projects implemented in the modeling served to reduce wave heights immediately in the restored areas and depending on storm characteristics, but sometimes cause slight reductions or increases in other adjacent areas because the wetlands are efficient sediment traps. More wetland area to trap sediment results in less sediment being delivered to the bay for deposition.

However, as demonstrated in the long term and short term to tidal range and tidal prism, increased wetland area decreases the volume of water that can penetrate into the basin during a short period of time such as during storm events. Less water can enter the basin with more wetland area, but at the same time, the wetlands are more efficient at retaining water, resulting in longer retention times after the high-water event (i.e., the more robust wetlands take longer to drain).

REGIONAL SYSTEM RESPONSE

Terrebonne and Barataria bays adjacent to Port Fourchon, the surrounding wetlands and tidal channels and bayous that bisect them, barrier islands fronting the bays, and the tidal inlets that separate them, all experience morphologic change brought about by SLR and wetland loss over the 30-year period of analysis. Additionally, coastal storms, including those occurring in the winter (cold fronts), continuously rework the sandy barrier shorelines and the nearshore environments of the headland, drive shoreface retreat and marsh edge erosion, and contribute to scour and expansion of tidal inlets.

March edge erosion increases the bay area by gradual widening as well as gradual disintegration and submergence of land bridges and marsh islands that rim the upper bays resulting in the capture of formally semi-isolated water bodies, expanding the bays up-basin. This increase in bay area and reduction of friction that marsh islands provide to the attenuation of the tidal wave, increases the tidal prism (FitzGerald et al., 2008; Miner et al., 2009a). For tidal inlets to remain in morphologic equilibrium (Jarrett, 1976; O'Brien, 1969), they must enlarge to support this higher volume of water that is exchanged daily during the tidal cycle (FitzGerald et al., 2007; Miner et al., 2009a). The increase in water volume exchange introduces higher fluxes of dissolved and particulate substances, such as nutrients, salinity, and sediment, all of which can have broader implications to the system (FitzGerald et al., 2018). With continued increase in sea level and deepening of backbarrier bays, the tidal range increases (Gehrels et al., 1995), which increases the tidal prism further, creating a feedback loop that enlarges inlets more (Miner et al., 2009a). Inlets widen and deepen at the expense of barrier island sand, which gradually evolves to create a system that is more open and more exposed to influences from the coastal ocean, facilitating water exchange of higher magnitude with the coastal ocean (Georgiou & Schindler, 2009; Hart & Murray, 1978). During winter storms, the exchange of water through inlets is more vigorous, compared to the exchange during astronomical conditions (Feng & Li, 2010; Huang & Li, 2017; Li et al., 2019), which increases salt exchange (Li et al., 2009), and can contribute to salinity increase (Schindler, 2010). The modeled results of this study align with these previous works on tidal prism and the primary consequences of expanding tidal prism as predicted in the model are: 1) increased salinity in the upper basin, 2) increased efficiency in exporting clay-sized sediment from the basin, and 3) larger tidal inlets that are increasingly more efficient at facilitating 1 and 2.

Tidal range increases for the FWOA base environmental scenario and across grouped alternatives evaluated with the model. In Terrebonne Bay to the west of Port Fourchon, tidal range increases by 15%, while for Barataria Bay and Bayou Lafourche, tidal range increases by 30% and 12% respectively for the sum of the dominant constituents (Table 20, Table 21). Moreover, tidal phase changes range from 3-7%, delaying or speeding up the tidal wave by up to 28 minutes from 2020 through 2050. While the tidal phase changes are minor, tidal range changes are appreciably higher with potential consequences for velocity excursion that can entrain and mobilize sediment. The differences in tidal range and phase

between scenarios appear to be minor, with negligible tidal range impacts (less than 2%) and tidal phase impacts of up to 8 minutes (Table 21). Moreover, these small changes are only relevant to Bayou Lafourche, likely due to the proximity of the Bayou to the restoration projects. For Terrebonne and Barataria bays, tidal range and phase changes across alternatives are undetectable. The proximity of the restoration to the back barrier wetlands close to the hydraulic divide between Terrebonne and Barataria bays, suggest that the small or undetectable reduction in the tidal range and phase, is likely due to the large size of the bays, degraded barrier islands, and the ample conveyance for redirecting the tidal wave.

Tidal prism also increases for the FWOA base case environmental scenario, as well as across AGs. For Terrebonne and Barataria bays, from 2020 through 2050, tidal prism increases appreciably with 39% and 52% respectively, corresponding to an inlet cross sectional area increase of 53% and 118% respectively (Table 23), results that agree with historical (1880-2007) inlet cross-sectional area increase documented by Miner et al., (2009). The lower reaches of Bayou Lafourche near Belle Pass, experienced an increase in tidal prism (from 2020 through 2050) of approximately 17%, corresponding to a cross-sectional area increase of approximately 32%. Evaluating tidal prism increase for inlets proximal to the Port and to Belle Pass, tidal prism increases are respectively 64% for East Timbalier and Raccoon Pass (west of the Port), and 55% for Caminada Pass, suggesting that the additional tidal prism resulting from the loss of wetlands is captured mostly by the proximal tidal inlets, and less so by tidal inlets located distally. This result is corroborated further by examining the next tidal inlets farther west and east, Little Pass Timbalier (westward) and Barataria Pass (eastward), which experience a tidal prism increase of 38% and 21% respectively (Table 23) This suggests that the tidal inlets proximal to the wetland loss do indeed capture more of the tidal prism, compared to their distal counterparts And, wetland restoration proximal to a tidal inlet can also mitigate for tidal prism increase at that inlet.

Following the reasoning discussed above, from the FWOA experiments, and utilizing theory (O'Brien 1969), reversing wetland loss via restoration, reduces bay area and thus tidal prism, a consequence that would be reflected in tidal inlets and the tidal prism they convey. For instance, AG have many various projects located along the spine of Bayou Lafourche, north near Leeville, and to the west and east but proximal to the port. As such, following simple rules of prism-inlet area relationships, tidal inlets proximal to these projects should experience a reduction in tidal prism.

Table 24 shows the calculated tidal prism from model results, showing that Belle Pass is the only tidal inlet that exhibits appreciable decrease in tidal prism. Specifically, Belle Pass tidal prism is reduced by 1% (±2%) for year 2020 for AG2, and up to 10% (±2%) for AG3. By year 2050, tidal prism for Belle Pass is reduced by 8% (±2%) for AG2, and up to 4% (±2%) for AG3. The remaining inlets do not show a change that is more than 1%, which is well within the model uncertainty, and thus experience negligible tidal prism reductions due to AG2 and AG3. The explanation for this response is that the projects are very close, or surrounding the Port, and the closest inlet currently conveying tidal flow is Belle Pass. Another explanation is that the change in the tidal prism is small proportional to the tidal prism of the Barataria-Terrebonne Basin, and thus a few relatively small projects reversing wetland loss are not sufficient to invoke significant change in the tidal prism. However, as evidenced by the sediment fluxes across inlets (e.g. Figure 48, Figure 49, Figure 50, Figure 51), even small changes in tidal range, tidal prism, and cross-sectional area, can have local effects on the velocity and instantaneous flow, which can cause sediment

fluxes to differ between alternative groupings. Given the small changes in tidal prism, it is unlikely that sediment impacts would be regional and widespread, except for clays, the smallest sediment fraction. The Mississippi River Delta, including the study area, has a significant amount of clay dispersed throughout the back barrier lagoons, wetlands, and the vast network of bayous. Clays remain in suspension longer and can be transported farther than any other sediment type. By 2050, the system becomes more ebb dominant compared to 2020 (net flux exporting the system), which contributes to more sediment (clays) being lost from the system. Moreover, with the gradual expansion of inlets and loss of barrier islands, the increased exchange of water will continue to increase the amount of clay sediment exported from the back barrier (Figure 51). This process can have significant implications for the regional sediment budget for the Barataria-Terrebonne Basin (with transferable findings to the rest of the Mississippi River Delta Plain) creating a permanent sediment deficit. As such, the expansion of basin can have irreversible consequences on the sediment budget and further highlights the role of regional sediment management in mitigating the effects of the regional transgression of these systems.

Annual average salinity patterns differenced between 2050 and 2020 (FWOA from 2020 to 2050; Figure 44) corroborates the tidal prism increase discussed previously, showing widespread saltwater intrusion albeit asymmetric, and increases of salinity at the headwaters of the estuaries, with less if any salinity increase toward the coast. Around the wetlands surrounding the Port, by 2050, salinity is reduced over time, due to the higher connectivity between Barataria Bay and Terrebonne Bay, created by wetland loss in the area. Changes in salinity, as well as water levels have implications for vegetation species transitions, which in turn, influences carbon pools because higher salinity wetlands have lower methane emissions as discussed above.

THE VALUE OF COLLABORATIVE MANAGEMENT IN BUILDING COMMUNITY RESILIENCE

Community resilience is closely related to the concept of adaptive capacity, defined as the ability of a system to adjust to change, moderate the effects, and cope with a disturbance (Cutter et al., 2008). In natural resource-dependent communities like those around Port Fourchon, resilience is often tied to the ability of residents to pursue natural resources in alternate areas or to shift the object of natural resource collection (Colten et al., 2012). This ability to shift to alternate areas is particularly important when working with renewable natural resources, such as fisheries. For communities that are reliant upon mineral resources such as oil and gas, where the location of the resource is often fixed, community resilience is more closely tied to the ability to protect those resources, and the infrastructure necessary for their extraction and transport, in place.

The projects co-developed by the ECG through this research were specifically designed to maximize co-benefits, including the protection of the primary natural resources that residents and local stakeholders rely upon, fisheries, and oil and gas. Several of these co-benefits were assessed directly through numerical modeling. The ability of the projects to build wetlands, including saltmarsh and mangroves, and to reduce wave impacts on infrastructure was examined for each project grouping. Recognizing that there is a social cost of carbon associated with the release of greenhouse gasses that will impact communities in the future, each project was assessed to determine its ability to serve as a sink or a source. One key resource

that the coast requires is a workforce and communities to sustain that workforce. The ECG recognized this, and each of the project alternatives was examined and assessed for its ability to protect surrounding homes and camps from storm surge and flooding.

Beyond providing protection for communities, wetlands are tied to the region's history and cultural heritage. Restored wetlands can provide enhanced opportunities for recreation and education. These more intangible aspects of coastal protection and restoration are not as readily modeled but no less important when it comes to building community resilience. All of these co-benefits were considered during each step of this research, from the initial conceptualization of the project footprints to the final social valuation and ranking of project alternatives. The framework developed and operationalized through this research represents a key advancement in the collaborative management of coastal protection and restoration planning and provides a framework and tools that can be leveraged to enhance resilience within the study area and adapted for other locations globally.

LITERATURE CITED

Alizad, K., Hagen, S. C., Morris, J. T., Bacopoulos, P., Bilskie, M. V., Weishampel, J. F., & Medeiros, S. C. (2016). A coupled, two-dimensional hydrodynamic-marsh model with biological feedback. *Ecological Modelling*, *327*, 29–43.

Allison, M. A., Carruthers, T. J. B., Clark, R., Di Leonardo, D. R., Hemmerling, S. A., Meselhe, E. A., Moss, L. C., Weathers, H. D., White, E. D., & Yuill, B. T. (2018). *Partnership for Our Working Coast: Port Fourchon Phase 1 Technical Report* (p. 215). Baton Rouge, LA.: The Water Institute of the Gulf. Produced for and funded by: Shell, Chevron, Danos, and the Greater Lafourche Port Commission.

Alymov, V., Cobell, Z., de Mutsert, K., Dong, Z., Duke-Sylvester, S., Fischbach, J., Hanegan, K., Lewis, K., Lindquist, D., McCorquodale, J. A., Poff, M., Roberts, H., Schindler, J., Visser, J. M., Wang, Z., Wang, Y., & White, E. D. (2017). *2017 Coastal Master Plan: Appendix C: Modeling Chapter 4 - Model outcomes and interpretations* (Version Final) (pp. 1–448). Baton Rouge, Louisiana: Coastal Protection and Restoration Authority.

Ardaman & Associates. (2017). *Field and Laboratory Data Collection Phase West Fourchon Marsh Creation & Nourishment* (Draft) (p. 176). Lafourche Parish: Ardaman & Associates. Prepared for Coastal Protection and Restoration Authority.

Ardaman & Associates. (2018a). *Caminada Headlands Back Barrier Marsh Creation Increment ll (BA-193)* (Design Report No. 17–2810) (p. 190). Lafourche & Jefferson Parishes, Louisiana: Ardaman & Associaties, Prepared for the Coastal Protection and Restoration Authority.

Ardaman & Associates. (2018b). *Design Report West Fourchon Marsh Creation & Nourishment (TE-134)* (Design Report No. 17–2803) (p. 100). Lafourche Parish, LA: Ardaman & Associaties, Prepared for the Coastal Protection and Restoration Authority.

Ardaman & Associates. (2018c). *Geotechnical Engineering Report Caminada Headlands Back Barrier Marsh Creation Increment l (BA-171) Marsh Fill Settlement Re-Evaluation* (Geotechnical Engineering Report No. 17- 2810B) (p. 42). Lafourche & Jefferson Parishes, Louisiana: Ardaman & Associates. Prepared for Coastal Protection and Restoration Authority.

Barataria-Terrebonne National Estuary Program (BTNEP). (2018). *BTNEP: Comprehensive Conservation and Management Plan* (p. 310). Barataria-Terrebonne National Estuary Program (BTNEP).

Barnes, S. R., Bond, C., Burger, N., Anania, K., Strong, A., Weilant, S., & Virgets, S. (2015). *Economic Evaluation of Coastal Land Loss in Louisiana* (p. 119). Baton Rouge, LA: Louisiana State University, Economics & Policy Research Group.

Barra, M. P., Hemmerling, S. A., & Baustian, M. M. (2020). A model controversy: Using environmental competency groups to inform coastal restoration planning in Louisiana. *The Professional Geographer*, *72*(4), 511–520.

Baustian, M. M., Jung, H., Bienn, H. C., Barra, M., Hemmerling, S. A., Wang, Y., White, E. D., & Meselhe, E. A. (2020). Engaging Coastal Community Members about Natural and Nature-Based Solutions and Assessing Their Ecosystem Functions. *Ecological Engineering*.

Baustian, M. M., Stagg, C. L., Perry, C. L., Moss, L. C., & Carruthers, T. J. B. (2021). Long-Term carbon sinks in marsh soils of coastal Louisiana are at risk to wetland loss. *Journal of Geophysical Research: Biogeosciences*, *126*(3).

Beasley, B. S., Georgiou, I. Y., Miner, M. D., & Byrnes, M. R. (2019). Coupled Barrier System Shoreline and Shoreface Dynamics, Louisiana, USA. *Coastal Sediments 2019*, 15.

Bernard, H. R. (2017). *Research methods in anthropology: Qualitative and quantitative approaches*. Rowman & Littlefield.

Bethel, M. B., Brien, L. F., Esposito, M. M., Miller, C. T., Buras, H. S., Laska, S. B., Philippe, R., Peterson, K. J., & Parsons Richards, C. (2014). Sci-TEK: A GIS-Based Multidisciplinary Method for Incorporating Traditional Ecological Knowledge into Louisiana's Coastal Restoration Decision-Making Processes. *Journal of Coastal Research*, *297*, 1081–1099.

Byrnes, M. R., Berlinghoff, J. L., Griffee, S. F., & Lee, D. M. (2018). *Louisiana Barrier Island Comprehensive Monitoring Program (BICM): Phase 2 – Updated Shoreline Compilation and Change Assessment, 1880s to 2015* (Final Report) (p. 46 p. plus appendices). Baton Rouge, LA: Prepared for the Louisiana Coastal Protection and Restoration Authority by Applied Coastal Research and Engineering.

Byrnes, M. R., Britsch, L. D., Berlinghoff, J. L., Johnson, R., & Khalil, S. (2019). Recent subsidence rates for Barataria Basin, Louisiana. *Geo-Marine Letters*, *39*(4), 265–278.

Cardoch, L., Jr., J. W. D., & Ibanez, C. (2002). Net primary productivity as an indicator of sustainability in the Ebro and Mississippi Deltas. *Ecological Applications*, *12*(4), 1044.

Clough, J., Polaczyk, A., & Propato, M. (2016). Modeling the potential effects of sea-level rise on the coast of New York: Integrating mechanistic accretion and stochastic uncertainty. *Environmental Modelling and Software*, *84*, 349–362.

Clough, J. S. (2016). SLAMM Technical Documentation, 100.

Coastal Engineering Consultants Inc. (2016). *TE-118 East Timbalier Island Restoration Project: Numerical modeling of restoration alternatives* (Draft No. CEC File No. 15.225) (p. 102). Baton Rouge, LA: Coastal Engineering Consultants Inc. Prepared for Coastal Protection and Restoration Authority.

Coastal Protection and Restoration Authority. (2017). *CPRA Marsh Creation Design Guidelines*. Coastal Protection and Restoration Authority.

Coastal Protection and Restoration Authority. (2022, February). Fiscal Year 2023 Annual Plan: Integrated Ecosystem Restoration and Hurricane Protection in Coastal Louisiana. Coastal Protection and Restoration Authority.

Cobell, Z., & Roberts, H. (2021). *Storm surge and waves: model updates for the 2023 Coastal Master Plan* (No. Version 1) (p. 56). Coastal Protection and Restoration Authority.

Cobell, Z., Sable, S., & Rose, K. A. (2020). *Calcasieu Ship Channel Salinity Control Measures Project (CS-0065): Larval Transport Modeling* (No. CS-0065) (p. 106). Baton Rouge, LA: The Water Institute of the Gul. Produced for and funded byCoastal Protection and Restoration Authority.

Cobell, Z., Zhao, H., Roberts, H. J., Clark, F. R., & Zou, S. (2013). Surge and wave modeling for the Louisiana 2012 Coastal Master Plan. *Journal of Coastal Research*, (67), 88–108.

Colten, C. E., Hay, J., & Giancarlo, A. (2012). Community Resilience and Oil Spills in Coastal Louisiana. *Ecology and Society*, *17*(3).

Colten, C. E., Simms, J. R. Z., Grismore, A. A., & Hemmerling, S. A. (2018). Social justice and mobility in coastal Louisiana, USA. *Regional Environmental Change*, *18*(2), 371–383.

Couvillion, B. (2017). *2017 Coastal Master Plan Modeling: Attachment C3-27: Landscape Data. Version Final.* (pp. 1–84). Baton Rouge, LA: Coastal Protection and Restoration Authority.

Couvillion, B. R., Beck, H., Schoolmaster, D., & Fischer, M. (2017). Land Area Change in Coastal Louisiana (1932 to 2016), 26.

CPRA. (2022). CIMS Coastal Basin Metadata.

Craig, N. J., Turner, R. E., & Day, J. W. (1979). Land loss in coastal Louisiana (U.S.A.). *Environmental Management*, *3*(2), 133–144.

Cramer, G. W., Day, J. W., & Conner, W. H. (1981). Productivity of four marsh sites surrounding Lake Pontchartrain, Louisiana. *American Midland Naturalist*, *106*(1), 65.

Crooks, S., Sutton-Grier, A. E., Troxler, T. G., Herold, N., Bernal, B., Schile-Beers, L., & Wirth, T. (2018). Coastal wetland management as a contribution to the US National Greenhouse Gas Inventory. *Nature Climate Change*.

Curtis, J. W., Curtis, A., & Hemmerling, S. A. (2018). Revealing the invisible environments of risk and resiliency in vulnerable communities through geospatial techniques. In A. Barberopoulou (Ed.), *Tsunamis: Detection, Risk Assessment and Crisis Management* (pp. 245–273). Hauppauge, NY: Nova Science Publishers.

Cutter, S. L., Barnes, L., Berry, M., Burton, C., Evans, E., Tate, E., & Webb, J. (2008). A place-based model for understanding community resilience to natural disasters. *Global Environmental Change*, *18*(4), 598–606.

Darby, F. A., & Turner, R. E. (2008). Effects of eutrophication on salt marsh root and rhizome biomass accumulation. *Marine Ecology Progress Series*, *363*, 63–70.

Day, J. W., Lane, R., Moerschbaecher, M., DeLaune, R., Mendelssohn, I., Baustian, J., & Twilley, R. (2013). Vegetation and soil dynamics of a Louisiana estuary receiving pulsed Mississippi River water following Hurricane Katrina. *Estuaries and Coasts*, *36*(4), 665–682.

de Groot, R., Brander, L., van der Ploeg, S., Costanza, R., Bernard, F., Braat, L., Christie, M., Crossman, N., Ghermandi, A., Hein, L., Hussain, S., Kumar, P., McVittie, A., Portela, R., Rodriguez, L. C.,

ten Brink, P., & van Beukering, P. (2012). Global estimates of the value of ecosystems and their services in monetary units. *Ecosystem Services*, *1*(1), 50–61.

Delaune, R. D., & Smith, C. J. (1984). Carbon cycle and the rate of vertical accumulation of peat in the Mississippi River deltaic plain. *Southeast. Geol.; (United States)*, *25:2*.

DeLaune, R. D., Smith, C. J., & Patrick, W. H. (1983). Methane release from Gulf coast wetlands. *Tellus B: Chemical and Physical Meteorology*, *35*(1), 8–15.

DeLaune, R. D., Smith, C. J., & Tolley, M. D. (1984). The effect of sediment redox potential on nitrogen uptake, an aerobic root respiration and growth of *Spartina alterniflora* Loisel. *Aquatic Botany*, *18*, 223–230.

DeMyers, C., Hemmerling, S. A., & Aarons, A. (2020). *Barataria-Terrebonne National Estuary System Climate Change Adaptation Plan*. Thibodaux, LA: The Water Institute of the Gulf. Prepared for the Barataria-Terrebonne National Estuary Program.

Dingler, J. R., Reiss, T. E., & Plant, N. G. (1993). Erosional patterns of the Isles Dernieres, Louisiana, in relation to meteorological influences. *Journal of Coastal Research*, *9*(1), 112–125.

Dismukes, D. E. (2021). *Louisiana 2021 Greenhouse Gas Inventory* (p. 404).

Domke, J., Hoefler, T., & Nagel, W. E. (2011). Deadlock-Free Oblivious Routing for Arbitrary Topologies. In *2011 IEEE International Parallel & Distributed Processing Symposium* (pp. 616–627). Anchorage, AK, USA: IEEE.

Edwards, K. R., & Mills, K. P. (2005). Aboveground and belowground productivity of *Spartina alterniflora* (Smooth Cordgrass) in natural and created Louisiana salt marshes. *Estuaries*, *28*(2), 252–265.

Egbert, G. D., & Erofeeva, S. Y. (2002). Efficient inverse modeling of barotropic ocean tides. *American Meterological Society*, *19*, 183–204.

Escoffier, F. (1940). The Stability of Tidal Inlets. *Shore and Beach*, *8*(4).

Eustis Engineering Services, LLC. (2015). *Final Geotechnical Exploration State of Louisiana Coastal Protection and Restoration Authority Caminada Headlands Back Barrier Marsh Creation Project Offshore Work* (No. Contract No. 2503-13-14, Task No.1, Amendment No.1) (p. 134). Lafourche Parish, LA: Eustis Engineering Services, LLC. Prepared for Coastal Protection and Restoration Authority.

Feijtel, T. C., DeLaune, R. D., & Patrick Jr, W. H. (1985). Carbon flow in coastal Louisiana. Marine Ecology Progress Series. *Marine Ecology Progress Series. Oldendorf*, *24*(3), 255–260.

Feng, Z., & Li, C. (2010). Cold-front-induced flushing of the Louisiana Bays. *Journal of Marine Systems*, *82*(4), 252–264.

FitzGerald, D. M., Fenster, M. S., Argow, B. A., & Buynevich, I. V. (2008). Coastal impacts due to sea-level rise. *Annual Review of Earth and Planetary Sciences*, *36*, 601–647.

FitzGerald, D. M., J. Hein, C., Hughes, Z. J., Kulp, M. A., Georgiou, I. Y., & Miner, M. D. (2018). Runaway barrier island transgression concept: Global case studies. In L. J. Moore & A. B. Murray (Eds.), *Barrier Dynamics and Response to Changing Climate* (pp. 3–56). Cham: Springer International Publishing.

FitzGerald, D. M., Kulp, M. A., Hughes, Z. J., Georgiou, I. Y., Miner, M. D., Penland, S., & Howes, N. C. (2007). Impacts of rising sea level to backbarrier wetlands, tidal inlets, and barrier islands: Barataria coast, Louisiana. In *Coastal Sediments '07* (pp. 1179–1192). New Orleans, Louisiana, United States: American Society of Civil Engineers.

Fitzpatrick, C., Jankowski, K. L., & Reed, D. J. (2021). *2023 Coastal Master Plan: Determining subsidence rates for use in predictive modeling* (Version I) (p. 70). Baton Rouge, Louisiana: Coastal Protection and Restoration Authority.

Flocks, J. G., Ferina, N. F., Dreher, C., Kindinger, J. L., FitzGerald, D. M., & Kulp, M. A. (2006). High-resolution stratigraphy of a Mississippi subdelta-lobe progradation in the Barataria Bight, north-central Gulf of Mexico. *Journal of Sedimentary Research*, *76*(3), 429–443.

Flynn, K. M., Mendelssohn, I. A., & Wilsey, B. J. (1999). The effect of water level management on the soils and vegetation of two coastal Louisiana marshes. *Wetlands Ecology and Management*, *7*(4), 193–218.

Fugro. (2018). *LNG plant borings - Fugro data sheets* (p. 42).

Gagliano, S. M., Meyer-Arendt, K. J., & Wicker, K. M. (1981). Land loss in the Mississippi River deltaic plain. *Transactions of the Gulf Coast Association of Geological Societies*, *31*, 295–300.

Gahagan & Bryant Associates, Inc. (2013). *Caminada Moreau Subsidence Study Phases 1-3 Project Report* (p. 467). Lafourche Parish, LA.

Ganju, N. K., Defne, Z., & Fagherazzi, S. (2020). Are Elevation and Open-Water Conversion of Salt Marshes Connected? *Geophysical Research Letters*, *47*(3), e2019GL086703.

Gehrels, W. R., Belknap, D. F., Pearce, B. R., & Gong, B. (1995). Modeling the contribution of M2 tidal amplification to the Holocene rise of mean high water in the Gulf of Maine and the Bay of Fundy. *Marine Geology*, *124*(1), 71–85.

GeoEngineers. (2010). *Geotechnical Data Collection Report Caminada Headland Beach and Dune Restoration Project (BA-45). LaFourche and Jefferson Parishes, Louisiana.* (Geotechnical Data Collection Report No. 16715- 012– 00) (p. 415). Lafourche Parish, LA: GeoEngineers. Prepared for Taylor Energy, Inc.

GeoEngineers. (2017). *Desktop Geotechnical Evaluation and Phase 2 Scoping: Federal Navigation Improvements-Port Fourchon* (No. 22642- 001– 00) (p. 118). Lafourche Parish, LA: GeoEngineers. Prepared for GIS Engineering, Inc.

GeoEngineers. (2019). *Port Fourchon Deepening Project: Section 203* (No. 22642- 001– 00). Baton Rouge, LA: GeoEngineers. Prepared for GIS Engineering, Inc.

GeoEngineers LLC. (2018, October 8). Geotechnical Data Report: East Leeville Marsh Creation and Nourishment (BA-0194). Coastal Protection and Restoration Authority.

Georgiou, I. Y., FitzGerald, D. M., & Stone, G. W. (2005). The Impact of Physical Processes along the Louisiana Coast. *Journal of Coastal Research*, 72–89.

Georgiou, I. Y., & Schindler, J. K. (2009). Wave forecasting and longshore sediment transport gradients along a transgressive barrier island: Chandeleur Islands, Louisiana. *Geo-Marine Letters*, *29*(6), 467–476.

Georgiou, I. Y., Yocum, T. E., Amos, M. L., Kulp, M. A., & Flocks, J. (2019). *Louisiana Barrier Island Comprehensive Monitoring Program 2015-2019 Coastal Surface-Sediment Characterization Analysis: Methods and Results.* (p. 38). New Orlean, LA: Prepared for the Louisiana Coastal Protection and Restoration Authority (CPRA), Pontchartrain Institute for Environmental Sciences, University of New Orleans.

GIS Engineering, LLC. (2018). *Port Fourchon Belle Pass channel deepening project, Fourchon, Louisiana, draft environmental impact statement* (EIS) (p. 147). New Orleans, LA: U.S. Army Corps of Engineers, New Orleans District.

GIS Engineering, LLC. (2018). *Port Fourchon Belle Pass Channel Deepening Project, Fourchon, Louisiana, Draft Environmental Impact Statement* (Draft Environmental Impact Statement) (p. 147). GIS Engineering, LLC.

GIS Engineering, LLC. (2019). *Port Fourchon Belle Pass Channel Deepening Project* (No. 22642- 001–00).

Gotham, K. F. (2016). Coastal Restoration as Contested Terrain: Climate Change and the Political Economy of Risk Reduction in Louisiana. *Sociological Forum*, *31*, 787–806.

Greater Lafourche Port Commission. (2020). Port Fourchon: Port Facts.

Hart, W. E., & Murray, S. P. (1978). Energy balance and wind effects in a shallow sound. *Journal of Geophysical Research: Oceans*, *83*(C8), 4097–4106.

Hemmerling, S. A., Barra, M., & Bienn, H. C. (2017a). *Restore the Earth Foundation Reforestation Social Return on Investment Report: Pointe-aux-Chenes Wildlife Management Area*. Baton Rouge, LA: The Water Institute of the Gulf.

Hemmerling, S. A., Barra, M., & Bienn, H. C. (2017b). *Restore the Earth Foundation Reforestation Social Return on Investment Report: Tensas River National Wildlife Refuge*. Baton Rouge, LA: The Water Institute of the Gulf.

Hemmerling, S. A., Barra, M., Bienn, H. C., Baustian, M. M., Jung, H., Meselhe, E. A., Wang, Y., & White, E. D. (2020a). Elevating local knowledge through participatory modeling: Active community engagement in restoration planning in coastal Louisiana. *Journal of Geographical Systems*, *22*(2), 241–266.

Hemmerling, S. A., Barra, M., Bienn, H. C., Baustian, M. M., Jung, H., Meselhe, E., Wang, Y., & White, E. (2020b). Elevating local knowledge through participatory modeling: active community engagement in restoration planning in coastal Louisiana. *Journal of Geographical Systems*, *22*(2), 241–266.

Hemmerling, S. A., Barra, M., & Bond, R. H. (2020c). Adapting to a smaller coast: Restoration, protection, and social justice in coastal Louisiana. In S. Laska (Ed.), *Louisiana's Response to Extreme Weather: A Coastal State's Adaptation Challenges and Successes* (pp. 113–144). Cham, Switzerland: Springer International Publishing.

Hemmerling, S. A., DeMyers, C. A., & Carruthers, T. J. (2022a). Building Resilience through Collaborative Management of Coastal Protection and Restoration Planning in Plaquemines Parish, Louisiana, USA. *Sustainability*, *14*(5), 2974.

Hemmerling, S. A., DeMyers, C. A., & Carruthers, T. J. B. (2022b). Building Resilience through Collaborative Management of Coastal Protection and Restoration Planning in Plaquemines Parish, Louisiana, USA. *Sustainability*, *14*(5), 2974.

Hemmerling, S. A., DeMyers, C. A., & Parfait, J. (2021). Tracing the flow of oil and gas: A spatial and temporal analysis of environmental justice in coastal Louisiana from 1980 to 2010. *Environmental Justice*, *14*(2), 134–145.

Henry, K. M., & Twilley, R. R. (2013). Soil development in a coastal Louisiana wetland during a climate-induced vegetation shift from salt marsh to mangrove. *Journal of Coastal Research*, *29*(6), 1273–1283.

Herbert, E. R., Windham-Myers, L., & Kirwan, M. L. (2021). Sea-level rise enhances carbon accumulation in United States tidal wetlands. *One Earth*, *4*(3), 425–433.

Hiatt, M., Snedden, G., Day, J. W., Rohli, R. V., Nyman, J. A., Lane, R., & Sharp, L. A. (2019). Drivers and impacts of water level fluctuations in the Mississippi River delta: Implications for delta restoration. *Estuarine, Coastal and Shelf Science*, *224*, 117–137.

Hijuelos, A. C., Sable, S. E., O'Connell, A. M., & Geaghan, J. P. (2017). *2017 Coastal Master Plan: Attachment C3-12: Eastern oyster,* Crassostrea virginica*, habitat suitability index model* (Version II.) (pp. 1–23). Baton Rouge, LA: Coastal Protection and Restoration Authority.

Holcomb, S. R., Bass, A. A., Seymour, M. A., Lorenz, N. F., Gregory, B. B., Javed, S. M., & Balkum, K. F. (2015). *Louisiana Wildlife Action Plan* (No. LA WAP-October 2015). Baton Rouge. LA: Louisiana Department of Wildlife and Fisheries.

Holm, G. O., Perez, B. C., McWhorter, D. E., Krauss, K. W., Johnson, D. J., Raynie, R. C., & Killebrew, C. J. (2016). Ecosystem level methane fluxes from tidal freshwater and brackish marshes of the Mississippi River Delta: implications for coastal wetland carbon projects. *Wetlands*, *36*, 401–413.

Holmquist, J. R., Windham-Myers, L., Bernal, B., Byrd, K. B., Crooks, S., Gonneea, M. E., Herold, N., Knox, S. H., Kroeger, K. D., McCombs, J., Megonigal, J. P., Lu, M., Morris, J. T., Sutton-Grier, A. E., Troxler, T. G., & Weller, D. E. (2018). Uncertainty in United States coastal wetland greenhouse gas inventorying. *Environmental Research Letters*, *13*(11), 115005.

Hopkinson, C. S. (2018). Net Ecosystem Carbon Balance of Coastal Wetland-Dominated Estuaries: Where's the Blue Carbon? In *A Blue Carbon Primer*. CRC Press.

Hopkinson, C. S., Gosselink, J. G., & Parrando, R. T. (1978). Aboveground production of seven marsh plant species in coastal Louisiana. *Ecology*, *59*(4), 760–769.

Hopkinson, C. S., Gosselink, J. G., & Parrondo, R. T. (1980). Production of Coastal Louisiana Marsh Plants Calculated from Phenometric Techniques. *Ecology*, *61*(5), 1091–1098.

Huang, W., & Li, C. (2017). Cold front driven flows through multiple inlets of Lake Pontchartrain Estuary. *Journal of Geophysical Research: Oceans*, *122*(11), 8627–8645.

Huang, W., & Li, C. (2020). Contrasting Hydrodynamic Responses to Atmospheric Systems with Different Scales: Impact of Cold Fronts vs. That of a Hurricane. *Journal of Marine Science and Engineering*.

International Water Management Institute. (n.d.). World Water and Climate Atlas.

IPCC. (2007). *Climate change 2007: The Physical Science Basis: Contribution of Working Group I to the Fourth Assessment Report of the Intergovernmental Panel on Climate Change*. Cambridge ; New York: Cambridge University Press.

Jankowski, K. L., Törnqvist, T. E., & Fernandes, A. M. (2017). Vulnerability of Louisiana's coastal wetlands to present-day rates of relative sea-level rise. *Nature Communications*, *8*, 14792.

Jarrett, J. T. (1976). *Tidal prism-inlet area relationships* (Vol. 3). US Department of Defense, Department of the Army, Corps of Engineers ….

Johnson, D., & Geldner, N. (2020). *Storm Selection for the ICM - Updates & Improvements* (p. 10). Baton Rouge, Louisiana: Purdue University; Prepared for Coastal Protection and Restoration Authority.

Jung, H., Messina, F., Moss, L., Baustian, M. M., Duke-Sylvester, S., & Roberts, H. H. (2019). *TO51: Vegetetation Model and Integration Framework for Mid-Breton Outfall Management Model.* (Funded by the Coastal Protection and Restoration Authority under Task Orders 51). The Water Institute of the Gulf.

Kalnay, E., Kanamitsu, M., Kistler, R., Collins, W., Deaven, D., Gandin, L., Iredell, M., Saha, S., White, G., Woollen, J., Zhu, Y., Chelliah, M., Ebisuzaki, W., Higgins, W., Janowiak, J., Mo, K. C., Ropelewski, C., Wang, J., Leetmaa, A., Reynolds, R., Jenne, R., & Joseph, D. (1996). The NCEP/NCAR 40-Year Reanalysis Project. *Bulletin of the American Meteorological Society*, *77*(3), 437–472.

Kaswadji, R. F., Gosselink, J. G., & Turner, R. E. (1990). Estimation of primary production using five different methods in a *Spartina alterniflora* salt marsh. *Wetlands Ecology and Management*, *1*(2).

Keogh, M. E., Törnqvist, T. E., Kolker, A. S., Erkens, G., & Bridgeman, J. G. (2021). Organic Matter Accretion, Shallow Subsidence, and River Delta Sustainability. *Journal of Geophysical Research: Earth Surface*, *126*(12), e2021JF006231.

Kirby, C. J., & Gosselink, J. G. (1976). Primary production in a Louisiana Gulf Coast *Spartina alterniflora* marsh. *Ecology*, *57*(5), 1052–1059.

Kirwan, M. L., & Guntenspergen, G. R. (2010). Influence of tidal range on the stability of coastal marshland. *Journal of Geophysical Research: Earth Surface*, *115*(F2), F02009.

Kirwan, M. L., & Murray, A. B. (2007). A coupled geomorphic and ecological model of tidal marsh evolution. *Proceedings of the National Academy of Sciences of the United States of America*, *104*(15), 6118–6122.

Kirwan, M. L., Temmerman, S., Skeehan, E. E., Guntenspergen, G. R., & Fagherazzi, S. (2016). Overestimation of marsh vulnerability to sea level rise. *Nature Climate Change*, *6*(3), 253–260.

Krauss, K. W., Holm, G. O., Perez, B. C., McWhorter, D. E., Cormier, N., Moss, R. F., Johnson, D. J., Neubauer, S. C., & Raynie, R. C. (2016). Component greenhouse gas fluxes and radiative balance from two deltaic marshes in Louisiana: pairing chamber techniques and eddy covariance. *Journal of Geophysical Research: Biogeosciences*, *121*(6), 1503–1521.

Krueger, T., Maynard, C., Carr, G., Bruns, A., Mueller, E. N., & Lane, S. (2016). A transdisciplinary account of water research: Transdisciplinary account of water research. *Wiley Interdisciplinary Reviews: Water*, *3*(3), 369–389.

Kulp, M. A., Penland, S., Flocks, J. G., Kindinger, J. L., Dreher, C., & Ferina, N. (2002). Regional geology, coastal processes, and sand resources in the vicinity of East Timbalier Island.

Lane, R. R., Mack, S. K., Day, J. W., DeLaune, R. D., Madison, M. J., & Precht, P. R. (2016). Fate of soil organic carbon during wetland loss. *Wetlands*, *36*(6), 1167–1181.

Leonardi, N., Ganju, N. K., & Fagherazzi, S. (2016). A linear relationship between wave power and erosion determines salt-marsh resilience to violent storms and hurricanes. *Proceedings of the National Academy of Sciences*, *113*(1), 64–68.

Li, C., Huang, W., & Milan, B. (2019). Atmospheric cold front–induced exchange flows through a microtidal multi-inlet bay: Analysis using multiple horizontal ADCPs and FVCOM simulations. *Journal of Atmospheric and Oceanic Technology*, *36*(3), 443–472.

Li, C., Weeks, E., Huang, W., Milan, B., & Wu, R. (2018). Weather-induced transport through a tidal channel calibrated by an unmanned boat. *Journal of Atmospheric and Oceanic Technology*, *35*(2), 261–279.

Li, C., Weeks, E., & Rego, J. L. (2009). In situ measurements of saltwater flux through tidal passes of Lake Pontchartrain estuary by Hurricanes Gustav and Ike in September 2008. *Geophysical Research Letters*, *36*(19).

List, J. H., Jaffe, B. E., Sallenger, A. H., Williams, S. J., McBride, R. A., & Penland, S. (1994). *Louisiana barrier island erosion study; atlas of sea-floor changes from 1878 to 1989*.

Liu, K., Chen, Q., Hu, K., Xu, K., & Twilley, R. R. (2018). Modeling hurricane-induced wetland-bay and bay-shelf sediment fluxes. *Coastal Engineering*, *135*, 77–90.

Loren C. Scott & Associates, Inc. (2014). *The economic impact of Port Fourchon: An update* (Economic Impact) (p. 39). Baton Rouge, LA.

Louisiana Department of Wildlife and Fisheries. (n.d.). *An assessment of the principal commerical fisheries in Barataria Bay and its environs* (p. 40). Louisiana Department of Wildlife and Fisheries, Office of Fisheries.

Lugo, A. E., & Snedaker, S. C. (1974). The ecology of mangroves. *Annual Review of Ecology and Systematics*, *5*(1), 39–64.

Madhav, K. C., Oral, E., Straif-Bourgeois, S., Rung, A. L., & Peters, E. S. (2020). The effect of area deprivation on COVID-19 risk in Louisiana. *PLOS ONE*, *15*(12), e0243028.

Maptionnaire. (n.d.). *Maptionnaire Community Engagement Platform*.

Marani, M., D'Alpaos, A., Lanzoni, S., & Santalucia, M. (2011). Understanding and predicting wave erosion of marsh edges. *Geophysical Research Letters*, *38*(21).

Mariotti, G. (2020). Beyond marsh drowning: The many faces of marsh loss (and gain). *Advances in Water Resources*, *144*, 103710.

Mariotti, G., & Fagherazzi, S. (2010). A numerical model for the coupled long-term evolution of salt marshes and tidal flats. *Journal of Geophysical Research*, *115*(F1), F01004.

McBride, R. A., Penland, S., Hiland, M. W., Williams, S. J., Westphal, K. A., Jaffe, B. E., & Sallenger Jr., A. H. (1992). Analysis of barrier shoreline change in Louisiana from 1853 to 1989. In S. J. Williams, S. Penland, & A. H. Sallenger Jr (Eds.), *Louisiana from 1853 to 1989: Atlas of shoreline changes in Louisiana from 1985 to 1989* (pp. 36–97). U.S. Geological Survey.

McCorquodale, A., Georgiou, I., Davis, M. D., & Pereira, J. (2010). *Hydrology and Hydrodynamic Modeling of the Mississippi River in Southeast Louisiana*. New Orleans, LA: Pontchartrain Institute for Environmental Studies, University of New Orleans.

McKee, K. L., & Vervaeke, W. C. (2017). Will fluctuations in salt marsh-mangrove dominance alter vulnerability of a subtropical wetland to sea-level rise? *Global Change Biology*, *24*(3), 1224–1238.

McMann, B., Schulze, M., Sprague, H., & Smyth, K. (2017). *2017 Coastal Master Plan: Appendix A: Project definition* (Version Final) (p. 109). Baton Rouge, LA: Coastal Protection and Restoration Authority.

Meselhe, E. A., Baustian, M. M., & Allison, M. A. (2015). *Basin Wide model development for the Louisiana Coastal Area Mississippi River Hydrodynamic and Delta Management study* (No. Task Order 27.1) (p. 303). Baton Rouge, LA.: The Water Institute of the Gulf. Prepared for and funded by the Coastal Protection and Restoration Authority.

Meselhe, E. A., & Rodrigue, M. D. (2013). *Models performance assessment metrics and uncertainty analysis* (p. 27). Baton Rouge, LA: Louisiana Coastal Area Program.

Meselhe, E., Wang, Y., White, E., Jung, H., Baustian, M. M., Hemmerling, S. A., Barra, M., & Bienn, H. (2020). Knowledge-Based Predictive Tools to Assess Effectiveness of Natural and Nature-Based Solutions for Coastal Restoration and Protection Planning. *Journal of Hydraulic Engineering*, *146*(2), 05019007.

Miner, M. D., Kulp, M. A., FitzGerald, D. M., Flocks, J. G., & Weathers, H. D. (2009a). Delta lobe degradation and hurricane impacts governing large-scale coastal behavior, South-central Louisiana, USA. *Geo-Marine Letters*, *29*(6), 441–453.

Miner, M. D., Kulp, M., Penland, S., Weathers, H. D., Motti, J. P., McCarty, P., Brown, M., Martinez, L., Torres, J., Flocks, J. G., DeWitt, N. T., Ferina, N., Reynolds, B. J., Twitchell, D., Baldwin, W., Danforth, B., Worely, C., & Bergeron, E. (2009b). *Bathymetry and historical seafloor change 1869-2007 Part 1: South-central Louisiana and northern Chandeleur Islands, bathymetry methods and uncertainty analysis* (No. Volume 3, Part 1) (p. 45). U.S. Geological Survey, Pontchartrain Institute for Envionmental Sciences.

Morris, J. T., Sundareshwar, P. V., Nietch, C. T., Kjerfve, B., & Cahoon, D. R. (2002). Responses of coastal wetlands to rising sea level. *Ecology*, *83*(10), 2869–2877.

Mudd, S. M., Howell, S. M., & Morris, J. T. (2009). Impact of dynamic feedbacks between sedimentation, sea-level rise, and biomass production on near-surface marsh stratigraphy and carbon accumulation. *Estuarine, Coastal and Shelf Science*, *82*(3), 377–389.

National Geophysical Data Center. (2001). U.S. Coastal Relief Model - Central Gulf of Mexico.

National Ocean Partnership Program. (n.d.). National Ocean Partnership Program.

NCEP, NOAA, National Weather Service, & U.S. Department of Commerce. (1994, November 21). NCEP/NCAR Global Reanalysis Products, 1948-continuing. UCAR/NCAR - Research Data Archive.

Nielsen, J. G., Lueg, R., & Van Liempd, D. (2021). Challenges and boundaries in implementing social return on investment: An inquiry into its situational appropriateness. *Nonprofit Management and Leadership*, *31*(3), 413–435.

NOAA. (n.d.). Sea Level Trends - NOAA Tides & Currents.

Nyman, J. A., DeLaune, R. D., Pezeshki, S. R., & Patrick, W. H. (1995). Organic matter fluxes and marsh stability in a rapidly submerging estuarine marsh. *Estuaries*, *18*(1), 207–218.

Nyman, J. A., DeLaune, R. D., Roberts, H. H., & Patrick, W. H., Jr. (1993). Relationship between vegetation and soil formation in a rapidly submerging coastal marsh. *Marine Ecology Progress Series*, *96*, 269–279.

O'Brien, M. P. (1969). Equilibrium Flow Areas of Inlets on Sandy Coasts. *Journal of the Waterways and Harbors Division*, *95*(1), 43–52.

Osland, M. J., Day, R. H., & Michot, T. C. (2020). Frequency of extreme freeze events controls the distribution and structure of black mangroves (*Avicennia germinans*) near their northern range limit in coastal Louisiana. *Diversity and Distributions*, ddi.13119.

Osland, M. J., Enwright, N., Day, R. H., & Doyle, T. W. (2013). Winter climate change and coastal wetland foundation species: Salt marshes vs. mangrove forests in the southeastern United States. *Global Change Biology*, *19*(5), 1482–1494.

Patillo, M. E., Czapla, T. E., Nelson, D. M., & Monaco, M. E. (1997). *Distribution and abundance of fishes and invertebrates in Gulf of Mexico estuaries volume II: Species life history summaries* (No. 11). U.S. Department of Commerce, Nation Oceanic and Atmospheric Administration, National Ocean Service.

Pattillo, Mark E. & et al. (1997). *Distribution and abundance of fishes and invertebrates in Gulf of Mexico estuaries, Vol. II: Species life history summaries* (No. No. 11) (p. 377). Silver Spring, Md.: U.S. Dept. of Commerce, National Oceanic and Atmospheric Administration, National Ocean Service.

Pawlowicz, R., Beardsley, B., & Lentz, S. (2002). Classical tidal harmonic analysis including error estimates in MATLAB using T_TIDE. *Computers and Geosciences*, *28*.

Penland, S., Boyd, R., & Suter, J. R. (1988a). Transgressive depositional systems of the Mississippi delta plain: A model for barrier shoreline and shelf sand development. *Journal of Sedimentary Petrology*, *58*(6), 932–949.

Penland, S., Ramsey, K. E., McBride, R. A., Mestayer, J. T., & Westphal, K. A. (1988b). *Relative sea level rise and delta-plain development in the Terrebonne Parish region* (Coastal Geology Technical Report No. No. 4) (p. 140). Baton Rouge, LA.: Louisiana Geological Survey.

Penland, S., & Suter, J. R. (1988). Barrier island erosion and protection in Louisiana: a coastal geomorpological perspective. *Transactions of the Gulf Coast Association of Geological Societies*, *38*, 331–342.

Penland, S., Wayne, L., Britsch, L. D., Williams, S. J., Beall, A. D., & Butterworth, V. C. (2001). *Process Classification of Coastal Land Loss between 1932 and 1990 in the Mississippi River Delta Plain, Southeastern Louisiana* (No. 418). U.S. Geological Survey.

Penland, S., Wayne, L., Britsch, L., Jeffress Williams, S., Beall, A., & Caridas Butterworth, V. (2000). *GEOMORPHIC CLASSIFICATION OF COASTAL LAND LOSS BETWEEN 1932 AND 1990 IN THE MISSISSIPPI RIVER DELTA PLAIN, SOUTHEASTERN LOUISIANA* (Open-File Report). Louisiana Marine Coastal Geology Program.

Pezeshki, S. R., & DeLaune, R. D. (1991). A comparative study of above-ground productivity of dominant U.S. Gulf Coast marsh species. *Journal of Vegetation Science*, *2*(3), 331–338.

Pham, H. T. (2014). *The Rate And Process Of Mangrove Forest Expansion On Above- And Belowground Carbon Relations In Coastal Louisiana* (Dissertation). North Carolina Agricultural and Technical State University.

Poffenbarger, H. J., Needelman, B. A., & Megonigal, J. P. (2011). Salinity influence on methane emissions from tidal marshes. *Wetlands*, *31*(5), 831–842.

Pontchartrain Conservancy. (n.d.). Barataria Basin Hydrocoast Map Archives.

RAE. (2017). *Tampa Bay Blue Carbon Assessment* (p. 373). Restore America's Estuaries.

Reynolds, B. M., Wren, P. A., & Gayes, P. T. (2007). Decadal evolution of shoreface geometry in South Carolina, USA. In *Coastal Sediments' 07* (pp. 1787–1798).

Sabatier, F., Samat, O., Ullmann, A., & Suanez, S. (2009). Connecting large-scale coastal behaviour with coastal management of the Rhône delta. *Geomorphology*, *107*, 79–89.

Salem, M. E., & Mercer, D. E. (2012). The Economic Value of Mangroves: A Meta-Analysis. *Sustainability*, *4*(3), 359–383.

Sallenger Jr., A. H. (2000). Storm impact scale for barrier islands. *Journal of Coastal Research*, *16*(3), 890–895.

Sapkota, Y., & White, J. R. (2021). Long-term fate of rapidly eroding carbon stock soil profiles in coastal wetlands. *Science of The Total Environment*, *753*, 141913.

Sasser, C. E., Evers-Hebert, E., Holm, G. O., Milan, B., Sasser, J. B., Peterson, E. F., & DeLaune, R. D. (2018). Relationships of Marsh Soil Strength to Belowground Vegetation Biomass in Louisiana Coastal Marshes. *Wetlands*, 1–9.

Sasser, C. E., & Gosselink, J. G. (1984). Vegetation and primary production in a floating freshwater marsh in Louisiana. *Aquatic Botany*, *20*(3), 245–255.

Sasser, C. E., Visser, J. M., Mouton, E., Linscombe, J., Hartley, S. B., Steinman, B. A., Abbott, M. B., Mann, M. E., Ortiz, J. D., Feng, S., & others. (2014). *Vegetation types in coastal Louisiana in 2013*. Reston, Virginia: U.S. Geological Survey.

Schindler, J. (2010, December). *Estuarine dynamics as a function of barrier island transgression and wetland loss: Understanding the transport and exchange process* (Master of Science in Earth and Environmental Science: Coastal Sciences). University of New Orleans, New Orleans, LA.

Siegismund, F., & Schrum, C. (2001). Decadal changes in the wind forcing over the North Sea. *Climate Research*, *18*, 39–45.

Smith, C. J., DeLaune, R. D., & Patrick Jr, W. H. (1983a). Carbon dioxide emission and carbon accumulation in coastal wetlands. *Estuarine, Coastal and Shelf Science*, *17*(1), 21–29.

Smith, C. J., DeLaune, R. D., & Patrick, W. H. (1983b). Nitrous oxide emission from Gulf Coast wetlands. *Geochimica et Cosmochimica Acta*, *47*(10), 1805–1814.

SROI Network. (2012). *A Guide to Social Return on Investment*. London, UK: Cabinet Office.

Stagg, C. L., & Mendelssohn, I. A. (2011). Controls on resilience and stability in a sediment-subsidized salt marsh. *Ecological Applications*, *21*(5), 1731–1744.

Stagg, C. L., Schoolmaster, D. R., Piazza, S. C., Snedden, G., Steyer, G. D., Fischenich, C. J., & McComas, R. W. (2016). A landscape-scale assessment of above- and belowground primary production in coastal wetlands: implications for climate change-induced community shifts. *Estuaries and Coasts*.

Stanley, J. G., & Sellers, M. A. (1986). *Species profiles: life histories and environmental requirements of coastal fishes and invertebrates (Gulf of Mexico)--American oyster* (No. TR EL-82-4) (p. 25). U.S. Army Corps of Engineers.

Stone, G. W., Liu, B., Pepper, D. A., & Wang, P. (2004). The importance of extratropical and tropical cyclones on the short-term evolution of barrier islands along the northern Gulf of Mexico, USA. *Marine Geology*, *210*(1–4), 63–78.

Stringer, L. C., Dougill, A. J., Fraser, E., Hubacek, K., Prell, C., & Reed, M. S. (2006). Unpacking "participation" in the adaptive management of social–ecological systems: a critical review. *Ecology and Society*, *11*(2).

Swarenzski, C. M., & Perrien, S. M. (2015). *Discharge, Suspended Sediment, and Salinity in the Gulf Intracoastal Waterway and Adjacent Surface Waters in South-Central Louisiana, 1997–2008* (Scientific Investigations Report No. 2015–5132) (p. 30). Reston, Virginia: U.S. Geological Survey.

Temmerman, S., Govers, G., Wartel, S., & Meire, P. (2003). Spatial and temporal factors controlling short-term sedimentation in a salt and freshwater tidal marsh, Scheldt estuary, Belgium, SW Netherlands. *Earth Surface Processes and Landforms*, *28*(7), 739–755.

Teo, W. S., Seow, T. W., Radzuan, I. S. M., Mohamed, S., & Abas, M. A. (2021). Social Return on Investment (SROI) for government flood recovery project in Kuala Krai, Kelantan. *IOP Conference Series: Earth and Environmental Science*, *842*(1), 012055.

The Water Institute of the Gulf. (2018). Partnership for Our Working Coast - Water Institute.

Törnqvist, T. E., Cahoon, D. R., Morris, J. T., & Day, J. W. (2021a). Coastal Wetland Resilience, Accelerated Sea-Level Rise, and the Importance of Timescale. *AGU Advances*, *2*(1), e2020AV000334.

Törnqvist, T. E., Cahoon, D. R., Morris, J. T., & Day, J. W. (2021b). Coastal Wetland Resilience, Accelerated Sea-Level Rise, and the Importance of Timescale. *AGU Advances*, *2*(1), e2020AV000334.

Törnqvist, T. E., Jankowski, K. L., Li, Y.-X., & González, J. L. (2020). Tipping points of Mississippi Delta marshes due to accelerated sea-level rise. *Science Advances*, *6*(21), eaaz5512.

U.S. Army Corps of Engineers, New Orleans District. (2021, November 2). Dredging/BU Spreadsheets.

US Department of Commerce, N. O. and A. A. (2018, April 24). National Data Buoy Center - Averaging Procedures for Wind Measurements.

US EPA. (2021). *Inventory of U.S. Greenhouse Gas Emissions and Sinks: 1990-2019* (No. EPA 430-R-210-005).

USACE. (1965, May 11). Interim Survey Report, Morgan City, Louisiana and Vicinity, serial no. 63. U.S. Army Corps of Engineers New Orleans District.

USACE. (2021, March 31). Engineering Manual Number 1110-2-1304: Civil Works Construction Cost Index System. U.S. Army Corps of Engineers.

USEPA. (2016). *EPA Fact Sheet: Social Cost of Carbon*. Washington, D.C.: U..S. Environmental Protection Agency.

Valentine, K., Bruno, G., Elsey-Quirk, T., & Mariotti, G. (2021). Brackish marshes erode twice as fast as saline marshes in the Mississippi Delta region. *Earth Surface Processes and Landforms*, *46*(9), 1739–1749.

Valentine, K., & Mariotti, G. (2019). Wind-driven water level fluctuations drive marsh edge erosion variability in microtidal coastal bays. *Continental Shelf Research*, *176*, 76–89.

Visser, J., & Duke-Sylvester, S. (2017). LaVegMod v2: Modeling Coastal Vegetation Dynamics in Response to Proposed Coastal Restoration and Protection Projects in Louisiana, USA. *Sustainability*, *9*(9), 1625.

Visser, J. M., Duke-Sylvester, S. M., Carter, J., & Broussard, W. P. (2013). A Computer Model to Forecast Wetland Vegetation Changes Resulting from Restoration and Protection in Coastal Louisiana. *Journal of Coastal Research*, *67*, 51–59.

Walker, N. D., & Hammack, A. B. (2000). Impacts of Winter Storms on Circulation and Sediment Transport: Atchafalaya-Vermilion Bay Region, Louisiana, U.S.A. *Journal of Coastal Research*, *16*(4), 996–1010.

Warner, J. C., Armstrong, B., Sylvester, C. S., Voulgaris, G., Nelson, T., Schwab, W. C., & Denny, J. F. (2012). Storm-induced inner-continental shelf circulation and sediment transport: Long Bay, South Carolina. *Continental Shelf Research*, *42*, 51–63.

Weaver, C. A., & Armitage, A. R. (2020). Above- and belowground responses to nutrient enrichment within a marsh-mangrove ecotone. *Estuarine, Coastal and Shelf Science*, 106884.

Whatmore, S. J. (2009). Mapping knowledge controversies: science, democracy and the redistribution of expertise. *Progress in Human Geography*, *33*(5), 587–598.

White, D. A., & Simmons, M. J. (1988). Productivity of the Marshes at the Mouth of the Pearl River, Louisiana. *Castanea*, *53*(3), 215–224.

White, D. A., Weiss, T. E., Trapani, J. M., & Thien, L. B. (1978). Productivity and decomposition of the dominant salt marsh plants in Louisiana. *Ecology*, *59*(4), 751.

White, E. D., Fitzpatrick, C., Freeman, A., Jankowski, K. L., & Pahl, J. W. (2021). *2023 Coastal Master Plan Modeling: ICM Boundary Conditions* (Forthcoming). Coastal Protection and Restoration Authority.

Wilson, C. A., & Allison, M. A. (2008). An equilibrium profile model for retreating marsh shorelines in southeast Louisiana. *Estuarine, Coastal and Shelf Science*, *80*(4), 483–494.

Wu, W., Yeager, K. M., Peterson, M. S., & Fulford, R. S. (2015). Neutral models as a way to evaluate the Sea Level Affecting Marshes Model (SLAMM). *Ecological Modelling*, *303*, 55–69.

Zedler, J. B. (2017). What's new in adaptive management and restoration of coasts and estuaries? *Estuaries and Coasts*, *40*(1), 1–21.